# Speed Control of Autonomous Amphibious Vehicles

DISSERTATION

zur Erlangung des Grades eines Doktors

der Ingenieurwissenschaften

vorgelegt von

M.Sc. Sailan Khaled

geb. in Sana,a

eingereicht bei der Naturwissenschaftlich-Technischen

Fakultät der Universität Siegen

Siegen, 2017

Gutachter der Dissertation:
Prof. Dr. Klaus-Dieter Kuhnert
Prof. Dr. Hubert Roth

Datum der mündlichen Prüfung:
20, December 2017

Gedruckt auf alterungsbeständigem holz- und säurefreiem Papier.

## CERTIFICATE OF AUTHORSHIP/ORIGINALITY

I certify that the work in this thesis has not previously been submitted for a degree nor has it been submitted as part of the requirements for a degree except as fully acknowledged within the text.

I also certify that the thesis has been written by me. Any help that I have received in my research work and in the preparation of the thesis itself has been acknowledged. In addition, I certify that all information sources and literature used are indicated in the thesis.

# Abstract

This thesis describes the development of a speed and steering control system for an autonomous amphibious vehicle use under extreme conditions for tactical distributed surveillance and autonomous motion on ground and water. It has been a research project of the Institute for Real-Time Learning Systems of Siegen University. The primary aim of the project is to design and develop speed and steering control systems for the DORIS Robot. The research is focused on controlling speed, steering, and obstacle avoidance using PID, Dead-Beat, and intelligent fuzzy logic control methods.

For controlling the steering of DORIS on ground, two DC motors were used, which act on two variable displacement hydraulic pumps that set the swashplate angles in the hydrostatic transmission system. The PID, Dead-Beat, and P-Dead-Beat controllers were each designed to control the DC motor's angular position, which in turn, controls the swashplate angle. Throughout the project, these types of controllers were tested on a separate hardware using PWM (Pulse-Width Modulation) for controlling the DC motor's angular position. A comparison identified the PID control method as the optimal one. The speed of the DC motor is an important factor for controlling the swashplate torque. It was analyzed and studied with respect to the impact of different surfaces during skidding and rolling. To control the steering of the vehicle optimally, an intelligent fuzzy logic controller was developed for producing the independent angular positions of the two DC motors, which control the different speeds of the left and right wheels of the vehicle. These different speeds cause the vehicle to skid-steer right or left per the fuzzy logic rules.

The speed of the vehicle is a function of the engine speed. A servo motor control system controls the engine speed, whereby a coupling between the servo-control loop and the engine control loop is achieved. To drive DORIS semi-autonomously, a tele-operating system was added to the whole design, using a PC and/or Joystick and the Robot Operating System (ROS). During the motion of the vehicle in an unknown and changing environment, the vehicle must be able to navigate successfully without colliding with obstacles in the surroundings. For this purpose, a fuzzy logic strategy was also developed to guide the Autonomous Amphibious Vehicle (AAV).

For driving the vehicle on water, a water-jet system is used. The steering control system was implemented based on a PID control approach.

All hardware systems, control architecture, sensor suite, current capabilities, future research, and applications of the AAV are described in this project.

# Zusammenfassung

Diese Arbeit beschreibt die Entwicklung einer Geschwindigkeits- und Lenkregelung für ein Amphibienfahrzeug, welches beispielsweise für Überwachungsaufgaben oder autonomes Fahren auf teilweise schwerbefahrbaren Untergründen zu Land und auf dem Wasser konzipiert wurde. Es ist ein Forschungsprojekt des Instituts für Echtzeit Lernsystems der Universität Siegen. Dabei ist das primäre Ziel der Entwurf und die Entwicklung einer Geschwindigkeits- und Lenkreglung zur Anwendung auf den mobilen Roboter „DORIS“ (Dual media Outdoor Robot Intelligent System). Darüber hinaus wurde darauf aufbauend eine Hindernisvermeidungsregelung entwickelt. Als Regelungssysteme wurden PID-Regler, Dead Beat-Regler und intelligente Fuzzy-Logik-Regler verwendet. Die Geschwindigkeitsreglung des hydraulisch angetriebenen Amphibienfahrzeugs DORIS wurde durch zwei Gleichstrommotoren realisiert, die jeweils die Winkelpositionen der Taumelscheibenpumpen am hydrostatischen Übertragungssystem stellen. Eine Kombination aus PID-, Dead-Beat- und P-Dead-Beat-Regler wurde entworfen und entwickelt, um die Gleichstrommotoren anzusteuern, sodass der Winkel der hydraulisch verstellbaren Taumelscheibenpumpe entsprechend eingestellt werden konnten. Des Weiteren wurden im Rahmen des Projektes diese Regelungstypen auf verschiedene Hardwaresystemen unter Verwendung von Pulsweitenmodulation (kurz PWM) getestet um die Winkelpositionen eines Gleichstrommotors zu kontrollieren. Ein Vergleich identifizierte den PID-Regler als das Optimum. Die Geschwindigkeitsreglung des Gleichstrommotors stellt einen wichtigen Faktor für die Steuerung des Drehmoments der Taumelscheibe dar. Dementsprechend wurde die Auswirkung des Taumelscheiben-Drehmoments bezüglich Roll- und Gleiteigenschaften des Fahrzeugs auf verschiedenen Untergründen analysiert. Für die optimale Steuerung des Lenkungssystems des Fahrzeugs wurde ein intelligenter Fuzzy-Logik-Regler entwickelt, um die zwei unabhängigen Winkelpositionen beider Gleichstrommotoren zu setzen, sodass unterschiedliche Drehzahlen bzw. Geschwindigkeiten für die linke und rechte Achse des Fahrzeugs erzeugt werden können. Diese durch Fuzzy-Logik-Reglung erzeugten unterschiedlichen Geschwindigkeiten erzeugen die entsprechenden Richtungsänderung des Fahrzeugs. Die Geschwindigkeit des Fahrzeugs ist eine Funktion aus der Motordrehzahl. Hierbei wird die Motordrehzahl mit Hilfe eines Servo-Motor-Regelungssystems gesteuert, wodurch eine Kopplung zwischen dem Servo-Regelkreis und dem Motor-Regelkreis erreicht wird. Um das Fahrzeug DORIS semi-autonom betreiben zu können, wurde dem Gesamtdesign ein

Funkfernsteuerungssystem hinzugefügt, welches ermöglicht, dass das Fahrzeug mit der Hilfe eines Eingabegerätes wie z.B. ein Joystick und/oder PC mit integriertem Roboter-Betriebssystems ROS (Robot Operation System), gesteuert werden kann. Während der Navigation des Fahrzeugs in einem unbekannten und sich ständig ändernden Umfeld, sollte das Fahrzeug in der Lage sein, Hindernissen erfolgreich auszuweichen, um Kollisionen zu vermeiden. Zu diesem Zweck wurde erneut eine Fuzzy-Logik-Strategie entwickelt, welche das autonome Amphibienfahrzeug navigiert. Um das Fahrzeug auf dem Wasser nutzen zu können, wurde ein Wasser-Jet-Antriebssystem mit einem Lenkungssystem basierend auf einem PID-Regler entwickelt und implementiert. Alle Hardwaresysteme, Regelungsarchitekturen, integrierte Sensor- und Stromversorgungseinheiten, zukünftige Forschungsausblicke und Anwendungsbereiche des autonomen Amphibienfahrzeugs sind in dieser Arbeit beschrieben.

# Acknowledgements

During my time as a Ph.D. student at the University of Siegen I have had the fortune of knowing and working with many amazing people. Their support and friendship has made my time here truly incredible.

First of all, I would like to thank my supervisor, Professor Dr. Klaus-Dieter Kuhnert for his constant guidance and support over the years. His wisdom, humor, and kindness are truly inspiring. He brought me into the field of ground vehicle control and taught me the principles of scientific work and writing. When my research suffered some setbacks, his encouragement let me persevere in my efforts. Without his careful guidance, this work would not have been possible.

Also, I would like to thank my thesis committee. They spent a lot of their valuable time to read and remark on my thesis, which guided and improved my thesis. I want to express my gratitude to my colleagues at the Institute of Real-Time Learning Systems for their cooperation and help, especially Jens Schlemper, who always discussed with me and served as a great source of inspiration for me. Thanks to Lars Kuhnert and Markus Ax who taught me about the robots' operation, electronic circuits and also helped me resolve many technical problems. I am grateful to Benjamin Meir who kindly provided me all kinds of support and help with my work. I would also like to thank Klaus Müller, Ievgen Smielik, Simon Hardt, Jan Kunze and Marc Steven Krämer for their encouragement, support and contributions to my experiments. My gratitude also goes to all of my friends who supported me.

Lastly, I would also like to thank my family, especially my parent and siblings, who gave me so much and helped me become who I am today. I thank my wife Bushra Abo-haider for being at my side throughout these years; she never had any complaint about my late nights at the lab and constantly provided comfort during difficult times. I am grateful to my daughter Khulood and my sons Amr and Omar who always gave me happiness and liveliness.

This thesis has also been funded by the ministry of higher education in Yemen and the Institute of Real-time Learning Systems at the University of Siegen. Their support is greatly acknowledged.

# Contents

# List of Figures

# List of Abbreviations

$V_y$ *Linear Speed in y direction (m/sec)*

$V_x$ *Linear Speed in x direction (m/sec)*

$R$ *Tire Radius (m)*

$\omega$ *Tire Rotational speed (rad/sec)*

$S_x$ *Longitudinal slip (m)*

$S_y$ *Lateral slip (m)*

$k_x$ *Slip coefficient in x direction*

$k_y$ *Slip coefficient in y direction*

$u$ *Friction coefficient*

$F_x$ *Longitudinal tire force (N)*

$F_y$ *Lateral tire force (N)*

$F_z$ *Force in z direction (N)*

$E_y$ *Curvature factor*

$F_r$ *Tractive Force (N)*

$m$ *Tire mass (kg)*

$g$ *Gravity (9.81 m/s2)*

$A$ *Vehicle front Area* ($m^2$)

$C_d$ *Drag coefficient*

$T_f$ *Torque produced by friction forces (N.m)*

$T_p$ *Torque relating to the pressure effect (N.m)*

$T_r$ *Torque relating to the rotation of the barrel (N.m)*

$J_b$ *swach plat inertia(kgm2)*

$\ddot{\theta_P}$ *Angular acceleration (rad/s2)*

$B_p$ *Damping coefficient of the swash plate yoke assembly*

$T_{fc}$ *Torque produced by the coulomb friction force(N.m)*

$K_{p1}$ *Pressure torque constant*

$K_{p2}$ *Pressure torque constant*

*Pp Pump pressure (N/m2)*

*S1 The simplified pump model constant*

*S2 The simplified pump model constant*

$Q_{Pump}$ *The hydraulic pump flow rate* $(m3/s)$

$V_g$ *Geometric displacement (m)*

$R_P$ *Piston pitch radius (m)*

$Z$ *Number of Pistons*

*d Piston Diameter(m)*

$N$ *Pump speed (rad/sec)*

$\gamma$ *Swash plate angle (degree)*

$K_p$ *PID controller Proportional part*

$K_i$ *PID controller Intergral Part*

$K_d$ *PID controller diferential Part*

$T_{dev}$ *The torque developed in the rotor (N.m)*

$V_T$ *Motor Voltage (V)*

$K$ *Constant depending on coil geometry,*

$\varphi$ *The magnetic flux density/pole (Tesla)*

$\omega_m$ *Motor Speed (rad/sec)*

$R_a$ *Armature resistance (*Ω*)*

$\rho$ *Slip rate*

$v_t$ *Theoretical speed of the vehicle (m/sec)*

$v$ *Actual speed of the vehicle (m/sec)*

$q$ *Location of the vehicle centre of gravity (m)*

$\theta$ *Lateral velocity of the vehicle centre of gravity (m/sec)*

$v_{Gx}$ *Longitudinal velocity of vehicle gravity centre (m/sec)*

$v_{Gy}$ *Lateral velocity of vehicle gravity centre (m/sec)*

$\rho_l$ *Slip rate of left side tires*

$\rho_r$ *Slip rate of right side tires*

$s_y$ *Offset of vehicle gravity centre*

$\omega_l$ *Rotational speed of left side tires (rad/sec)*

$\omega_r$ *Rotational speed of right side tires (rad/sec)*

$\rho$ *The density of liquid (kg/m3)*

$Q$ *The flow of jet pump (m3/s)*

$V_j$ *The jet velocity of flow at the spout (m/s)*

$V_i$ *The flow speed at entrance (m/s)*

$k$ *The ratio of jet velocity to entering speed*

$\zeta$ *the loss coefficient of system head*

$CG$ *vehicle gravity centre( 9.81 m/s2)*

$sx$, $sy$ *the position coordinates of the vehicle gravity centre*

$\omega r$ *rotational speed of right side tires(rad/sec)*

$\omega l$ *rotational speed of left side tires(rad/sec)*

$ks$ *rotational speed ratio*

$\tau$ *shear stress (Pascal)*

$j$ *shear displacement(m)*

*Vl longitudinal velocity of left side tires (m/sec)*

V *longitudinal velocity of right side tires (m/sec)*

*K shearing modulus of elasticity*

$\sigma$ *normal pressure stress (N/m2)*

$Fyr$ *longitudinal force of right sides tire(N)*

$Fyl$ *longitudinal force of left sides tire(N)*

$C_d$ *Aerodynamic drag coefficient.*

$\rho$ *Air density* ($kg.m^{-3}$)

*k Shear deformation modulus*

# Chapter 1

# Amphibious Vehicles

An amphibious vehicle (AV) is a vehicle that serves as a means of transportation and exploration on land as well as on water. Amphibian vehicles include amphibious bicycles, vehicles, All Terrain Vehicles, cars, buses, trucks, military vehicles, and hovercrafts. Classic landing crafts are not amphibious vehicles, as they do not offer any real land transportation at all, although they are part of amphibious assault. Over the last few years, there has been a growing emphasis on autonomous vehicles, "intelligent machines" capable of performing tasks in the world by themselves without explicit human control over their movement. These types of vehicles are self sufficient and capable of making on-the-fly decisions; they remove the human element.

For a variety of reasons, traversing to such places is important, some examples include collecting/analyzing water samples in possibly contaminated environments, mapping out landmarks and the geology of an area, search and rescue, delivering items/tools from one location to security surveillance, and filming animals in their natural environments. Not withholding, an Autonomous Amphibious Vehicle (AAV) could be used for either primarily terrestrial or aquatic purposes.

Given the rapid increase in vehicular technology, one may reasonably ask, "Where are the promised amphibious vehicles for land-water?" Many companies were founded in the 1960s, most notably, the ARGO company, to manufacture and commercialize the amphibious all-terrain vehicles (AATV) (Wikipedia, 2012). However, due to the oil crisis of 1973, poor quality product has resulted in a rapid decline in this type of AATVs, only a small number of manufacturers remain today. From the latter part of 1980s, amphibious vehicles exist only for military, research, hobby, and educational use. Today, the uses of these amphibious vehicles have been recognized as important logistic tools by the US marine as a single vehicle support line over land and water operations. However, the wait for a promising unmanned amphibious vehicle has proven to be an unexpected long and difficult one. The exponential increase in computer processing capability and other advancements have not led to improvements of general solutions to the machine vision, robotic sensory, and the ability to navigate autonomously. To date, many mobile robots have been built worldwide for outdoor navigation, some of which worked, some fewer which appear to have worked well,

and far fewer of which were actually transferred into regular use. Therefore, to achieve a routine deployment of autonomous robots for outdoor applications remains a great challenge.

## 1.1 State of the Art

Everyday more and more amphibious robotic are entering the real world. They are being put to work just about everywhere manual vehicles have been used in the past. From agriculture, mining operations, military and exploring, to inside factories and hospitals, they are increasing safety, efficiency, and performance in all tasks. The recent explosion of unmanned amphibious vehicle technology has been made possible by vast improvements in sensors, computers and research developments. There is now a greater understanding of the problems that need to be solved in order to allow autonomous robot to operate in the largely uncertain real world. Amphibious vehicles are designed to perform a variety of tasks, which they perform with varying levels of independence. While some amphibious vehicles are rigidly controlled by human operators, via teleportation and wireless input, others are sent about with little to no assistance. The structures and control strategies of the robots are different according to various environments.

The capability of autonomous and semi-autonomous platforms to function in the shallow water surf zone is critical for a wide range of military and civilian operations. A series of rugged all-terrain robotic vehicles dubbed Whegs™ as shown in figure 1.1 and 1.2 capable of fast running and climbing through the incorporation of all of the aforementioned biologically-inspired mechanisms to navigate terrain developed. Common to all robots in this line is a single drive motor that powers six multi-spoke appendages called wheel-legs. When three-spoke wheel-legs are used, neighbouring legs are offset by 60° yielding a nominal tripod gait. The spokes allow Whegs™ to climb over larger obstacles than a vehicle with similarly sized wheels [Boxerbaum, A.S., et al., 2005].

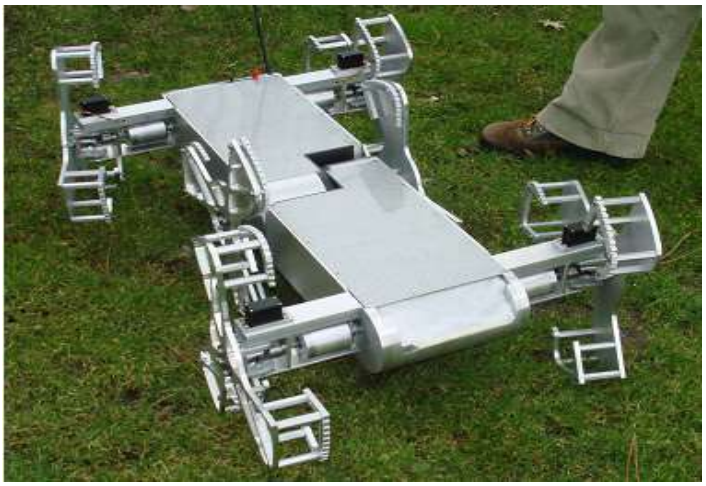

Figure 1.1 Wheg sT M IV

Figure 1.2 Wheg sT M II

Swimming and Crawling Amphibious Snake Robot for outdoor robotics tasks as shown in figure 1.3, taking inspiration from snakes and elongated fish such as lampreys, to use the robot as a test-bed for novel types of adaptive controllers based on the concept of central pattern generators, and to use the robot to investigate hypotheses of how locomotion-controlling neural networks are implemented in real animals [Crespi, A., et al., 2005].

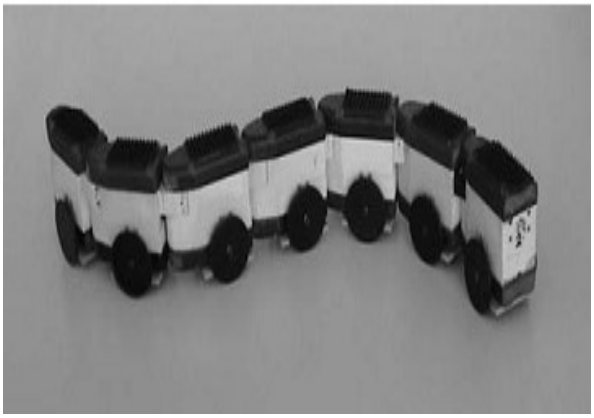

Figure 1.3 Snake Robot

An Autonomous Amphibious Vehicle (AAV) capable of traversing across aquatic and terrestrial environments as shown in figure 1.4 is used for either primarily terrestrial or aquatic purposes. Such purposes could include investigating icebergs, surveying ships in shipyards, traversing open waters, or collecting data in farm fields. The multi-purpose nature of AAVs makes them more appealing then autonomous terrestrial vehicles and autonomous on-water vehicles [Frejek, M., et al., 2008].

Figure 1.4 Autonomous Amphibious Vehicle (AAV)

AmphiRobot-II is an amphibious robot, which is capable of multi-mode motion as shown in figure 1.5, designed and controlled for a versatile amphibious robot. AmphiRobot-II inspired by various amphibian principles in the animal kingdom. In terms of the propulsion features of existing amphibians, a novel hybrid propulsive mechanism coupled with wheel-propeller fin movements is proposed that integrates fish- or dolphin-like swimming and wheel-based crawling. The robot is able not only to implement flexible wheel-based movements on land,

but also to perform steady and efficient fish- or dolphin-like swimming under water and can further switch between these two patterns via a specialized swivel device [Yu, J., et al., 2012].

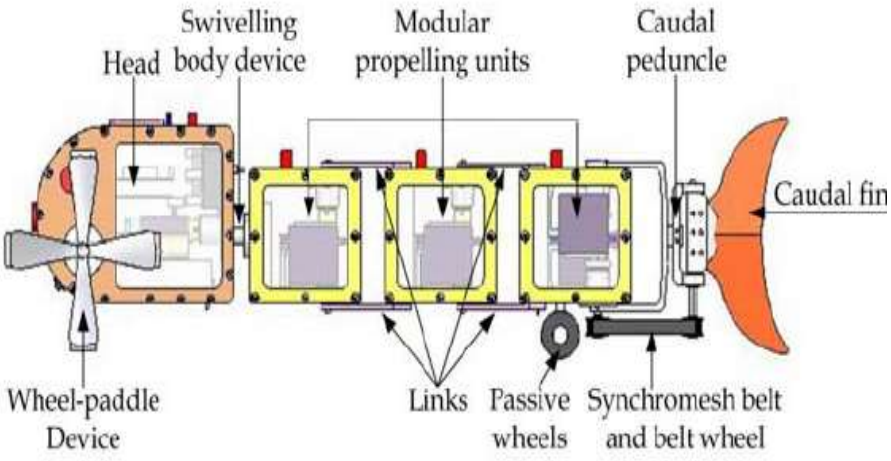


Figure 1.5 Multi-Mode Motion Amphibious Robot

Numerous natural disasters have occurred around the world that reflect the need for Autonomous Amphibious Vehicle (AAV) such as shown in figure 1.6; during the Indonesia Tsunami, earthquake in India and rainstorm in Guangzhou: in such dangerous situation, the rescue team will risk their life in saving other lives to reach the destination in time to save the victims who have been trapped in the scene. For some areas, marches, riverbanks, small lakes and flood areas are the main barriers that affect the efficiency of the rescue mission. Hence, Autonomous Amphibious Vehicle was developed [Tee, Y., et al., 2010].

Figure 1.6 Autonomous Amphibious Vehicle

In 1996, H. Greiner pioneered the study of amphibious robot by developing ALUV (Autonomous Legged Underwater Vehicle) that propels with six crab-like legs. For coral reefs protection and ocean exploration, G. Dudek, constructed the well-known "AQUA" that walks and swims with six flippers. Unlike the legged robots as mentioned above, snake-like amphibious robot was developed for exploration and inspection tasks in pipes and other narrow and dangerous environment. In 2002, an amphibious snake-like robot called "ACM-R5" was built based on the underwater snake-like robot "HELIX" [Luo, F., et al., 2010]. Multipurpose Autonomous Amphibious as in figure 1.7 Vehicle which could operate 3 terrains; land-sea-air, a 3-in1 amphibious vehicle has been developed [Yu, S.C., et al., 2011].

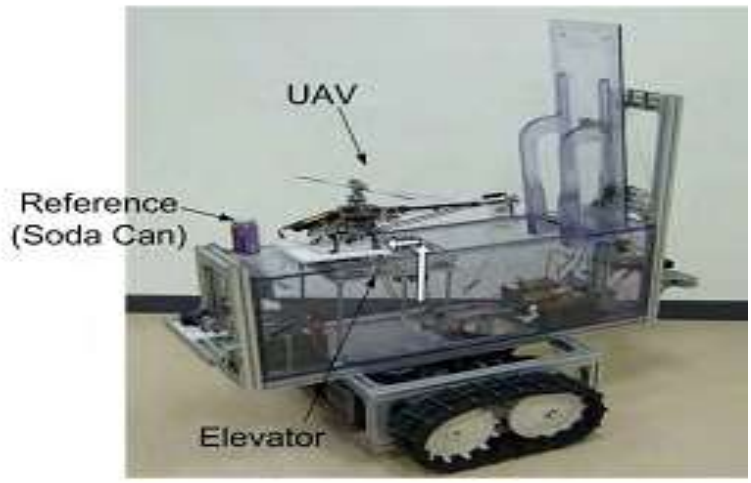


Figure 1.7 Multifunctional Autonomous Amphibious Vehicle

Serving as an outdoor demonstrator for the research programme at CAS is the ARGO, an Autonomous Amphibious Vehicle as shown in figure 1.8. The vehicle is retrofitted on the platform of the Conquest 8x8 that can achieve 30km/h on land and 3km/h on water. The power transmission system includes a water-cooled V-2 Kawasaki engine, continuous variable transmission (CVT), gearbox, differential and a chain system [Tran, T.H., et al., 2006].

Figure 1.8 ARGO 8x8 - an Autonomous Amphibious Vehicle

An all-terrain robotic platform based on an ARGO 6x6 amphibious petrol powered skid-steer vehicle was developed by Michael Clarke and Tom Blanchard as shown in figure 1.9. In addition, an Amphibious Robot for Operation in the Littorals called Sea-Dragon carries a tele-operated weapon and is controlled by the remote operator using standard R/C gear and camera feedback was designed [Clarke, M., et al., 2010].

Figure 1.9 ARGO 6x6 - an Autonomous Amphibious Vehicle

A small tracked unmanned amphibious vehicle called the DUKW-Ling as shown in figure 1.10 was designed and controlled, The DUKW-Ling is a 1/7th-scale model of a tracked amphibious vehicle which was developed by the Center for Innovation in Ship Design at the Naval Surface Warfare Center, Carderock Division [Marquardt, J.G., et al., 2014].

Figure 1.10 The DUKW-Ling Unmanned Amphibious Vehicle

A novel amphibious robot as show in figure 1.11 with wheel propeller- leg integrated driving devices, was developed by Shenyang Institute of Automation, which can realize both crawling locomotion on the ground and swimming locomotion in the water without changing its driving devices [Yu, J., et al., 2010].

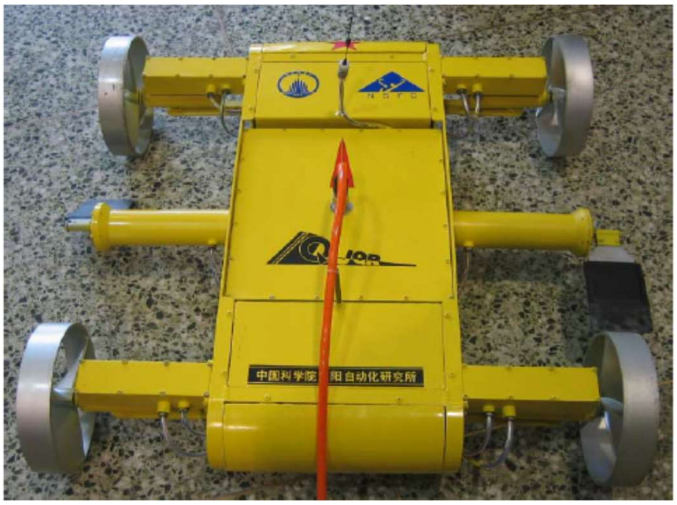

Figure 1.11 Wheel-Propeller-Leg Integrated Amphibious Robot

An amphibious walking robot shown in figure 1.12, which has some unique features in the structure and composition, was developed in order to experiment the proposed method in real sea. [Tanaka, T., et al., 2006].

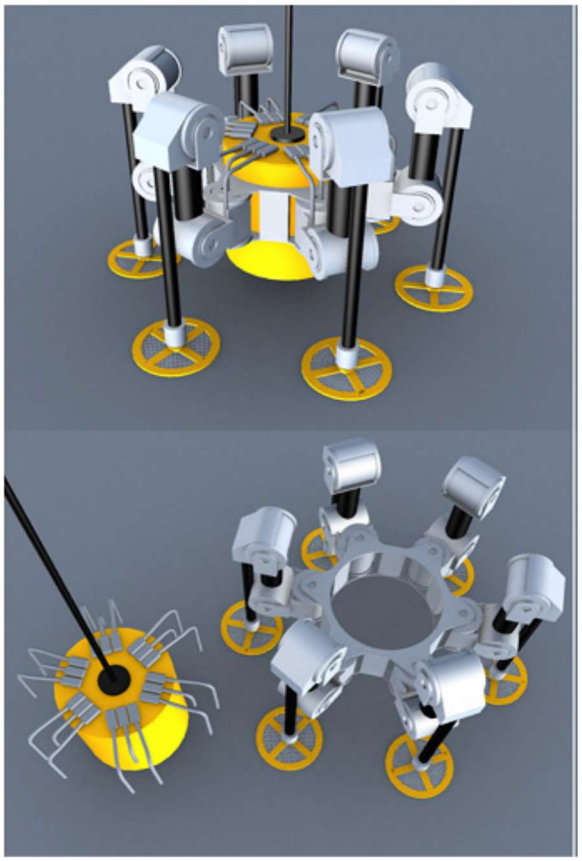

Figure 1.12 Amphibious Walking Robot

## 1.2 Research Areas in AAR Development

AAV research can be divided up into five areas: mobility, localisation, navigation, planning, and communication. Mobility deals with the vehicle mechanism design, the motion control technique, and the interaction between the vehicle and terrain. It is concerned with the kinematics and dynamics of the vehicle platform and the control algorithms for the vehicle as well as all actuators outfitted on the vehicle to obtain the desired motion on a certain terrain. This is the area where this research project is involved.

Localisation is related to estimation of the vehicle position and attitude in a fixed frame: for example, an earth-fixed coordinates system. It is concerned with robust algorithms for accurate estimation to deal with sensor uncertainties. Taking information from internal and external sensors as inputs, its outputs affect both navigation and mobility processes.

Navigation handles information obtained from environment sensors to build up a map of the environment. The representation of the environment is then used to control the vehicle in small area around the current vehicle position in order to follow a trajectory defined in a planning process. It also manages obstacle detection and avoidance. Mission and path

planning make use of all known information from prior maps, mission goals, sensory and control structures to generate trajectories, or way points and other actions for the vehicle to execute. However, due to the incomplete knowledge of the world in outdoor missions, the vehicle must use the environment information gathered along the local path to update or rebuild the trajectory.

Communication allows the vehicle to be connected with human operators and other vehicles or systems. Whether the vehicle is fully autonomous or not, it requires a communication link to co-operate with other vehicles or the base station in many missions.

## 1.3 Motivation and Research Objectives

This research is part of a larger project conducted at the institute of Real-Time Learning Systems at the University of Siegen. The project aims to develop a speed, motion and steering control system for an existing 8x8 skid-steering vehicle with equipped actuators and sensors to achieve semi and autonomous operations. This thesis focuses on motion control of the Autonomous amphibious vehicle. This project concentrates on the DORIS robot and practically develops the vehicle driveline system in which the vehicle can move in constant speed up to 25 km/hour and developed the proper controller that actuate the variable displacement hydraulic pump.

Whilst robotic platforms are wide spread, after significant investigations, it has become clear that the automation of DORIS robot and the methods of controlling the hydrostatic transmission system have never been attempted before. This has lead to a number of questions about the automation of such a vehicle and the effects to the different surfaces:

1. Can DORIS Robot be automated, and what complexity of Software and Hardware components are required?
2. What level of accuracy can be expected from a skid-steering system and to what extent is a control system more or less accurate than a human operator?
3. What effects does surfaces type have on the vehicle speed? The development of the control system is intended to provide answers to these questions, and will hopefully provide a solid robotic platform for further scientific study in the future. However, if the system is unable to control the DORIS Robot, or does so with little or no control, then this project will not be considered a failure. This would simply result in negative responses to most of the research questions posed. For example, it may simply be the case that it is not possible to automate such a robot or the non-reliability in the hardware.

## 1.4 Main Contribution

The goal of this dissertation is to implement speed control system to control the autonomous amphibious Vehicle in a real environment. The main contributions addressing key technical issues in speed control are listed as follows:

• I have studied, analysed and modeled the hydraulic system used to operate the Robot; electrical motor with gearbox producing high torque was proposed to control the hydraulic variable displacement pump; hydrostatic transmission with fixed hydraulic motor and variable displacement pump were used as propulsion system. The hydraulic pump swash plate angular position in small distance rotating (rotation), should be controlled accurately in order to control the Robot speed, which is a big challenge. The effect of surfaces on the torque applied on the swash plate was studied and analysed.

• Based on controlling the swash plate angular position connected to the DC motor I have developed two control systems, PID control system and Dead Beat control system and I have compared between the two methods and I also used mixed method of PID and Dead beat which is a P-Dead beat to control the angular position. With the P-Dead beat I have achieved a good result. Speed of the DC motor is controlled using PWM, the DC motor Torque is a function of Motor speed, the maximum torque from DC Motor should be able to open and close the swash plate during skid steer where the torque on the swash plate become too high.

• Adding the steering effect to drive the Vehicle left and right or around itself like skid steer Vehicles, is achieved using intelligent fuzzy logic controller where I have divided the steering wheel to 5 positions and the motors to 3 positions for forward and 3 positions for backward and with 15 fuzzy logic rules, I have implemented the fuzzy decision to each motor where the position of each DC Motor should be to give the action of skid steer.

• Because the engine speed is an important effect on the Hydraulic motor, I have coupled the steering control system and the engine speed control system with the servo control system. With this coupled system we can increase the hydraulic motor speed as well. A linear function to couple the high level control system with the high level control system was estimated.

• To convert the Vehicle to be semi-automated vehicle, a Tele-operation control system was implemented to drive the vehicle using PC, robot operating system (ROS) was used to

program and connect the joystick, the communication between the motors' controllers and the main processor was designed using SPI and UART communication protocols.

• Analysing, Modelling and design of object avoidance controller system for DORIS is achieved in this project, HOKUYO laser scanner integrated with ROS was used to detect obstacles in front of the vehicle.

• For driving the vehicle on water, a water jet system and water jet steering controller was analysed and designed, the mathematical model of water jet system was analysed and the PID controller was used to control the steering box of water jet motor.

## 1.5 Organisation of the Dissertation

This dissertation contains nine chapters, which describe in detail the main research involved, together with the contributions made. The first and second chapters give the general description about the amphibious vehicle and control system.

- Chapter 2 presents the control systems in amphibious autonomous vehicles and the state of the art.
- Chapter 3 discusses the hydrostatic transmission of the Autonomous Amphibious Vehicle speed control systems. The prolusion system, sensors, actuators and the electronic Boards are discussed. The effect of the torque on the hydraulic displacement pump swash plate is described and analyzed. In addition, I have studied the effect of swash plate angle with the hydraulic motor speed. The effect of surface type on the swash plate torque is analyzed also in this chapter.
- Chapter 4 describes controlling the variable displacement hydraulic pumps swash plate position. A swash plate lever is connected to a DC Motor shaft using flexible coupling. PID controller is designed to control the DC Motor position, in addition I have designed Dead beat controller and I have added P part from PID controller to the Dead Beat controller to have P-Dead Beat controller, the combination between those controllers is discussed. DC Motor speed should be controlled to meet the required swash plate torque; this is achieved by using PWM.
- Chapter 5 demonstrates the strategy of the steering control of DORIS robot like skid steer. The Steering wheel and Gas pedal are divided into many input points and Fuzzy rules are concluded for each input point where the DC Motors position should be, the

intelligent fuzzy logic controller give the decision to the DC Motors output. Different positions for the two DC Motors cause different speeds between the left and right wheels; these different speeds rotate the robot left right or around itself. To add the throttle engine open loop control system to the closed loop control system, coupling the low level control systems with a high level control system is discussed. A combination between steering wheel Gas pedal and servo motor is concluded.

- Chapter 6 demonstrates the Tele-operation control system. Robot operation system (ROS) is used to communicate between the PC client and the controller through wireless means, WIFI. I have divided the robot speed in this control strategy to 3 speeds for forward, 3 for backward, steering left, steering right and stop. By using the PC keyboard, the robot can be moved forward and backward, steered left and right.

- Chapter 7 demonstrates how to avoid static and dynamic obstacles using fuzzy logic strategy. In this strategy the laser scanner scanned the front area and give information about obstacles' angle and distance and with this information the fuzzy logic will control the hydraulic pump angular position that causes different angles for left and right hydraulic pumps swash plat, which causes skid steer of the robot to the left or to the right side.

- Chapter 8 shows the water jet system. I have developed and designed water jet system and I have designed and modeled the system to meet DORIS robot requirements. This chapter also demonstrates how to control the water jet steering system. I have proposed a PID controller to control the direction of the steering box which allows the Vehicle to rotate left and right on water.

- Chapter 9 describes the conclusion and future works. The problems of the old system and comparison between the hydrostatic transmission and electro hydraulic system are also described.

## 1.6 Publications

1. Sailan, K., "DC Motor Angular Position Control using PID Controller for the Purpose of Controlling the Hydraulic Pump," *International Conference on Control, Engineering, Information Technology (CEIT'13) Proceeding Engineering and Technology*, copyright IPCO, Vol. 1, pp. 22-26, 2013.
2. Sailan, K. and Kuhnert, K.D., "Design and Impliment of Powertrain Control System for the All Terrian Vehicle" *International Journal of Control, Energy and Electrical Engineering (CEEE)*, copyright IPCO, Vol.1, pp. 50-56, 2014.
3. Sailan, K., Kuhnert, K.D. and Sedighi, S., "Development of Electro-Hydraulic Servo Drive Train System for DORIS Robotm" *Scientific Cooperations International Workshops on Electrical and Computer Engineering Subfields*, Koc University, Istanbul (Turkey), 22.-23. August 2014.
4. Sailan, K.; Kuhnert, K.D. and Karelia, H., "Modeling, Design and Implement of Steering Fuzzy PID Control System for DORIS Robot," *International Journal of Computer and Communication Engineering*, Vol. 3, Issue No. 1, January 2014.
5. Sailan, K. and Kuhnert, K.D., "Speed Control of UGV using Electro Hydraulic Servo System and Fuzzy and PID controller," *International Journal of Advanced Computer Technology (IJACT)*, ISSN: 2319-7900, Vol. 3, Issue No. 5, October 2014.
6. Sailan, K. and Kuhnert, K.D., "Modeling and Design of Cruise Control System with Feedforward for All-Terrain Vehicles," *Second International Conference on Advanced Information Technologies and Applications* (ICAITA), pp. 339-349, 2013.
7. Sailan, K. and Kuhnert, K.D., "Speed Control of Unmanned Ground Vehicle for non Autonomous Operation," *International Journal of Materials Science and Engineering*, Vol. 3, Issued No. 1, pp. 44-48, March 2015.
8. Sailan, K., and Krämer, M.S., "Keyboard Tele-operation for Autonomous Amphibious Vehicle," *International Journal of Advanced Computer Technology*, ISSN: 2319-7900, Vol. 4, Issue No. 1, 2015.
9. Sailan, K.; Kazerouni, M.F. and Kuhnert, K.D., "Simulation of DORIS Robot HTS and the effect of the Swash Plate Torque on the DC Motor Actuator," *International Journal of Innovative Research in Advanced Engineering (IJIRAE),* ISSN 2349-2163, Vol. 2, Issue No. 4, April 2015.
10. Sailan, K.; Kuhnert, K.D. and Hardt, S., "Obstacle Avoidance Strategy using Fuzzy Logic Steering Control of Amphibious Autonomous Vehicle," *International Journal*

*of Innovative Science, Engineering & Technology (IJISET),* Vol. 2, Issue No. 10, October 2015.

11. Sailan, K.; Kuhnert, K.D.; Hardt, S. and Schlemper, J., "Design and Control of Water Jet System for the Amphibouse Autonomous Vehicles," *International Journal of Innovative Research in Computer and Communication Engineering*, Vol. 4, Issue No. 1, January 2016.

# Chapter 2

# Control Systems in Amphibious Vehicles

## 2.1 Introduction

Control systems engineers are concerned with understanding and controlling segments of their environment, often called systems, to provide useful economic products for society. The twin goals of understanding and controlling are complementary because effective systems control requires that the systems may be understood and modeled. Furthermore, control engineering must often consider the control of poorly understood systems such as chemical process systems. The present challenge to control engineers is the modelling and control of modern, complex, interrelated systems such as traffic control systems, chemical processes, and robotic systems. Simultaneously, the fortunate engineer has the opportunity to control many useful and interesting industrial automation systems. Perhaps the most characteristic quality of control engineering is the opportunity to control machines and industrial and economic processes for the benefit of society. Control engineering is based on the foundations of feedback theory and linear system analysis, and it integrates the concepts of network theory and communication theory. Therefore control engineering is not limited to any engineering discipline but is equally applicable to aeronautical, chemical, mechanical, environmental, civil, and electrical engineering. For example, a control system often includes electrical, mechanical, and chemical components. Furthermore, as the understanding of the dynamics of business, social and political systems increases, the ability to control these systems will also increase.

A control system is an interconnection of components forming a system configuration that will provide a desired system response. The basis for analysis of a system is the foundation provided by linear system theory, which assumes a cause–effect relationship for the components of a system. Therefore, a component or process to be controlled can be represented by a block, as shown in figure 2.1. The input–output relationship represents the cause-and-effect relationship of the process, which in turn represents a processing of the input signal to provide an output signal variable, often with power amplification. An open-loop control system utilizes a controller or control actuator to obtain the desired response, as shown in figure 2.1.

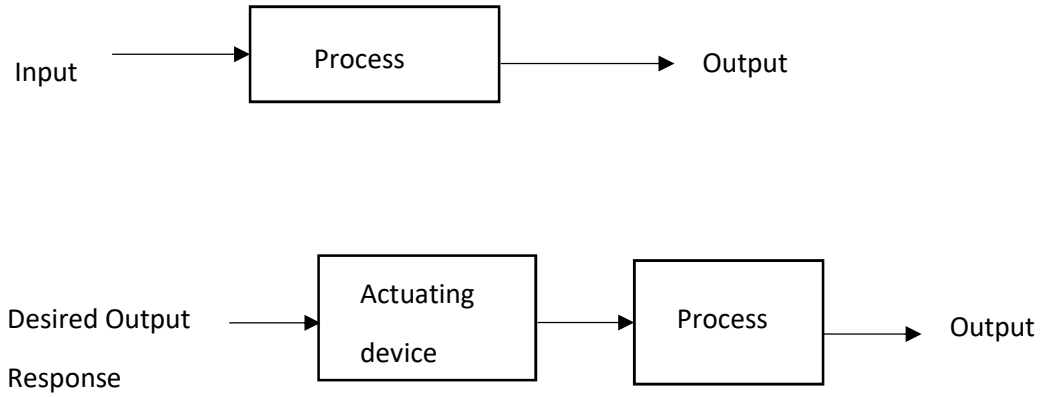


Figure 2.1 Control System Block Diagram

In contrast to an open-loop control system, a closed-loop control system utilizes an additional measure of the actual output to compare the actual output with the desired output response. The measure of the output is called the feedback signal. A simple closed-loop feedback control system is shown in figure 2.2. A feedback control system is a control system that tends to maintain a prescribed relationship of one system variable to another by comparing functions of these variables and using the difference as a means of control. A feedback control system often uses a function of a prescribed relationship between the output and reference input to control the process. Often the difference between the output of the process under control and the reference input is amplified and used to control the process so that the difference is continually reduced. The feedback concept has been the foundation for control system analysis and design [Dorf, R.C., et al., 2010].

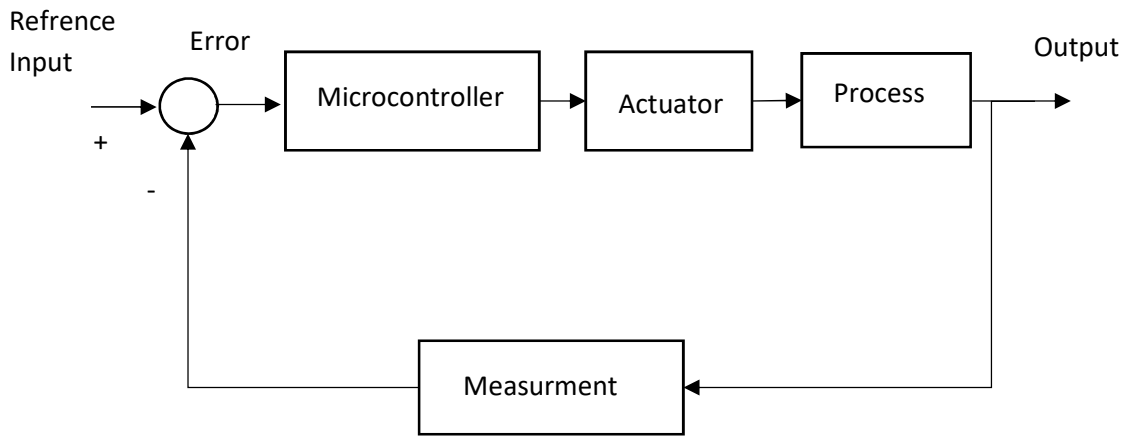


Figure 2.2 Closed-Loop Feedback Control System

## 2.2 Control System Design

The design of control systems is a specific example of engineering design. Again, the goal of control engineering design is to obtain the configuration, specifications, and identification of the key parameters of a proposed system to meet an actual need. The first step in the design process consists of establishing the system goals. For example, we may state that our goal is to control the velocity of a motor accurately. The second step is to identify the variables that we desire to control (for example, the velocity of the motor). The third step is to write the specifications in terms of the accuracy we must attain. This required accuracy of control will then lead to the identification of a sensor to measure the controlled variable. As designers, we proceed to the first attempt to configure a system that will result in the desired control performance. This system configuration will normally consist of a sensor, the process under control, an actuator, and a controller. The next step consists of identifying a candidate for the actuator. This will, of course, depend on the process, but the actuation chosen must be capable of effectively adjusting the performance of the process. For example, if we wish to control the speed of a rotating flywheel, we will select a motor as the actuator. The sensor, in this case, will need to be capable of accurately measuring the speed. We then obtain a model for each of these elements. The next step is the selection of a controller, which often consists of a summing amplifier that will compare the desired response and the actual response and then forward this error-measurement signal to an amplifier. The final step in the design process is the adjustment of the parameters of the system in order to achieve the desired performance. If we can achieve the desired performance by adjusting the parameters, we will finalize the design and proceed to document the results. If not, we will need to establish an improved system configuration and perhaps select an enhanced actuator and sensor. Then we will repeat the design steps until we are able to meet the specifications, or until we decide the specifications are too demanding and should be relaxed. The control system design process is summarized as

1. Understand the automation problem:

    a) What are the specifications to be achieved?
    b) Which variables can be manipulated by actuators?
    c) What are the output variables of interest?
    d) What should we measure?
    e) Which are the disturbances?

2. Choose sensors to measure the required feedback signals.

3. Choose actuators to drive the plant.

4. Get a simplified mathematical model or a reliable simulation model of the plant, sensors, and actuators.

5. Synthesize the control algorithm based on the developed models and the control criteria.

6. Test the design analytically by simulation

7. Validate on real process (implementation).

8. Iterate this procedure until a satisfactory physical system response results.

The controller design problem is as follows: Given a model of the system to be controlled (including its sensors and actuators) and a set of design goals, find a suitable controller, or determine that none exists. As with most of engineering design, the design of a feedback control system is an iterative and nonlinear process. A successful designer must consider the underlying physics of the plant under control, the control design strategy, the controller design architecture (that is, what type of controller will be employed), and effective controller tuning strategies. In addition, once the design is completed, the controller is often implemented in hardware; hence issues of interfacing with hardware can surface. When taken together, these different phases of control system design make the task of designing and implementing a control system quite challenging.

## 2.3 Control System Design Steps

The design of a controller that can alter or modify the behaviour and response of an unknown plant to meet certain performance requirements can be a tedious and challenging problem in many control applications. By plant, we mean any process characterized by a certain number of inputs u and outputs y, as shown in figure 2.3. The plant inputs u are processed to produce several plant outputs y that represent the measured output response of the plant. The control design task is to choose the input u so that the output response y(t) satisfies certain given performance requirements. Because the plant process is usually complex, i.e., it may consist of various mechanical, electronic, hydraulic parts, etc., the appropriate choice of u is in general not straightforward. The control design steps often followed by most control engineers in choosing the input u are explained below [Ioannou, P., 2003].


Figure 2.3 Plant Representation

Step 1. Modelling and simulation

The task of the control engineer in this step is to understand the processing mechanism of the plant, which takes a given input signal u(t) and produces the output response y(t), to the point that he or she can describe it in the form of some mathematical equations. A plant model may be developed by using physical laws or by processing the plant input/output (I/O) data obtained by performing various experiments.

Step 2. Controller Design

Once a model of the plant is available, one can proceed with the controller design. The controller is designed to meet the performance requirements for the plant model. Because the plant model is always an approximation of the plant, the effect of any discrepancy between the plant and the model on the performance of the controller will not be known until the controller is applied to the plant in Step 3.

Step 3. Implementation

In this step, a controller designed in Step 2, which is shown to meet the performance requirements for the plant model and is robust with respect to possible plant model uncertainties 4, is ready to be applied to the unknown plant. The implementation can be done using a digital computer, even though in some applications analogue computers may be used too. Another important aspect of implementation is the final adjustment, or often called the tuning, of the controller to improve performance by compensating for the plant model uncertainties that are not accounted for during the design process. Tuning is often done by trial and error, and depends very much on the experience and intuition of the control engineer [Ioannou, P. 2003].

## 2.4 Digital Control System

Most control engineering applications nowadays are computer based, where a digital computer or a microcontroller is used as the controller. Figure 2.4 shows a typical computer controlled system. Here, it is assumed that the error signal is analogue and an A/D converter is used to convert the signal into digital form so that it can be read by the computer. The A/D converter samples the signal periodically and then converts these samples into a digital word suitable for processing by the digital computer.

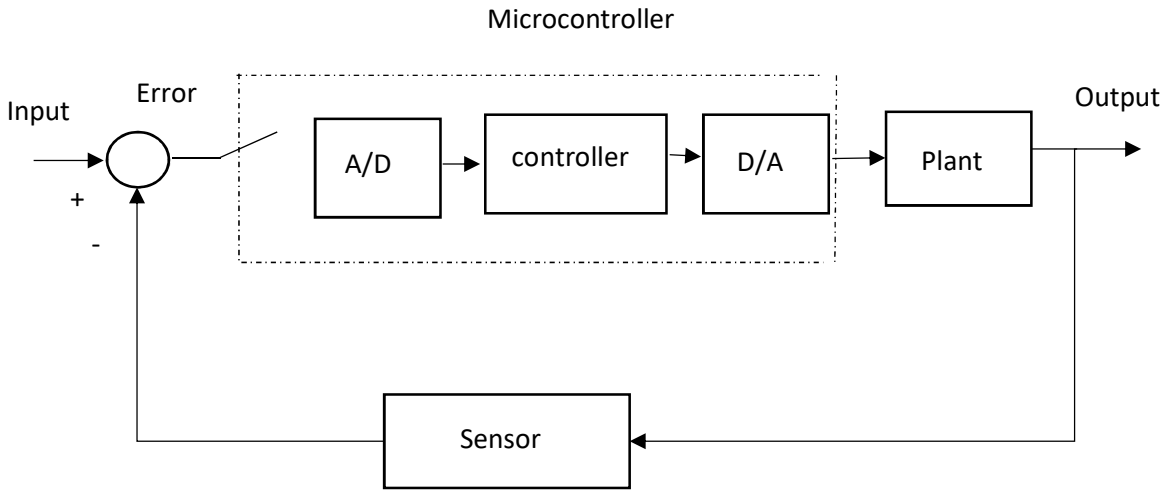


Figure 2.4 Typical Digital Control System

The computer runs a controller algorithm (a piece of software) to implement the required actions so that the output of the plant responds as desired. The output of a digital computer is a digital signal, and this is normally converted into analogue form by using a digital-to-analogue (D/A) converter. The operation of a D/A converter is usually approximated by a zero-order hold transfer function. There are many microcontrollers that incorporate built-in A/D and D/A converter circuits. These microcontrollers can be connected directly to analogue signals, and to the plant. In figure 2.4 the reference set-point, sensor output, and the plant input and output are all assumed to be analogue. Figure 2.5 shows the mathimatical block diagram of the system in figure 2.4 where the A/D converter is shown as a Sample and Hold which is the mathimatical discription of the A/D and D/A converters. Most modernmicrocontrollers include built-in A/D and D/A converters, and these have been incorporated into the microcontroller as in figure 2.6. The purpose of developing the digital control theory is to be able to understand, design and build control systems where a computer is used as the controller in the system. In addition to the normal control task, a computer can

perform supervisory functions, such as reading data from a keyboard, displaying data on a screen or liquid crystal display, turning a light or a buzzer on or off and so on [Dogan, I., et al., 2006].

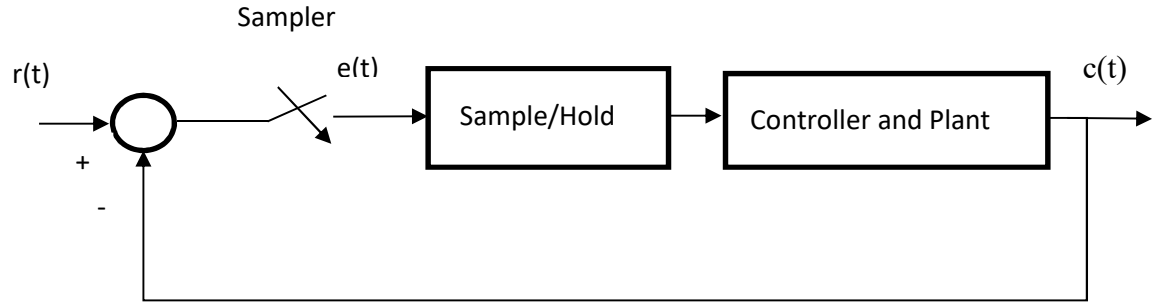


Figure 2.5 Block Diagram of the Digital Control System

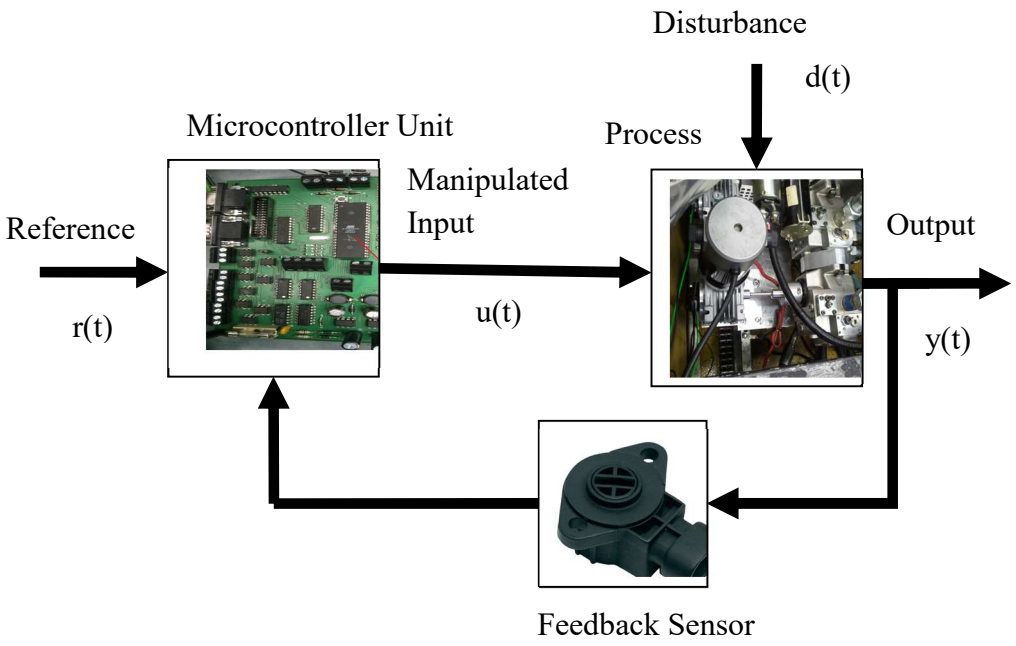


Figure 2.6 Block Diagram of the Computer Control System

## 2.5 Amphibious Vehicles Propulsion Control Systems

Propulsion is creating a force to move or rotate something. A propulsion system has a source of mechanical power such as engines, which are used to generate rotating or moving force such as wheel and axles, propellers, a propulsive nozzle, wings, fins or legs. Other components such as clutches, chains, gearboxes and so forth may be needed to connect the

power source to the force generating component. Many methods to generate force and produce speed for driving a vehicle and to control it are descped in detail.

### 2.5.1 Mechanical Propulsion System

Amphibious Vehicles use Diesel or Gasoline combustion engines. Power is transmitted from the engine to the wheels through a continuous variable transmission, gearbox, differential and a chain system. The vehicle wheels are connected by a chain system and driven by the left and right outputs of a differential. Two brake discs are attached to the outputs of the differential and can be operated separately. The differential and braking system enables turning the vehicle (skid-steering). The driveline of the vehicle is shown in figure 2.7 and 2.8. The vehicle uses an automatic torque converter known as a continuous variable transmission. It consists of a driver clutch located on the engine output shaft, a driven clutch located on the input shaft of the gearbox, and a drive belt. Both clutches comprise of a fixed face and a movable face. In acceleration, the driver clutch movable face travels towards the fixed face as the weights in the clutch are pushed outwards due to the centrifugal force. As the driver clutch faces get narrower, they grip the drive belt and move it towards the top of the driver clutch. At the same time, the driven clutch plates spread apart as the belt rides down between the faces. The tension in this clutch is also regulated by a spring. As the engine comes under load, the spring loaded cam on the driven clutch forces the clutch plates together.

The driver clutch can therefore be considered as a pulley whose radius is increased when accelerated, resulting in an increase of the output speed. Similarly, when the engine is under load, the driven clutch increases its radius and more torque can be transmitted to the wheels. At the engine idle speed, the centrifugal force is not enough to overcome the spring load between driver clutch faces and the clutch is completely disengaged. It is only engaged after the engine reaches a certain speed, in the manner of a conventional centrifugal clutch.

The gearbox has variable positions, and the output of gearbox engages directly to the case gear of the differential.

The differential distributes the torque from the gearbox to the left and right wheels. The two driving shafts of the differential are attached to the left and right brake discs. The torque difference enables the vehicle to turn [Ha, Q.P., et al., 2005].

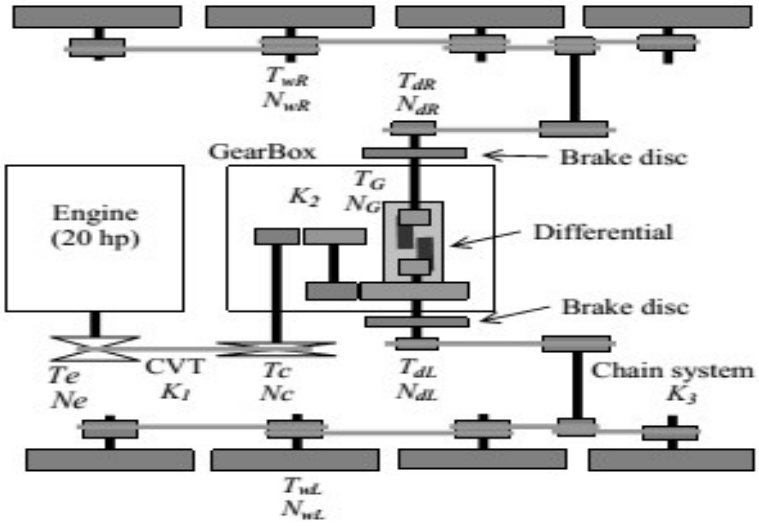


Figure 2.7 Mechanical driveline of Amphibious Vehicle

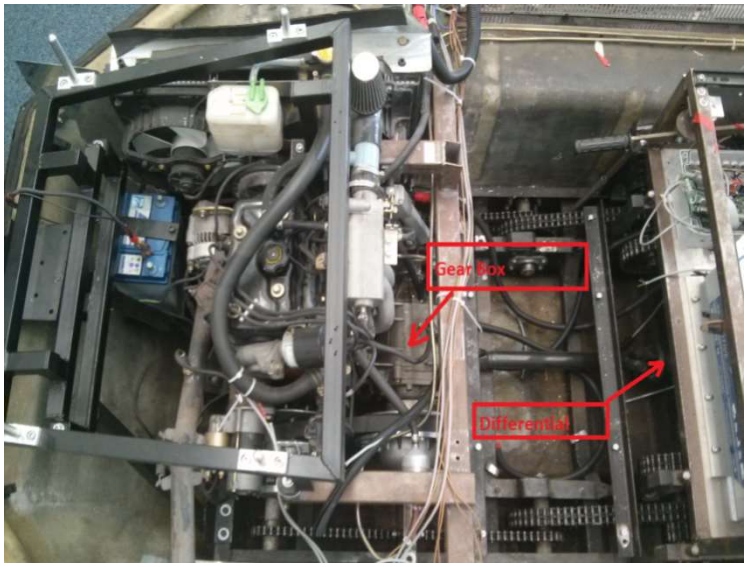


Figure 2.8 Mechanical driveline of Amphibious Vehicle

### 2.5.1.1 Control of Mechanical Propulsion System

Hydraulic Actuation

Hydraulic actuation driver performs many operations at the same time such as increasing or decreasing the speed, gear shifting, steering and braking. It needs a control system for interfacing a simple control lever with vehicle manual control linkages (accelerating pedal, steering and braking levers, and gear shifting lever) to be similar to the electric vehicles. The target of control module is to be operated as an interface between the driver control lever or the remote-control receiver unit and the vehicle conventional mechanical control linkages.

The control module is able to carry out the entire driver's work as shown in figure 2.9 from starting the engine, shifting gears for vehicle motion, sensing vehicle speed, steering, and braking, reverse direction of motion to opening and closing the ramp [A. Eliewa, et al., 2009].

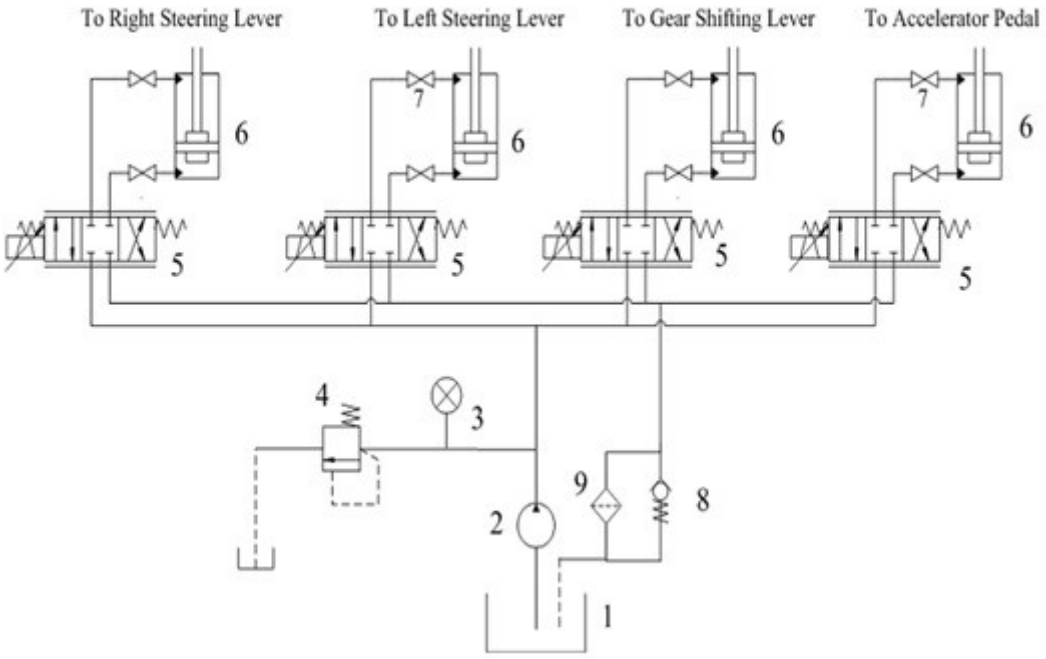


Figure 2.9 Hydraulic Actuator

Electrical actuation

The steering system on the amphibious vehicle operates through handlebars, which apply brake pads to a set of discs. These discs are directly connected via chains and sprockets to the wheels on either side of the vehicle. When the handlebars are moved, for example to a fully left position, the brakes on the left hand side are applied and the vehicle skids left. The simplest method of modifying this system for computer control would involve moving the handlebars using an appropriate electrical actuator.

### 2.5.2 Hydraulic Propulsion System

The Hydraulic Propulsion System consists of two systems, either hydrostatic system of electrical servo system; both systems are described in the project.

### 2.5.2.1 Hydrostatic Transmission

Hydrostatic transmission system has long been recognized for superior power transmission when variable output speed is required because they provide fast response, maintain precise speed under varying loads, and allow infinitely variable speed control from zero to maximum. A hydrostatic transmission is an entire hydraulic system in a single package pump, motor, and all required controls. These systems provide all the advantages of a conventional hydraulic system which are:

- adjustable speed, torque, and power
- smooth and controllable acceleration
- stalled without damage
- controllability

There are two general hydrostatic transmission configurations: split or closed coupled. Split hydrostatic transmission systems consist of a power unit with the hydraulic pump, heat exchangers, filters, valves, and controls mounted on a reservoir. The hydraulic motor is remotely mounted and connected to the power unit through hose or tubing. Closed hydraulic circuits typically utilize a variable displacement pump and fixed motor. This combination provides a constant torque output at a fixed maximum pressure over the pump's full speed range. Speed and direction are controlled with a variable displacement over centre pump. Power from overhauling loads is regenerated back into the pump prime mover. Motor speed is limited to the maximum speed permitted by full pump displacement [Klocke, C., 2012].

### 2.5.2.2 Control of Hydrostatic Transmission

The evolution of control methods for hydrostatic machines is similar to many other paths evolution has taken. As with other subject areas, the pace of the evolution of hydrostatic machines is a balance between technology and value.

Hydrostatic transmissions utilizing variable displacement components. Figure 1.12 shows a cross-section of a closed circuit variable displacement axial piston pump with swash plate [Klocke, C., 2012].

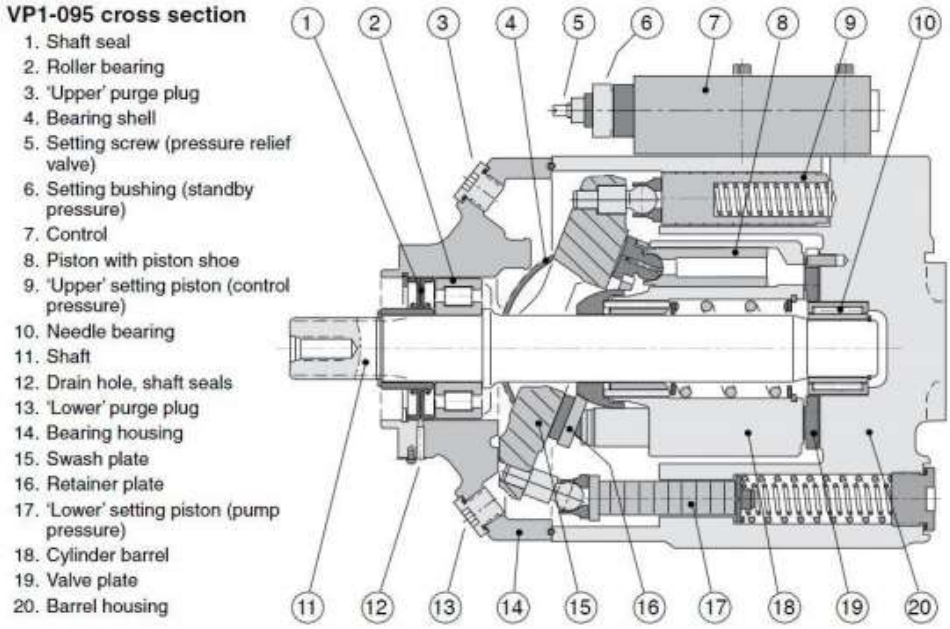


Figure 2.10 Variable Displacement Axial Piston Pump

First to be discussed is a simple closed circuit hydrostatic system comprised of a variable pump and fixed motor. The speed of the motor shaft is determined by the following three factors:

1. Pump Speed
2. Pump Displacement
3. Motor Displacement

Pump speed is usually a fixed ratio to the Vehicle engine speed. For a system consisting of a fixed displacement hydraulic motor, variable displacement hydraulic pump, and fixed engine speed, the motor shaft speed will be controlled by the pump displacement. Different methods will be examined of how to control the swash plate position of the variable displacement hydraulic pump [Klocke, C., 2012].

Direct control

Direct Displacement Control means to position the variable hydrostatic pump swash plate between maximum displacement in one direction and maximum displacement in the opposite direction. This is normally accomplished by attaching a lever directly to the swash plate as shown in figure 2.11.

The motion range required for the Direct Displacement Control lever equal to the swash plate displacement and is typically between 15 to 18 degrees from the centre position, depending on the design of the variable displacement pump.

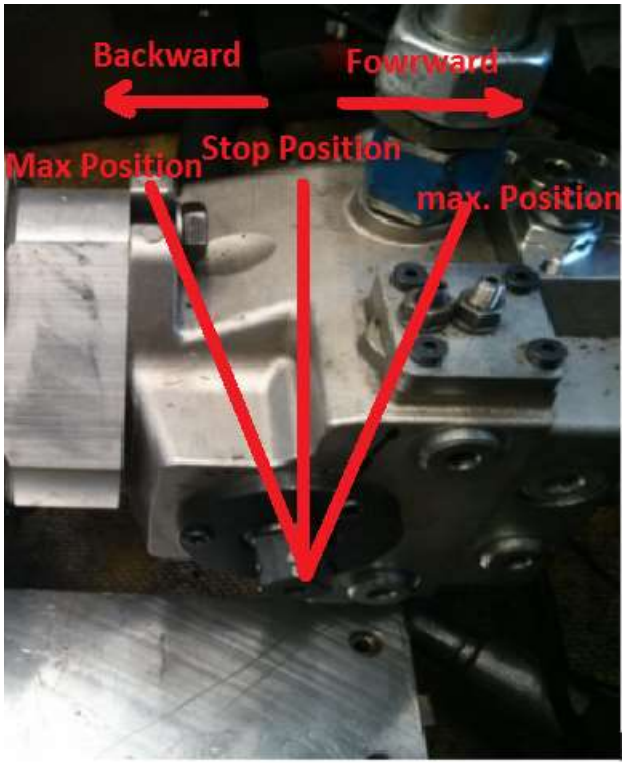


Figure 2.11 Position of the Pump Swash Plate

Servo Control

Servo systems consist of one or more control pistons used to apply a force to the swash plate and a device to regulate the pressure applied to the control piston. Servo pressure is typically regulated by a proportional three-position four-way valve, although other systems may use different designs. Typically, a low pressure source on the variable displacement hydraulic pump is used to supply the servo system. Designs also may use system pressure or other medium or high pressure sources on the pump or machine to feed the servo system.

The means of controlling the servo system has many methods. The input signal or control method of the servo valve is typically one of the following:

1. Mechanical Input
2. Hydraulic Input
3. Electrical Input

Mechanical Input

Replacing a Direct Displacement Control pump with one having Mechanical Input for the servo valve drastically reduces the forces required by the operator. A servo valve with Mechanical Input requires 2-5 Nm of control torque to reach maximum hydraulic displacement pump. The Mechanical Input generally provides a position input command to the servo valve that generates the required servo pressure to move the swash plate to the commanded position.

Hydraulic Input

A servo valve with hydraulic input can be designed for any signal pressure range. Typically, most hydraulic input servo systems utilize low pressure as the signal pressure source and the supply pressure to the servo valve. Hydraulic Input servo systems provide the flexibility of adding additional logic and/or control valves in series or parallel with the operator input. Designs utilizing system pressure to supply the servo system are more common on motors and very large pumps. The advantage of system pressure input is the reduction in control piston size to generate the same force as with a low pressure source. The Hydraulic Input provides a pressure input to the servo valve that generates the required servo pressure to move the swash plate to the commanded position.

Electrical Input

A servo system with electrical input can be designed for almost any type of input signal. These have been either low current DC or high current PWM with 12 or 24volt supply. The Electrical Input provides current to a solenoid that is converted to a force acting on the pilot valve or spool of the servo valve. This force caused the pilot valve or spool to generate servo pressure to position the swash plate to the desired position.

Digital control

Digital Control of variable displacement pump lever is an enabler for more sophisticated control systems as shown in figure 2.12. With the use of electronics, control types can be changed at the touch of a button or automatically without operator input. A basic control type can be “over-ridden” or merged with other sensors and electronics. The obvious benefit is increased machine performance. Sensors can detect changes in operating conditions providing information to the electronic control system which results in optimized performance and function of the system, more quickly and more accurately than the best-skilled operator could control the machine [Klocke, C., 2012].

Figure 2.12 Digital Controller

### 2.5.3 Hydraulic Motor Control

Motor controls have the same general descriptions and classifications as pump controls. In general, variable displacement motors may have Load Dependent or Load Independent Controls with mechanical, hydraulic or electrical input signals. An additional variant for motors is the option of two-position control. Motors generally have Direct Displacement Control available only for smaller displacements. Motors generally do not have Mechanical Input. Consequently, the majority of variable motors have servo valves with Hydraulic or Electric Input. As with pumps, electric input signals for motors are typically either low current DC or high current PWM with 12 or 24 V.

### 2.5.4 Electro Hydraulic Servo System (EHSS)

EHSS as shown in figure 2.13 is used in many industrial applications, because of its ability to handle large inertia and torque loads and, at the same time, achieve fast responses and a high degree of both accuracy and performance depending on the desired control objective, an EHSS can be classified as either a position, velocity or torque EHSS, the electro-hydraulic actuator can use either proportional valve or servo valve, it converts electrical signal to hydraulic power. There are electro-hydraulic valve actuators, which move rotary motion valves such as ball, plug and butterfly valves through a quarter-turn or more from open to close. There are also valve actuators, which move linear valves such as gate, globe, diaphragm and pinch valves by sliding a stem that controls the closure element. Usually, valve actuators are added to throttling valves, which can be moved to any position as part of a control loop. Important specifications for electro-hydraulic valve actuators include actuation time, hydraulic fluid supply pressure range and acting type. Other features for these

actuators include over-torque protection, local position indication and integral pushbuttons and controls. The applications of electro-hydraulic actuators are important in the field of robotics, suspension systems and industrial process. This is because it can provide precise movement, high power capability, fast response characteristics and good positioning capability [Angue-Mintsa, H., et al., 2011].

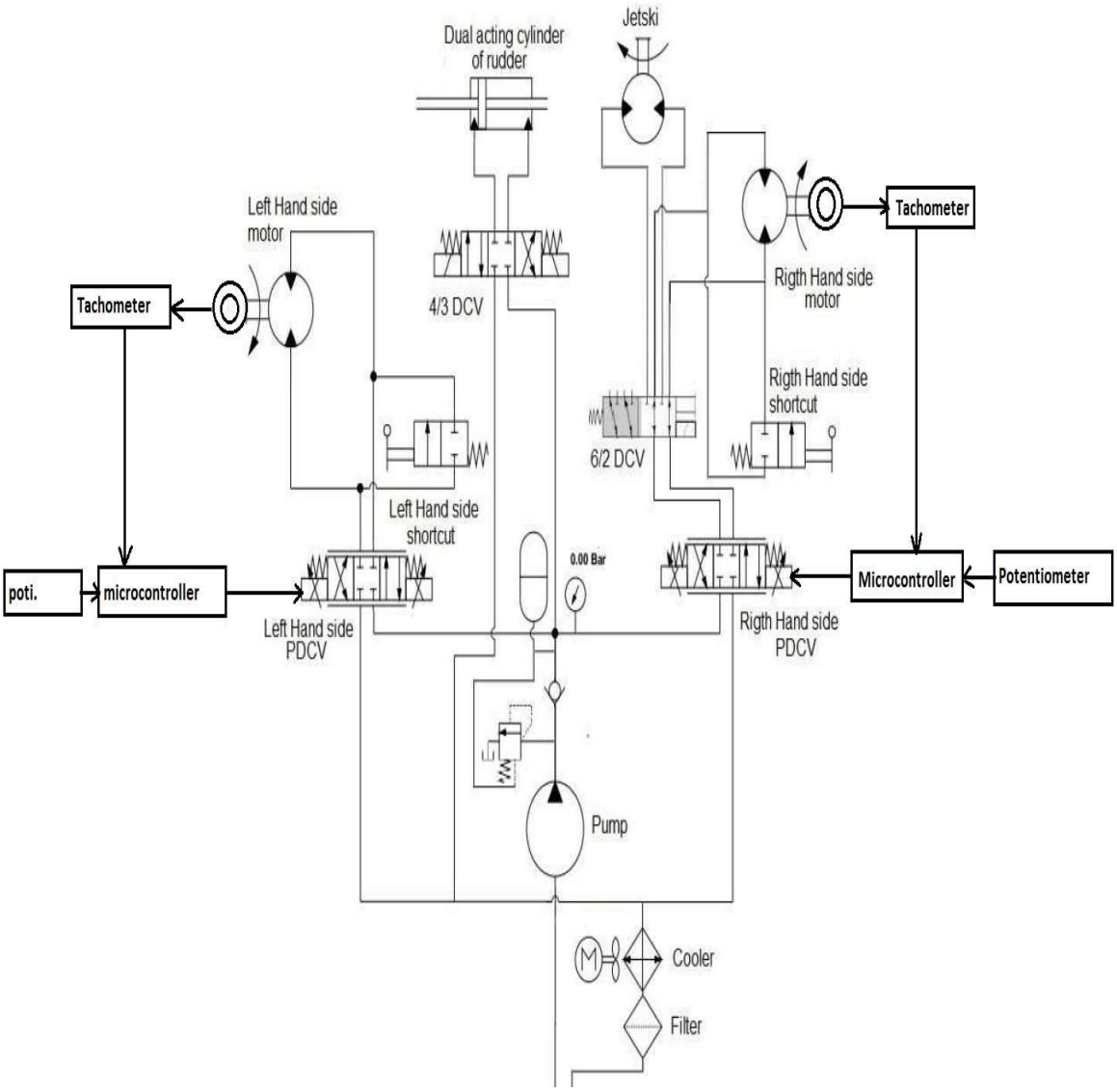


Figure 2.13 Electro Hydraulic System

# Chapter 3

# Hydrostatic Transmission Control System

The DORIS Robot shown in figure 3.1 is an 8-wheeled, skid-steering, amphibious all-terrain vehicle powered by a 29 KW gasoline engine. It is capable of operating for up to 5 hours on one fuelling and has a top speed of about 25 miles per hour. Speeds as low as a few inches per second can also be sustained indefinitely. Payload capacity is about 800 kg, and a variety of implements can be installed in its bed. The drive train is hydrostatic drive train system consisting of two variable-displacement pumps driven by the engine output shaft and two fixed-displacement hydrostatic motors driving the left and right rear axles, respectively. The four wheels on each side of the vehicle are linked together by drive chains. Each pump-motor combination drives one side of the vehicle, resulting in independent control of the speed on the left and right sets of wheels. The vehicle is operated by controlling the throttle lever for engine power and rotating the Two DC Motor that control the swash plat of the variable displacement pump forward for forward motion and backward for backward motion, this has been done using two Pedals one for forward and the other for backward driving mode. Steering is accomplished by rotating the DC Motors in deferent positions according to fuzzy rules this will give a different motor speed and will skid the vehicle left or right. The DC Motors positions correspond to wheel speed, so care must be taken to avoid moving the control levers too quickly and stalling the engine.

The variable displacement pumps behave like a continuously variable transmission, allowing the vehicle to be driven at any ratio of wheel speed to engine speed. This reduction ratio is set by the position of each pumps' swash plate control lever, which is connected to a DC Motor with coupling. The left and right wheels may also be driven at continuously differing speeds, allowing turns of any radius. The engine is designed to operate continuously at a speed that depends on the load and on the required maximum speed. The hydraulic variable transmission system eliminates the need for clutch, gearshift, and brake actuators, which enormously simplifies remote operation. The interconnection between the system parts is shown in figure 3.1b.

Figure 3.1 DORIS Robot

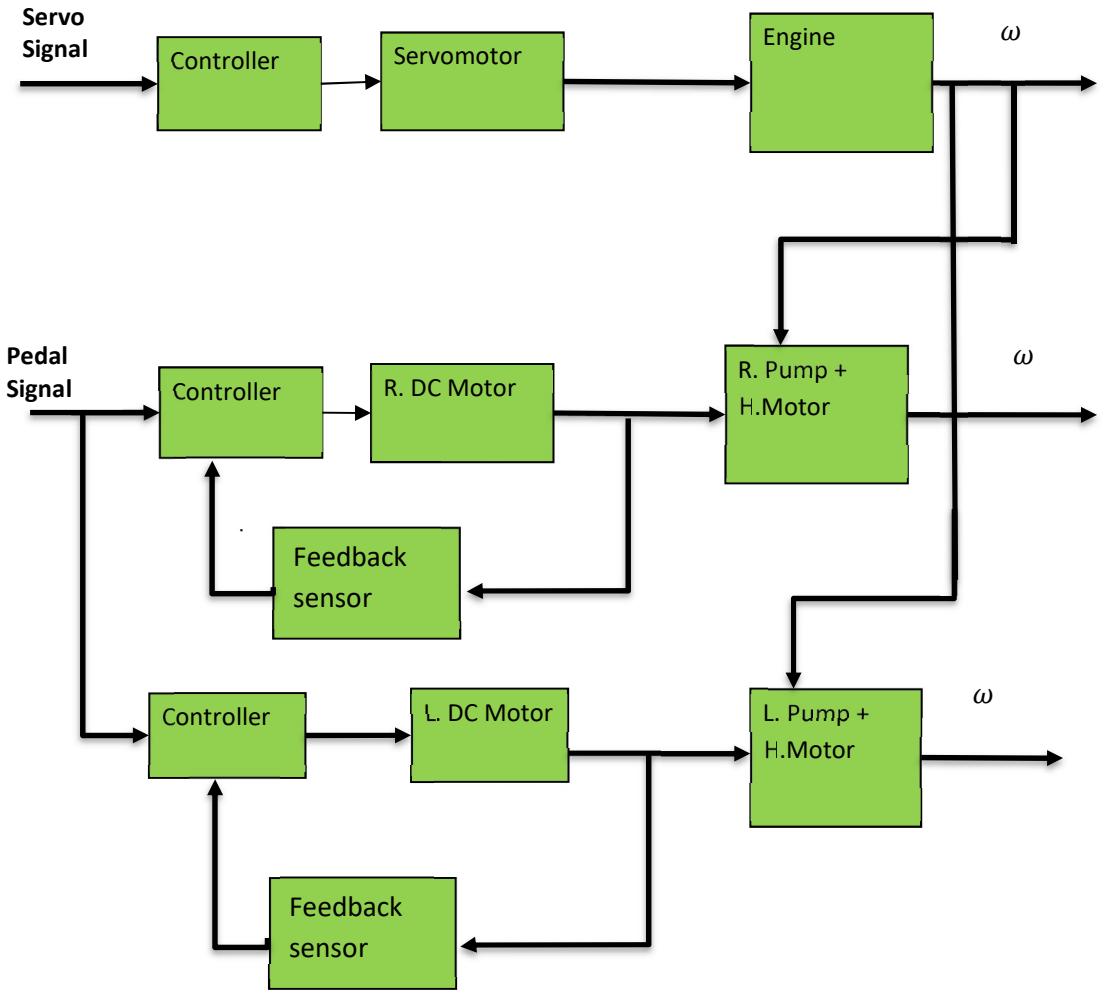


Figure 3.1b DORIS Interconnection Block Diagram

## 3.1 Petroleum Internal Combustion Engine

DORIS uses Gasoline engine (Suzuki engine) as shown in figure 3.2. Such engines have more mechanical complexity than an electrical system with a motor and battery.

This presents various challenges, and also some opportunities. One clear problem will be that the vehicle will periodically need re-fuelling as more conventional options such as solar power will not be possible; this will greatly impact the potential for long periods of autonomy. In addition, there will be almost certainly timing issues with the engine that will need to be monitored and accounted. One possible example of this is the time between the increase in throttle and the resulting acceleration. However, there are some advantages that should also be noted. Having a petrol engine effectively means an unlimited amount of electrical power, which is available for computer equipment while there is sufficient petrol. In addition, the various mechanical components (such as wheel drive chains) could pose possible targets for sensors to be able to measure speed without necessarily requiring any mechanical modifications to the wheel axles or the engine itself. The used engine power and torque shown in figure 3.3 [Suzuki datasheet].

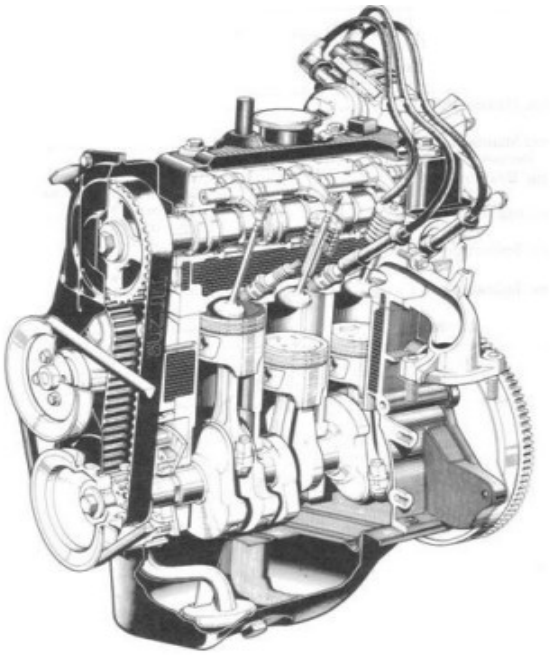

Figure 3.2 Suzuki Engine with 3 cylinders

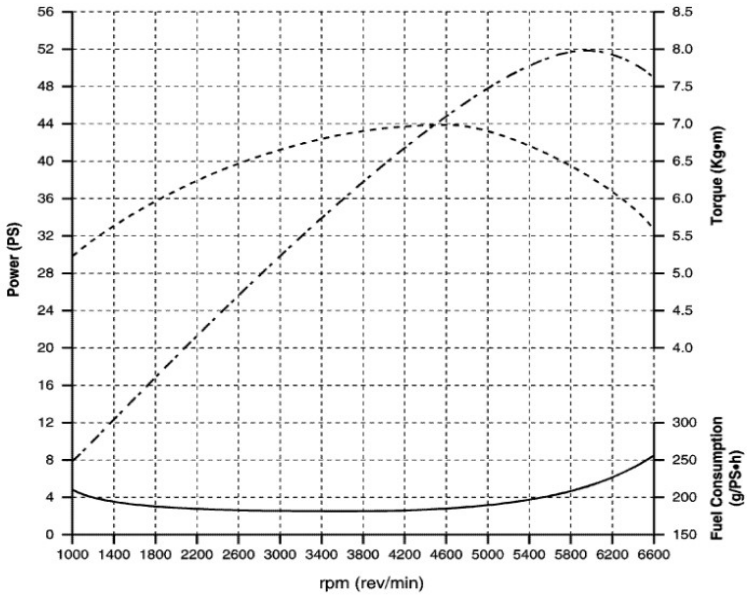


Figure 3.3 Power chart of Suzuki engine with 3 cylinders

## 3.2 Microcontroller

The ATmega16 as shown in figure 3.4 is a low-power CMOS 8-bit microcontroller based on the AVR enhanced RISC architecture. By executing powerful instructions in a single clock cycle, the ATmega16 achieves throughputs approaching 1 MIPS per MHz allowing the system designed to optimize power consumption versus processing speed. The ATmega16 provides the following features: 16K bytes of In-System Programmable Flash Program memory with Read-While-Write capabilities, 512 bytes EEPROM, 1K byte SRAM, 32 general purpose I/O lines, 32 general purpose working registers, a JTAG interface for Boundary-scan, On-chip Debugging support and programming, three flexible Timer/Counters with compare modes, Internal and External Interrupts, a serial programmable USART, a byte oriented Two-wire Serial Interface, an 8-channel, 10-bit ADC with optional differential input stage with programmable gain (TQFP package only), a programmable Watchdog Timer with Internal Oscillator, an SPI serial port, and six software selectable power saving modes. The Idle mode stops the CPU while allowing the USART, Two-wire interface, A/D Converter, SRAM, Timer/Counters, SPI port, and interrupt system to continue functioning. The Power-down mode saves the register contents but freezes the Oscillator, disabling all other chip functions until the next External Interrupt or Hardware Reset. In Power-save mode the Asynchronous Timer continues to run, allowing the user to maintain a timer base while the rest of the device is sleeping. The ADC Noise Reduction mode stops the CPU and all I/O modules except Asynchronous Timer and ADC to minimize

switching noise during ADC conversions. In Standby mode, the crystal/resonator Oscillator is running while the rest of the device is sleeping; this allows very fast start-up combined with low-power consumption. In Extended Standby mode, both the main Oscillator and the Asynchronous Timer continue to run [Atmel datasheet, 2012].

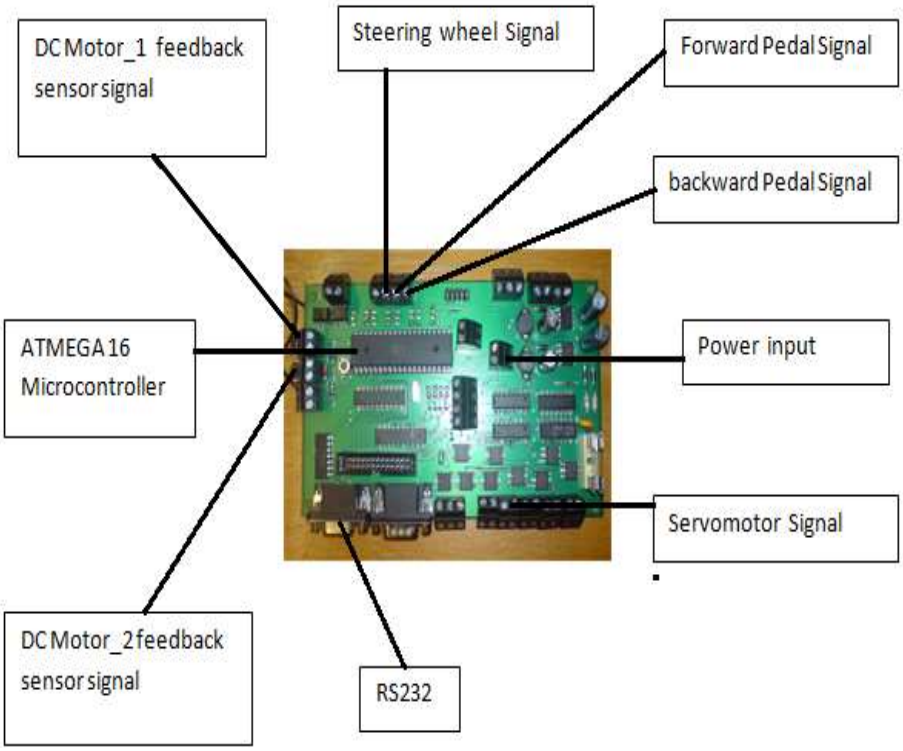


Figure 3.4 The Microcontroller Board

## 3.3 Motor Driver

An H-Bridge as shown in figure 3.5 is an electronic power circuit that allows motor speed and direction to be controlled. Often motors are controlled from some kind of brain or microcontroller to accomplish a mechanical goal [Sieben, V. 2003]. The microcontroller provides the instructions to the motors, but it cannot provide the power required to drive the motors. An H-bridge circuit inputs the microcontroller instructions and amplifies them to drive a mechanical motor. This process is similar to how the human body generates mechanical movement, the brain can provide electrical impulses that are instructions, but it requires the muscles to perform mechanical force. The muscles represent both the H-bridge and the motor combined. The H-bridge takes in the small electrical signal and translates it into high power output for the mechanical motor.

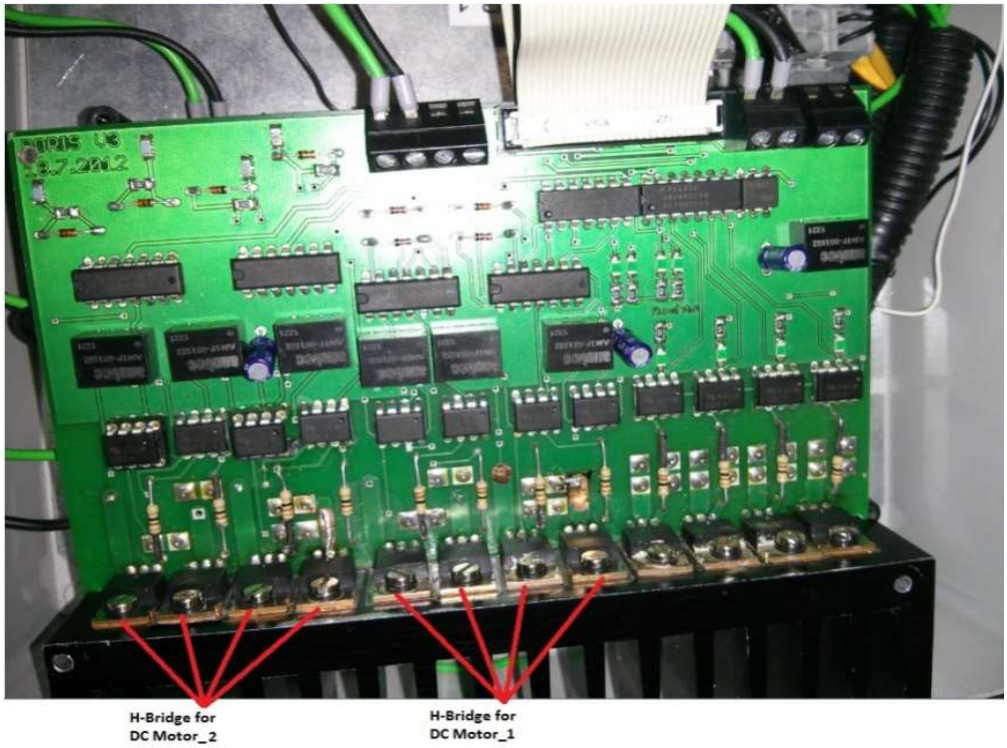


Figure 3.5 Motor Driver Circuit

## 3.4 Limit Switches

To prevent the DC motors getting burnt when the motor position goes more than the maximum swash plate points for any reason, a motor circuit for that purpose is designed as shown in figure 3.6, using limited switches with diodes. A limit switch is an electromechanical device that consists of an actuator mechanically linked to a set of contacts. When an object comes into contact with the actuator, the device operates the contacts to make or break an electrical connection. It can determine the presence or absence of an object. It was first used to define the limit of travel of an object.

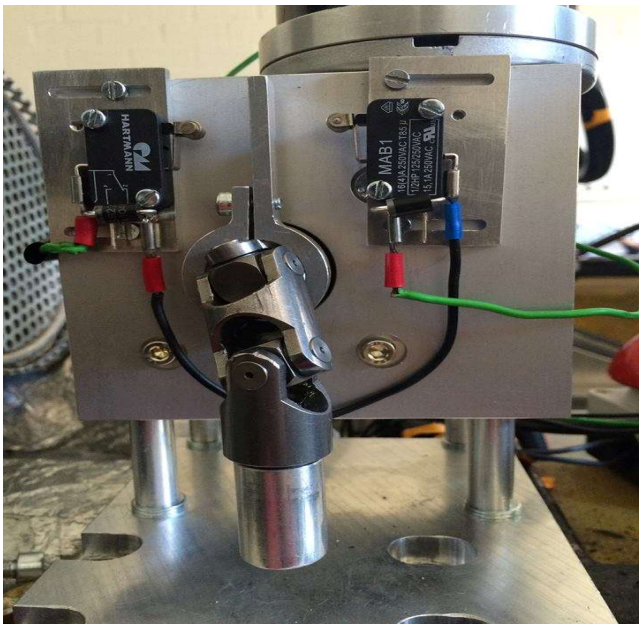


Figure 3.6 Limited Switches

When the Motor is at the end of its range, the switch connects the diode in the circuit. The diode at the actuated switch will block DC power in the direction that it was travelling, so the motor is turned off. If you move the Pedal to the other direction, the polarity changes so the diode can conduct electricity as if it were a wire. The motor turns on and goes the other direction.

## 3.5 Variable Displacement Pump

Axial piston pump is the common variable displacement pump used in the hydrostatic transmission systems due to their fast dynamic response and high efficiency compared to other pump designs. Swash plate on a ball bearing is positioned on the shaft which connects pump to the DC motors power source as shown in figure 3.7. Odd numbered pistons and piston shoes placed in cylinder barrel and rigidly connected to swash plate. Cylinder barrel and pistons rotate with the shaft while the valve plate is stationary. There are suction and delivery ports on valve plate over which pistons periodically pass during operation. When the piston starts its suction stroke, piston moves over suction port of valve plate and sucks the fluid under suction pressure, when the piston comes to end of suction port, it is fully retracted. On the contrary, when the piston comes to delivery port, it starts extending and pushes the fluid out of cylinder. Displacement of the pump depends on extension rate of pistons inside cylinder barrel. Volume difference of pistons during suction and delivery ports determines the displacement of the pump; extension rate of the piston is maximum and thus maximum flow is delivered to system. When swash plate angle is in zero position, there is

no volume difference during the suction and delivery of the pistons. Consequently, displacement of the pump is zero for zero angle of swash plate; the swash plate angle is nearly ± 18 degree.

Figure 3.7 The Hydraulic Pumps

## 3.6 DC Motors

Two DC Motors were used to actuate the swash plate with the specifications listed in table 3.1 and shown in figure 3.8, the DC Motors have a gearbox with 60 times amplification torque to be able to open and close the swash plate lever.

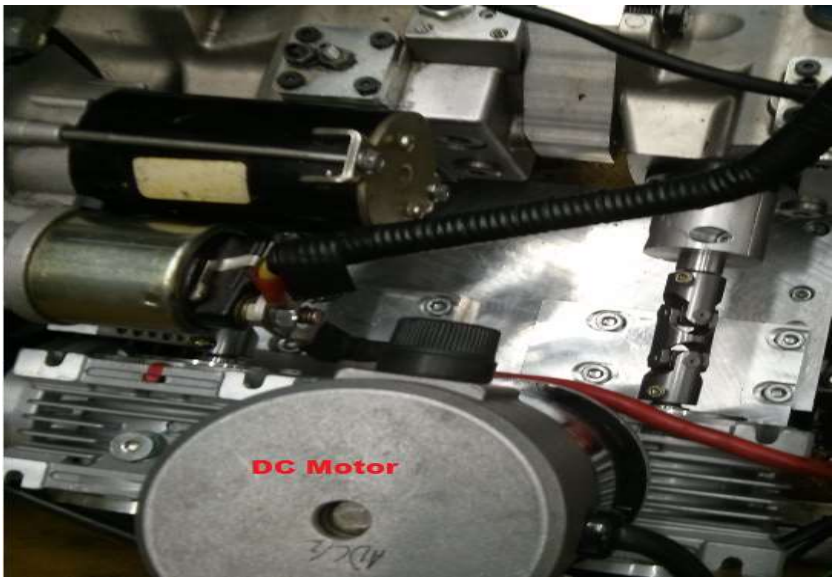


Figure 3.8 12V DC Motor

Table 3.1 DC Motors specifications

| Parameters | Motor 1 | Motor2 | Unit |
|---|---|---|---|
| Operating Voltage | 12 | 12 | V |
| Rated Current | 9.2 | 9.2 | A |
| Max. Power | 75 | 75 | W |
| Max. Speed | 3000 | 3000 | RPM |
| Max. Torque | 1 | 1 | Nm |
| Rated Torque | 0.25 | 0.25 | Nm |
| Rotor Inertia | 52 | 52 | gcm2 |
| Terminal Resistance | 1.8 | 1.8 | Ohm |
| Inductance | 2.4 | 2.4 | mH |
| Mech. Time Constant | 15 | 15 | ms |
| Electr. Time Constant | 1.3 | 1.3 | ms |
| Speed Constant | 300 | 300 | rpm/Ncm |
| Torque Constant | 2.45 | 2.45 | Ncm/A |
| Thermal Resistance | 16 | 16 | K/W |
| Thermal Time Constant | 10 | 10 | min |
| Axial Play | < 0.01 | < 0.01 | mm |

## 3.7 Feedback Sensors

This angular position sensor as shown in figure 3.9 used in many applications like throttle and valve position sensing, User interface controls, Pedal position sensing, Implement position sensing, Gear selection, Joystick position. The sensors electrical output signal ranges from 0 to 120 degree as shown in figure 3.10 and the sensor is provided with return spring. Two sensors are attached to the DC Motors to measure the swash plate position and send the signal back to the microcontroller. For the Jet-ski motor feedback sensor angular position sensor also used.

Figure 3.9 Angular Position Sensor

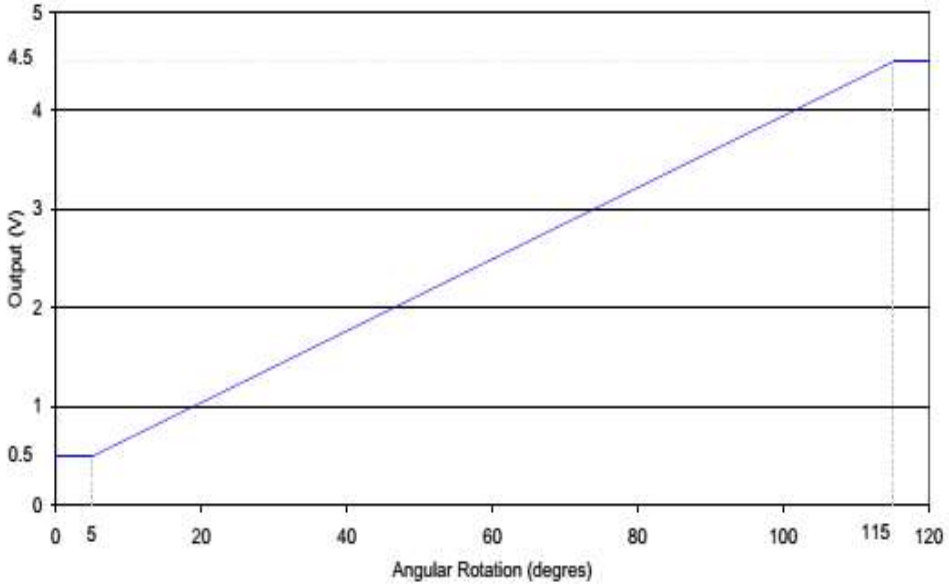


Figure 3.10 Sensor Electrical Signal

## 3.8 Angular Position Sensors

Position sensor as shown in figure 3.11 is an important sensor for measuring angular displacement or linear displacement, which is called as the angular potentiometer or the linear potentiometer, respectively. So it has successfully been applied in many engineering areas, such as the control of the ultrasonic motor, steering position, pedal positions, medical instrument and bioengineering, the dexterous control of the robot hand, the multi-fan hovering system, the diagnosis of the electronic products, etc. [Zhang, X.D. et al., 2005]. In this project there are three position sensors, two to detect the gas pedal position and the brake pedal position and one for the steering position.


Figure 3.11 Angular Position Sensor

## 3.9 Hydraulic Motors

The hydraulic motors used on the Vehicle are Danfoss OMR 160 hydraulic pump as shown in figure 3.12 with the specifications listed (Table 3.2) below.

Table 3.2 Hydraulic motor specifications

| Connection | 1/2 "female thread |
|---|---|
| Geometric displacement | 159.6 cc |
| Max. Speed | 375 rev/min |
| Max. Torque | 380 Nm |
| Max. Power | 12.5 KW |
| Max. pressure drop | 175 bar |
| Max. Oil flow | 60 l/min |
| Max. Starting Pressure | 7 bar |

Figure 3.12 Danfoss OMR 160 Hydraulic Motor

## 3.10 Throttle Engine Servomotor

The primary input for controlling the speed for an internal combustion engine vehicle is the closing and opening of the throttle plate. As depicted in figure 3.13, servomotor has been introduced in the cable connecting the throttle lever to the throttle plate; this preserves a rider's ability to manually control the throttle using the lever, while allowing autonomous control via the R/C servo. The choice of an R/C servo for throttle actuation is based on its low cost, small size, internal closed-loop position control, low power consumption and easy control signal generation [Trebi-Ollennu, A., et al., 1999].

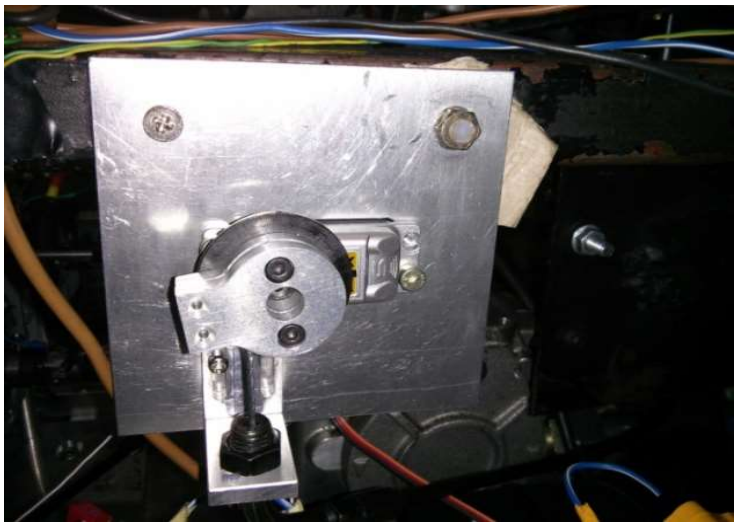

Figure 3.13 Throttle Servo Motor

## 3.11 Arduino Board

This is an open source tool for making computers that can sense and control more of the physical world than a desktop computer would. It's a physical computing platform based on a simple micro-controller board, and a development environment for writing software for the board. Arduino can be used to develop interactive objects, taking inputs from a variety of switches or sensors, and controlling a variety of lights, motors, and other physical outputs. Arduino projects can be stand-alone, or they can communicate with software running on your computer (e.g. Flash, Processing, Max MSP). The boards can be assembled by hand or purchased pre-assembled; the open-source IDE can be downloaded for free. Arduino micro-controller is shown in figure 3.14. It has 14 digital input/output pins (of which 6 can be used as PWM outputs), 6 analogue inputs, a 16MHz ceramic resonator, a USB connection, a power jack, an ICSP header, and a reset button. It contains everything needed to support the micro-controller; connect it to a computer with a USB cable or power it with an AC-to-DC adapter or battery to get started. All the modules in the circuit are connected to Arduino module. The Board is provided with current sensor to measure the DC Motors current [Krishnamurthi, K., et al., 2015]

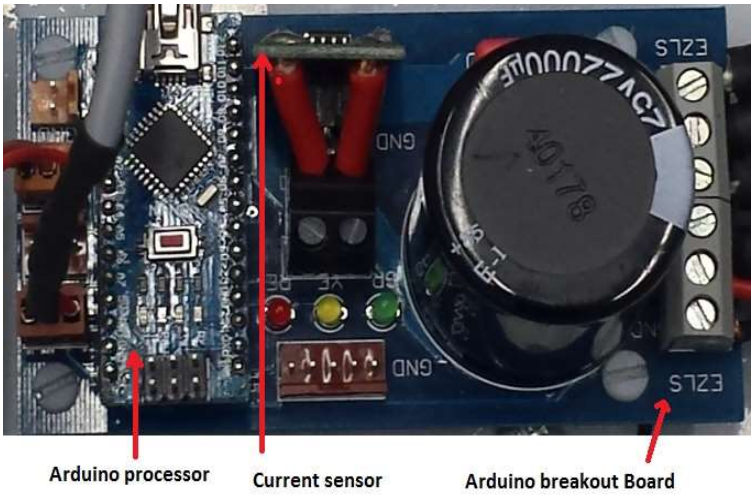


Figure 3.14 Arduino Board

## 3.12 MD Motor Driver

The models of the motor drivers used in this project are MD30C and MD10A. MD30C is use to drive medium to high power brushed DC motor. Meanwhile, MD10C is used to drive low current motor suitable to control linear actuator, it can control both clockwise and anticlockwise direction.

In this project, two MD30C motor drivers were used to control the speed and direction of motors as a hydraulic pump actuator as shown in figure 3.15 and one MD10C to control linear actuator as shown in figure 3.16. The direction of motor can be easily controlled by just giving logic value 1 or 0 to directional pin to cause the motor to turn clockwise or anticlockwise. For controlling the speed of motor, PWM value will determine the speed of the motor.

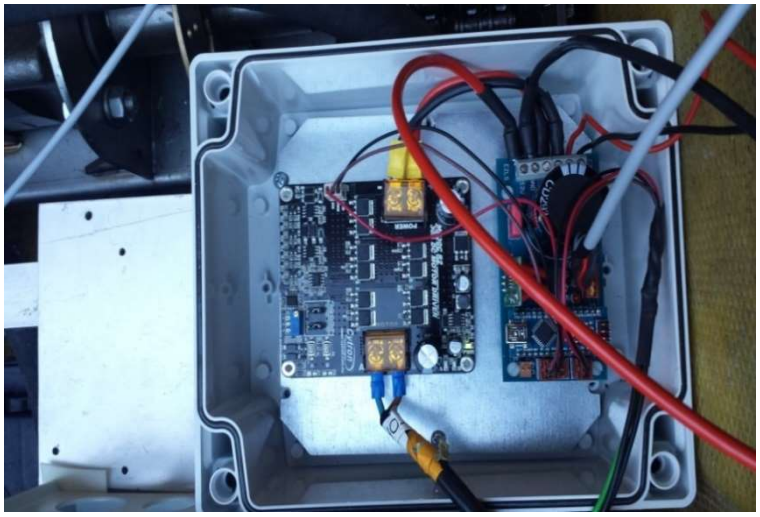

Figure 3.15 Motor Driver MD30C


Figure 3.16 Motor Driver MD10C with Arduino Board and current sensor

## 3.13. Control System Circuit

Two control system circuits were implemented in the real time system, the old system was using just one control Board and one motor driver to control the motors and read the sensors

values as shown in figure 3.18, this board acts as a slave and raspberry Pi as a master. In the new system a single board and motor driver was made for each motor and one board to read the analogue and digital signal and send it to the master, four slaves and one master were used in the new system as shown in figure 3.17.

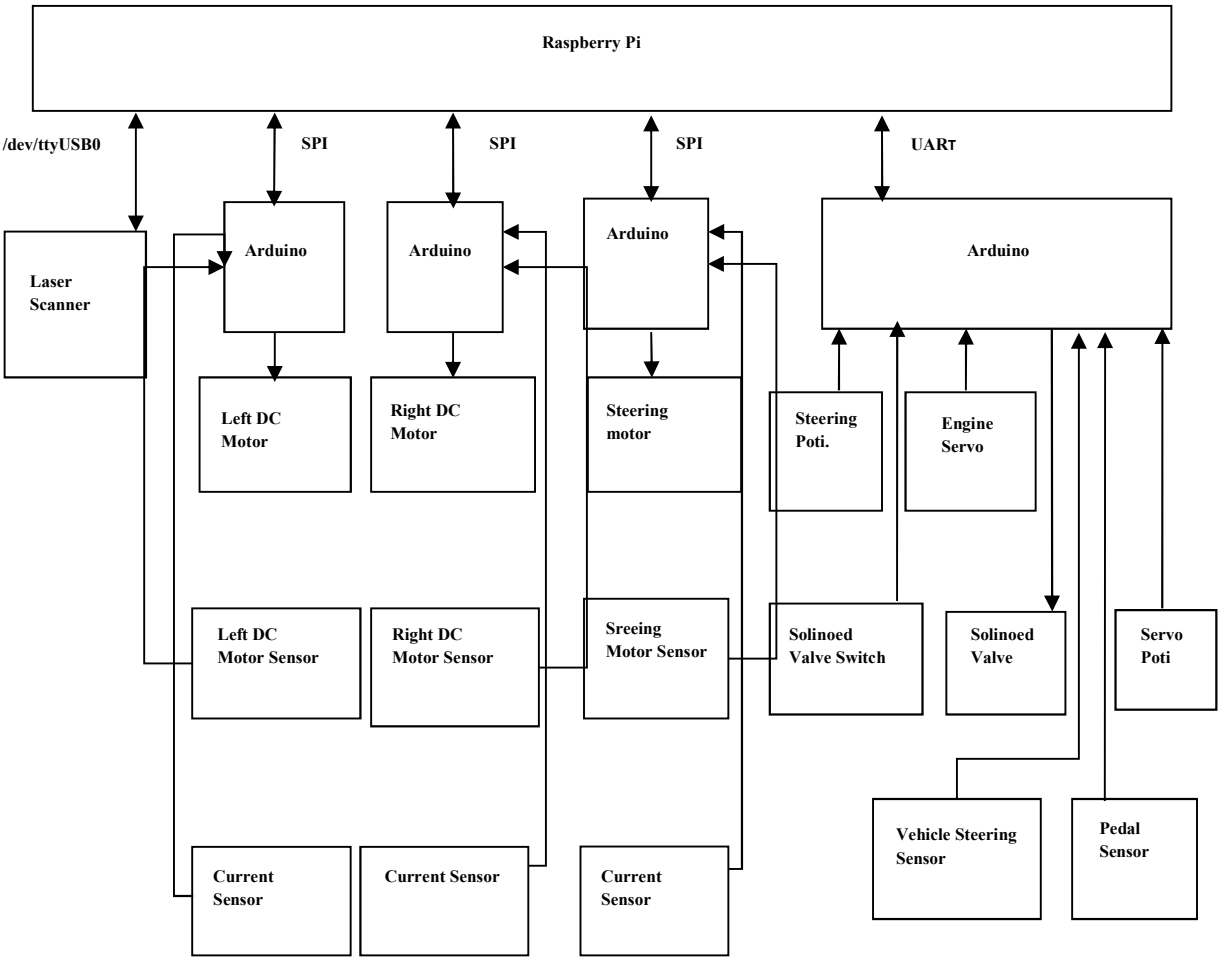


Error! Bookmark not defined.

Figure 3.17 The New Control System Block Diagram

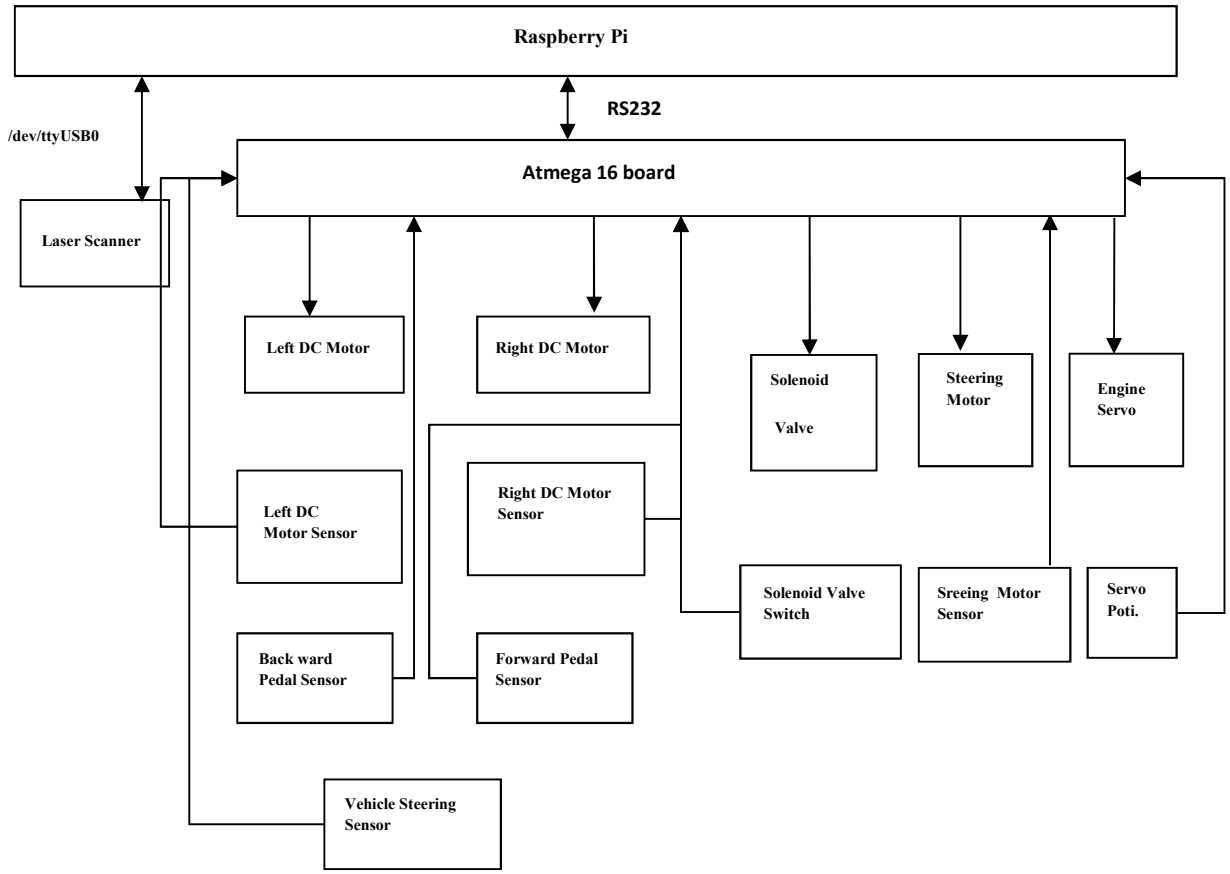


Figure 3.18 The Old Control System Block Diagram

## 3.14 Hydrostatic Transmission System

The gasoline engine that delivers the power to the machine is connected to the variable displacement pump via a drive coupling. Inside the variable displacement pump there is a swash plate that determines whether the vehicle is moving forward, backwards or is stationary, the angle of the swash plate also controls how much oil that flows out from the pump to the hydraulic Motor. In the swash plate a number of pistons are attached, an angle of the swash plate will make the pistons go back and forward with the rotation. An increase of the angle makes the stroke of the pistons longer which results in larger flow of oil out of the pump. The flow out of the pump is a product of the rotation of the pump and the displacement of the pump, where the displacement is determined by the swash plate angle. The flow created by the pump passes through a security valve that ensures that the pressure is not too high. After that it is connected to the hydraulic motor. A hydraulic motor is basically the same thing as a hydraulic pump, but it works in the opposite way, consequently the hydraulic motor is converting the flow back into rotation of the wheels. The hydraulic motor is a fixed displacement motor. These two swash plates are used to achieve the

demanded speed from the driver, if really high speed is desired then the Swash plate angle as well as the volume of the pump decreases, and the flow passes through a smaller volume and the rotation increases. A hydrostatic transmission as shown in figure 3.19 and 3.20 has advantages compared to a normal mechanical transmission line. Hydrostatic transmission is generally used in low-speed and high-torque applications. The reason is the continuously variable transmission, which makes it possible to achieve desired torque. A CVT is a little bit less efficient than a mechanical transmission but the possibility to drive at an optimal combination of torque and speed makes the gasoline engine to work in more efficient range, and therefore the whole vehicle becomes more efficient. The choice of torque and speed can be reached with high accuracy. Another motive is that a hydraulic motor produces up to ten times more power compared to an electrical motor with the same dimensions.

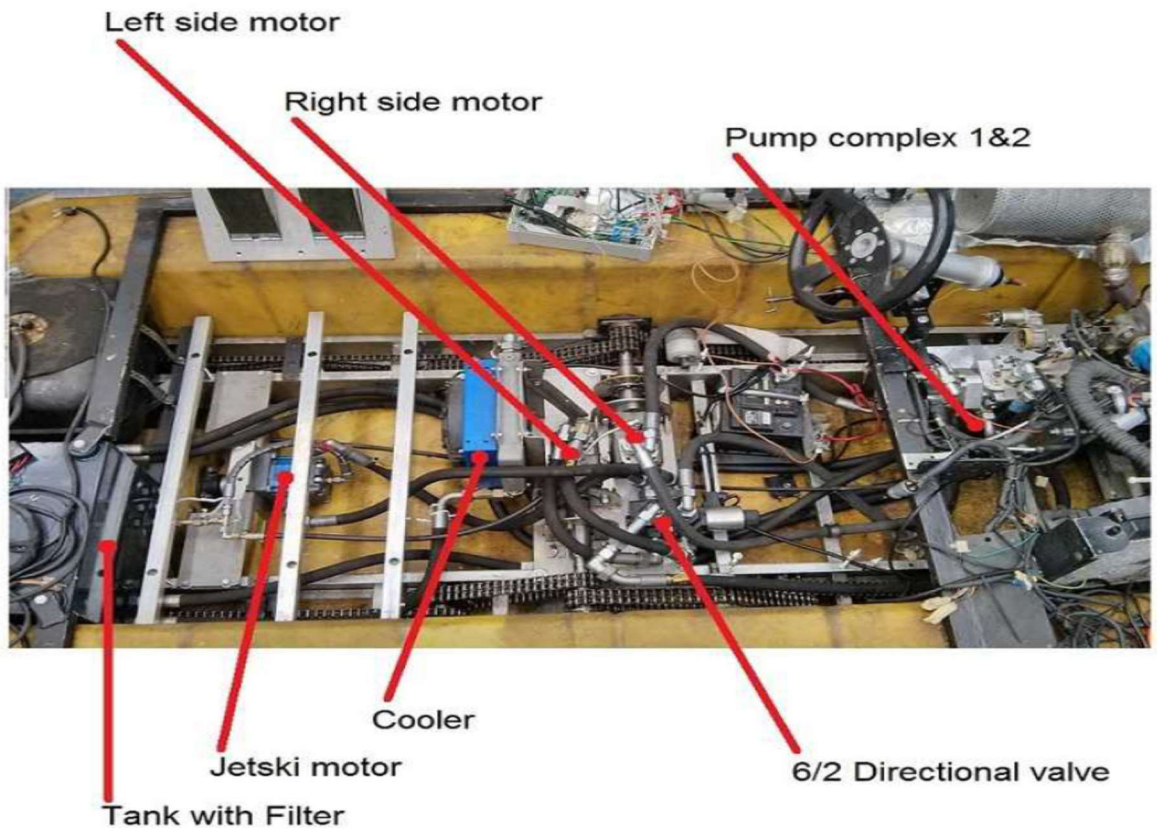


Figure 3.19 DORIS Hydraulic Circuit

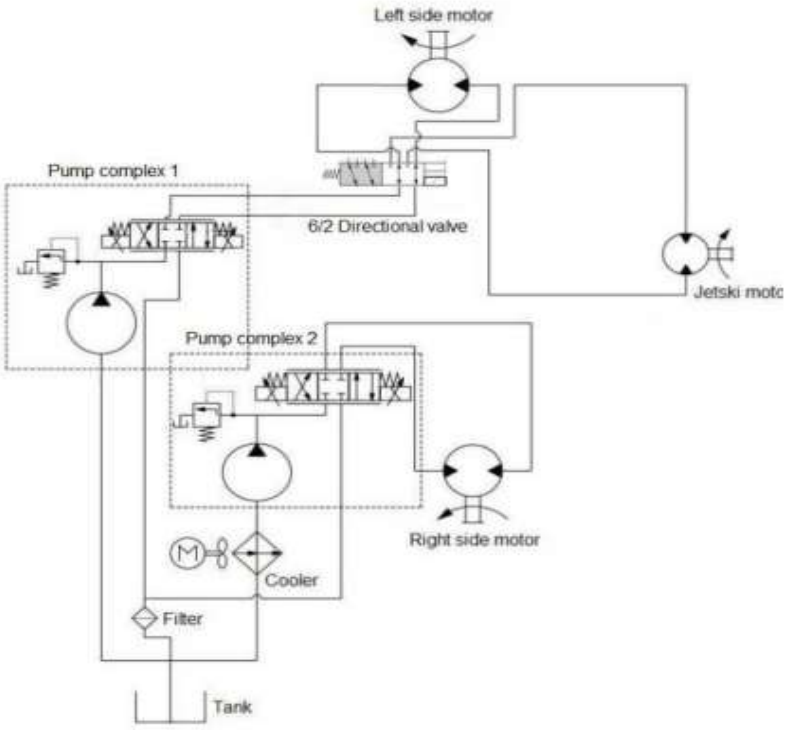


Figure 3.20 Hydrostatic Transmission Circuit

## 3.15 Hydraulic Transmission System Model

A dynamic model of the hydrostatic transmission has been created with simulation tools; SimHydraulics and Simulink/Matlab to analysis and study the effect of the surfaces during skid steering. A steady-state model of the hydrostatic transmission system has also been created in order to carry out steady-state simulation of the hydrostatic transmission system. The results from the steady state simulation give an indication if the dynamic models give a rational result or not. The steady-state simulation does not include any dynamic behavior of the system such as compressibility of fluid and pressure peaks. SimHydraulics is a block package under the Simscape toolbox in Simulink which is used to model up a hydraulic system. There are also used blocks from SimMechanics, another block package under Simscape, to model the mechanical components connected to the hydraulic system. The SimHydraulics model is shown in figure 3.21. The motor and load contains the hydraulic motor, the pressure measurement and the velocity measurement. The inertia is provided and the torque and rotational speed are measured. The pump system contains the variable displacement pump, the gasoline engine, the pump gets rotational speed and control signal in, and provides the system with flow.

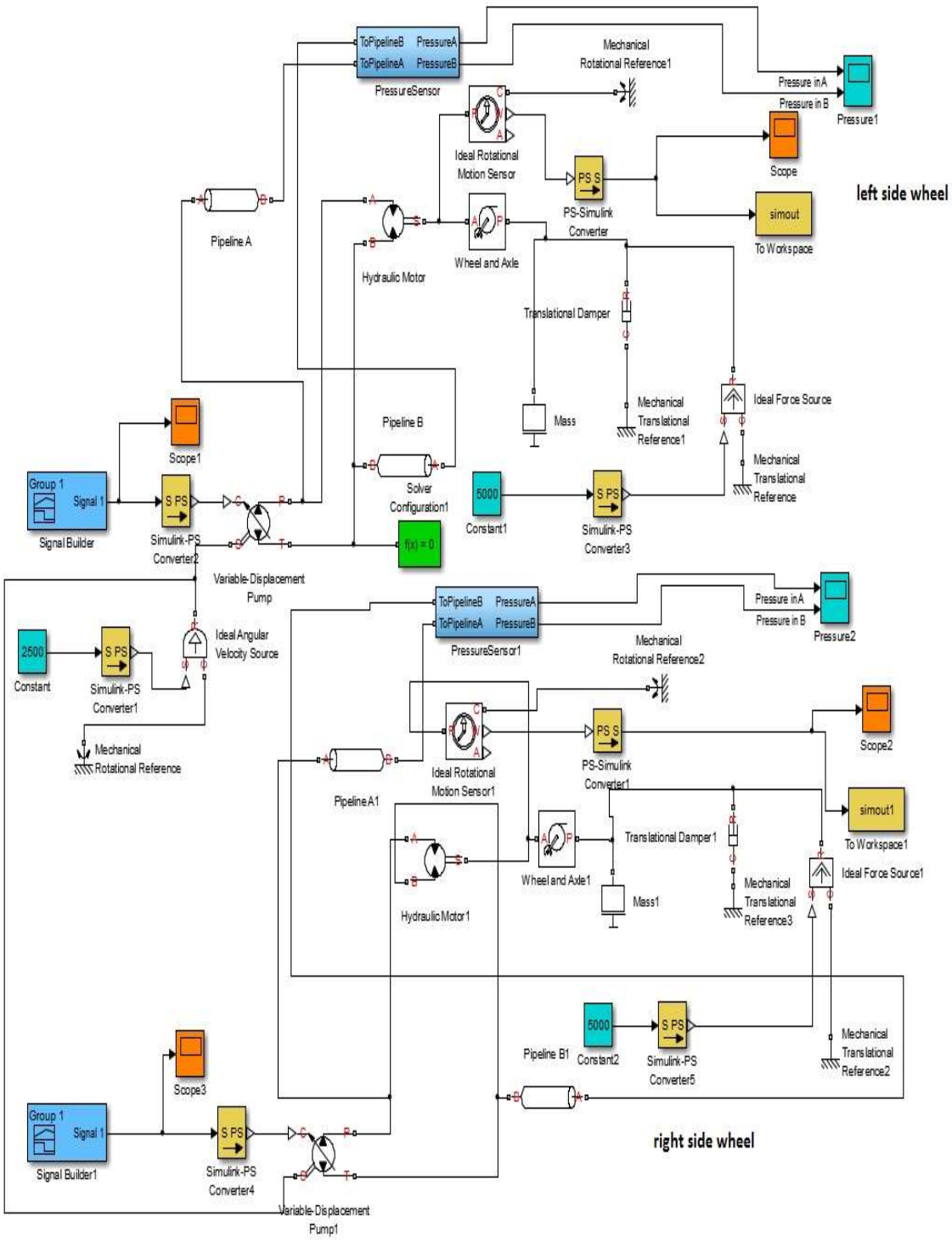


Figure 3.21 Hydrostatic Transmission System Model

## 3.16 Tire Model

Tire model is very important for Vehicle control systems where tire generates the forces that drive and manoeuvre the vehicle. Regardless of the inability of the linear model to provide the wheel tractive force, which is the most important factor in skid steer is that the linear

model could not properly describe the overall vehicle dynamic behaviour in some driving conditions. It is well known that the most accurate tire model is the magic formula model but it is also the one requiring the longest computation time for the determination for the coefficients. The tire model used in this simulation study is relatively more complex than a simple linear model, which is called unite semi-empirical tire model. From this model, longitudinal and lateral tire force can be calculated by slip ratio directly. The tire-road relative slip velocity Vs can be calculated by longitudinal speed Vx and lateral vehicle speed Vy and the wheel angular speed ω as shown in figure 3.22 [Shuang, G., et al., 2007].

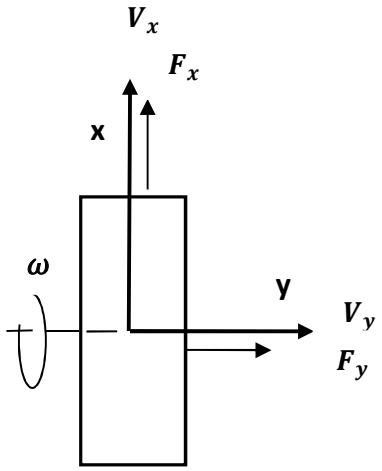


Figure 3.22 Wheel Speed

$$V_s = \sqrt{(V_x - \omega R)^2 + V_y^2} \tag{3.1}$$

Longitudinal slip

$$S_x = \frac{V_x - \omega R}{\omega R} \tag{3.2}$$

Lateral slip

$$S_y = \frac{V_y}{\omega R} \tag{3.3}$$

Infinitude relative longitudinal slip

$$\delta_x = \frac{k_x S_x}{\mu} \tag{3.4}$$

Infinitude relative lateral slip

$$\delta_y = \frac{k_y S_y}{\mu} \tag{3.5}$$

Infinitude total slip

$$\delta = \sqrt{{\delta_x}^2 + {\delta_y}^2} \tag{3.6}$$

The longitudinal tire force and the lateral tire force is:

$$F_x = -\frac{\delta_x}{\delta} F_z \, \mu \left[1 - e^{-\delta - E_y.\delta^2 - \left({E_y}^2 + \frac{1}{12}\delta^3\right)}\right] \tag{3.7}$$

$$F_y = -\frac{\delta_y}{\delta} F_z \, \mu \left[1 - e^{-\delta - E_y.\delta^2 - \left({E_y}^2 + \frac{1}{12}\delta^3\right)}\right] \tag{3.8}$$

For moving the vehicle forward and backward where there is no steering the tractive force is.

$$F_r = \mu mg + 1/2\rho v^2 C_d A \tag{3.9}$$

**3.17 Simulation Results**

The simulation studies are made with respect to the specified loads during rolling and skid steer on a various surfaces to show how the effect of the surface on the swash plate torque is produced from the pressure difference, friction and swash plate inertia as in equation (3.10). Figure 3.23 shows the swash plate strock with time and figure 3.24 shows the speed of the wheel for rolling for various surfaces; the speed is around 27m/sec with small changes between them, on sand the speed decreased a bit, while during skid steering the speed decreased to 25 m/sec as shown in figure 3.25. Figure 3.26 shows the pressure difference for rolling on various surfaces, the pressure difference becomes high on dry concrete surface because of the rolling coefficient and for asphalt and concrete, no big difference. Figure 3.27 shows the pressure during skid steer on various surfaces, the pressure difference is high on concrete surface and less on ice. Table 3.4 summarizes the pressure difference for the various surfaces during rolling and skid steer [Denis Corriveau, 1987], the result is calculated according to the value from table 3.3 and for 10degree swash plate angle and 2500 rpm gasoline engine speed. Figure 3.28 shows the effect of the engine speed on the hydraulic pump pressure difference, more engine speed less hydraulic pump pressure difference less swash plate torque because of that engine speed is coupled with the hydrostatic transmission speed system.

Table 3.3 Rolling and Friction coefficient for various surfaces [engineering toolbox]

| | Rolling coefficient | Friction coefficient |
|---|---|---|
| Sand | 0.3 | 0.65 |
| Asphalt | 0.03 | 0.55 |
| Concrete | 0.01 | 0.8 |
| Earth road | 0.04 | 0.68 |
| Hard-packed snow | 0.013 | 0.2 |

Table 3.4 Pressure and Torque on various surfaces and for 10 degree swash angle

| | Max.ΔP (Skid) | Max.ΔP (Rolling) | Max.T (Skid) | Max.T (Rolling) |
|---|---|---|---|---|
| Sand | 45 bar | 15 bar | 13.32 N.m | 7.36 N.m |
| Asphalt | 38 bar | 4 bar | 12 N.m | 5.1 N m |
| Concrete | 58 bar | 3.5 bar | 16.1 N.m | 5 N.m |
| Earth road | 51 bar | 8.2 bar | 14.68 N.m | 6 N.m |
| Hard-packed snow | 18.7 bar | 6.6 bar | 8.13 N.m | 5.6 N.m |

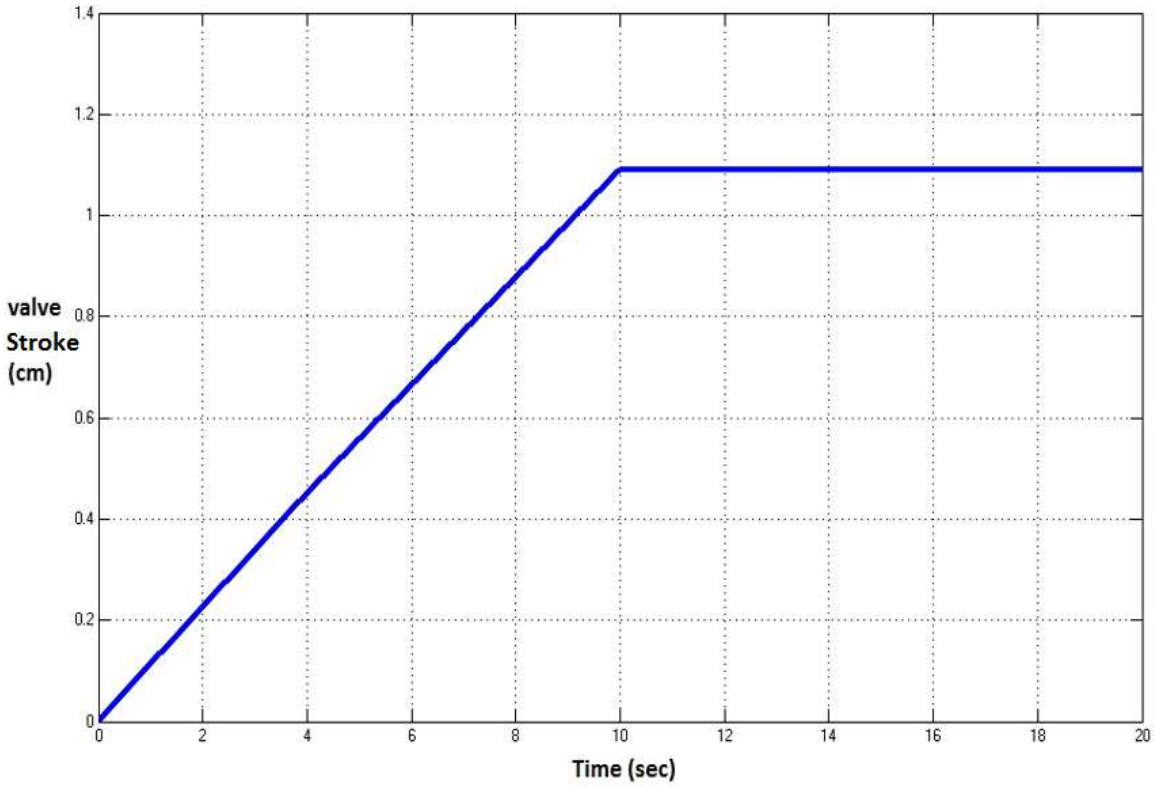


Figure 3.23 Valve Stroke

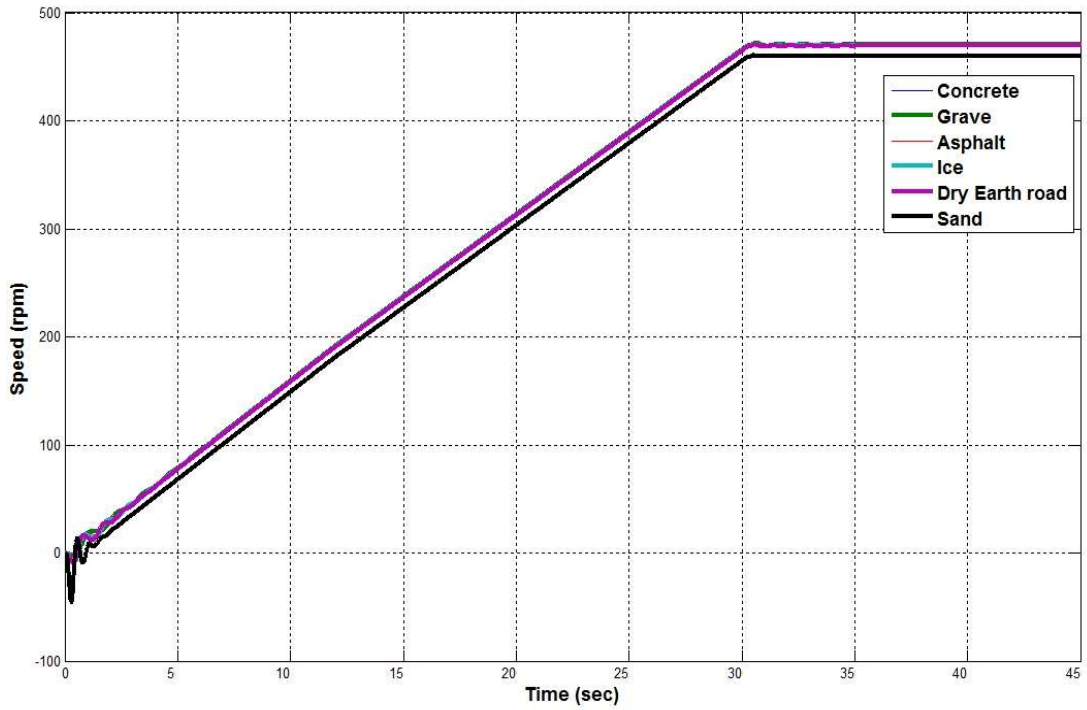


Figure 3.24 Wheel speed for rolling

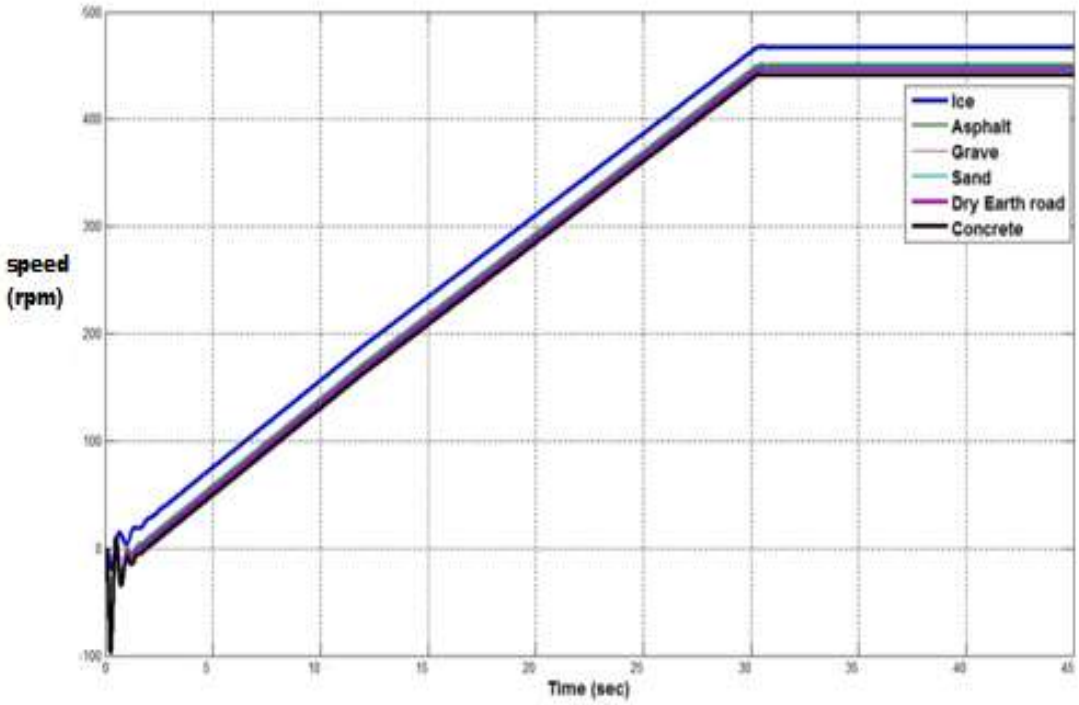


Figure 3.25 Wheel speed for skid steer

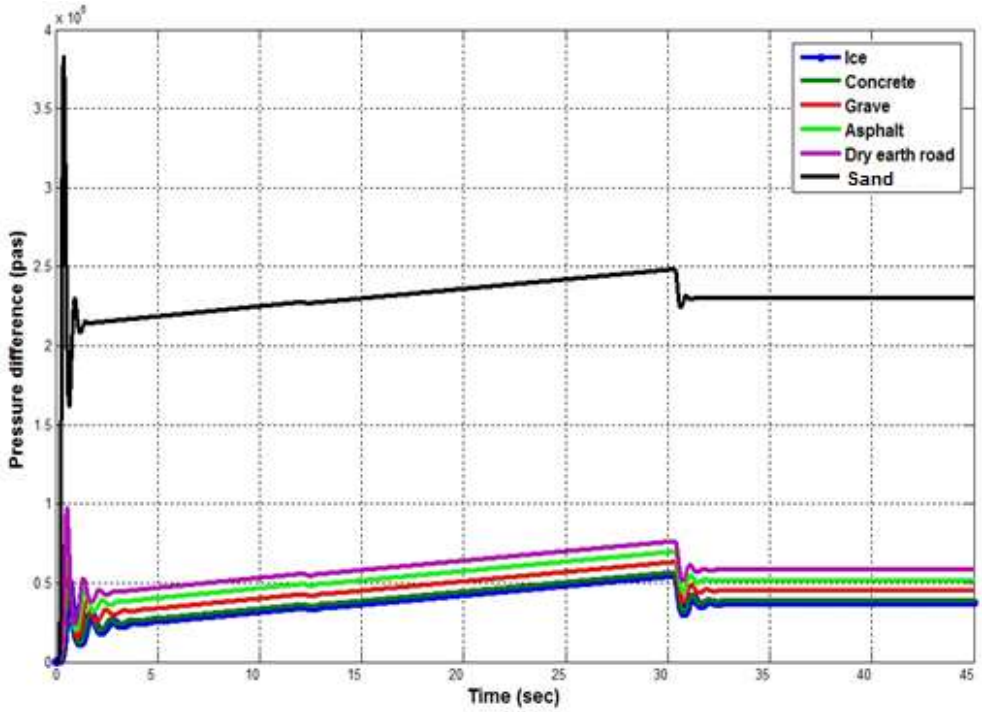


Figure 3.26 Pressure difference for rolling wheel

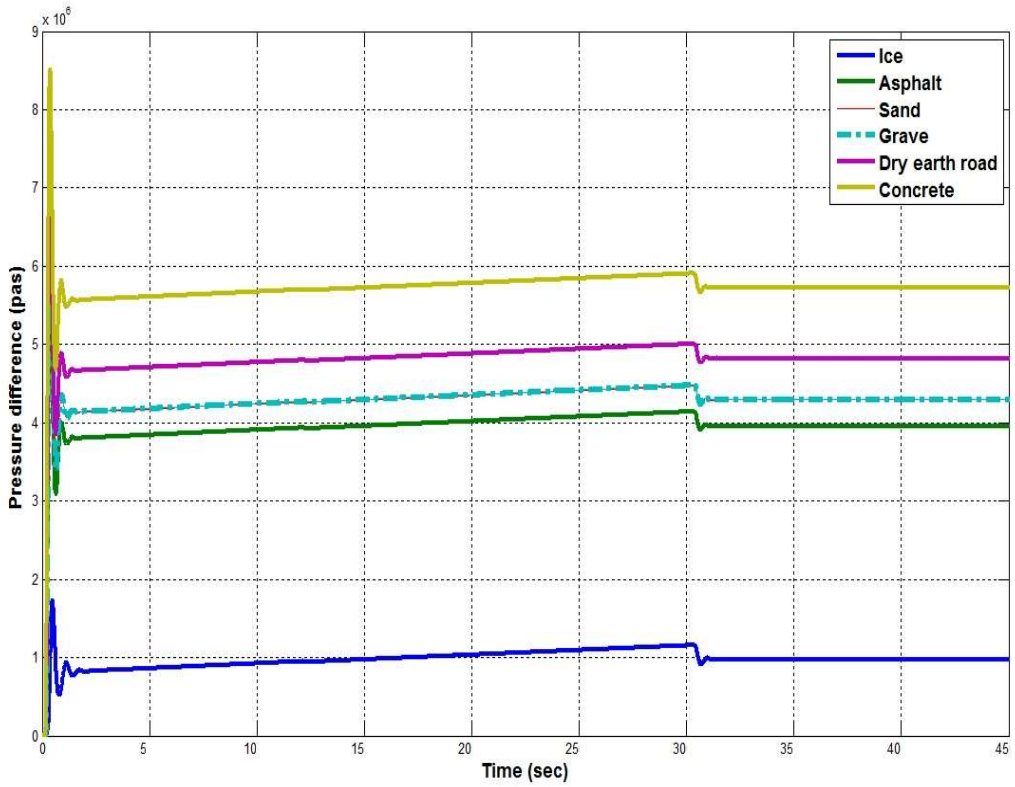


Figure 3.27 Pressure difference for wheel skid steer

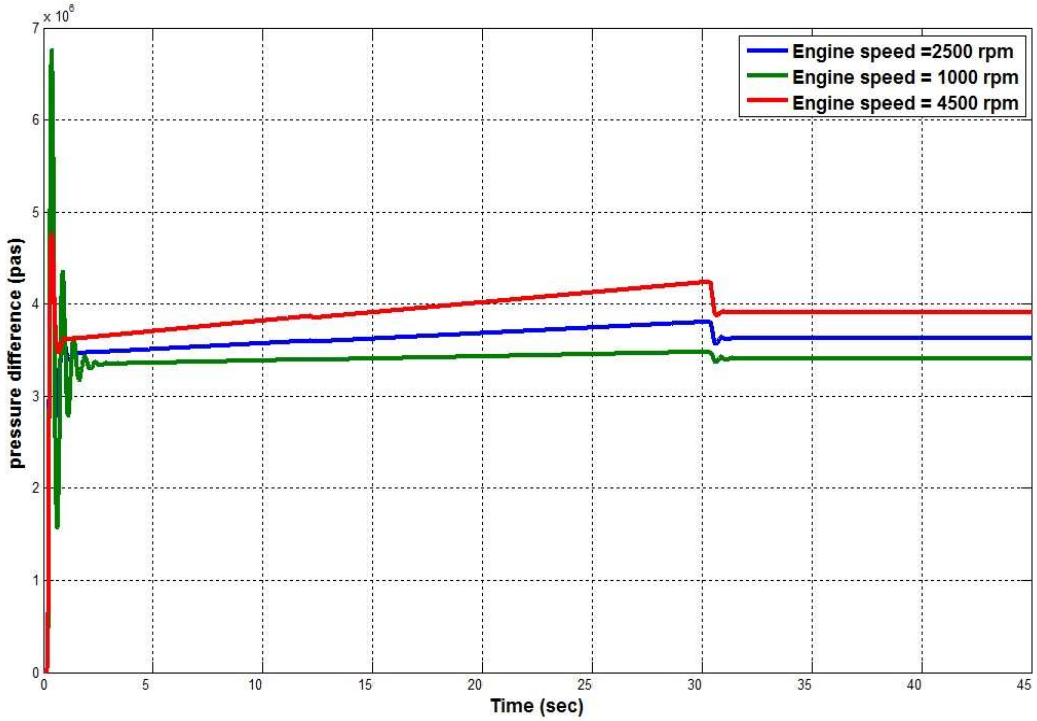


Figure 3.28 Pressure difference for skid steer on asphalt for difference engine speed

## 3.18 Swash Plate Torque

Figure 3.29 illustrates the components and forces that have an effect on the total torque. The load exerted by the swash plate can be divided into the following torques:

- Torque produced by friction forces, Tf,
- Torque relating to the pressure effect, Tp,
- Torque relating to the rotation of the barrel, Tr and
- Torque required to overcome the swash plate inertia $J_b \ddot{\theta}_P$

$$T_d = J_b \ddot{\theta}_P + T_f - T_p - T_r \tag{3.10}$$

Where Jp is the average moment of inertia of swash plate yoke assembly and Td is the torque applied to the yoke by the stepper motor [Magdy M. Abdelhameed et al., 2014].

The friction torque includes coulomb friction, viscous damping friction and stiction. The stiction friction is assumed to be negligible. Hence the friction torque can be represented by

$$T_f = \sin(\dot{\theta}_p) T_{fc} + \dot{\theta}_p B_P \tag{3.11}$$

Where Tfc is the torque produced by the coulomb friction force, Bp is the damping coefficient of the swash plate yoke assembly.

However, the torque applied to the swash plate due to the pressure effect is significant. This torque is a function of both the pump pressure and swash plate angle and can be written as

$$T_p = K_{p1} P_p - K_{p2} P_p \theta_p \tag{3.12}$$

Where $K_{p1}$ , $K_{p2}$ $are$ the pressure torque constants and Pp is the pump pressure.

When the pump is in operation, there is a torque applied to the swash plate by the piston slippers. This force is a result of the inertia of pistons and the shoe plate and is known to be a function of the swash plate angle. Therefore, this torque is related to the rotation of the barrel and can be represented as

$$T_r = -S_1 - S_2 \theta_p \tag{3.13}$$

Where S1and S2 are the simplified pump model constants. Substituting Equations (3.11) - (3.13) in (3.10):

$$T_d = J_b \ddot{\theta}_P + \sin(\dot{\theta}_p) T_{fc} + B_p \dot{\theta}_p - K_{p1} P_p - K_{p2} P_p \theta_p - S - S_2 \theta_p \tag{3.14}$$

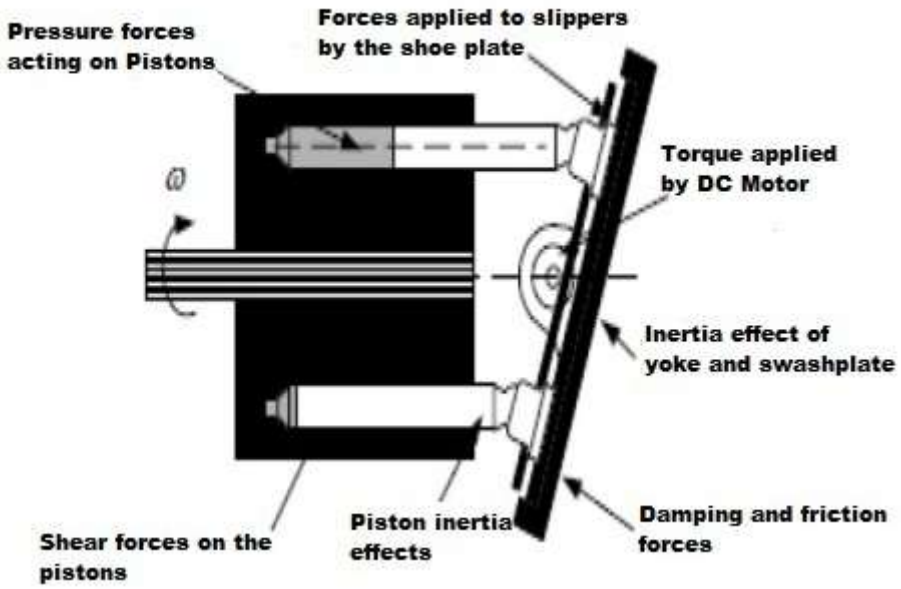


Figure 3.29 Swash Plate mechanism

The swash plate is actuated using DC Motor and the torque applied on the yoke, the torque produced by friction and by the rotation of the barrel is calculated manually as shown in figure 3.30. And the torque produced by pressure difference is calculated using simulation and by adding the pressure difference torque to the result from manual calculation we get the overall torque applied on the swash plate.

The motor to the gear box ratio is concluded experimentally by rotating the motor manually and getting the number of rotation from the gear box.

DC Motor Max. Torque =1 N.m [from motor specifications].

Gear box ratio=60.

Gearbox output max Torque = 60x 1= 60 N.m.

Hydraulic Pump swash plate Torque produced by friction and by the rotation of the barrel =2.0 Kg .9.81 m/s².0.21 m = 4.3 N.m, from this calculation the DC Motor System Torque is enough to open the Hydraulic Pump swash plate. The most important torque is produced from the pressure difference between the input and output hydraulic pump pressure, this difference happens during skid steering specially for a sharp angle which causes some times, slip between the DC motor shaft and the coupling and produce extra stress on the shaft key. Figure 3.31 shows the swash plate torque with the pressure difference for rolling and figure 3.32 shows the swash plate torque with the pressure difference for skid steer. For skid steer the torque reaches maximum on the dry concrete.

Figure 3.30 Measure Swash Plate Torque manually

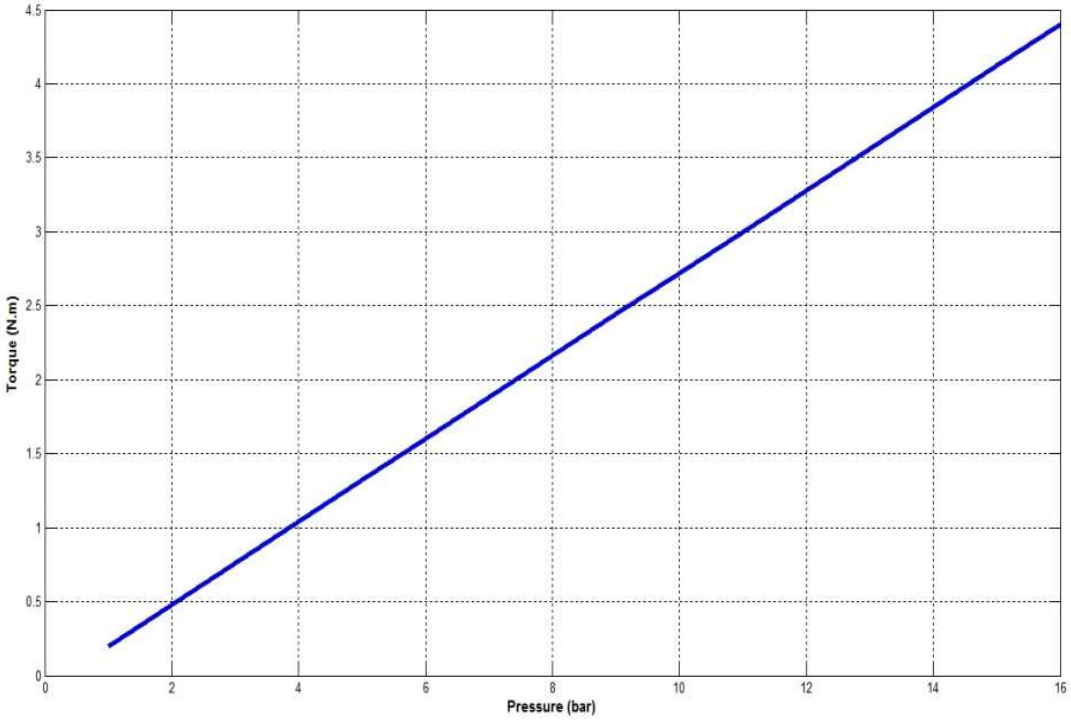


Figure 3.31 Pressure difference and Swash Plate Torque for Rolling

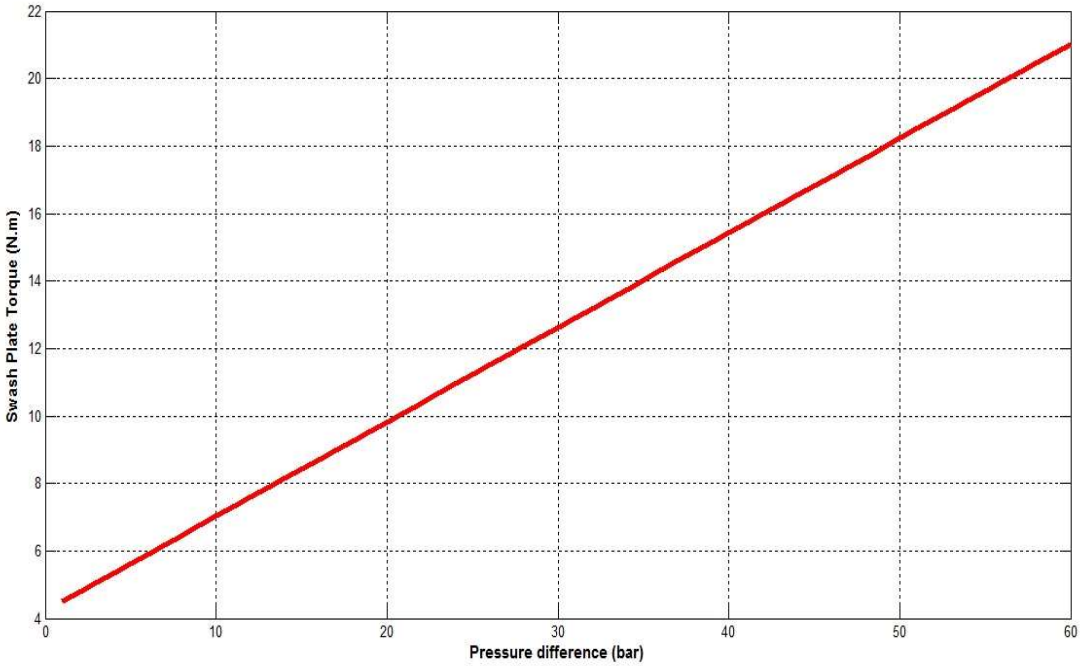


Figure 3.32 Pressure difference and Swash Plate Torque for skid steer

## 3.19 Swash Plat Angle

In axial piston pumps, where the cylinders and the drive shaft are parallel, the pistons are nested in a circular array within a common cylindrical block at equal intervals about the *x*-axis. Here, the reciprocating motion is created by the swash plates which is sometimes referred as cam plate or wobble plate as well. The swash plate lies in a plane that cuts across the center line of the drive shaft and cylinder barrel and does not rotate. In a fixed-displacement pump, the swash plate will be rigidly mounted in a position so that it intersects the center line of the cylinder barrel at an angle approximately $18^0$ from perpendicular. Variable-delivery axial piston pumps are designed so that the angle that the swash plate makes with a perpendicular to the center line of the cylinder barrel may be varied from 0 to $18^0$ to one or both sides. From figure 3.33, the relationship between the swash plate angle of the variable displacement pump and the hydraulic motor speed in the hydrostatic transmission circuit is estimated.

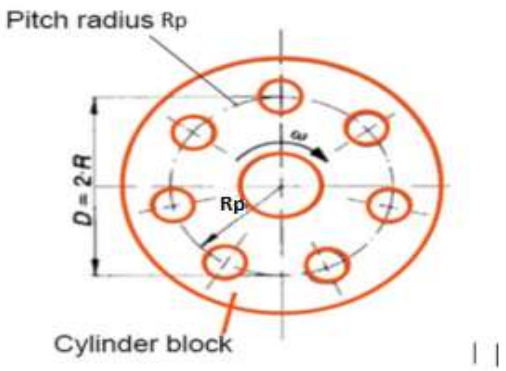


Figure 3.33 Cylinder Block of Variable Displacement Pump

If the piston pitch radius is defined by R then geometric displacement q of an axial piston pump with straight cylinder block bore is then given by [Will Guo,2010]:

$$V_g = \frac{\pi}{2} D^2 Z R_P \tan(\gamma) \tag{3.16}$$

The hydraulic pump flow rate defined as:

$$Q_{Pump} = \frac{V_g N}{1000} \tag{3.17}$$

And by substitute 3.16 in 3.17 the flow rate as a function of the swash plate angle become:

$$Q_{Pump} = \frac{\pi}{2} D^2 Z R_P \tan(\gamma) \frac{N}{1000} \tag{3.18}$$

The hydraulic motor speed is:

$$N_{Motor} = \frac{1000 Q f}{V_g motor} \tag{3.19}$$

Assume that there is no leakage in the circuit so the flow from the pump is equal to the flow rate to the hydraulic motor.

$$Q_{Pump} = Q_{Motor}$$

By adding (3) to (4) the speed of the hydraulic motor as a function of swash plate angle defined as:

$$N_{Motor} = \frac{\frac{\pi}{2} D^2 Z R_P \tan(\gamma) N f}{V_g motor} \tag{3.20}$$

Where

D: the piston diameter (cm) = 1.2 cm

Z: number of pistons = 9

$R_P$: pitch radius (cm) = 3 cm

γ: swash plate angle (degree)

$V_g$ : geometric dispalcement ($cm^3$) = 159.7 $cm^3$

N: Hydraulic pump speed (rpm) = gasoline engine speed = 1200 rpm

$f$ : Efficiency

With D=1.2cm, Z=9, Rp=cm, $V_g$ =159.7 [OMS Danfoss hydraulic motor datasheet],N=1200 rpm [Suzuki engine 3 cylinders data sheet]

Figure 3.34 shows the relation between the swash plate angle and the hydraulic motor speed, the relation is proportional relation and for one degree difference angle the speed increased around 8 rpm more ,to avoid this difference speed between the both motors which cause the vehicle to skid left and right side, the DC Motor actuator with the shaft and coupling between the swash plate pivot and the gearbox should not have any tolerance because to open the swash plate with $18^0$ angle, the shaft travels 4 mm; this traveling distance is the controlled value and one degree difference happened in 0,25mm traveling distance, so we should not have this small tolerance to avoid any difference in speed between left and right that cause the vehicle to skid right or left instead of forward and backward.

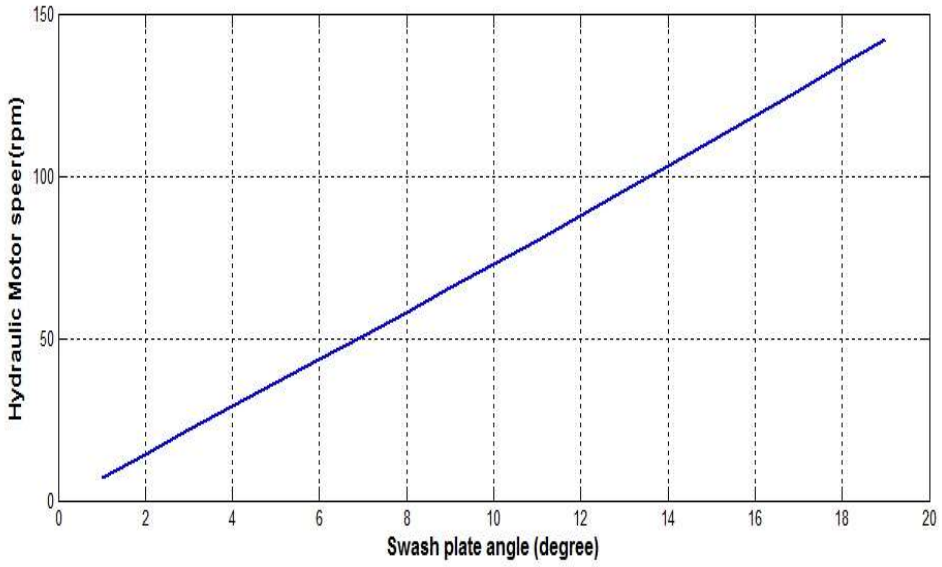


Figure 3.34 The Swash Plate Angle and Hydraulic Motor Speed

# Chapter 4

# Position control of swash plate Angle

DC motor angular position systems are usually controlled by proportional integral-derivative (PID) control algorithms with PID coefficients tuned for optimizing operation [Lin, P.I.H., et al., 1994]. The objective of a PID controller in a position control system is to maintain a position set point at a given value and be able to accept new set-point values dynamically. Modern position control environments require controllers that are able to adapt with parameter variations and system uncertainties. An alternative method to control the DC Motor position is Dead Beat control system; both methods as well as their combination, resulting in a P-Dead Beat controller are described in detail in this part.

To implement a PID controller, the proportional gain KP, the integral gain KI and the derivative gain KD must be determined carefully [Bindu, R., et al., 2012]. Controlling the DC motor without using the PID controller will give some oscillation in the signal and because the system is nonlinear, controlling by function is the best way to control the nonlinear systems and PID controller is a good choice to achieve this task. To implement the Dead Beat controller a sampling time is used to settle the steady state error in a finite time. Sampling time depends on the microcontroller frequency and the choice prescaler. Two DC motors used to control the two hydraulic pump swash plates which rotating in limited angle between +18 to -18 degree. To open the hydraulic pump swash plat the torque apply from the motor should be enough to overcome the overall swash plat torque and has be done by controlling the motor speed, the more motor speed the more torque. Controlling the speed is done by using PWM (Pulse Width Modulation), all of these are written in C-code using AVR studio and loaded into the ATmega16 microcontroller.

## 4.1 System Mathematical Model

DC motor electrical circuit shown in figure 4.1. A simple mathematical relationship between the shaft angular position and voltage input to the DC motor may be derived from physical laws. In the point of control system, DC motor can be considered as single input single output plant (SISO) [Bindu, R., et al., 2012]. Therefore, complications related to multi-input system are discarded. DC motors have the field coil in parallel with the armature, the current in the

field coil and the armature are independent of one another, and as a result, these motors achivied the desired speed and position

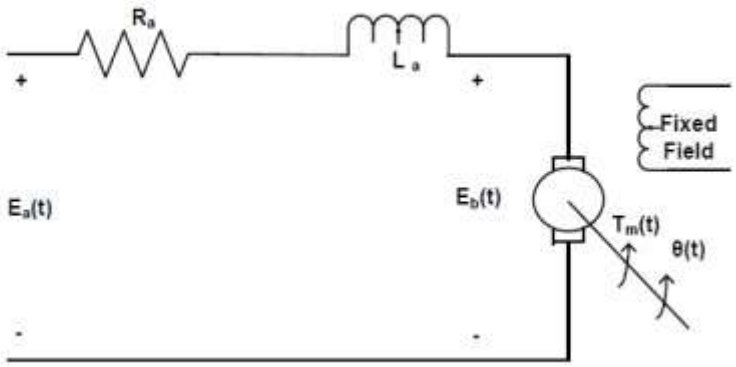


Figure 4.1 Schematic Diagram of a DC Motor

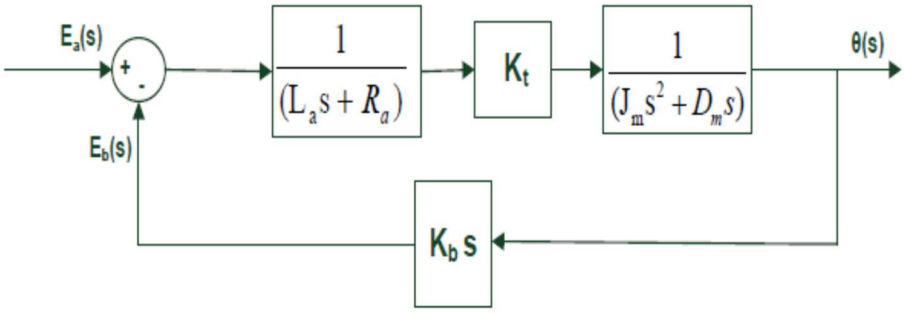


Figure 4.2 Block Diagram representation of a DC motor

The dynamic behaviour of the DC motor is given by the following equations [Meshram, P.M., et al., 2012], and can be represented by the block diagram shown in figure 4.2.

$$E_a(s) = R_a I_a(s) + L_a s\, I_a(s) + E_b(s)$$

$$T_m(s) = K_t I_a(s)$$

$$E_b(s) = K_b\, s\, \theta(s)$$

$$T_m(s) = (J_m\, s^2 + D_m\, s)\theta(s)$$

Where,

Ra=Armature resistance in ohm (Ω)

La=Armature inductance (H)

ia=Armature current (A)

ea=Armature voltage (V)

eb=Back EMF (V)

Kb=Back EMF constant (volt/ rad/sec)

Kt=Torque constant (N.m/A)

Tm=Torque developed by the motor (N.m)

θ(t)=Angular displacement of shaft ( rad)

J=Moment of inertia of the motor and load (K-g$m^2$/rad )

Dm=Frictional constant of motor and load ( Nm/ (rad/sec)).

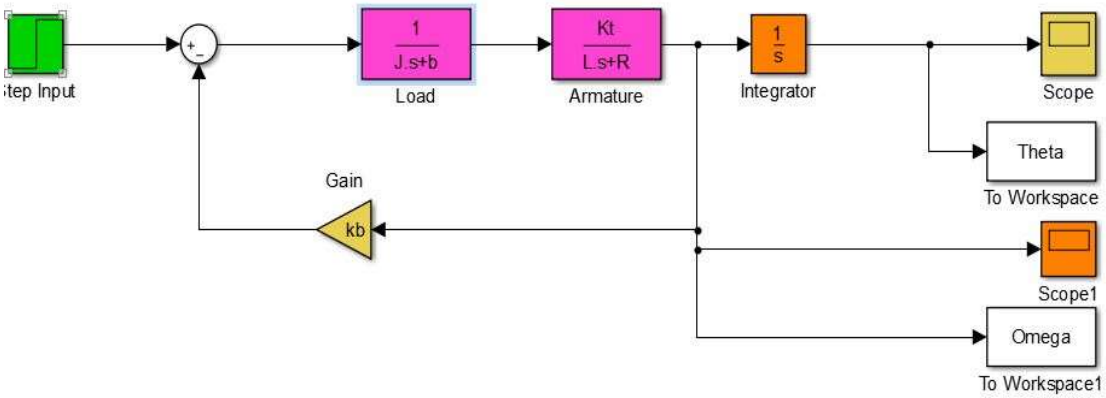


Figure 4.3 Simulink Block Diagramd of the DC Motor

After simplification and taking the ratio of $\frac{\theta(s)}{E_a(s)}$ the transfer function will be as below,

$$G(s) = \frac{Kt}{\big((Js + b)(Ls + R) + Kt\,Kb\big) * s} \tag{4.1}$$

The rotor and the shaft are assumed to be rigid. Consider the DC Motor specification in table 3.1The transfer function is:

$$G(s) = \frac{1}{0.05s^2 + 3.8s + 0.78} * \frac{1}{s}$$

## 4.2 PID Controller

Proportional-integral-derivative (PID) controllers are widely used in industrial control systems because of the reduced number of parameters to be tuned [Basilio, J.C., et al., 2002]. They provide control signals that are proportional to the error between the input signal and the actual output, to the integral of the error, and to the derivative of the error, namely

$$U(t) = K_p \left[ e(t) + \frac{1}{T_i} \int_0^t e(\tau)\, d\tau + T_d \frac{d}{dt} e(t) \right] \tag{4.2}$$

Where U(t) and e(t) denote the control and the error signals respectively, and Kp, Ti and Td are the parameters to be tuned. The corresponding transfer function is given as

$$U(s) = K_p \left[ 1 + \frac{1}{T_i(s)} + T_d\,(s) \right] \tag{4.3}$$

These functions have been enough to the most control processes. Because the structure of PID controller is simple, it is the most extensive control method to be used in industry. The PID controller is mainly to adjust an appropriate proportional gain (Kp), integral gain (Ki), and differential gain (Kd) to achieve the optimal control performance. The PID controller is shown in Figure 4.4 and the Simulink block diagram for the system is as shown in figure 4.3. Transfer function can also be expressed as

$$K(s) = \frac{U(s)}{E(s)} = K_p + \frac{K_i}{S} + K_d\, S \tag{4.4}$$

The main features of PID controllers are the capacity to eliminate steady-state error of the response to a step reference signal (because of integral action) and the ability to anticipate output changes (when derivative action is employed). Tuning the PID controller is achieved experimentally on the plant. A lot of experiment has been carried out before getting the best result for Kp, Ki and Kd.

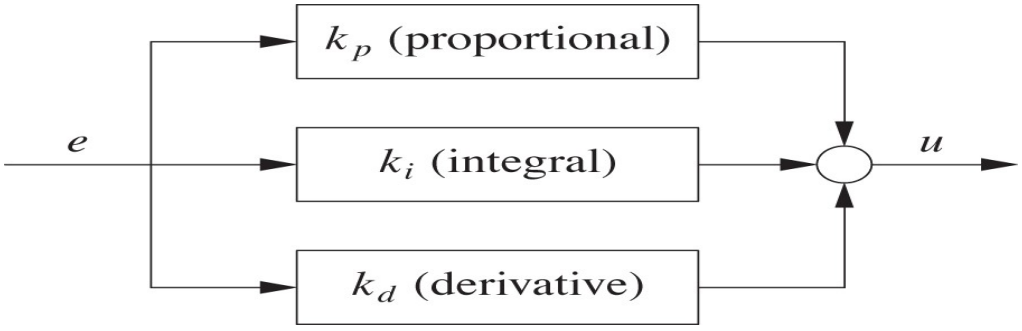


Figure 4.4 PlD Controller Block Diagram

## 4.3 Speed Control of a DC Motor

In order to effectively use a D.C. motor for any application, it is very important to understand its characteristic curves. For every motor, there is a specific Torque/Speed curve. The relation between torque and speed is important in choosing a DC motor for a particular application. Figure 4.6 shows a torque/speed curve of a DC motor. Note that torque is inversely proportional to the speed of the output shaft. In other words, there is a trade off between how much torque a motor delivers, and how fast the output shaft spins.

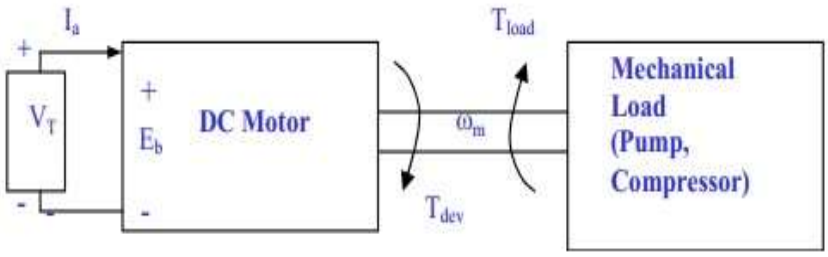


Figure 4.5 DC Motor and Mechanical Load

The torque developed in the rotor as shown in figure 4.5 is [Gupta, R. 2012]:

$$T_{dev} = \frac{K\varphi}{R_a}\,(V_T - K\varphi\omega_m)$$

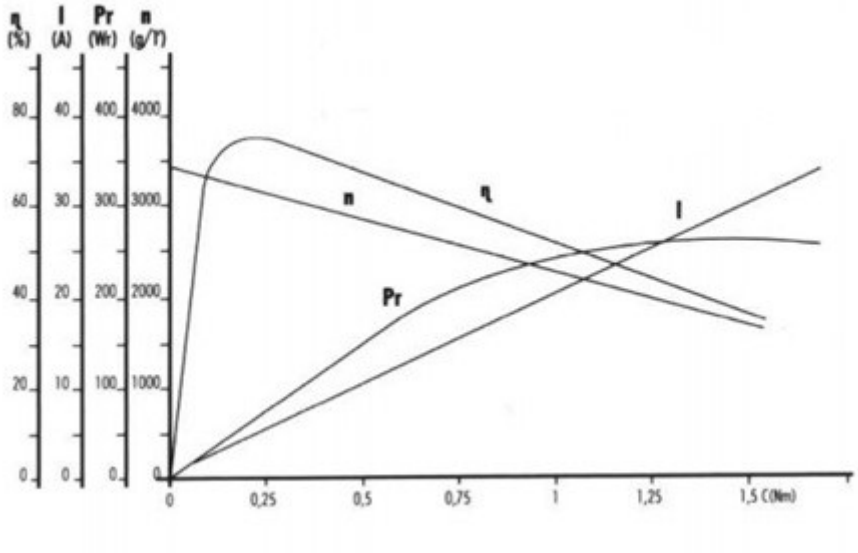


Figure 4.6 Motor Speed and Torque Relationship

In essence, there are four ways to vary the speed of DC motors:

1. By using mechanical gears to achieve the desired speed. This method is generally beyond the capability of most home workshops.

2. Reducing the motor voltage with a series resistor. However, this is inefficient and reduces torque. As the current drawn by the motor increases, the motor load increases too. More current means a larger voltage drop across the series resistor and therefore less voltage to the motor.

3. Using a transistor to continuously vary the voltage to the motor. This works well but a substantial amount of heat is dissipated in the power transistor.

4. By applying the full supply voltage to the motor in bursts or pulses, eliminating the voltage losses in the series resistor or transistor. This is called Pulse Width Modulation PWM and it is the method used in the project circuit. It is a very efficient way of providing intermediate amounts of electrical power between fully on and fully off. Short pulses means the motor runs slowly. Longer pulses make the motor run faster. The main advantage of a PWM circuit over a resistive power controller is the efficiency. One additional advantage of PWM is that the pulses reach the full supply voltage and will produce more torque in a motor by being able to overcome the internal motor resistances more easily. Finally, in a PWM circuit, common small potentiometers may be used to control wide varieties of the loads whereas large and expensive high power variable resistors are needed for resistive controllers [Mohammed, J.A., et al., 2013].

### 4.3.1 Speed control with PWM

One essential aspect of controlling motors is the ability to change the speed of rotation and the amount of torque produced. One simple but usually impractical means of achieving this is to adjust the supply voltage up and down as required. However, it is more effective and common to use the PWM concept, by adjusting the duty cycle of the signal, the time fraction it is "on", the average power can be varied, and hence the motor speed [ Wang, W.A., et al., 2010]. This is a control technique where power to the motor is switched on and off rapidly, at rates high enough that the effects of the switching can be negligible (less power is wasted as heat and smaller heat-sinks can be used). The resulting effective voltage is then the average fraction of the time the power is on. This technique is also used in many other applications. Figure 4.7 illustrates the PWM concept. Figures 4.8, 4.9, 4.10 shows the DC

Motor in a different Duty cycles. The drive signal is switched on and off with a given period and is in the “on” state for a fixed fraction of the period. This “on” time is referred to as the “duty cycle” and is stated as a percentage, calculated as

$$\text{Duty Cycle (\%)} = \frac{\text{On Time}}{\text{One Time} + \text{Off Time}}\ 100$$

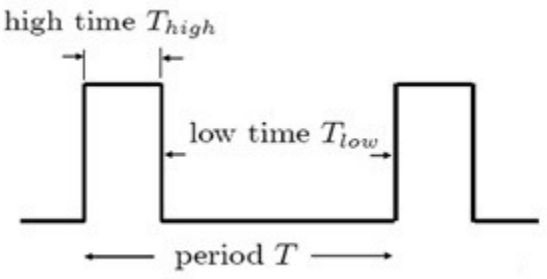


Figure 4.7 Duty cycle

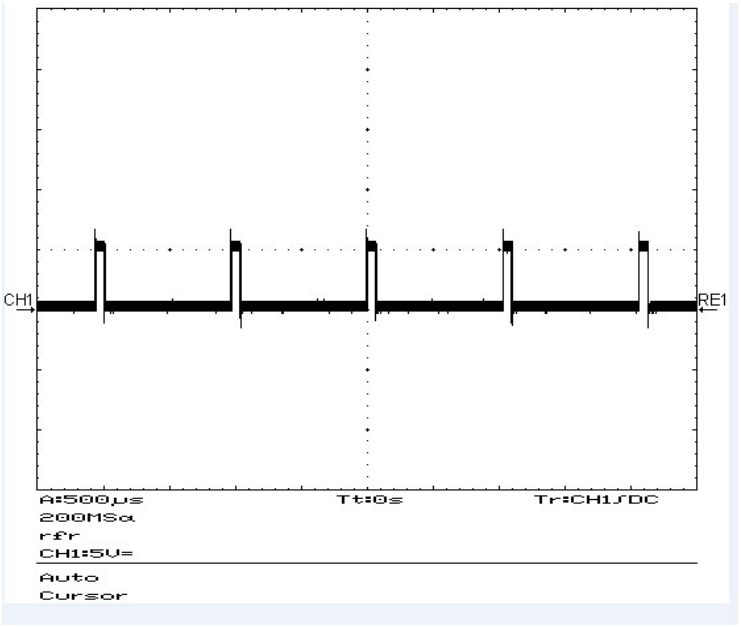


Figure 4.8 5% DC Motor Duty cycle

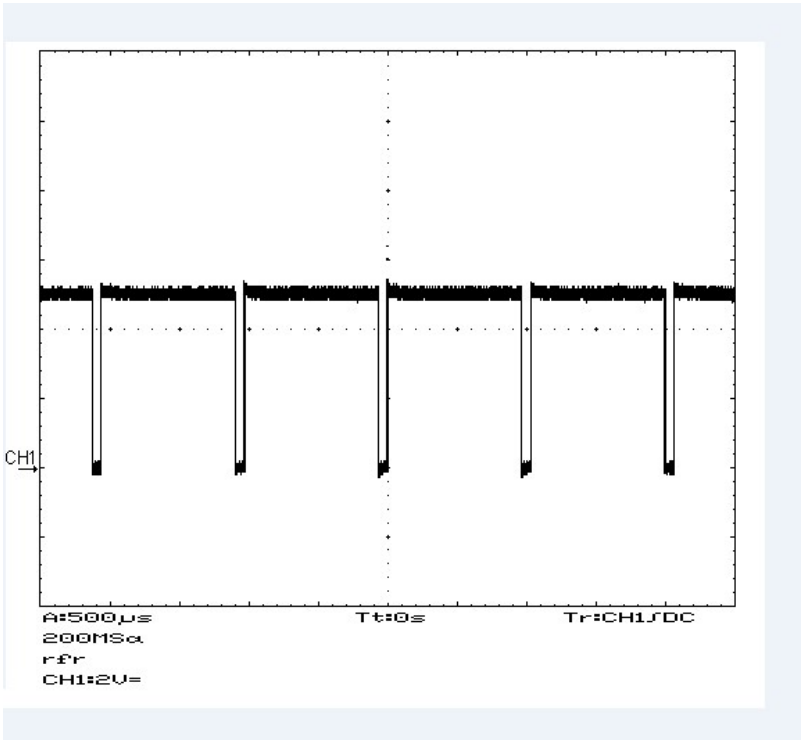


Figure 4.9 90% DC Motor Duty cycle

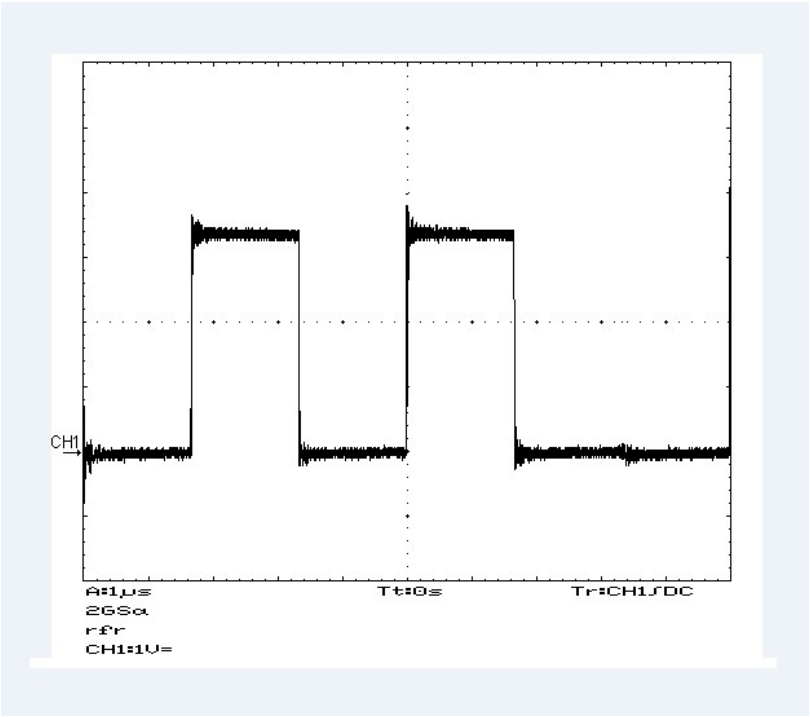


Figure 4.10 50% DC Motor Duty cycle

### 4.3.2 PWM Implemented in AVR

Generate stable and accurate pulse width modulated (PWM) signals on an AVR can easily be achieved using the waveform generator modes of the timer peripherals as shown in figure 4.11, however only a limited number of channels can be implemented. If a large number of PWM channels are required then a software solution must be used, and the intention of this application is to demonstrate a method for providing a very low jitter PWM signals. Software generation of PWM requires a certain amount of processing time to manage the signal level decision process, so it is only suitable for low base frequency waveform generation. Signals of this type are suitable for DC control applications such as brush-type DC motor speed control, analogue meter driving, or any situation requiring a low-dynamic DC control voltage.

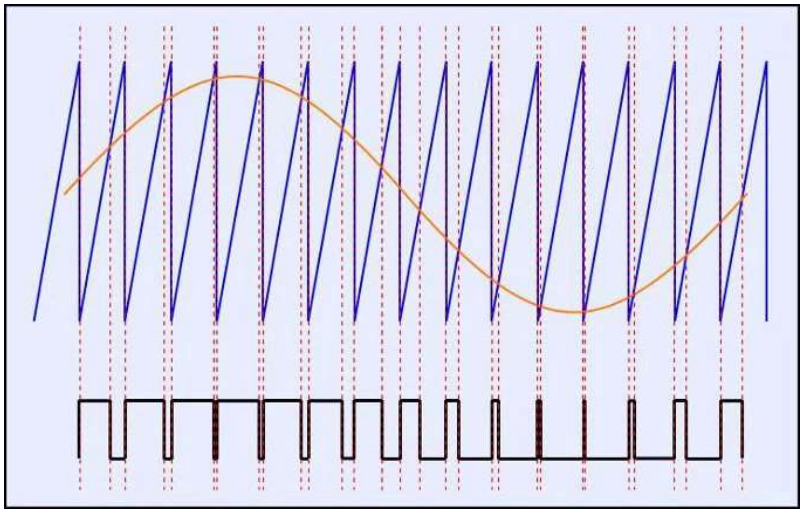

Figure 4.11 Generate wave form in AVR microcontroller

## 4.4 Graphical Display Interface

A low cost PC based real time data logging and displaying system can be used in the laboratories for measurement, monitoring and storage of data for slowly varying signals in science and engineering stream. Data logging, displaying and recording is a very common measurement application. In its most basic form, data logging is the measurement and recording and displaying of physical or electrical parameters over a period of time. For proper acquisition of the data by the PC, graphical display and saving into a file an application program is developed in Visual Studio 6.0. It uses the MSComm component to communicate through the COMM port of the PC. The data acquired is analysed and split into four values having four digits each, since it has 10bit resolution it can read a value from

0 to 1023 for a channel. Controlling the DC motors position is needed to adjust the Pedals and steering wheel positions. To do this step displaying the sensors value is important. To show and visualize the sensors data from the input and output sensors a program in visual studio developed as shown in figure 4.12 where the data from feedback sensors, steering sensor and pedals sensors are displayed.

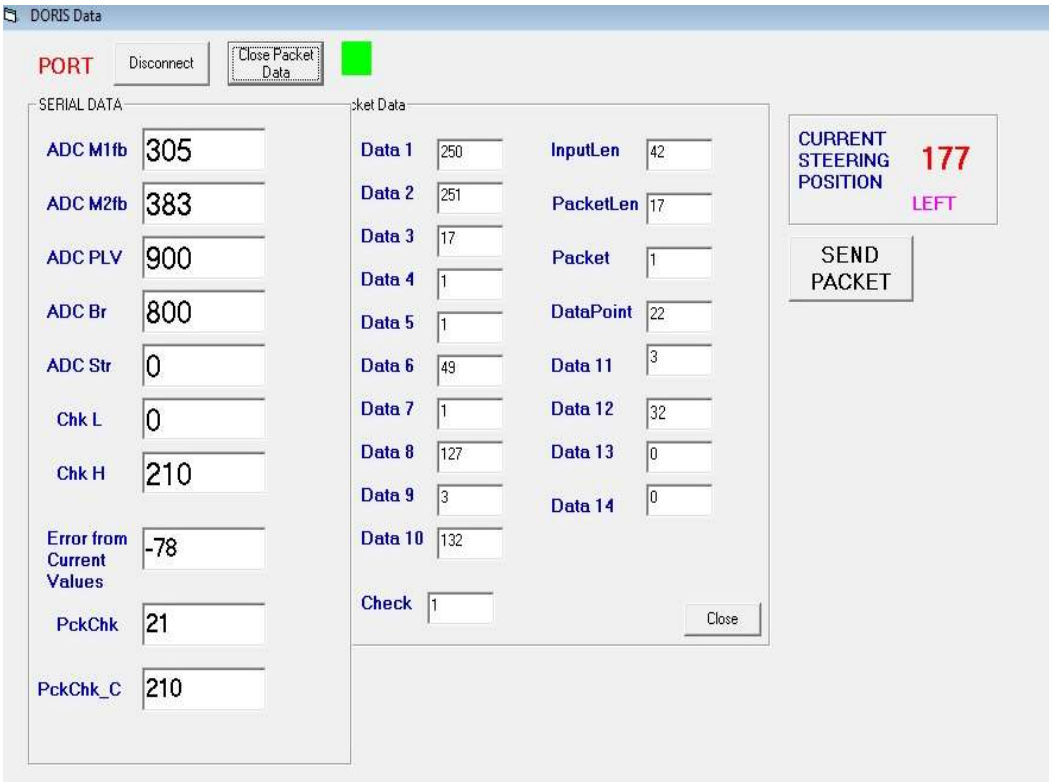


Figure 4.12 Graphical Display Interface

## 4.5 Dead-Beat Controller

In digital control systems, the controller is realized by an intelligent device, normally by a microcontroller. The task of the microcontroller is to realize the controller algorithm and to handle the signals used for operation of the controller (filtering, ADC (analogue to digital converter), signal conditioning interfaces).

As the controller algorithm is realised by software, there is a possibility to apply different special, more sophisticated control algorithms. One of these algorithms ensures the accurate settling of the output signal during a finite, small number of the sampling periods. In literature, this algorithm is referred as the dead-beat controller algorithm. To understand the essence of the method we consider a stable plant without dead time. The reference signal is a unit step. [Hetthéssy, J. 2004].

In the sequel a design procedure is derived in three steps. This solution satisfies the practical requirements as well. In the first step, the controller is designed for the fastest behaviour when the output signal is settled in one sampling step. It will be seen that with this design with typical sampling times, the control signal could be extremely high, moreover in most cases oscillations occur between the sampling points. In the second step the design is modified to avoid inter sampling oscillations. It will be shown that cancellation of zeros outside of the unit circle is the reason for oscillations. Zeros of the plant pulse transfer function is separated for cancellable and non-cancellable ones and only the cancellable zeros will appear in the controller algorithm. This modification of the algorithm increases the settling time. If the control signal is still higher than allowed, the solution can be refined using a design polynomial. In this case the settling time is increased further (but still remains finite). The design is executed in the 'z' operator domain as shown in figure 4.13. Interesting feature of the design method is the fact that it removes undesirable time domain properties (oscillations, too high values of the control signal) by considerations done in the 'z' operator domain. The basic task is the design of a sampled data controller [Hetthéssy, J. 2004].

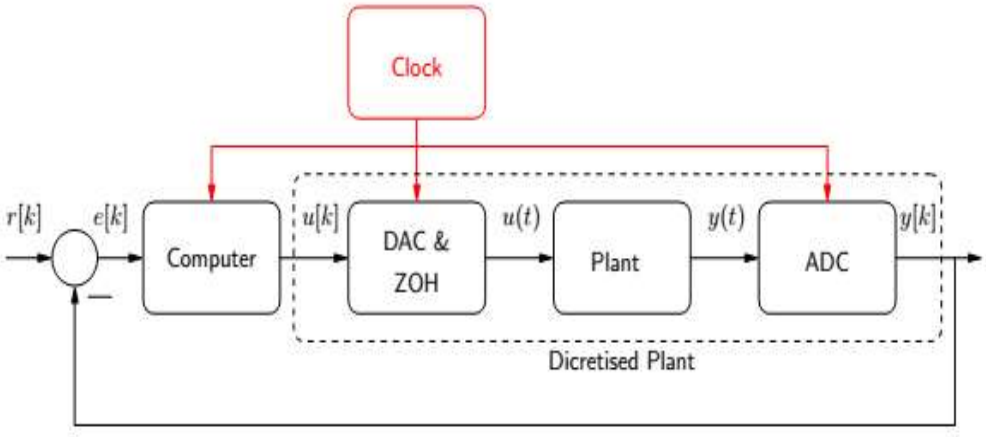


Figure 4.13 Digital Time Discrete Controller

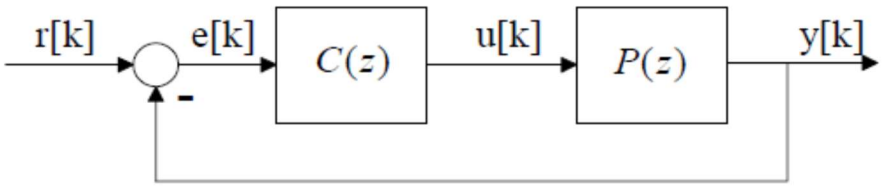


Figure 4.14 Dead Beat Controller

To get the transfer functions for figure 4.14, let us analyse realisation aspects. The pulse transfer function of the controller is:

$$C(z) = \frac{b_3\, z^3 + b_2\, z^2 + b_1\, z + b_0}{z^3 + az^2 + a_1\, z + a_0} \tag{4.5}$$

The z-transfer function is a third order transfer function and the Dead Beat controller will reach final state in four sample intervals. The coefficients $b_3$ , $b_2$ , $b_1$ , $b_0$ , $a_0$ , $a_1$ and $a_2$ are found from the plant parameters. In order to use the shift operator $z^{-1}$ let us divide both the numerator and the denominator by third power of z

$$C(z) = \frac{b_3 + b_2\, z^{-1} + b_1\, z^{-2} + b_0\, z^{-3}}{1 + a_2\, z^{-1} + a_1\, z^{-2} + a_0\, z^{-3}} \tag{4.6}$$

As

$$C(z) = \frac{Z\{u[k]\}}{Z\{e[k]\}}$$

With cross-multiplication we get

$$u[k] + a_2\, u[k-1] + a_1\, u[k-2] + a_0\, u = b_3\, e[k] + b_2\, e[k-1] + b_1 e[k-2] + b_0 e[k-3]$$

$$u[k] = b_3\, e[k] + b_2\, e[k-1] + b_1 e[k-2] + b_0 e[k-3] - a_2\, u[k-1] - a_1\, u[k-2] - a_0\, u[k-3] \tag{4.7}$$

### 4.5.1 Dead- Beat Controller Design

Dead-Beat Control is characterized by establishing a zero tracking error in a finite number of discrete steps [Barber, R., et al., 2013]. The condition for this is that the resulting transfer function of the closed loop between the output signal and the input signal (supposed to be a sampled unit step) be a one-step shift, namely the shift operator $z^{-1}$

$$T(z) = \frac{C(z)P(z)}{1 + C(z)P(z)} = Z^{-1} \tag{4.8}$$

Hence the controller pulse transfer function is expressed as

$$C(z) = \frac{T(z)}{P(z)\big(1 - T(z)\big)} = \frac{1}{P(z)(z-1)} \tag{4.9}$$

Express P(z) as a ratio of two polynomials:

$$P(z) = \frac{B(z)}{A(z)}$$

Then

$$\mathrm{C(z)} = \frac{\mathrm{A(z)}}{\mathrm{B(z)(z-1)}} \tag{4.10}$$

The discrete transfer function of the DC Motor in z domain is:

$$\mathrm{C(z)} = \frac{0.06\mathrm{z} - 0.06}{\mathrm{z}^2 - 1.35\,\mathrm{z} + 0.3}$$

In order to use this controller, several points must be:

1. Since multiple poles are obtained in closed loop on the origin, this controller is very sensitive to variations in the system parameters.

2. Although this controller is designed to obtain a zero tracking error response in a determined number of samples, lower transient responses can be displayed depending on the input type. The optimal control will work appropriately only for the input type for which it has been designed.

3. Initially, the sampling period does not affect the calculation of the controller terms. However, variations in the sampling period can cause dynamic changes in the system and even the instability.

4. If a dead-beat response has only been requested in the sampling instants, oscillations may occur even if the control system is internally stable considered [Barber, R., et al., 2013].

## 4.6 Experimental results

The experimental results of the proposed position controlled system are compared with simulated results in figure 4.15, in order to confirm the satisfied results thus obtained. It can observe that the response to the input signal is fast with small error and damped oscillation.

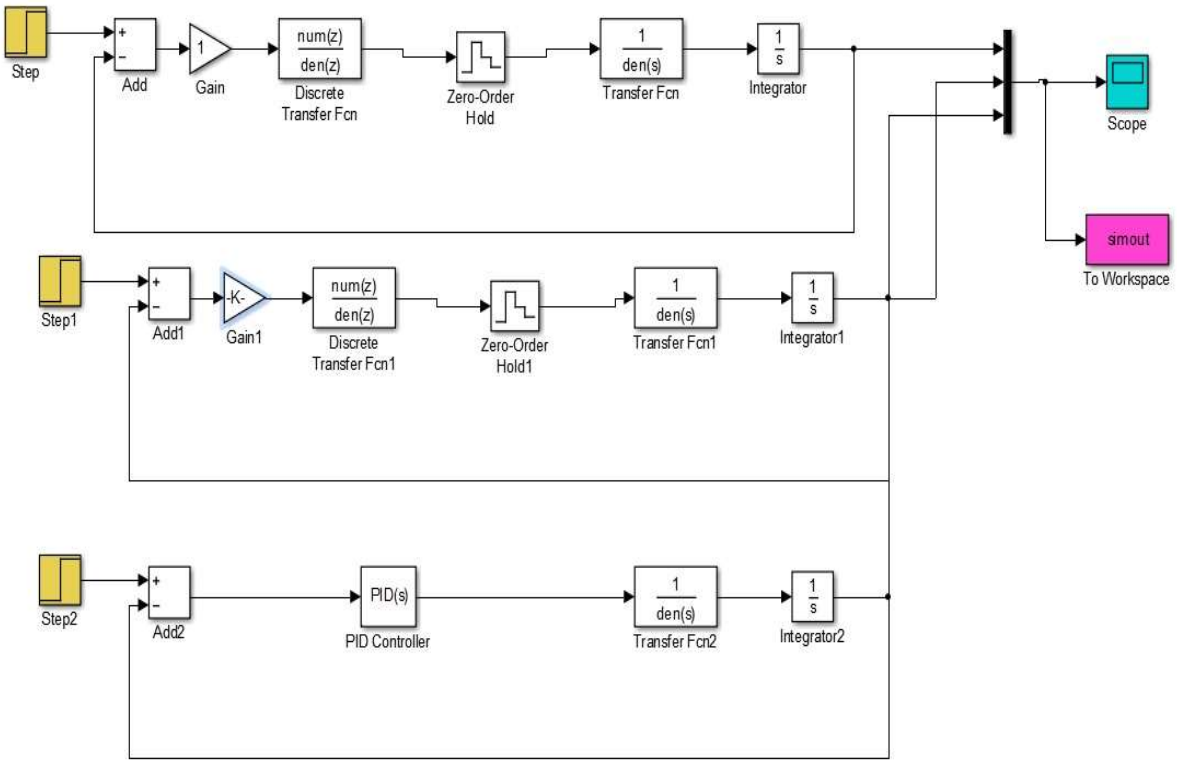


Figure 4.15 Simulink of Dead-Beat Controller

The overshoot of the proposed position controlled system using PID controller is smaller than the overshoot of a system without PID controller as shown in figure 4.16. Using PID parameters of kp = 0.055, kd = 0.015 and ki = 0, gives a good signal as shown in figure 4.17. A proportional Dead Beat control is a combination of a Dead Beat controller with proportional action.The only design parameter in Dead Beat controller is the sampling period that influence the magnitude of the contrl signal.when dead beat controller is used ,the magnitude of the control signal increases as the sampling period decreases,other wise ,a larger overshoot occurs .Thus,it is importent to choose the sampling period carefully when using Dead Beat control. .From Shannon's Sampling Theorem, the sampling frequency should be at least twice the bandwidth of the closed-loop system and based on this theorem the sampling time is 0.01 sec. besides increasing the sampling period,adding an extend proportional part to the Dead Beat controller reduces the overshoot. The proportional gain calculated expermintally on the plant.

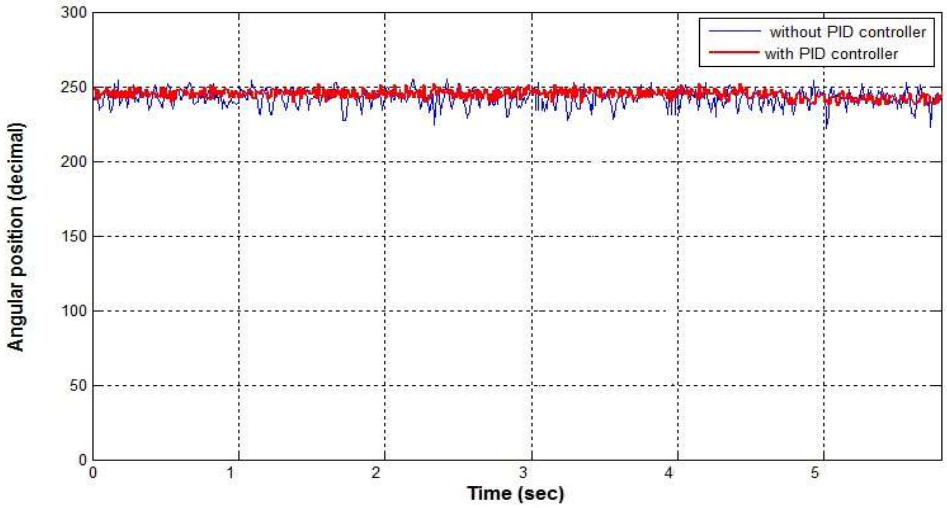


Figure 4.16 The System with and without PID

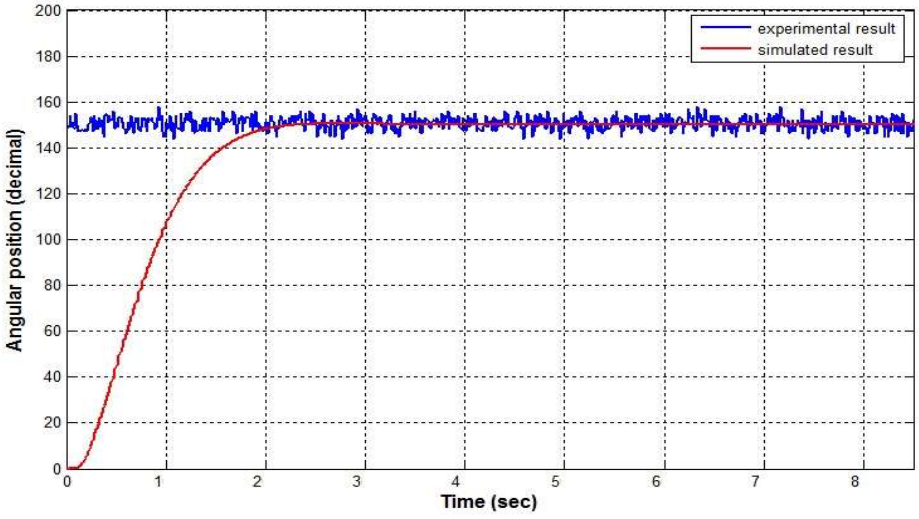


Figure 4.17 Angular Position with kp = 0.055, kd = 0.015, ki = 0

From the result shown in figure 4.17, the PID controller gives a good steady state error and small overshoot comparing with the system without PID controller. by using PID parameters of kp = 0.06, kd = 0.02 and ki = 0.02 this will not give a good result with a big error in the beginning as shown in figure 4.19 and by connecting the DC Motor to the pump shaft the resistance from the pump swash plate gives an error in the beginning for some millisecond and then become constant as shown in figure 4.20. Several DC Motor angular positions is

shown in figure 4.18 and the best PID parameters choice that was achieved experimentally and compared in Simulink are seen in figure 4.21. Figure 4.22 shows the angular position using Dead Beat controller while figure 4.23 shows the angular position using P-Dead Beat controller where this signal is better than using just Dead Beat controller, figure 4.24 summarize the PID, Dead Beat and P-Dead Beat controller and the relation between these controllers are shown in table 4.1. Figure 4.25 shows the PID controller with several PID parameters. From the table down, we can see that the rising time for P-Dead Beat and Dead Beat controllers are faster than the PID controller but the settling time and overshoot for P-Dead Beat controller is better; overshoot in PID controller is smaller than the others but contains more steady state error because the integral part in the simulated model is nearly zero (PD). The sensor noise (sigma) is 0.521 degree as shown and calculated from figure 4.26 and the ADC sampling time for ATmega16 microcontroller is 1500 samples per second. The position set point adjusted mechanically via several adjusted screws between the Motor body and the sensor. The time constant measured in the experiment is 63 ms, which is around 68% from the rising time.

Table 4.1 Controllers specifications

| | PID | Dead Beat | P Dead Beat |
|---|---|---|---|
| Steady state error | 5% | 2% | 2% |
| Rising time | 0.1sec | 0.06 sec | 0.08 sec |
| Settling time | 0.15sec | 0.35 sec | 0.2sec |
| Over shoot | 5% | 30% | 10% |

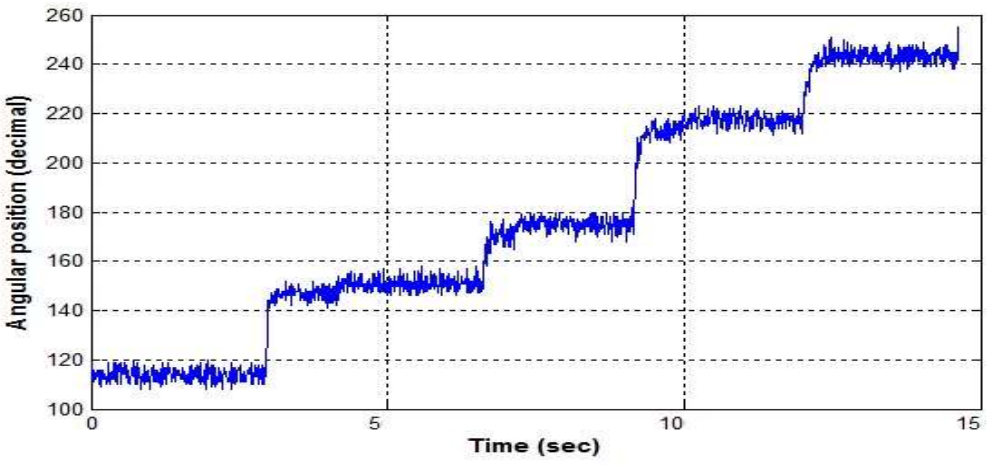


Figure 4.18 Angular Position with several Input Signals

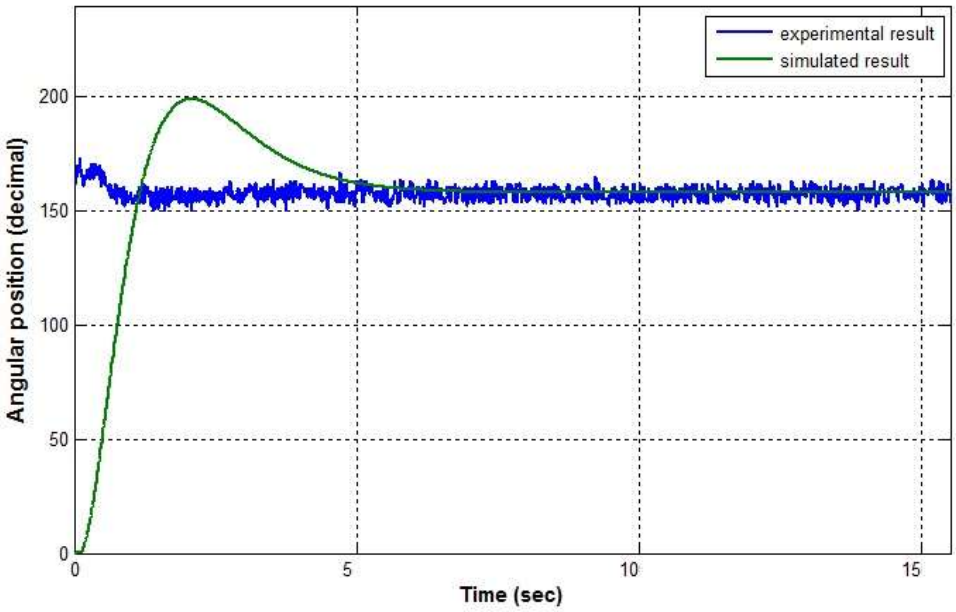


Figure 4.19 Angular position with kp = 0.06, kd = 0.02, ki = 0.02

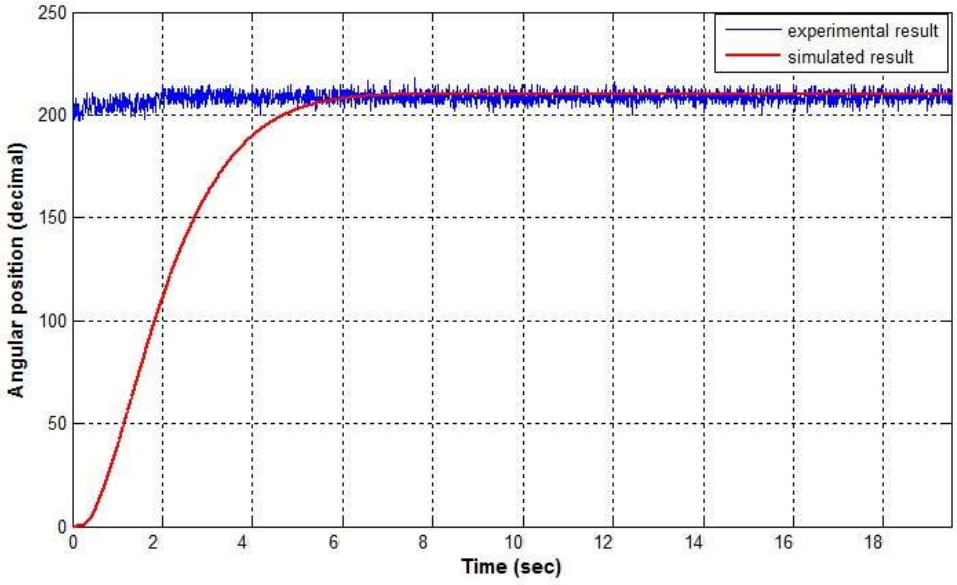


Figure 4.20 Angular Position when connected to the Hydraulic Pump

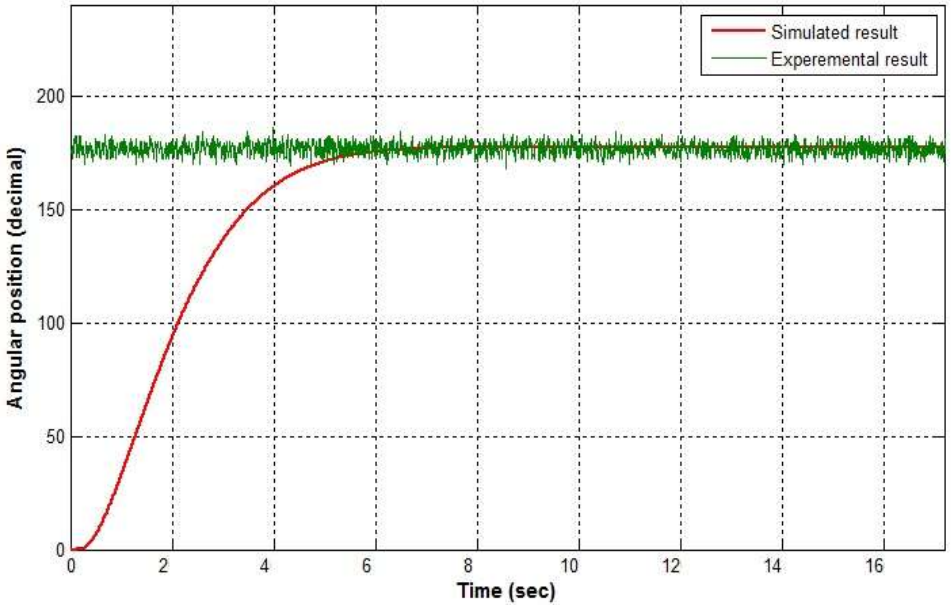


Figure 4.21Angular Position with kp = 0.05, kd = 0.01, ki = 0

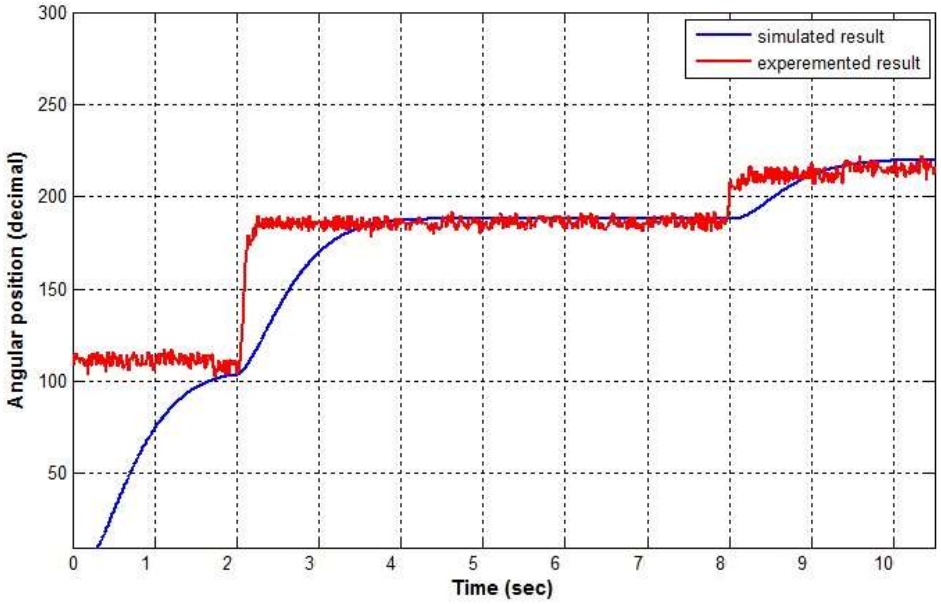


Figure 4.22 Dead beat controller response to step input

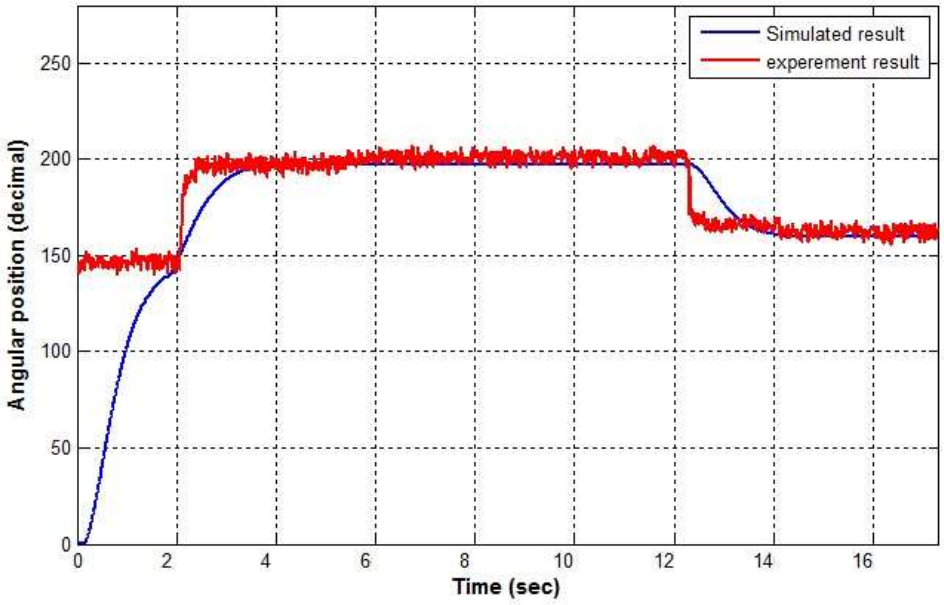


Figure 4.23 P Dead beat controller response to step input

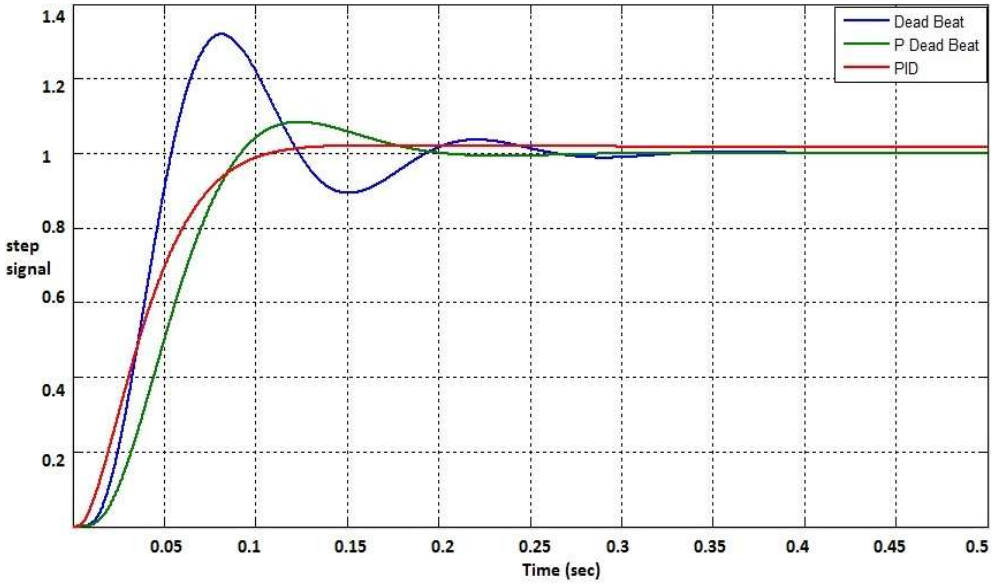


Figure 4.24 Simulated Controllers Response to Step Input

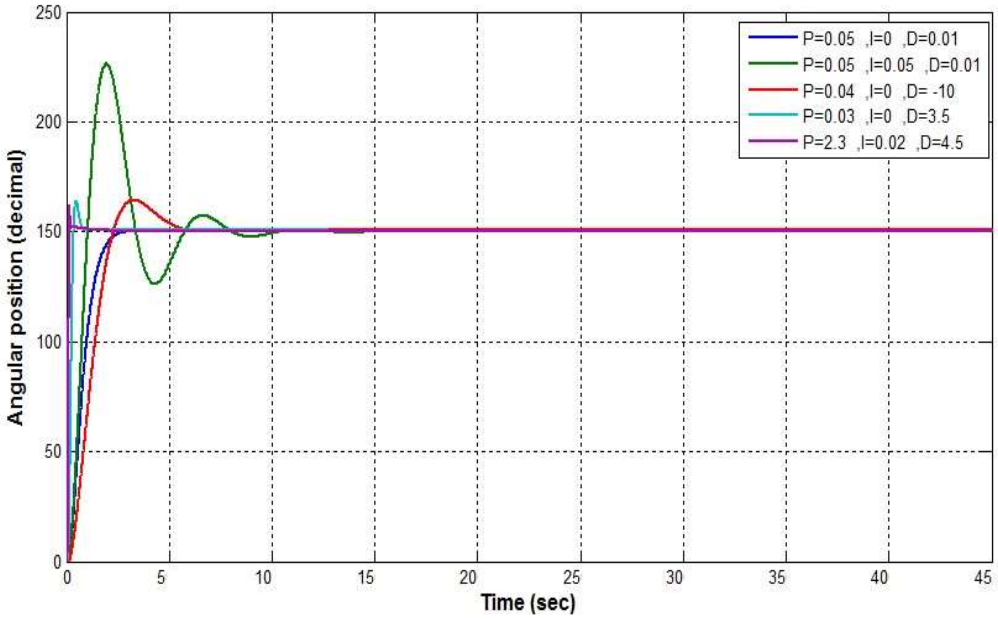


Figure 4.25 Several simulated PID parameters

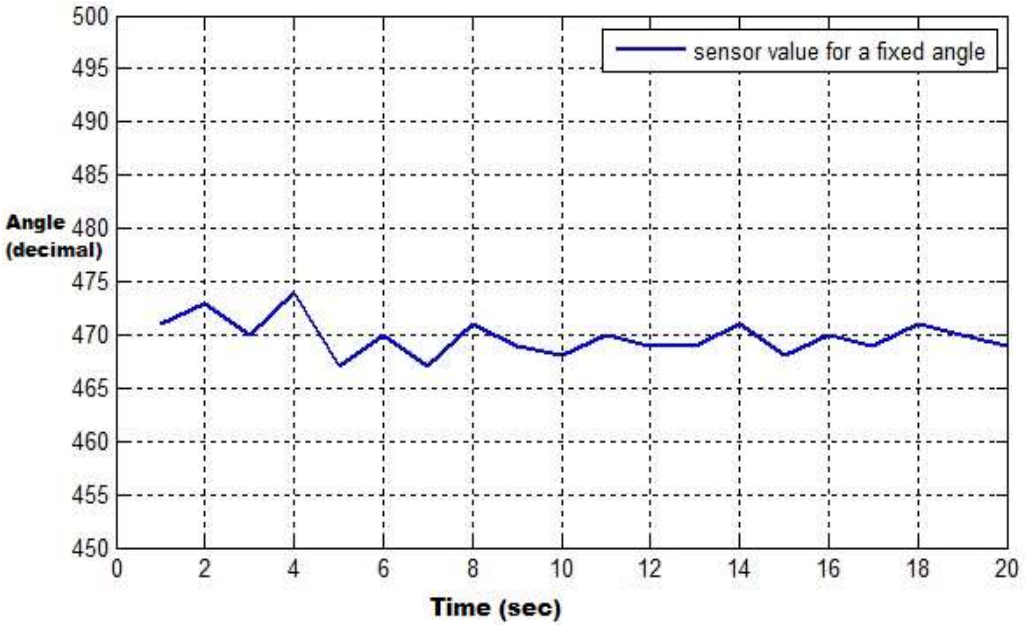


Figure 4.26 Sensor noise

# Chapter 5

# Steering Control System

Controller design for any system needs some knowledge about the system. Usually this involves a mathematical description of the relation among inputs to the process, its state variables, and its Output. This description is called the model of the system. The model can be represented as a set of transfer functions for linear time invariant systems or other relationships for non-linear or time variant systems. Modelling of complex systems may be a very difficult task.

In a complex system such as a multiple input and multiple outputs system inaccurate models can lead to unstable systems, or unsuitable system performance. Fuzzy Logic Control (FLC) is an effective alternative approach for systems, which are difficult to model. The FLC uses the qualitative aspects of the human decision process to construct the control algorithm. This can lead to a robust controller design [Shukla, S., et al., 2010]. To steer the Vehicle left and right one side should have different speed than the other side for that a steering control system using intelligent fuzzy logic Controller was designed and developed.

When considering the problem of accurate path following, skid steer autonomous amphibious robots are difficult to model; in fact, the wheels of the autonomous amphibious robots need to skid laterally in order to follow a curved path. Moreover, the Instantaneous Center of Rotation (ICR) of skid steer autonomous amphibious robots may move out of robot wheelbase, causing loss of motion stability. A survey of literature reveals that although a large amount of research has been performed on Ackermann-steered and differential drive WMRs, in terms of mathematical Modelling and control, a few works exist on 8-wheel differentially skid steer autonomous amphibious robots. Several approaches have been developed to solve this problem through direct control of the robot's dynamics [Nazari, V., et al., 2008].

## 5.1 Analysis of Skid Steering

Different tire speed produces skid steering, as shown in figure 5.1. As the speed of the tire on the right side is greater than the left side, the vehicle steers to the left; tire on the right side needs traction in the driving direction during steering process, and the tires on the left side have a braking effect in the steering range. Thereby, it forms a steering torque, which

balances the resistance torque generated between the tire and the ground in constant speed motion state. In order to analyse the speed, force, and torque of the driving wheel in the steering process, the following assumptions are made [Ren, F., et al., 2014]:

- the vehicle is travelling on a uniform flat ground;
- the steering process is at constant speed;
- ignore the centrifugal force;
- the load of the tires on both sides of the vehicle is the same;
- ground pressure evenly distributes in the length of the drive tires touching the ground;
- the driving resistance of both sides of the driving wheel is the same;
- centre of gravity of the vehicle is located at the intersection of the symmetrical axis. The travelling speed of the left is $v_l$, the travelling speed of the right is $v_r$, and the vehicle will do the rotary movement around the steering centre M. In reality most of this assumption are not applied, the vehicle travels on un uniform flat ground, the load on each tire is not the same, the centrifugal force should not be ignored, centre of gravity does not located on the intersection of the symmetrical.

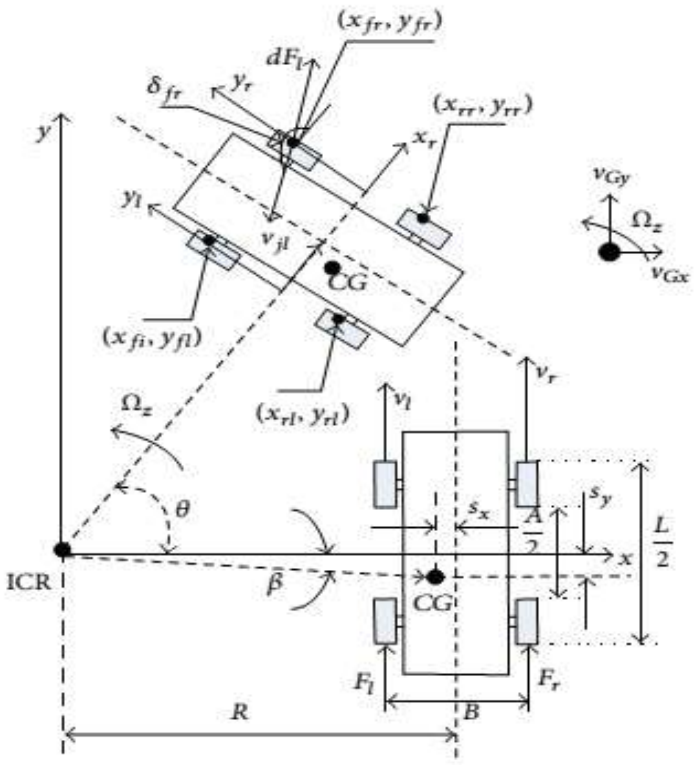


Figure 5.1.Skid Steer Dynamic

The kinematics equation in the process of steering is

$$q = S(q)v + A(q)v_y \tag{5.1}$$

Where

$q = [x_c \;\; y_c \;\; \theta]^T$ , $S(q) = \begin{bmatrix} \cos\theta & 0 \\ \sin\theta & 0 \\ 0 & 1 \end{bmatrix}$, $A(q) = [-\sin\theta \quad \cos\theta \quad 0]^T$ , $v = [v_x \quad \omega]^T$

, $q$ is the location of the vehicle center of gravity, $x_c$ and $y_c$ are the location coordinates of the vehicle center of gravity, $\theta$ is the angle between the vehicle traveling direction and the $x$-axis, $v_x$ is the longitudinal velocity of the vehicle center of gravity, and $v_y$ is the lateral velocity of the vehicle center of gravity.

When the vehicle turns in a small steering radius, the left side tires slip in the opposite direction and the right side tires slip in the same direction. The measure is slip rate. Slip rate can be expressed as:

$$\rho = \frac{\mathrm{v_t} - \mathrm{v}}{\mathrm{v_t}} \tag{5.2}$$

Where $\rho$ is slip rate, $v_t$ is theoretical speed of the vehicle and $v$ is actual speed of the vehicle. Considering the vehicle will slip during the steering process, the relations between slip rate and vehicle steering speed can be deduced. Considering the slipping of the tire, the steering radius $R$ and the rotation angular velocity Ω are derived as follows. When the longitudinal slip ratios $\rho_o$and $\rho_i$ on both sides of the tires are taken into account in the model, the rotation angular velocity Ω are given by:

$$\Omega = \frac{r\omega_o(1-\rho_o) + r\omega_i(1-\rho_i)}{2R}$$

The change of vehicle tire slip rate can be qualitatively analyzed by (5.3) when the vehicle speed is changing.

$$\begin{bmatrix} v_{Gx} \\ v_{Gy} \\ \dot{\Omega} \end{bmatrix} = \begin{bmatrix} \frac{r}{2}(1-\rho_l) & \frac{r}{2}(1-\rho_r) \\ \frac{rs_y}{B}(1-\rho_l) & -\frac{rs_y}{B}(1-\rho_r) \\ \frac{r}{B}(1-\rho_l) & -\frac{r}{B}(1-\rho_r) \end{bmatrix} \begin{bmatrix} \omega_l \\ \omega_r \end{bmatrix} \tag{5.3}$$

Where $v_{Gx}$ is the longitudinal velocity of vehicle gravity center, $v_{Gy}$ is the lateral velocity of vehicle gravity center, $\rho_l$ is the slip rate of left side tires, $\rho_r$ is the slip rate of right side tires, r is tire radius, $s_y$ is offset of vehicle gravity center , $\omega_l$ is rotational speed of left side tires, and $\omega_r$ is rotational speed of right side tires. The kinetic equations in stable steering process are as follows.

To analyze the dynamics of the vehicle in steering process, the relationship between shear stress and shear deformation should be known as shown in

$$\tau = \delta\mu\left(1 - e^{-j/k}\right) \tag{5.4}$$

Take an infinitesimal element of tire grounding area for analysis; the traction suffered by an infinitesimal element of the left and right sides of the tire is shown in

$$dF_r = \tau_r dA = \delta_r\mu\left(1 - e^{-j_r/k}\right) dA \tag{5.5}$$

$$dF_l = \tau_l dA = \delta_l\mu\left(1 - e^{-j_r/k}\right) dA \tag{5.6}$$

The longitudinal force of left and right tires shown in (5.7, 5.8) can be obtained by integrating the tire grounding area

$$F_{yr} = -\int_{\frac{A}{2}}^{\frac{L}{2}}\int_{-\frac{b}{2}}^{\frac{b}{2}}\delta_l\mu\left(1-e^{-\frac{j_r}{k}}\right)\sin\lambda_{fr}dx_{fr}dy_{fr} - \int_{-\frac{A}{2}}^{-\frac{L}{2}}\int_{-\frac{b}{2}}^{\frac{b}{2}}\delta_r\mu\left(1-e^{-\frac{j_r}{k}}\right)\sin\lambda_{rr}dx_{rr}dy_{rr} \quad (5.7)$$

$$F_{yl} = -\int_{\frac{A}{2}}^{\frac{L}{2}}\int_{-\frac{b}{2}}^{\frac{b}{2}}\delta_{fl}\mu\left(1-e^{-\frac{j_l}{k}}\right)\sin\lambda_{fl}dx_{fl}dy_{fl} - \int_{-\frac{A}{2}}^{-\frac{L}{2}}\int_{-\frac{b}{2}}^{\frac{b}{2}}\delta_{rl}\mu\left(1-e^{-\frac{j_l}{k}}\right)\sin\lambda_{rl}dx_{rl}dy_{rl} \quad (5.8)$$

The steering torque in steering process shown in (5.9, 5.10) can be obtained by the left and right sides of the resistance taking the vehicle center for moment:

$$M_r = \frac{B}{2}F_{yr} \quad (5.9)$$

$$M_l = \frac{B}{2}F_{yl} \quad (5.10)$$

The main research of vehicle with the ground dynamics is the interaction between the tires and the ground. As the skid steer amphibious vehicle is equipped with rubber tires, the magic formula uses to establish the dynamics model of the vehicle with the ground [Maclaurin, B. 2011]. Magic formula is a semi empirical formula. It deduces from the physical prototypes of the tire and can accurately describe the mechanical characteristics of the tire. It has been adopted by the majority of scholars who studied tire and ground distraction, and the model has been applied to the multi-body dynamics simulation software.

The basic expression forms of magic formula are as follows:

$$y(x) = Dsin\{C\ arctan[Bx - E(Bx - arctan(Bx))]\} \quad (5.11)$$

$$C = 1 \pm \left(1 - \frac{2}{\pi}arcsin\frac{y_a}{D}\right)$$

$$B = \frac{BCD}{CD}$$

$$E = \frac{Bx_p - tan(\pi/2C)}{Bx_p - arctan(B_{xm})}$$

Where y is the side force, longitudinal force, or self-aligning and x is longitudinal slip. D is the peak value, C is termed the shape factor, BCD is the longitudinal or lateral slip stiffness, $xm$ is the value of x at the peak value of y and E is termed the curvature factor.

## 5.2 Fuzzy Logic Controller Description

Fuzzy logic control is a control algorithm based on a linguistic control strategy, which is derived from expert knowledge. Fuzzy logic control doesn't need any difficult mathematical

calculation like the others control system like PID and Dead Beat control systems. While the other control systems use difficult mathematical calculation to simulate the expert knowledge. Although it doesn't need any difficult mathematical calculation, but it can give good performance in a control system. Thus, it can be one of the best available answers today for a broad class of challenging controls problems. A fuzzy logic control usually consists of the following as shown in figure 5.2. [Jamshidi, M., et al., 1993]:

1. Fuzzification: This process converts or transforms the measured inputs called crisp values into the fuzzy linguistic values used by the fuzzy reasoning mechanism.

2. Knowledge Base: A collection of the expert control rules (knowledge) needed to achieve the control goal.

3. Fuzzy interface engine: This process will perform fuzzy logic operations and produce the control action according to the fuzzy inputs.

4. Defuzzification unit: This process converts the result of fuzzy reasoning mechanism into the required crisp value.

### 5.2.1 Differences between Probability and Fuzzy Logic

The lack of a probability distribution or the difficulty of obtaining one, or because only the opinion of an expert expressed in ambiguous linguistic terms may be available, are often quote as reasons to select Fuzzy logic over stochastic methods, finding a suitable probability distribution can be an accurate, time consuming and difficult task. This difficulty has led some researchers to conclude that Fuzzy logic might then be better than probability theory, as Fuzzy logic membership functions can be drawn from a little information. This is the reason for choosing a Fuzzy logic over a probability (stochastic) distribution, because no reason is given why or how a Fuzzy logic distribution could be estimated more easily than a probability (stochastic) distribution. [Riedewald, F. 2011].

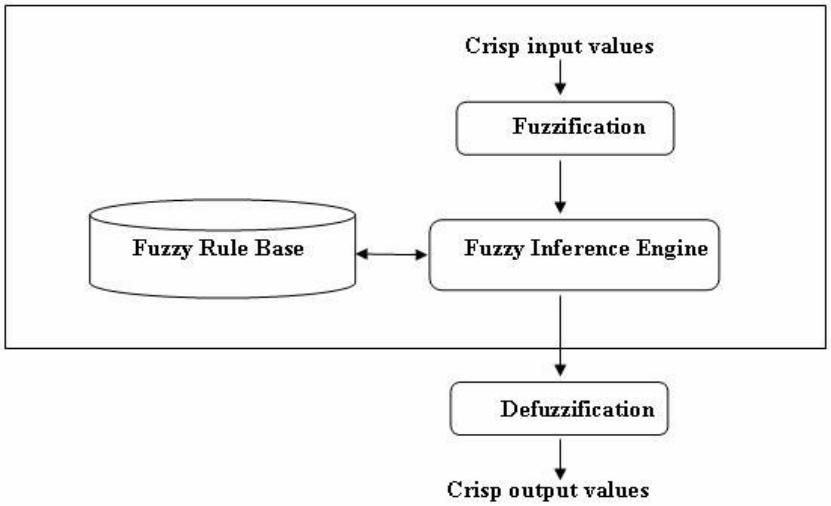


Figure 5.2 Fuzzy Logic Controller

## 5.3 Fuzzy Steering Strategy Design

The intelligent Fuzzy logic steering controller is shown in figure 5.3. There are two inputs, including the Gas or Break Pedal as input 1 according to the desired driving mode either forward by using the Gas Pedal or backward by using the Brake Pedal and the steering wheel angle as input 2. The Fuzzy logic steering controller can handle the two DC motors position to produce desired Hydraulic pump fluid speed through the swash plate valve position. Herein, the controller is only designed to achieve the reference DC motor position, three driving modes were designed; stop mode when the pedal is in the zero position, middle speed when the pedal is in the middle position and full speed when the pedal is in the full position. These three modes are repeated also for driving backward by using the brake pedal and the steering wheel was divided into 5 positions; two for right turning, middle and full and two for left turning, middle and full. The steering wheel angle is between 90 degrees and –90 degrees, i.e., the driver does not really turn, therefore, the stop mode is excited and the motor stay in its position according to the pedal signal. Secondly, if the assist mode is excited, the assist motor position can be obtained through an assist fuzzy inference mechanism. Larger steering wheel angle is referred to larger Vehicle turning needed. If the steering wheel is in the zero angle, the vehicle will move forward or backward, if the steering wheel is turned right to the middle and gas or brake pedal in the middle, the right DC motor should stay in the middle and the left DC motor should move backward to the zero position according to fuzzy rule. DC Motor's position is controlled by PID Controller or Dead Beat controller as shown in figure 5.3.

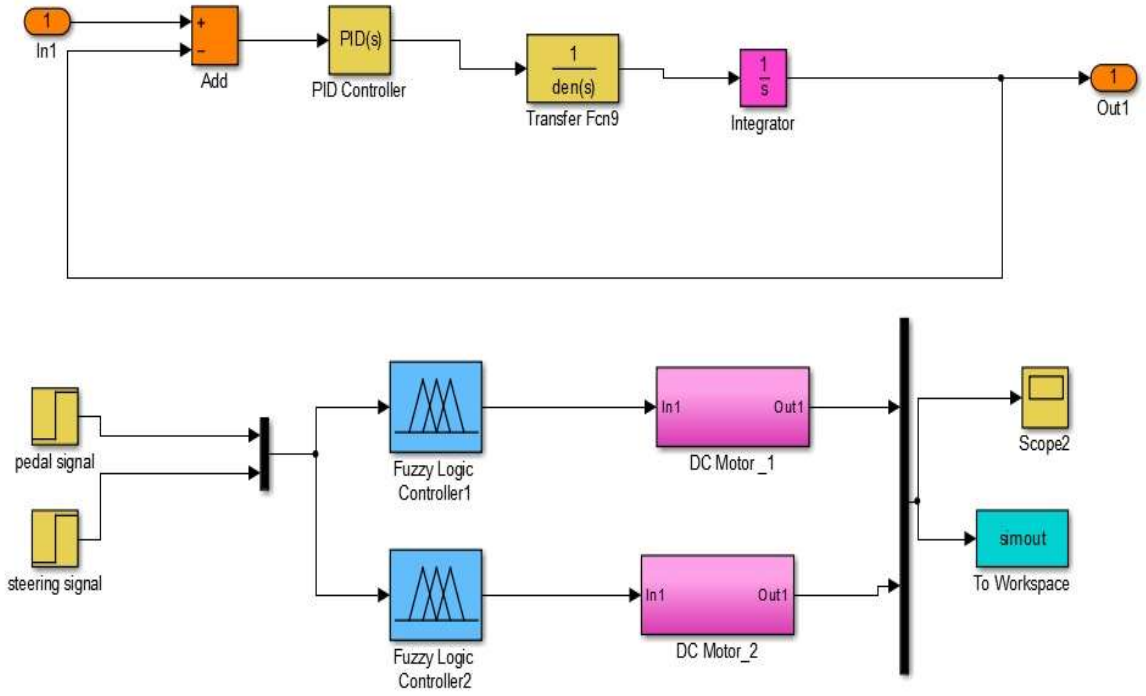


Figure 5.3 Simulation diagram of Fuzzy Logic Controller

Figure 5.4 shows the flow chart of the Fuzzy logic controller; the sequence of the Fuzzy logic controller starts by reading the signal from Gas Pedal which has been set up to be for forward driving mode. If there is a signal from the Gas Pedal, the forward mode will start, if there is a signal from the Brake Pedal the backward mode will start and if there is no signal from both Pedals, the two DC Motors are stopped. By adding the steer signal the controller checks if the steer is right or left.

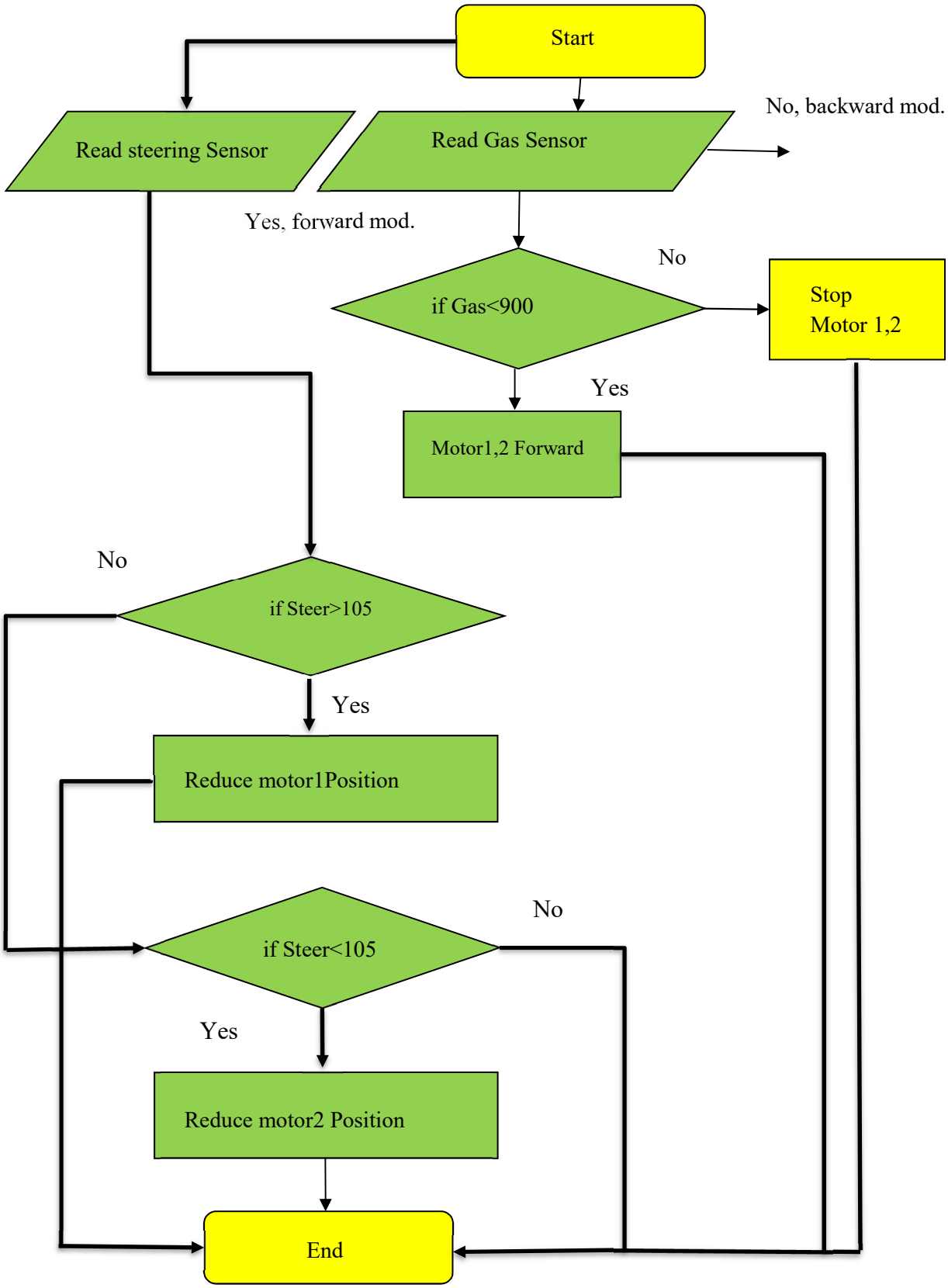


Figure 5.4 Steering Control System Flow Chart

## 5.4 Fuzzy Logic Inference System Design

Basically, a fuzzy logic system consists of one or more inputs and a single output. Each rule describes a connection between the input and the output. Through the fuzzy inference engine, each rule maps the input fuzzy sets to an output fuzzy set. Finally, the output fuzzy set is translated to a crisp value by the defuzzification process. [Chang, S.H., et al., 2009]. The steering wheel angle and the Gas Pedal position are the inputs and the DC motor position is the output of the fuzzy inference mechanism. Input from Pedal can be divided to 3 levels and input from steering divided into 5 levels; output variables can be divided into 3 levels. Input 1 is defined as full, middle and zero and for output, full_r, middle_r and zero that make vehicle drives forwards, input from steering defined as zero, full_l, full_r, middle_l, and middle_r. In order to improve defuzzification speed, Trimf (Triangular Membership Function) is chosen as membership function and the weight is equal to one [Zhang, J., et al., 2007]. Figures 5.5 a, b, c show the membership functions of steering and Gas input and DC Motor output for forward driving and Figures 5.6 a, b, c show the membership functions of steering and Brake input and DC Motor output for backward driving. Table 5.1 shows the assist fuzzy rule base. Fifteen fuzzy rules for each motor achieved the control goal represented as

Rules for Motor_1

Rule 1: IF (Gas is M) AND (Steering is ZE) THEN (Motor_1 is M_r)

Rule 15: IF (Gas is F) AND (Steering is M_L) THEN (Motor_1 is ZE)

Rules for Motor_2

Rule 1: IF (Gas is M) AND (Steering is ZE) THEN (Motor_1 is M_r).

Rule 15: IF (Gas is F) AND (Steering is M_L) THEN (Motor_1 is F_r).

Where:

Middle right = M_r, Middle left = M_L, Full Left = F_L.

Full right = F_r, F = Full, M = Middle, ZE = Zero.

Table 5.1 Fuzzy rule for forward driving

| Gas | Steering | Mot_1 | Mot_2 |
|---|---|---|---|
| Middle | Zero | Middle_r | Middle_r |
| Middle | Middle_r | Middle_r | Zero |
| Middle | Full_r | Middle_r | Zero |
| Full | Zero | Full_r | Full_r |
| Full | Middle_r | Full_r | Zero |
| Full | Full_r | Full_r | Zero |
| Zero | Zero | Zero | Zero |
| Zero | Middle_r | Zero | Zero |
| Zero | Full_r | Zero | Zero |
| Zero | Middle_l | Zero | Zero |
| Zero | Full_l | Zero | Zero |
| Middle | Middle_l | Zero | Middle_r |
| Middle | Full_l | Zero | Middle_r |
| Full | Full_l | Zero | Full_r |
| Full | Middle_l | Zero | Full_r |

Table 5.2 shows the assist fuzzy rule base for backward driving. Fifteen fuzzy rules for each motor achieved the control goal represented as

Rules for Motor_1

Rule 1: IF (Break is M) AND (Steering is ZE) THEN (Motor_1 is M_r).

Rule 15: IF (Break is F) AND (Steering is M_L) THEN (Motor_1 is ZE)

Rules for Motor_2

Rule 1: IF (G Break is M) AND (Steering is ZE) THEN (Motor_1 is M_r).

Rule 15: IF (Break is F) AND (Steering is M_L) THEN (Motor_1 is F_r).

Where:

Middle right = M_r, Middle left = M_L, Full Left = F_L

Full right = F_r, F = Full, M = Middle, ZE = Zero

Table 5.2 Fuzzy rule for backward driving

| Break | Steering | Mot_1 | Mot_2 |
|---|---|---|---|
| Middle | Zero | Middle_r | Middle_r |
| Middle | Middle_r | Middle_r | Zero |
| Middle | Full_r | Middle_r | Zero |
| Full | Zero | Full_r | Full_r |
| Full | Middle_r | Full_r | Zero |
| Full | Full_r | Full_r | Zero |
| Zero | Zero | Zero | Zero |
| Zero | Middle_r | Zero | Zero |
| Zero | Full_r | Zero | Zero |
| Zero | Middle_l | Zero | Zero |
| Zero | Full_l | Zero | Zero |
| Middle | Middle_l | Zero | Middle_r |
| Middle | Full_l | Zero | Middle_r |
| Full | Full_l | Zero | Full_r |
| Full | Middle_l | Zero | Full_r |

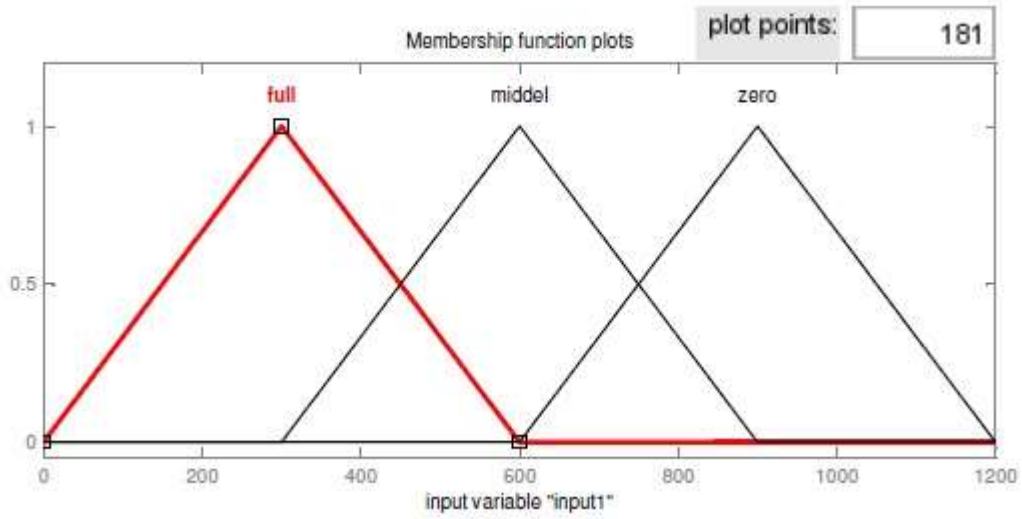


Figure 5.5a Membership function of gas pedal

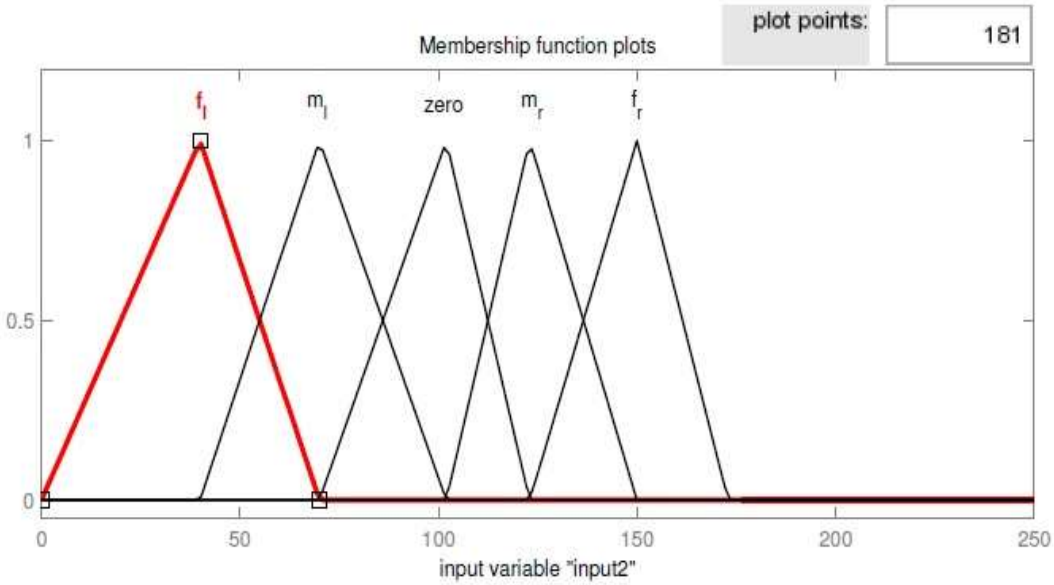


Figure 5.5b Membership function of steering wheel

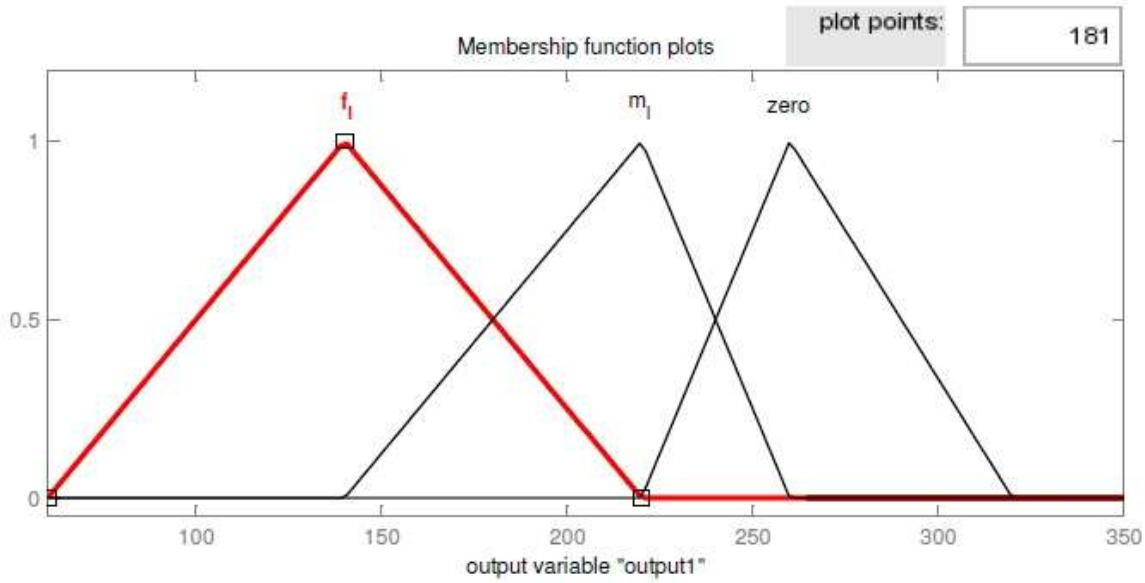


Figure 5.5c Membership function of DC Motor position

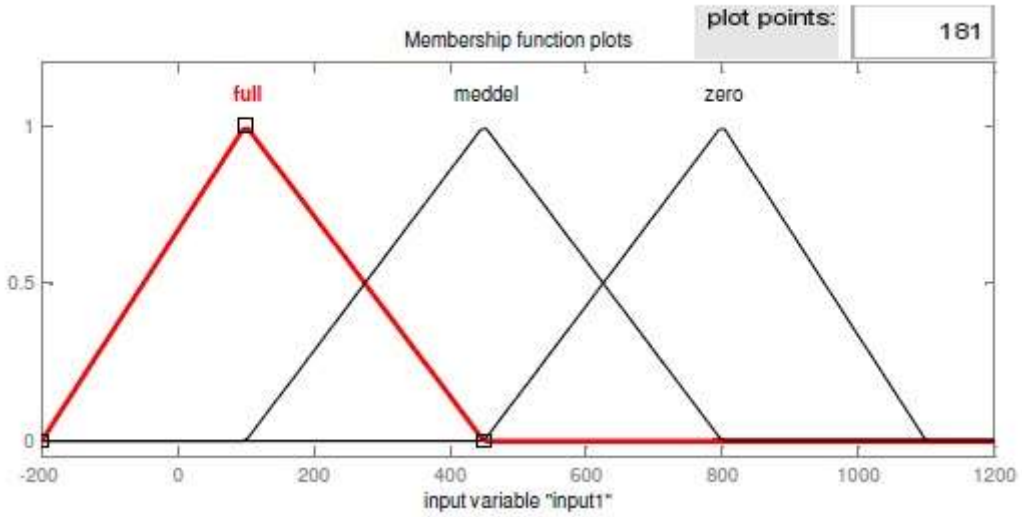


Figure 5.6a Membership function of brake pedal

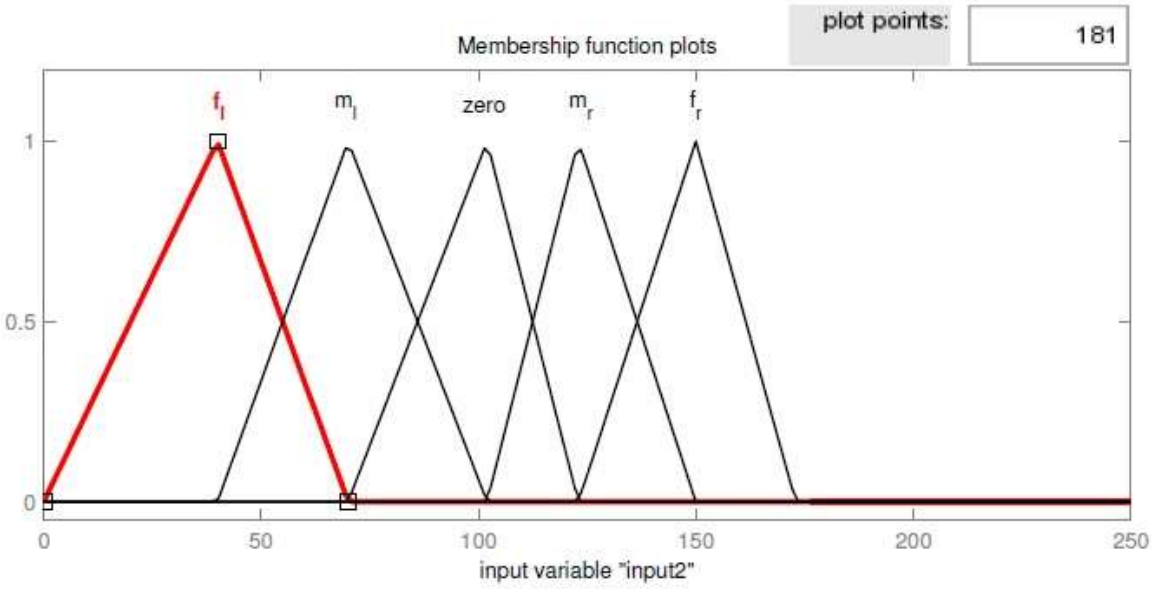


Figure 5.6b Membership function of steering wheel

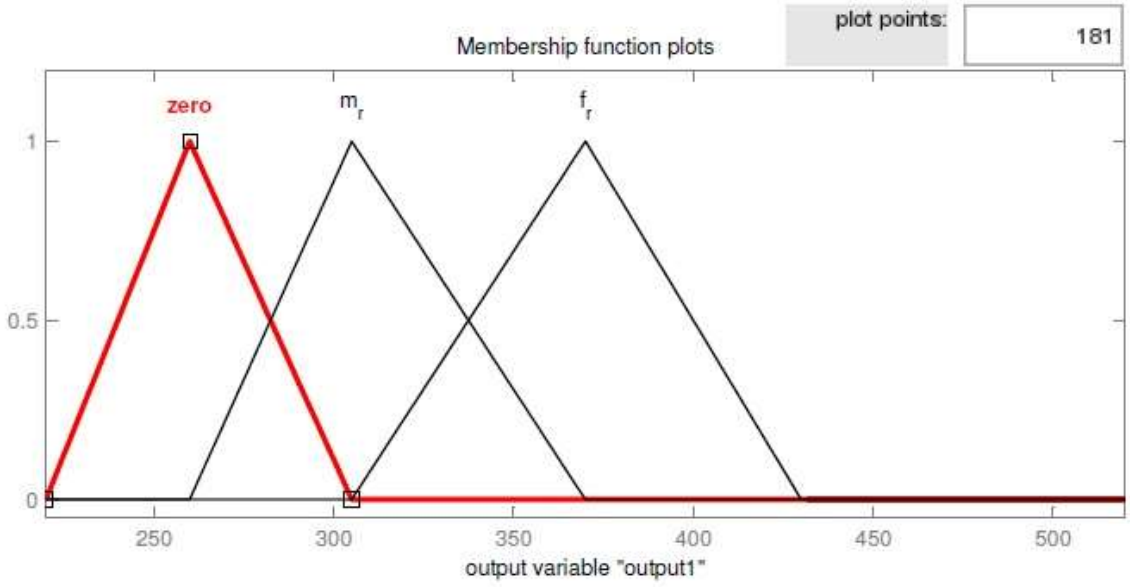


Figure 5.6c Membership function of DC Motor position

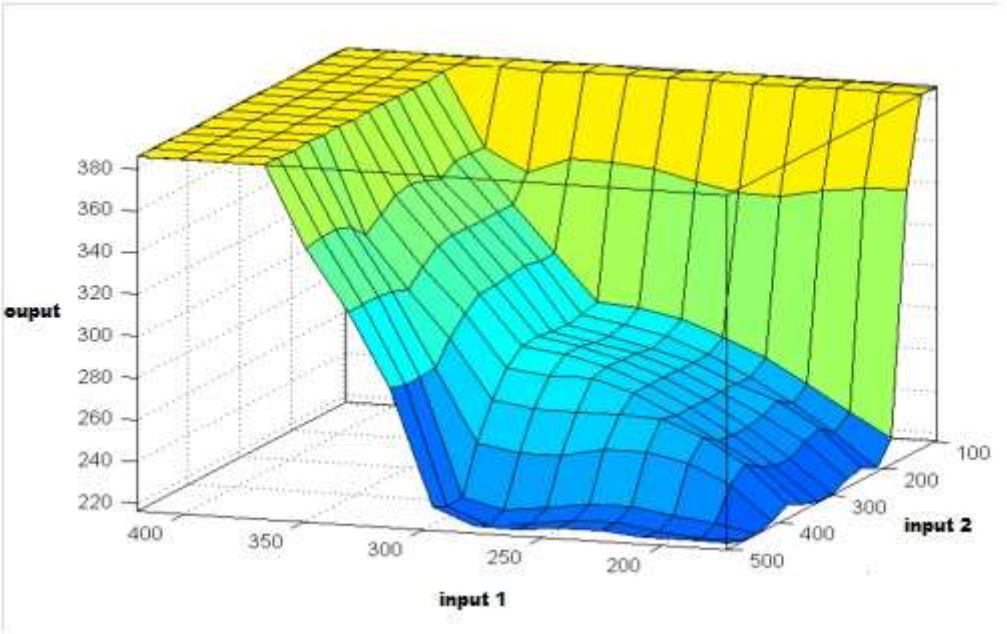


Figure 5.7 Response Surface of Motor position

One of the testing examples is shown in figures 5.8 a, b. If we select the input 1 to be in the range of full and input 2 middle right, the resulting Motor 1 position would be in the full range and Motor 2 will be in the zero position [Kenaya, R., et al., 2010]. Figure 5.7 shows the relation between the Gas, wheel steering and the output. The inputs is the same for both motors but the output is different according to the rule table and for backward the same thing just replacing the signal from Gas pedal with the signal from Brake Pedal with the same value input and the output will be in the range of backward side.

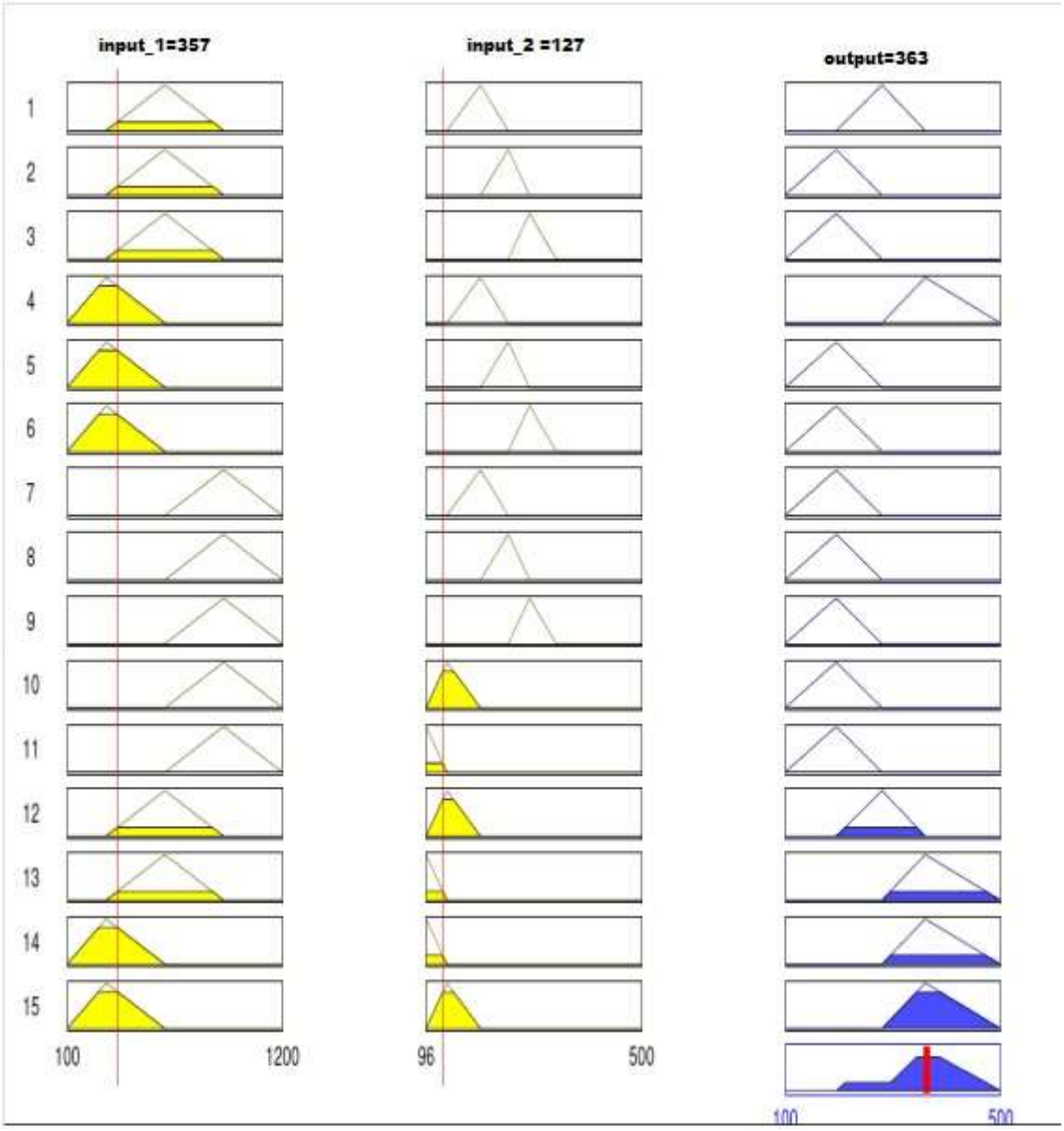


Figure 5.8a Fuzzy Rule result for Motor_1

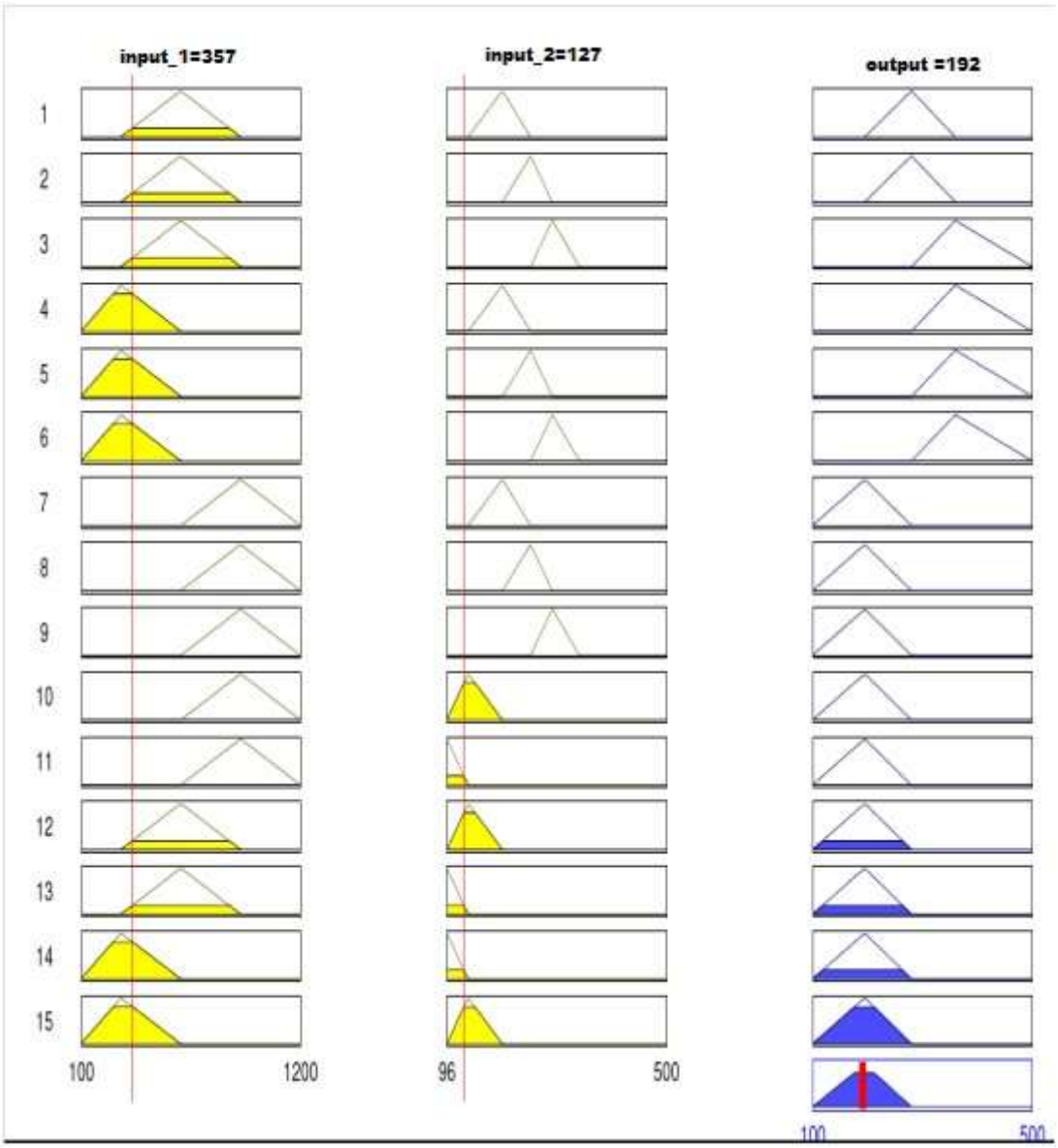


Figure 5.8b Fuzzy Rule result for Motor_2

For two input variables and fifteen rules, the output of the fuzzy logic system can be represented as [Nhivekar, G.S., et al., 2011]

$$\text{Defuz} = \frac{\sum_{i=1}^{15} P[i]\, W[i]}{\sum_{i=1}^{15} W[i]}$$

P[i] is the peak value of ith output membership function. W[i] is the weight associated with this rule.

## 5.5 Coupled Control System

### 5.5.1 Low Level Control and Vehicle Automation

The first step to convert the vehicle into a semi autonomous amphibious robot is automating all onboard actuating functions and placing them under closed-loop control. The task is simplified for the vehicle considered here since all drive functions (accelerating, braking and turning) are controlled through the two DC Motors connected to the hydraulic pumps and one servo motor to control the gasoline engine throttle. The speed is controlled by controlling the swash pump position which is connected to the DC Motors as shown in figure 5.9 and by adjusting the engine throttle valve through the servo motor.

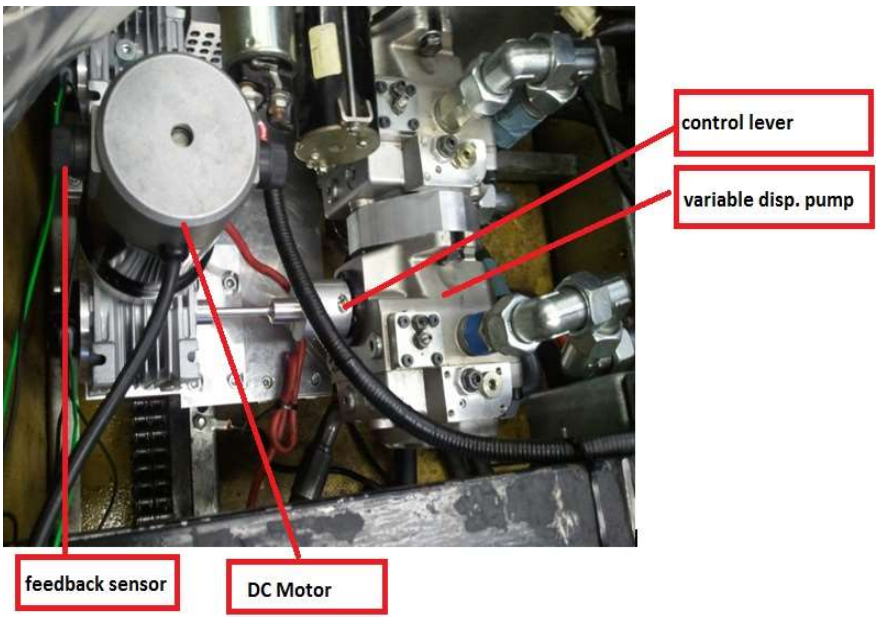


Figure 5.9 The Pump Actuators

Thus, complete automation of the vehicle is accomplished with the addition of just two feedback loops, which are identical, their required sensors, and actuators as shown in figure 5.10; and one open loop for control of the engine speed. The low-level controls shown in figure 5.11 consist of two feedback loops and one open loop around the three components of the drive system: an engine speed controller, and left and right wheel speed controllers.

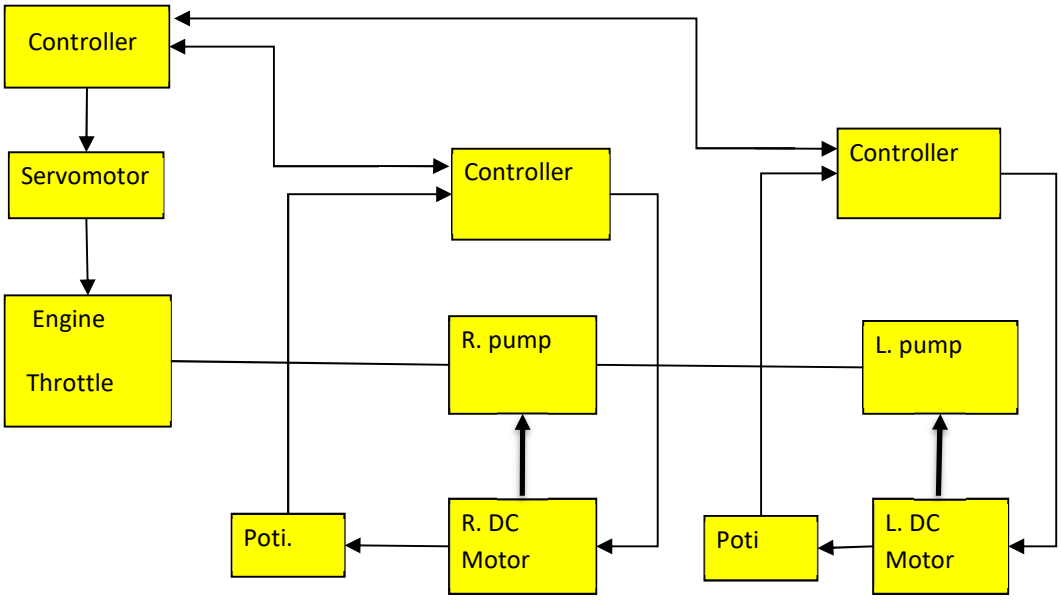


Figure 5.10 The Automated Drive Train

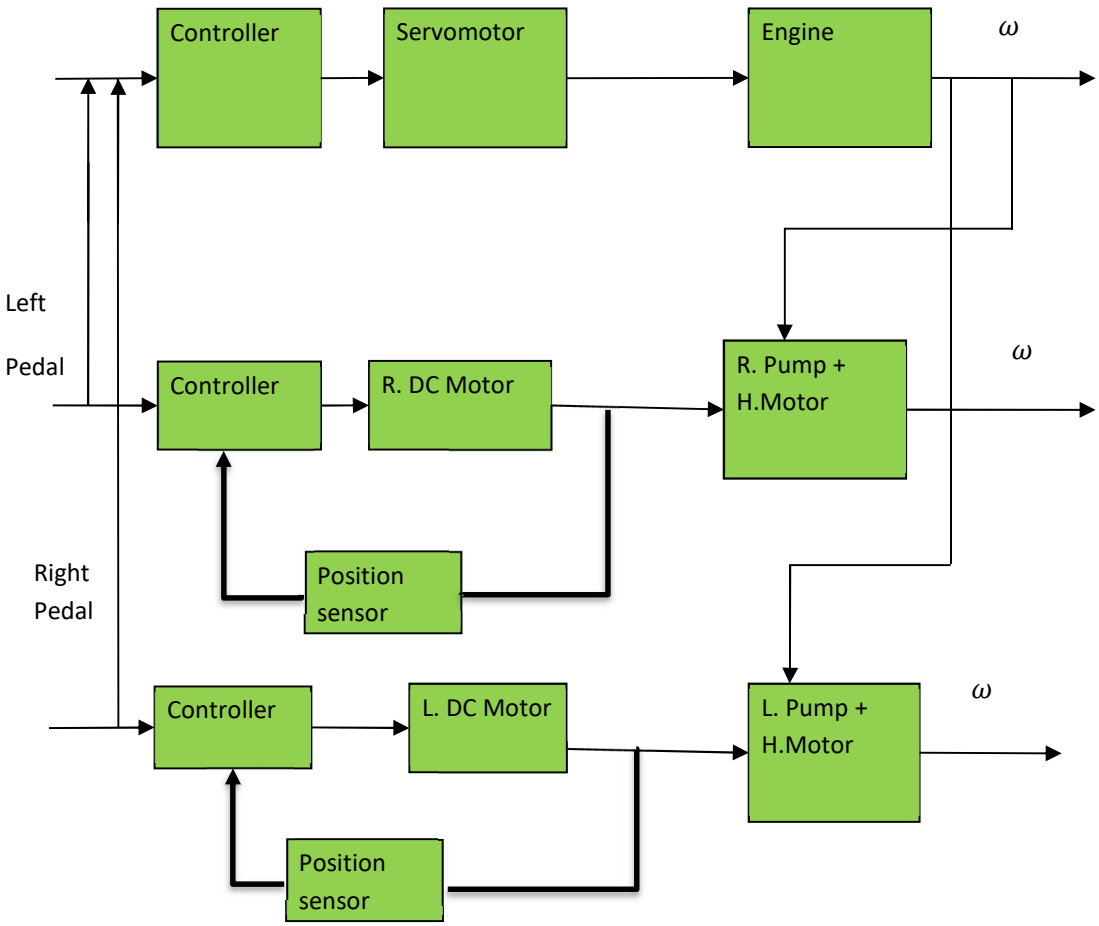


Figure 5.11 Coupled Control System

The automated drive train is shown schematically in figure 5.10. It consists of the engine with an open loop speed controller and two sets of hydraulic pump-motor systems each with a closed loop swash plate position controller. The hydraulic pumps produced disturbance on the engine since they must overcome inertia and drag on the vehicle. The engine acts as a speed disturbance to both pumps, since the wheel speed is directly proportional to engine speed. Fortunately, only a slight change to the low level control architecture is required to decouple the three systems. Relying on the drive controllers exclusively to govern the speeds of the wheels results in incorrect responses to terrain variation disturbances like the skid steer disturbance. This problem provides another compelling reason for decoupling the low level control loops in the manner described above. When the Vehicle encounters a hill, the added load reduces the vehicle's speed. Wheel speed drive controllers would respond by moving the throttle lever toward higher displacement, since this should result in higher wheel speed and compensate for the disturbance. Actually, this is analogous to shifting DORIS into a higher throttle position for driving up a steep hill. Moving the controls forward results in less drive force rather than more, since it increases the wheel speed to engine speed. The correct response is to increase the DC Motors angular position and apply more engine throttle. On a very steep hill, the drive controls must sometimes be moved forward for the vehicle to move faster uphill [Jacob, J.S. 1998].

### 5.5.2 Implement the open loop Control System

It is beyond the scope of this chapter to describe in detail the design and implement of the two feedback control loops and servo open loop. The servo motor throttle engine actuator is connected to the engine leaver and coupled to the two pedals as an open loop for controlling the engine speed, the two closed loop control position, DC Motors control the position of the variable displacement swash pump between -18 to +18 degree. The driven signal comes from the two Pedals one for driving the Vehicle forward and the other to drive the Vehicle backward and two feed-back sensors attached to the Motors sends the actual position to the microcontroller which processes the error between the input signal and the output signal, the servo motor control signal gets some disturbance from the two DC Motors due to the electromagnetic interference (EMI) which is not a desired signal. There are numerous EMI filters that could be considered for noise reduction but the most popularly used are the LC inductor filter and the π filter [Jayasree, P.V.Y., et al., 2012], for that a low pass filter was used to eliminate the EMI, and because the servo motor has independent power supply, the Ground line of the servo motor should connect to the Ground of the microcontroller to

prevent the servo noise. The low level control system should be coupled with the high level control system. The signal from the Gas Pedal with the steering wheel signal and servo position should be combined together to have a linear function connecting these variables (S,G,St). Matlab tools were used to determine this relationship. Table 5.3 shows the Gas Pedal positions, Steering wheel positions and where the servo position should be to have a good engine speed. Table 8 shows the combined system for brake pedal.

Table 5.3 Gas, Steering and Servo relationship

| Gas | Steering | Servo | Gas | Steering | Servo |
|---|---|---|---|---|---|
| Middle | Zero | zero | 600 | 102 | 520 |
| Middle | Middle_r | Middle | 600 | 123 | 400 |
| Middle | Full_r | Full | 600 | 145 | 300 |
| Full | Zero | Zero | 300 | 102 | 520 |
| Full | Middle_r | Middle | 300 | 123 | 400 |
| Full | Full_r | Full | 300 | 145 | 300 |
| Zero | Zero | Zero | 900 | 102 | 520 |
| Zero | Middle_r | Zero | 900 | 123 | 520 |
| Zero | Full_r | Zero | 900 | 145 | 520 |
| Zero | Middle_l | Zero | 900 | 80 | 520 |
| Zero | Full_l | Zero | 900 | 60 | 520 |
| Middle | Middle_l | Middle | 600 | 80 | 400 |
| Middle | Full_l | Full | 600 | 60 | 300 |
| Full | Full_l | Full | 300 | 60 | 300 |
| Full | Middle_l | Middle | 300 | 80 | 400 |

The linear function combined the Gas, steering and servo from Table 5.4 and using Matlab tools is

$$S = 545 - 0.34\,G + 0.0166\,St \tag{5.13}$$

Table 5.4 Break, Steering and Servo relationship

| Break | Steering | Servo | Gas | Steering | Servo |
|---|---|---|---|---|---|
| Middle | Zero | zero | 452 | 102 | 520 |
| Middle | Middle_r | Middle | 452 | 123 | 400 |
| Middle | Full_r | Full | 452 | 145 | 300 |
| Full | Zero | Zero | 108 | 102 | 520 |
| Full | Middle_r | Middle | 108 | 123 | 400 |
| Full | Full_r | Full | 108 | 145 | 300 |
| Zero | Zero | Zero | 800 | 102 | 520 |
| Zero | Middle_r | Zero | 800 | 123 | 520 |
| Zero | Full_r | Zero | 800 | 145 | 520 |
| Zero | Middle_l | Zero | 800 | 80 | 520 |
| Zero | Full_l | Zero | 800 | 60 | 520 |
| Middle | Middle_l | Middle | 452 | 80 | 400 |
| Middle | Full_l | Full | 452 | 60 | 300 |
| Full | Full_l | Full | 108 | 60 | 300 |
| Full | Middle_l | Middle | 108 | 80 | 400 |

The linear function combined the Brake, steering and servo from Table 5.4 and using Matlab tools is

$$S=289 + 0.225\ B + 0.021\ St \tag{5.14}$$

Figure 5.12 shows the linear function connecting the Gas pedal, Steering wheel and servo motor position and figure 5.13 shows the linear function connecting the Gas pedal, Steering wheel and servo motor position

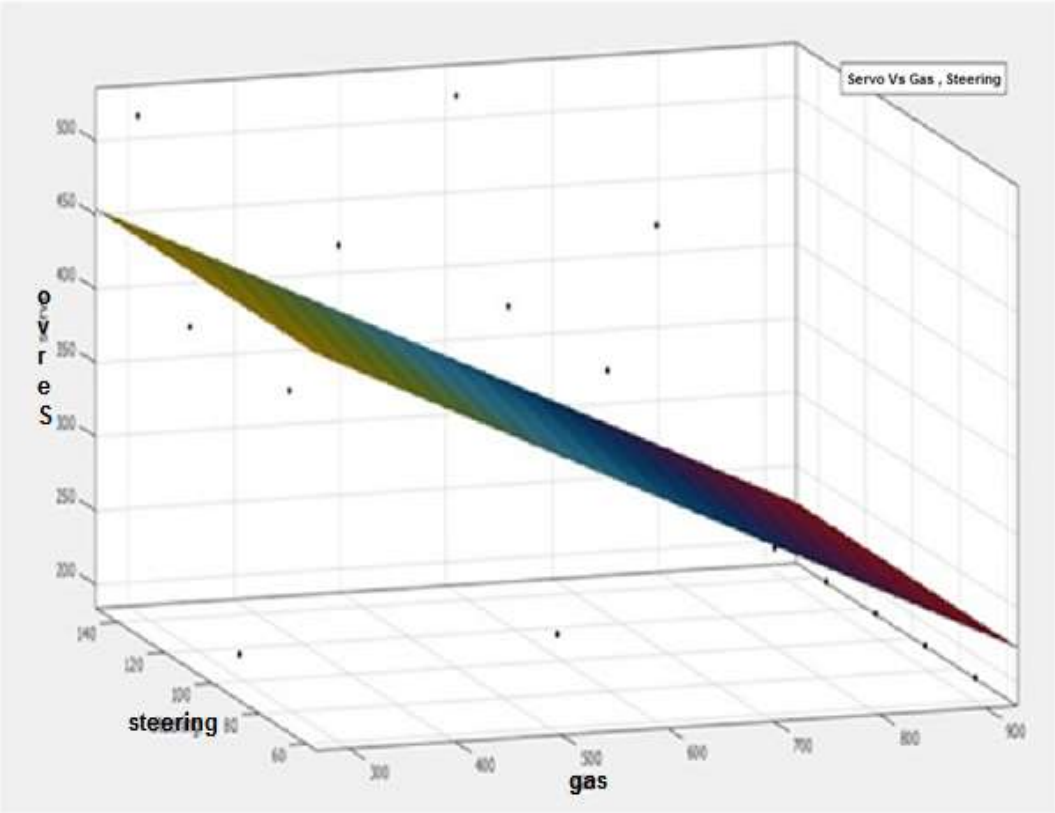


Figure 5.12 The relation between gas, steering and servomotor

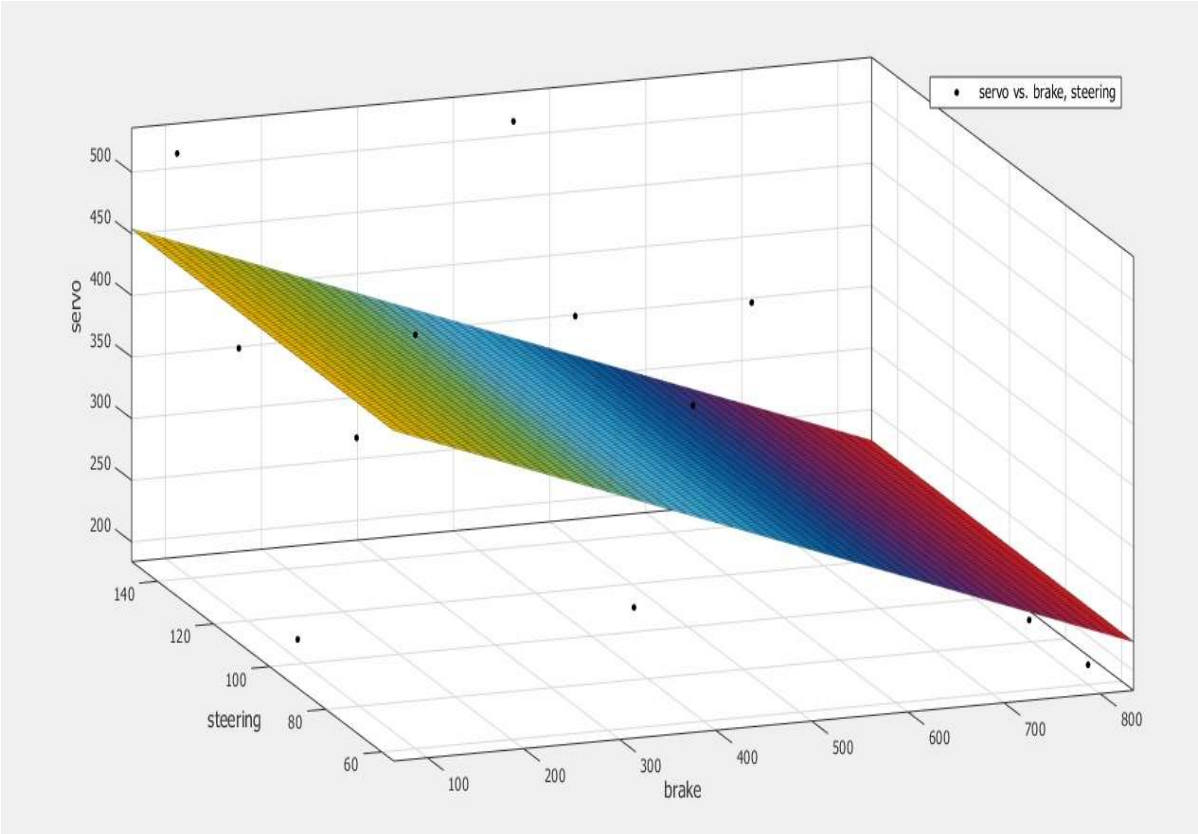


Figure 5.13 The relation between brake, steering and servomotor

## 5.6 Experiments and Results

Figures 5.14b, 5.15b and 5.16b show three experimental test results for driving forward that display the two DC Motors' positions which control the hydraulic pump flow rate. The more the hydraulic pump swash plat angular position is increased the more hydraulic motor speed and wheel speed are increased. For no turning mode it can be seen that both DC Motors are in the same position for driving forward without turning and for small turning mode, one DC Motor is stopped in the zero position and the other DC Motor in another angular position to give right turn. The full turning action is done by stopping one DC Motor in the zero position and the other Motor is moved to the full angular position that makes it turn full right. This result can be compared with the simulated result in figure 5.14a, 5.15a and 5.16a. Figure 5.17 shows the state of DC Motor _1 and _2 during turning left backward, DC Motor_2 is in the backward position and DC Motor_1 in a zero position this combination make the vehicle rotate to the backward left side. Figure 5.18 shows the relationship between Motor_1, Gas and Steering during steering action and Figure 5.19 shows the relationship between Motor_2, Gas and Steering. Figure 5.20 shows the effect of DC Motors electromagnetic interference (EMI) on the servo motor control signal this problem solved by adding R/C low

pass filter between the servo motor signal line and ground line. Figure 5.21 shows the control signal after filtering and eliminating the effect of EMI, this figure is for a middle throttle angle that meet the middle gas pedal position while figure 5.22 shows the servo signal in small throttle angle position that meet the small gas pedal position. Figure 5.23 shows steering scenes during driving the Vehicle manually.

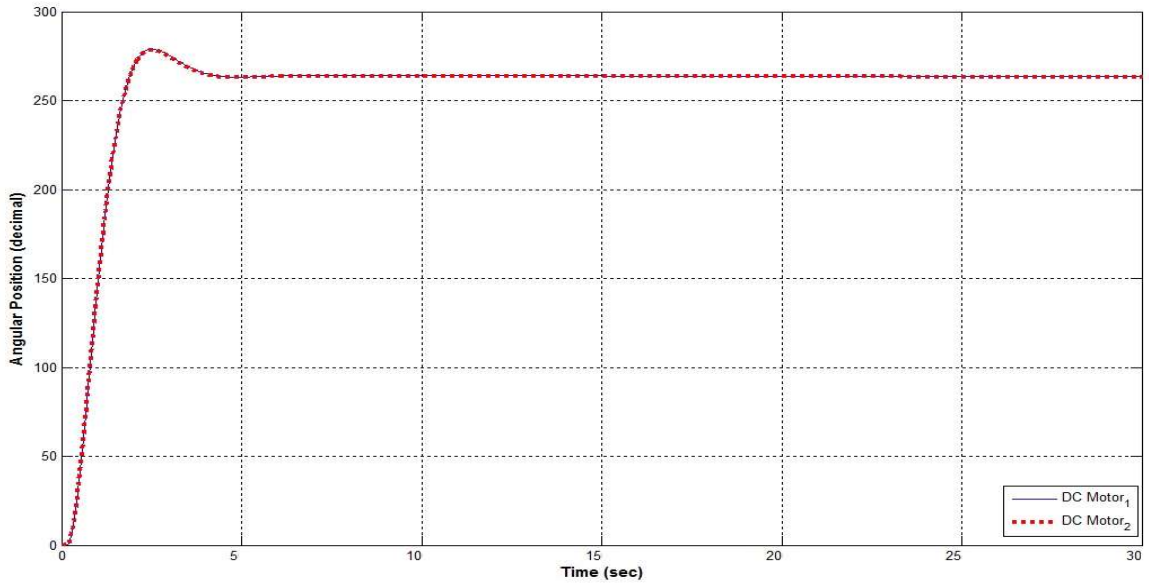


Figure 5.14a No turning simulated

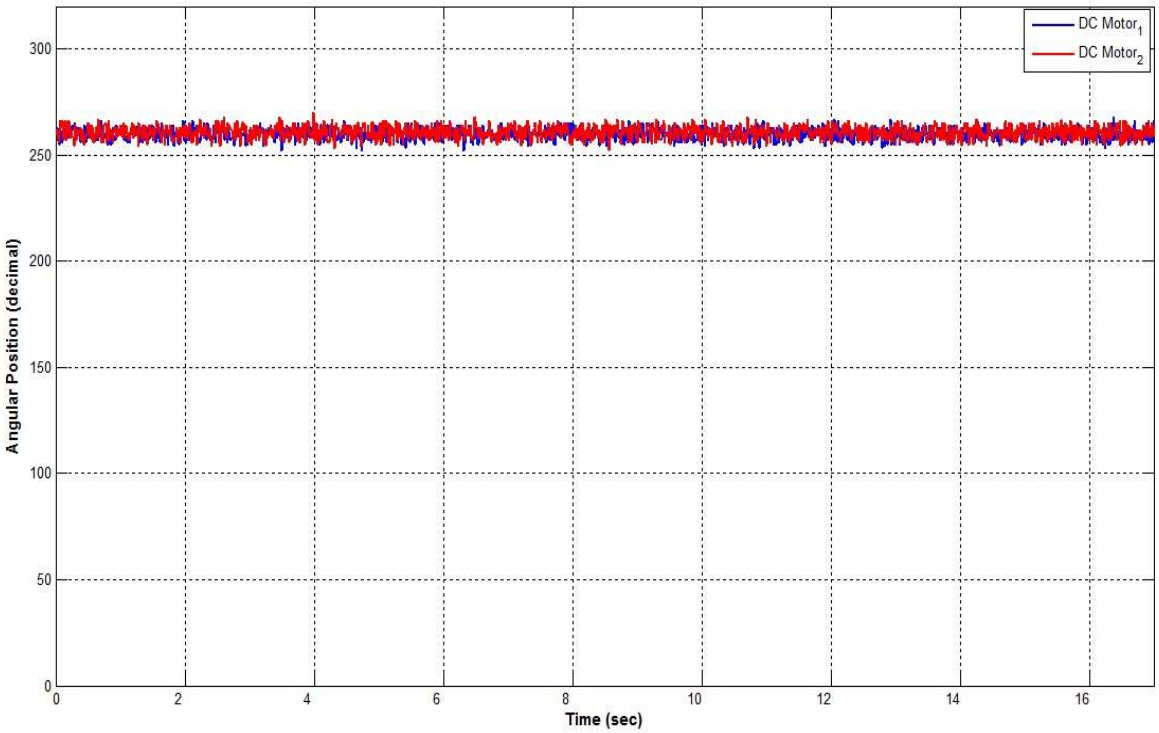


Figure 5.14b Without turning experimental result

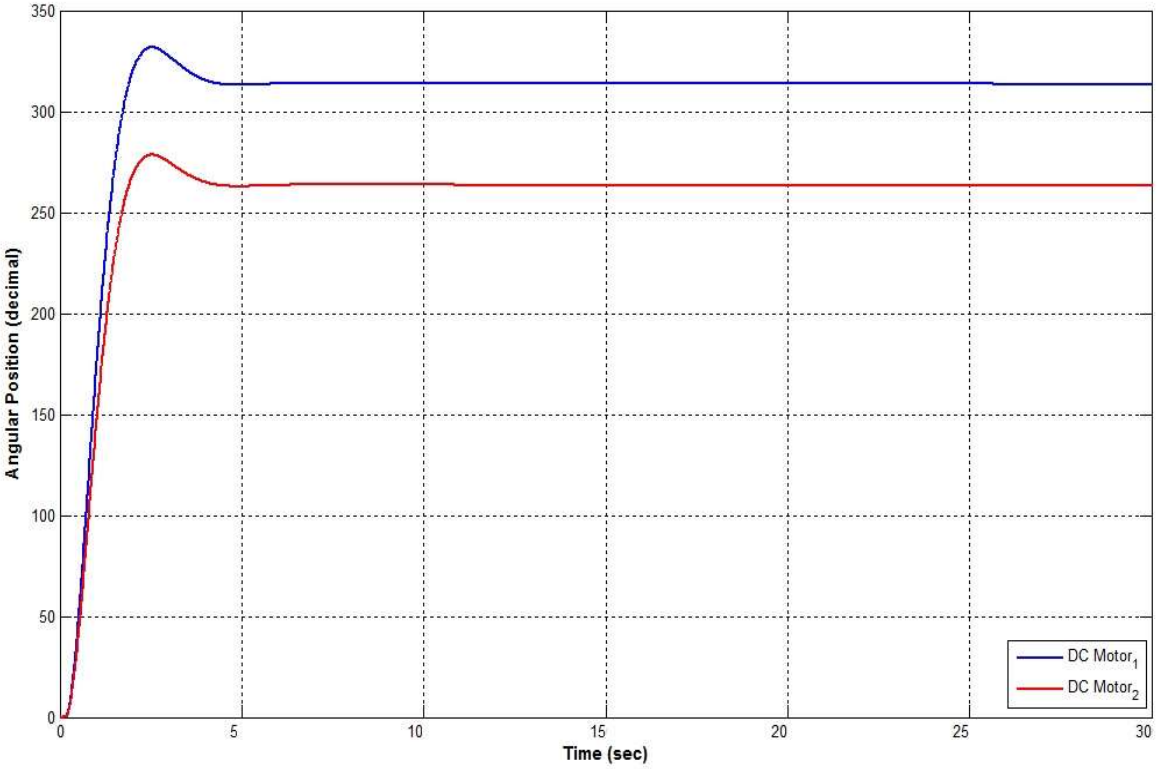


Figure 5.15a Big right turning simulated

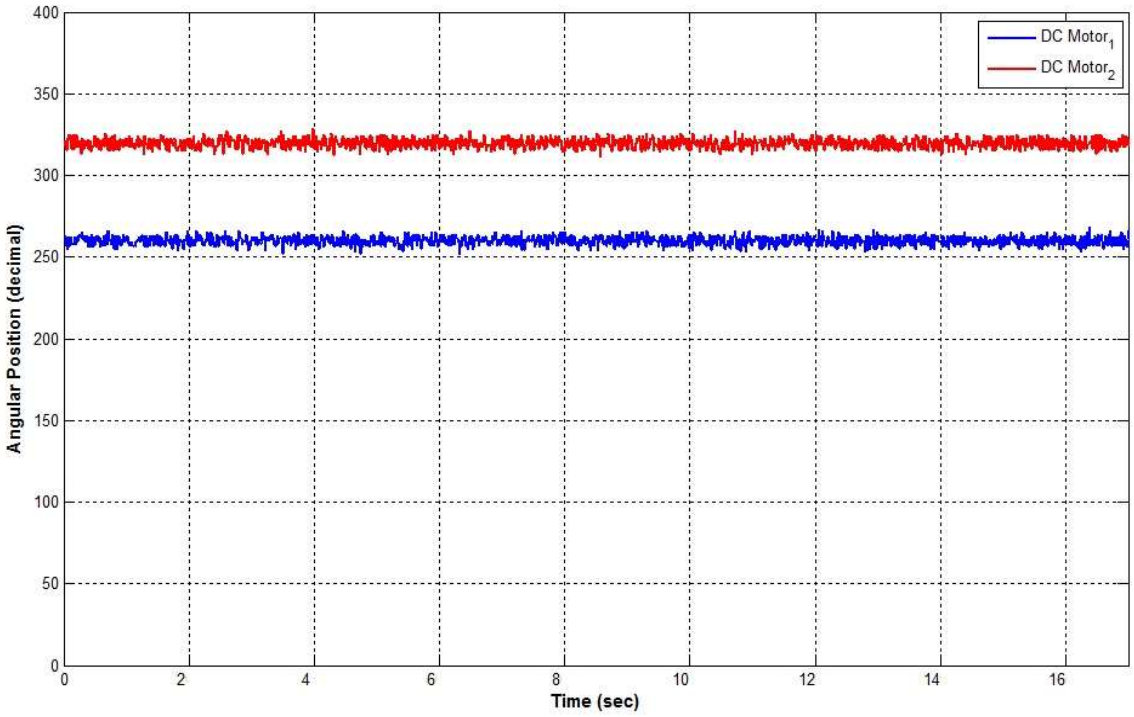


Figure 5.15a Small right turning experimental result

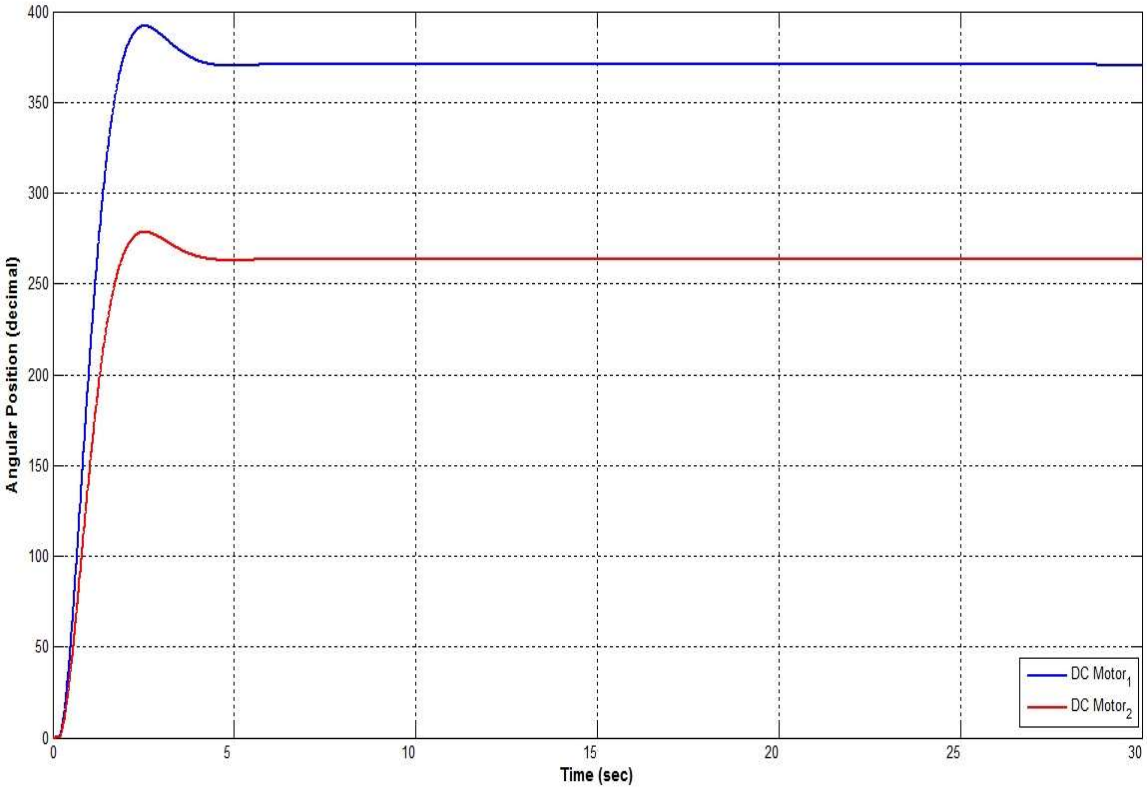


Figure 5.16a Full right turning simulated

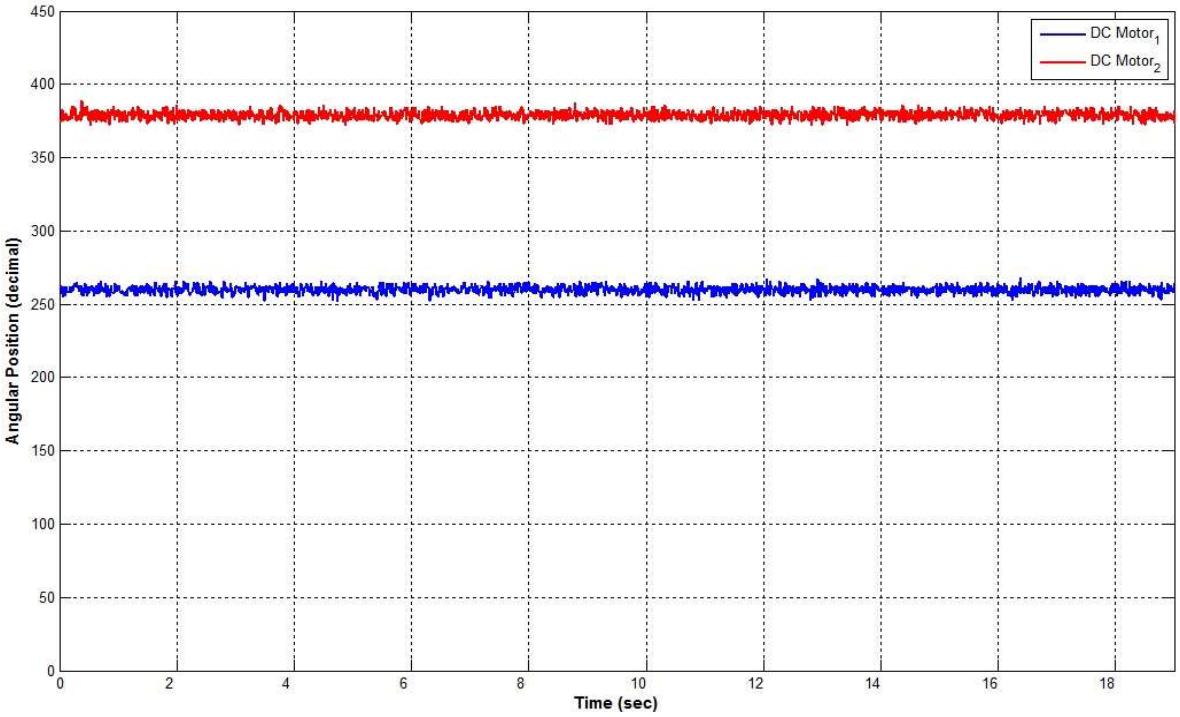


Figure 5.16b Full right turning experimental result

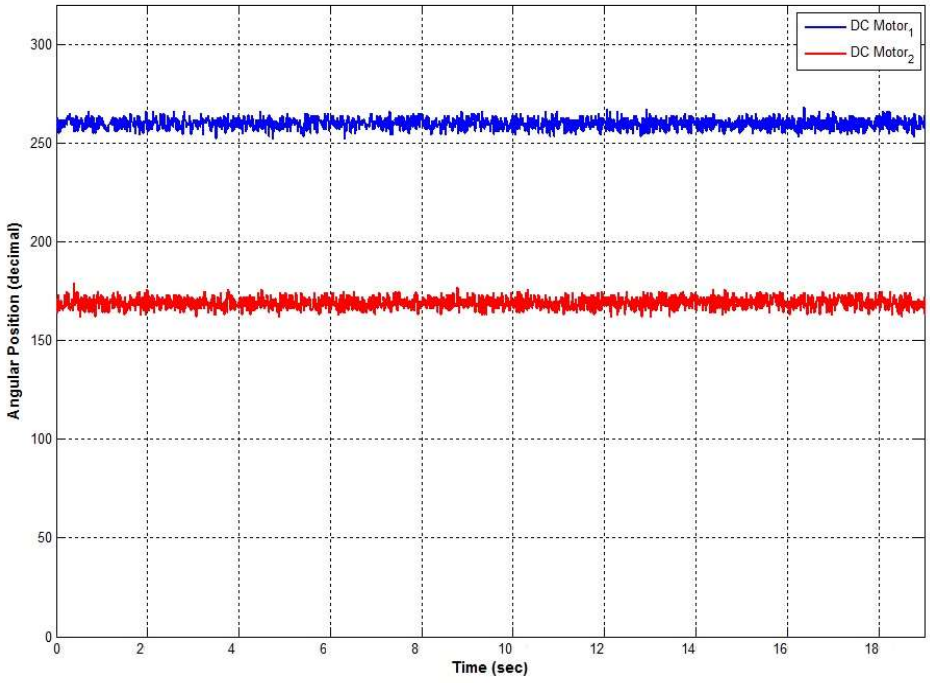


Figure 5.17 Left turning experimental result

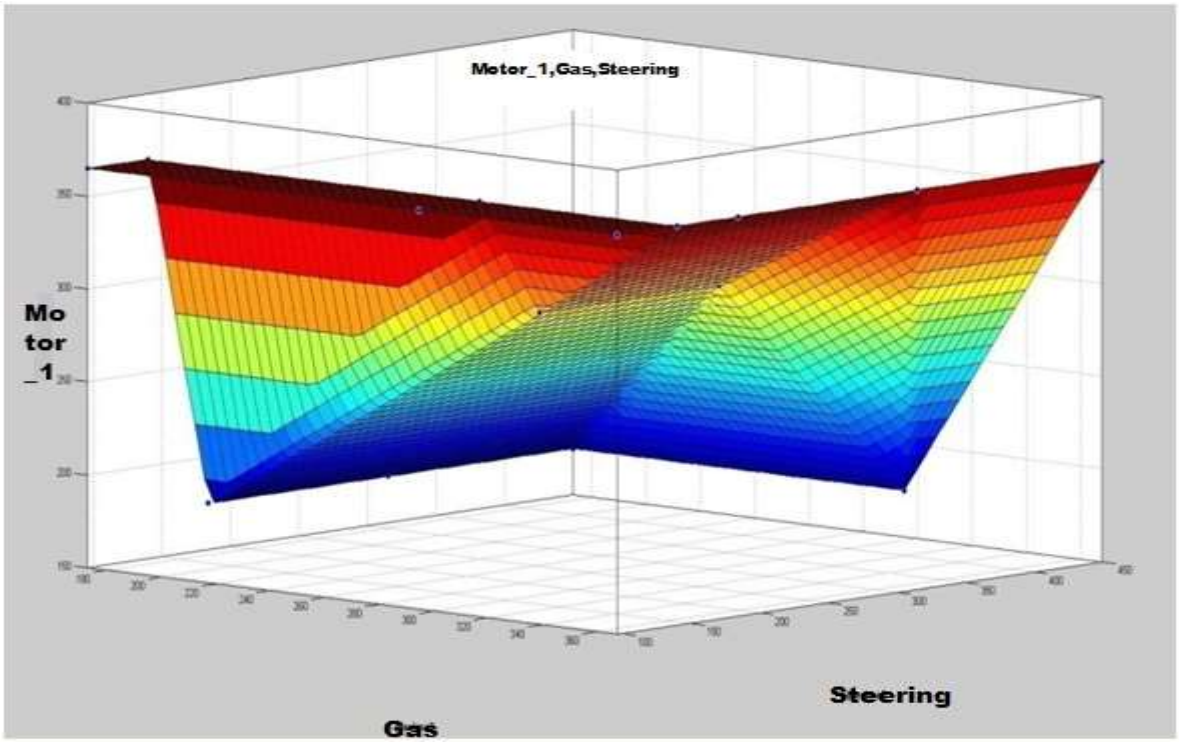


Figure 5.18 Relationship between Motor_1, gas and steering

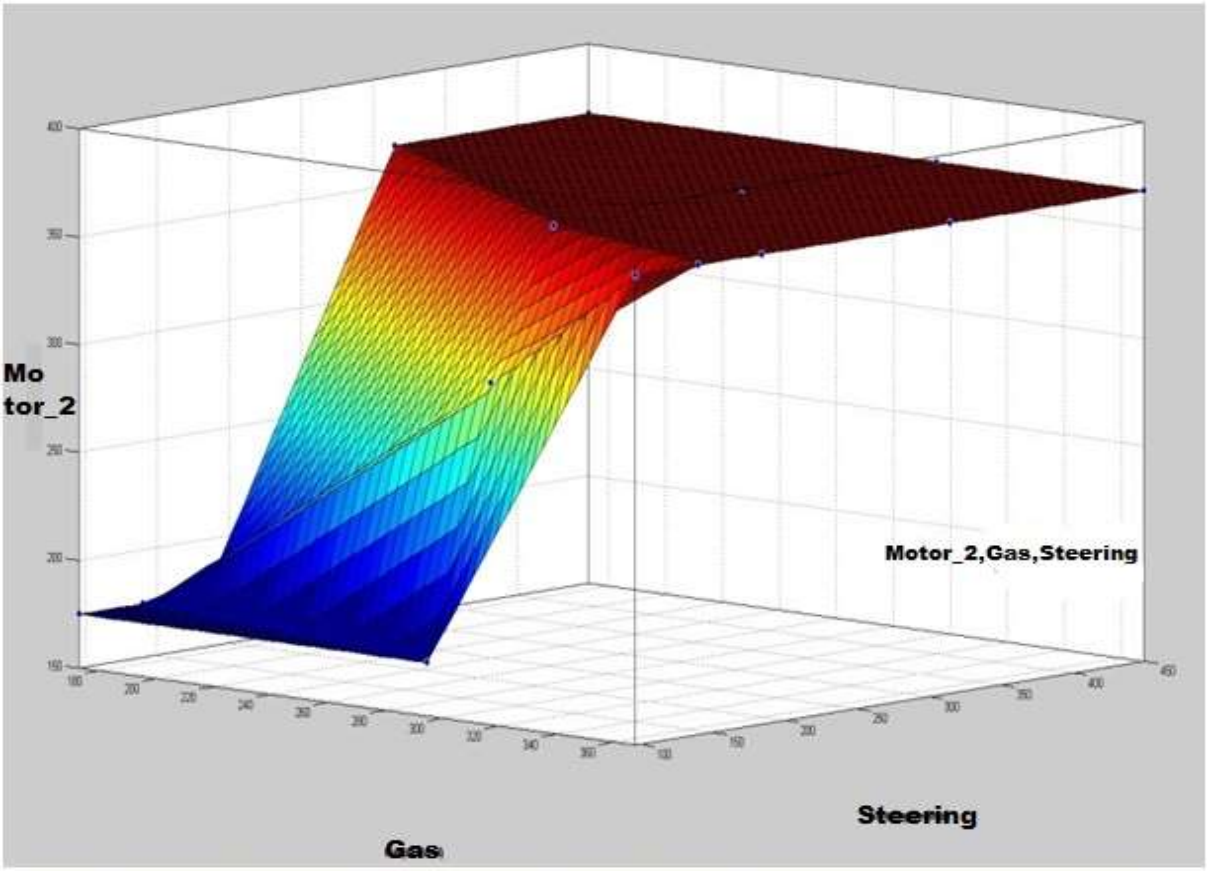


Figure 5.19 Relationship between Motor_2, gas and steering

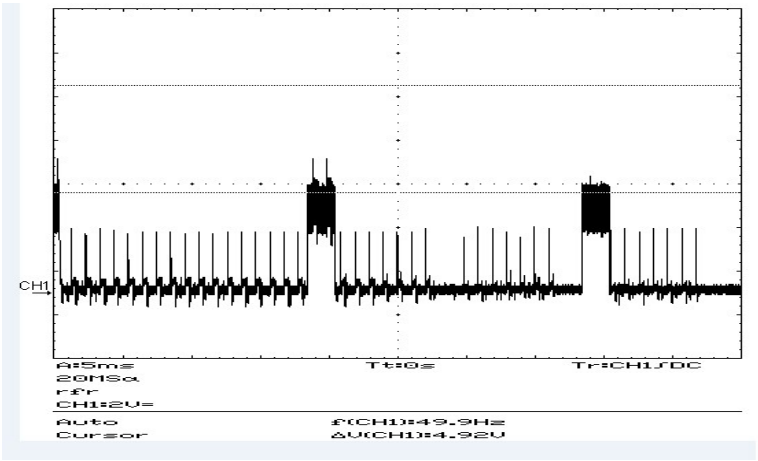


Figure 5.20 12% Servo Motor Duty Cycle with noise

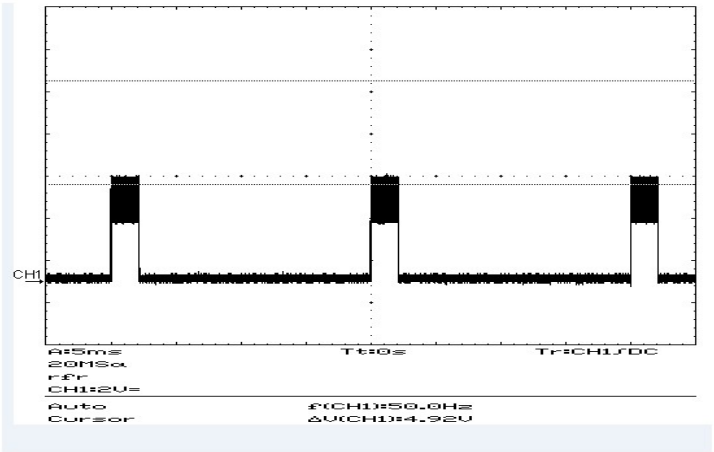


Figure 5.21 12% Servo Motor Duty Cycle

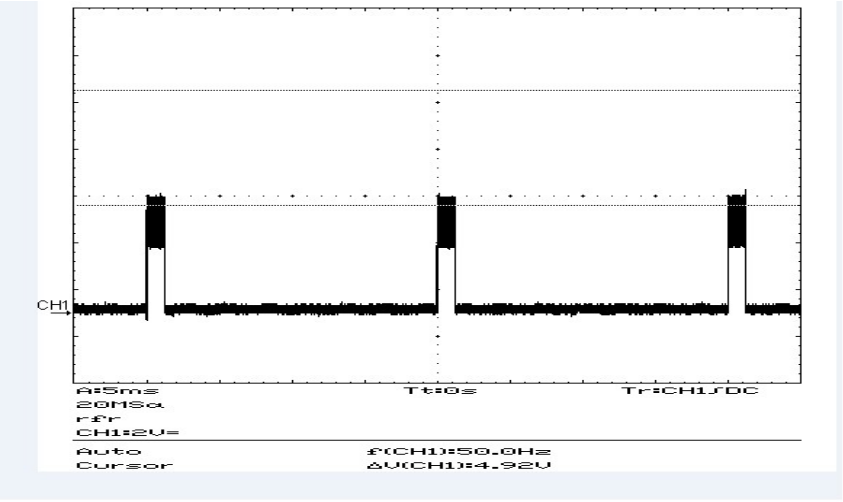


Figure 5.22 5% Servo Motor Duty Cycle

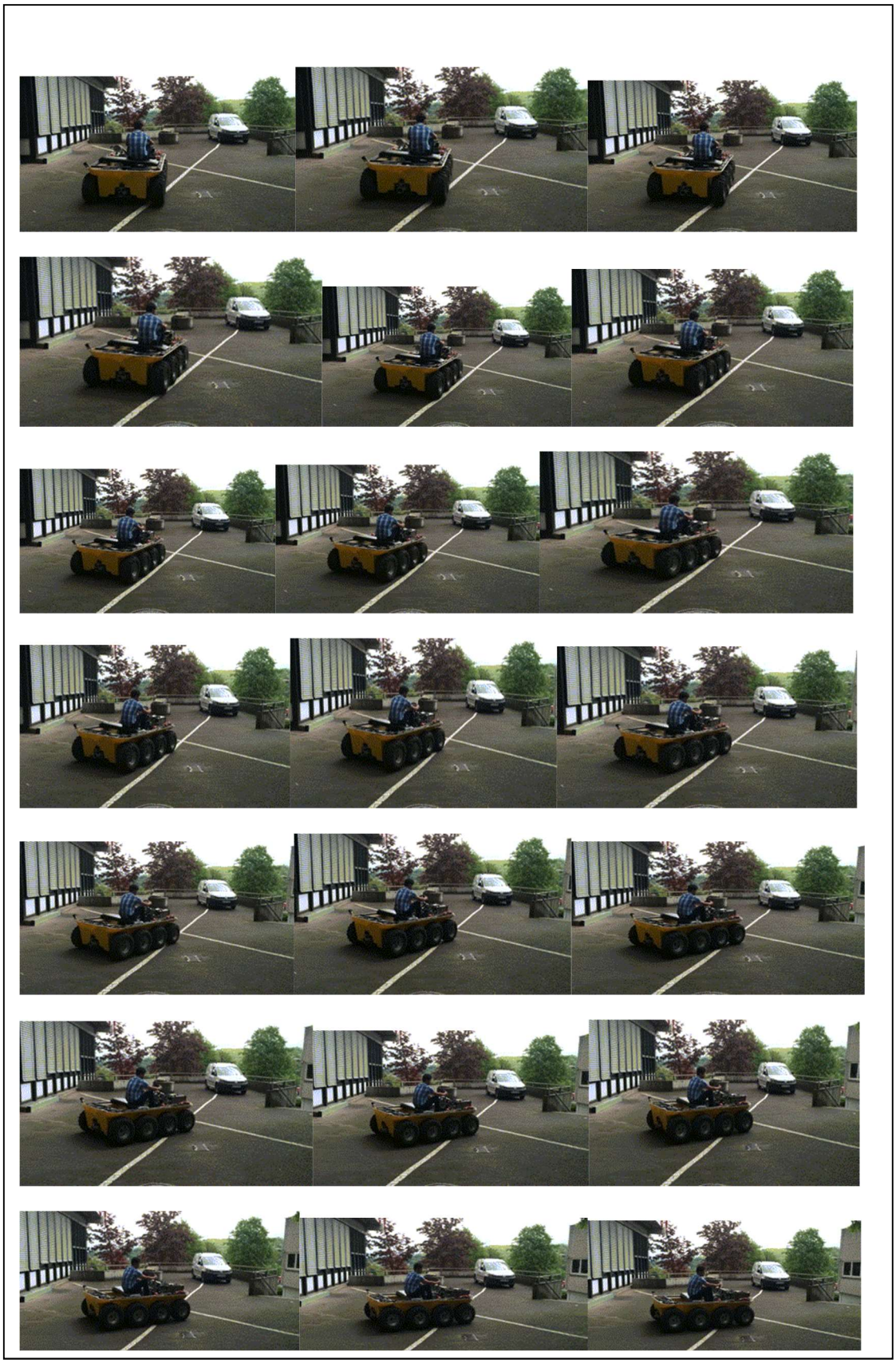

Figure 5.23 Steering scene

# Chapter 6

# Tele-Operation and Communication System

Tele-operation system is a kind of system which controls agents, e.g. robotic vehicles, Drones, etc., from a remote location through wireless signals such as Wi-Fi, GPS, cellular phone signals, Bluetooth, etc. [Fong,T., et al., 2001]. The system has advantages by being able to replace humans working in dangerous and unreachable environments to reduce mission failure and avoid casualties. In order to perform well, human-robot interactions need to be designed and provided for users as convenient and efficient as possible. Most of the human-robot interactions for tele-operation are in the form of traditional systems based on hand controllers, e.g. joystick, keyboard, mouse, touchpad, etc. In the process of tele-operation, generally, the users are required to sit in front of a computer and view real-time vehicle movements. Then, the user sends control commands manually, e.g. by pressing keys, touching the screen, or clicking the mouse, to the agent towards completion of specific tasks [Yu, M., et al., 2014]. Vehicle teleopertation first appeared in the early 1900's, but it was not until the 1970's that systems became widely used. Today, vehicle tele-operation is used for applications in the air, on the ground and underwater. Since development occurred over different periods and domains, it is not surprising that vehicle tele-operation is referred to by numerous terms (ROV, RPV, UAV, UGV). However, regardless of system type, many common characteristics and features exist [Fong, T., et al., 2001]. We classify tele-operated ground vehicles into three categories: exploration rovers, Unmanned Ground Vehicles (UGV), and hazardous duty. Exploration rovers are ground vehicles designed to remotely perform science tasks such as in-situ sensing and sample collection. The first exploration rovers were the Soviet Lunokhods, which explored the moon in the early 1970's [Carrier, D., et al., 1992]. Since then, NASA has produced numerous research vehicles (the Rocky series, Dante I/II, Nomad, etc.) and has landed on Mars. UGVs are primarily used for tasks requiring remote navigation such as reconnaissance or surveillance. In the early 1980's, the Naval Ocean Systems Center developed the Tele-Operated Dune Buggy and the Tele-Operated Vehicle. Both were driven with stereo video and replicated controls. During the 1990's, the Tactical UGV program produced several vehicles, which could be driven using either rate or waypoint-based control [Gage, D., et al., 1995].

## 6.1 ROS

Robotic middleware solutions migrated to a thin-design paradigm that supports the development of modular components and increases the ability to reuse existing code. Several frameworks follow this new paradigm with the Robot Operating System (ROS) being one of the most popular. Since its release in 2007, several hundred packages have been published. Despite the clear benefits that ROS introduced to the robotic community, the concept of ROS is not particularly new, but it is actually comparable to existing solutions such as, e.g., the Inter Process Communication (IPC) library. ROS provides mainly a communication interface between independent pieces of a framework together with a platform to share released code. In order to implement their algorithms on a particular robotic platform, robot cists are still forced to develop the appropriate drivers and controllers and to link them into a reliable framework. While drivers for several hardware components have been gratefully shared by other scientists through ROS, the development of an appropriate control framework still remains a challenging and time-consuming task, for example in the popular research field on Unmanned Ground Vehicles [Volker Grabe, et al., 2013].

Robot Operating System (ROS) is used as the middleware for the robotic platform. Safety features, at both the software and hardware level, are pre-built into the robot thus providing the basic measures for ensuring its safe operation in human environments. The ROS middleware also provides easy access to the open-source library of various robotics algorithms, which can be used off-the-shelf or customized for the mobile base.

## 6.2 Major Components of the Tele-Operation System

The hardware used to drive the amphibious vehicle semi-autonomous consists of the following components:

### 6.2.1 PC and Joystick Controller

The client PC shows in figure 6.1 is a standard personal computer running Linux and robot operating system (ROS) with networking enabled, and the necessary drivers installed. Beside the PC, the joystick is used also to drive the Robot.


Figure 6.1 PC and Joystick Controller

### 6.2.2 Raspberry Pi

The Raspberry Pi as shown in figure 6.2 is a credit card sized computer. It runs a full version of the Linux Operating System. Its files are held on SD card typically holding between 2 and 32 Giga-bytes of data. When connected to a power supply, a USB keyboard and mouse, and attached to a TV via an HDMI cable, it behaves like a regular laptop running Linux. Programs for it can be written in various languages such as Python, C++ and Java. Systems such as Squeak and Scratch are fun to use and well worth looking.

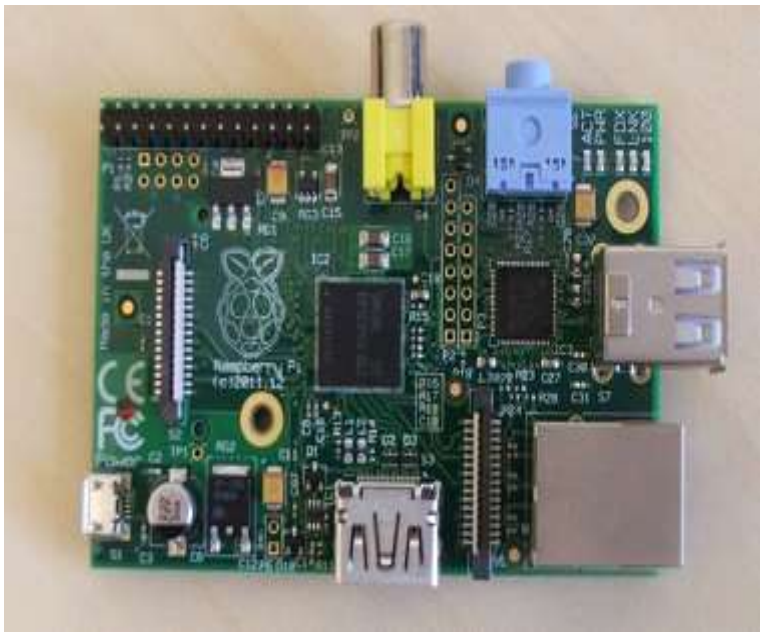

Figure 6.2 Raspberry Pi Platform

## 6.3 Software

A tele-operation system was chosen because it allows much more flexibility in programming.It also allows for easy warless control; provides a reduced need for specialist hardware; and wireless communications have already been well established [Guptal, G.S. 2009]. The programs have been written in C, the same program runs on both the server and the client computer. However, one is set as the server and the other as client at runtime. The server listens to its set ports waiting for a connection from the client. The client needs the IP address of the server and the port number it is listening to, and then can establish a link. The wireless communications are handled by ADHOC through WIFI. Once communications have been established, the client and server computers can send each other the necessary control commands. The control command is sent from the PC to the client PC, which is a raspberry pi through WIFI and from the raspberry pi to the microcontroller through the serial communication as shown in figure 6.3.Erforderliche Parameter fehlen oder sind falsch.

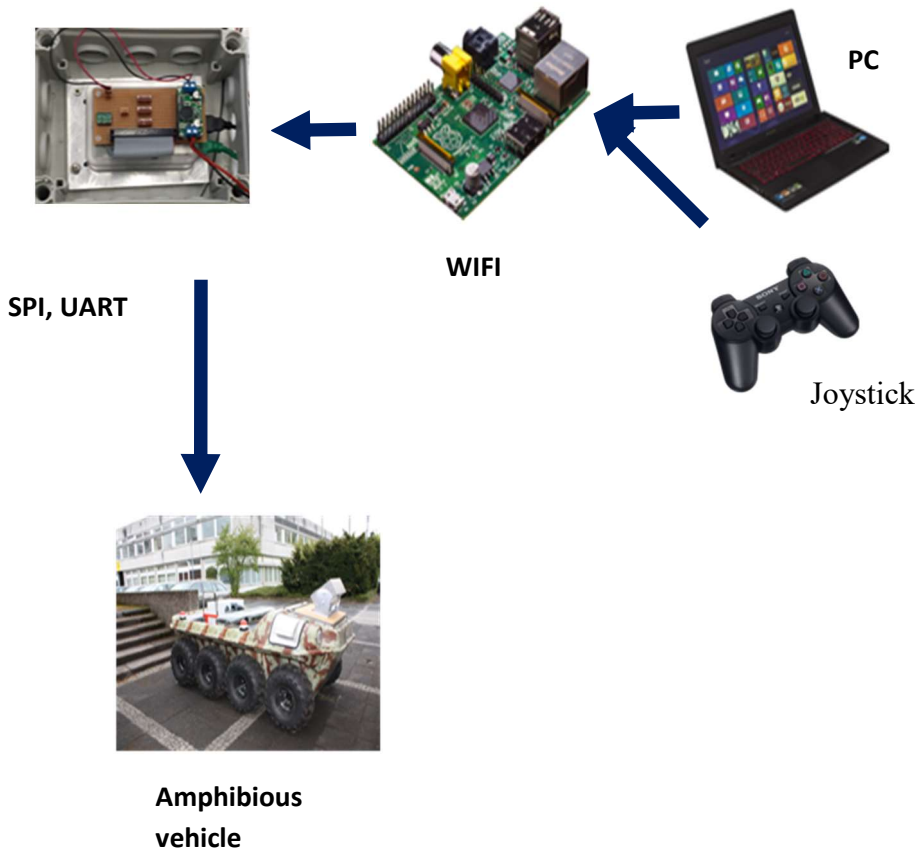


Figure 6.3 Hardware structure of keyboard tele-operation

Tele-Operation of the robot includes 2 parts, one is a listener and another one is a publisher. The setting is like this, we have two nodes running. One is a publisher, which takes keyboard input and keeps sending keyboard event command out. A second node, a listener, keeps listening to keyboard events command then print it out on the computer screen and also send it to the microcontroller via UART. For Joystick a joy node is installed in ROS Package which is used to send the controlling commands according to the adjusted buttons, in the microcontroller, a UART communication sitting is made to get the keyboard events. The DC Motors positions that set the hydraulic pump speed and the wheel speed is divided to four speeds for forward driving and four for backward driving.

To stop the Tele-operation of the robot, the user should press the key “S” on the keyboard. At this moment the robot stops and waits for the user commands indicating the movement direction. The commands and the corresponding movement directions to be carried out by the robot are shown in table 6.1.

Table 6.1 Tele-operation keyboards commands

| **Keyboard button** | **PS3 button** | **speed** |
|---|---|---|
| f | 4 | Forward speed_1 |
| g | 5 | Forward speed_2 |
| h | 6 | Forward speed_3 |
| j | 7 | Forward speed_4 |
| r | 12 | backward speed_1 |
| t | 13 | backward speed_2 |
| z | 14 | backward speed_3 |
| u | 15 | backward speed_4 |
| e | 11 | Left Skid steer |
| x | 10 | Right Skid steer |
| w | 9 | Right spot turn |
| y | 8 | Left spot turn |
| s | PS | Vehicle stop |

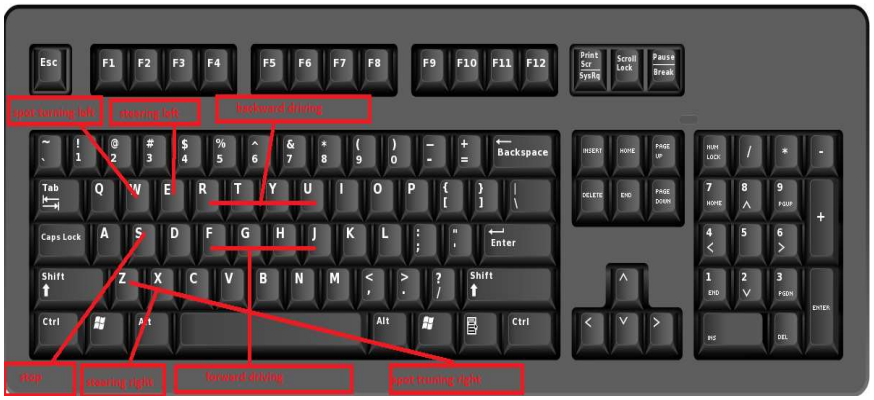


Figure 6.4 Keyboard speed command

The control commands sent from the keyboard to drive the robot and to steer the robot is shown in the figure 6.4 where the keyboard event is used to control servo motor and the two DC Motors. One node written in C language on the pc called PC node, receives the keyboard commands and publishes this event through the keyboard publisher to the raspberry pi where another node written on the raspberry pi board called pccontroll receives the published event. The subscriber receives the keyboard event and sends it to the microcontroller. In the microcontroller a function treat the keyboard events and drive the motors and servo to drive the robot forward, backward and steer the robot. Figure 6.5 shows the control structure of the Tele-operation System.

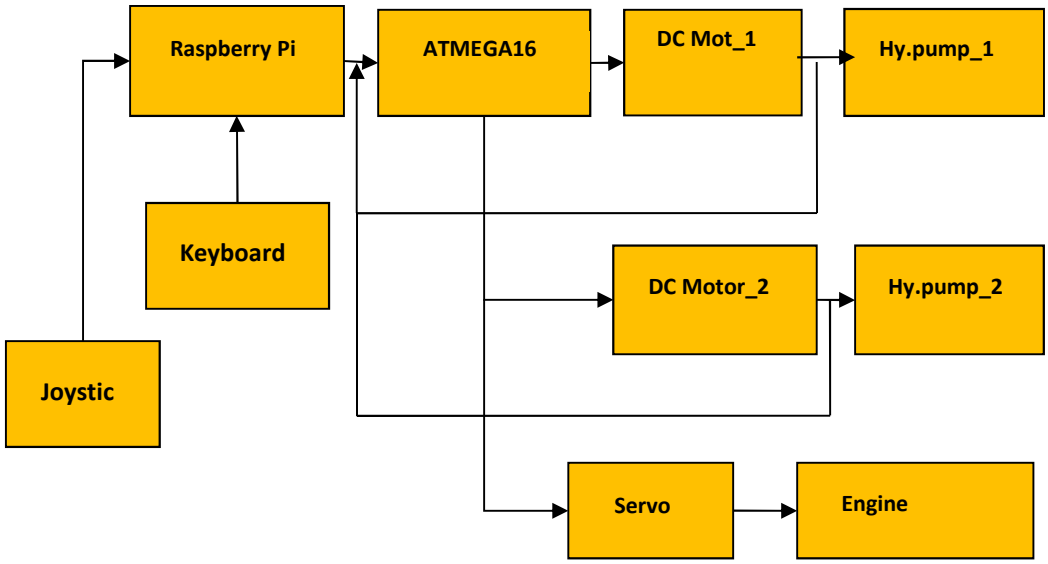


Figure 6.5 Control structure

## 6.4 The Nodes

Everything on the ROS system is based on nodes, messages, topics and services. The nodes are processes that execute a specific task. Two nodes were created to do the communication task between the PC and the control system which is used to send the letters in table 6.1 to the raspberry Pi node which does the communication between the pc and the control system through UART. It is like a software module, while Nodes can use the topics to communicate with each other and use the services to do some simple and external operations. The nodes usually manage low complexity tasks. It is possible to represent the nodes in a graphical representation as shown in figure 6.6.

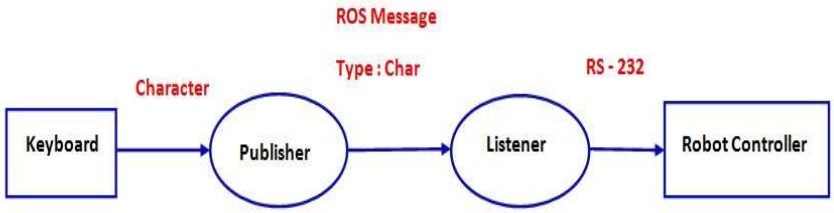


Figure 6.6 ROS message flow diagram

## 6.5 Network Communication

In microcontrollers and sensor networks as shown in figure 6.7, microcontrollers and sensor networks are generally connected together, which provides built-in linearization, error correction, and access to the network. The interface between the microcontroller nodes becomes important to achieve easy deployment, low power, low cost, and high reliability. Some digital interfaces, which were not originally designed for microcontroller networks, such as I2C, SPI and RS-232, have been widely used in robotics and the industry, however, some specific characteristics of the microcontroller network require more features for the interface. Energy efficiency may be of importance if thousands of nodes operate unattended for a long period of time. In some applications the configuration of the system needs to be done automatically and, therefore, hot swap functions become necessary for the microcontroller's network. The interface between the microcontrollers should be carefully chosen to meet the requirements of the application. ISO-OSI network model defines 7 layers of communication: physical, data link, network, transport, session, presentation and application layer. The SPI standard defines only the bottom two layers of this network

model. In SPI, the data is exchanged between two devices; it can be daisy chained so that the data is exchanged between more than two devices. Typical SPI configuration: (a) Peer-to-Peer, (b) Loop. Commonly used configuration allows exchange of data between two devices. Depending on the capabilities of the devices, either of the communicating devices can be a master, but master has always to provide the clock to the slave. The data is exchanged between four devices, device1, device2, device3 and device4 device n, connected in a loop topology. SPI only defines the physical and data link layer of ISO-OSI network model. The connection and media between the devices indicates the physical layer. The Data link layer defines the way in which the devices are connected and the connections include the input and output lines such as clock, data in and data out. Data link layer in SPI is implied in the connection itself and no provision is made for location or address information. In the simplest form, two computers exchange data among themselves. In contrast with other serial protocols, communications on SPI is always an exchange of data and not read or write: in other words, read and write occur simultaneously. SPI is a master slave network and hence there are no collisions, arbitration issues, or packet loss, which needs to be handled in the other device communication networks [Mayannavar, S., et al., 2008].

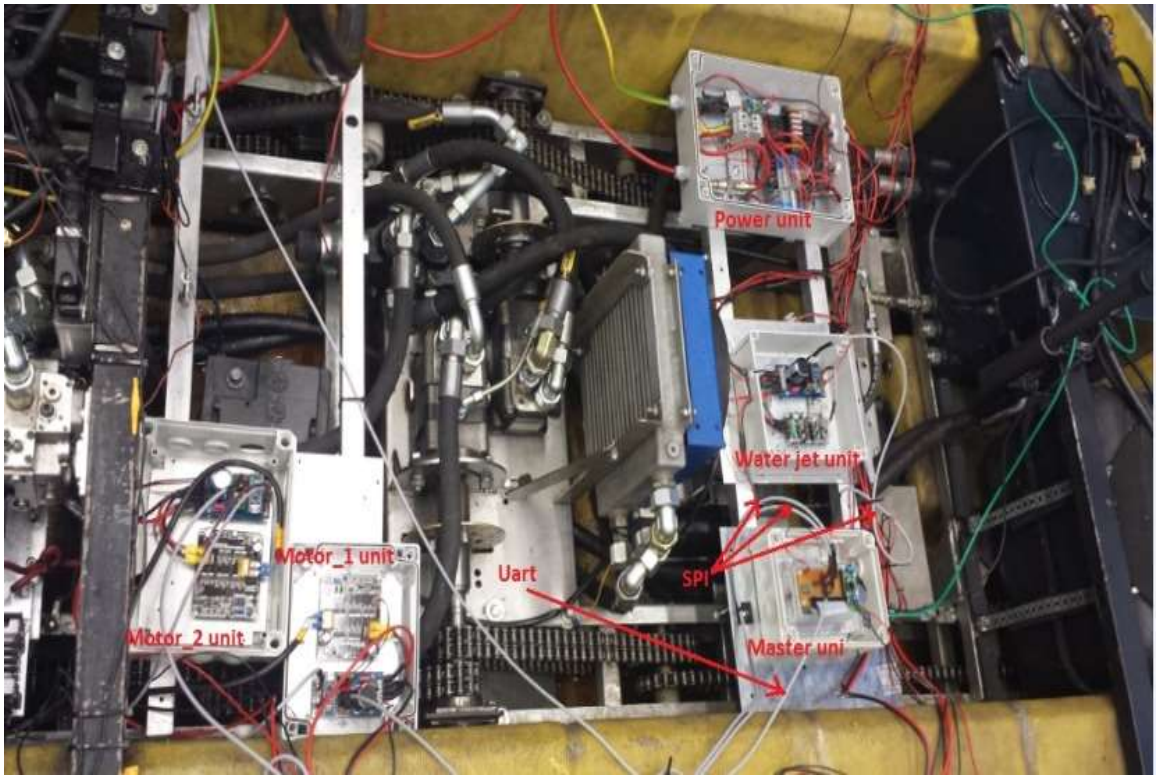


Figure 6.7 Network block diagram

### 6.5.1 Serial Peripheral Interface (SPI)

Serial peripheral interface (SPI) as shown in figure 6.8 is one of the most commonly used serial protocols for both inter-chip and intra-chip low/medium speed data-stream transfers. It is used to communicate between a microcontroller and other devices like external EEPROMs, DACs, ADCs, etc. In the world of communication protocols, SPI is often considered as little communication protocol. It is important not to forget the purpose of each protocol. Ethernet, USB, and SATA are meant for outside the box communications and data exchanges between whole systems while SPI is aptly suited for communication between integrated circuits for low/medium data transfer speed with on-board peripherals. In SPI the data exchange takes place between the master and the slave device. The master device provides a clock signal to attain synchronisation. The instance of when the data can change and when the data is valid for reading is controlled by the clock signal. The clock line is controlled by the master device. Data transfer happens only when there is a clock chang. During the case of a device transmitting a data, the incoming data must be read before an attempt to transmit again, an exchange of data always takes place between the devices. In SPI protocol, a device cannot be just a transmitter only device or a receiver only device. The master device controls the clock line SCK and the data exchange between the devices are controlled by SCK clock line. The working of the SPI module is essentially based on the contents of an eight-bit serial shift register present in both the Master and the Slave. The transmissions take place based on the clock signal, which is generated by the master. The Master, when it wants to send a byte of data to the Slave, places the byte in its shift register and similarly, the Slave can place the content in its shift register. As eight clock pulses are generated, the bits contained in the Master's shift register are transferred by means of the MOSI line to the Slave's shift register and the slave transfers its shift register content by means of the MISO signal line back to the master. So the contents of the two shift registers get exchanged. SPI uses the following signals for transmissions across its interface:

SS: This stands for Slave Select. When it goes high, the corresponding slave device will be selected. The slave select line is used by master device to select which slave to initiate communication with the master.

SCK: This stands for serial clock. This signal synchronises the transmissions taking place across the bus.

MOSI: It is serial single bit data line, which the SPI master generates based on internally shifted value of the master data register.

MISO: It is serial single bit data line, by which the SPI slave communicates with the master. It sends out the serially shifted out bits from the slave data register [Choudhury, S., et al., 2014].

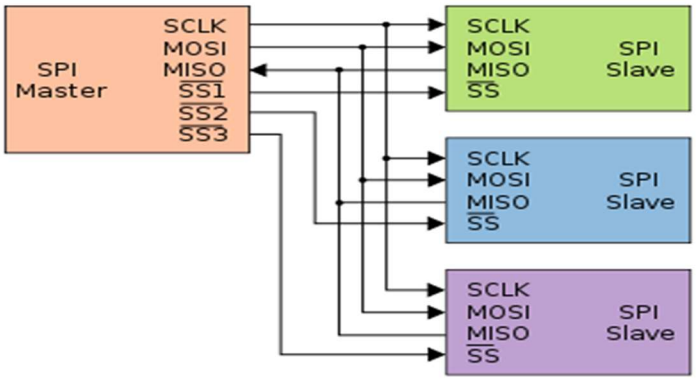


Figure 6.8 Serial peripheral interfaces

### 6.5.2 Serial Communication

A uenevesal asynchronouse receiver transmitter is an integrated circuit that plays the most important role in serial communication. A UART is a circuit that sends parallel data through serial lines. UARTs are used in association with the serial communication EIA standard RS-232 or RS-425. The main function of a UART is parallel-serial conversion during transmission and serial-parallel conversion during reception. In contrast, parallel communication needs a multi-bit address bus and is convenient only for short distance transmission. Serial communication is another means used widely because of its simple design and long possible transmission distance. The communication parameters such as baud rate and synchronisation error also have great impact on system performance, in order to overcome these difficulties, a UART controller can be designed which can transmit and receive data between equipment with different baud rates; the fact that a clock signal is not sent with the data complicates the design of a UART. Figure 6.9 shows the block diagram of serial communication between two computers using UART. Basic UART communication needs only two signal lines (TxD, RxD) to achieve full-duplex serial data transmission. When transmitting, the UART converts the incoming multi-bit data stream into serial data stream and sends it serially via the TxD pin of RS232 [Kumar, S. 2013].

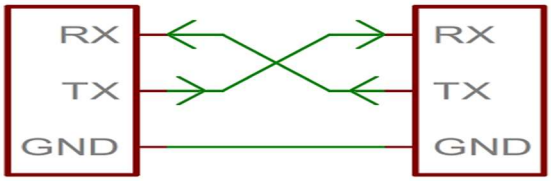


Figure 6.9 UART

## 6.6 Experiments and Results

The illustrated figures show the DC Motor angular position for motor 1 and 2 where each Motor controls the hydraulic pump swash plate position. These positions give us different hydraulic pump speeds and different robot speeds. Figure 6.10 shows the both motors in stop position where the robot is not working, figure 6.11 and 6.12 shows the DC Motors in different positions, this combination speed make the robot to skid right and figure 6.13 shows the DC Motors position to skid the vehicle left. Figure 6.15 shows the DC Motors in the same position but less angular position than the stop mode, this makes the swash plate open and the hydraulic motors and robot wheel will rotate forward, with this combination the robot will move forward. Figure 6.14 shows the robot in the backward driving mode. Figure 6.16 shows the swash plate angular position for both motors response to the input signal from the PC or from the Joystick, where the step response time is very short. Figure 6.17 shows the scene of the skid steering for right side in the real world, where a driving on the ground is achieved will figure 6.18 shows the skid steer for left side in the real world.

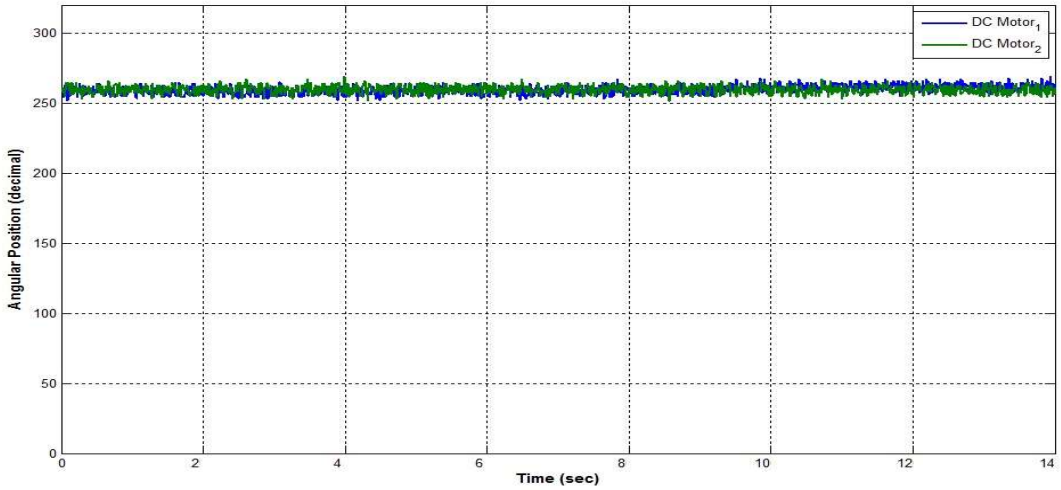


Figure 6.10 Swash Plate position in stop mode

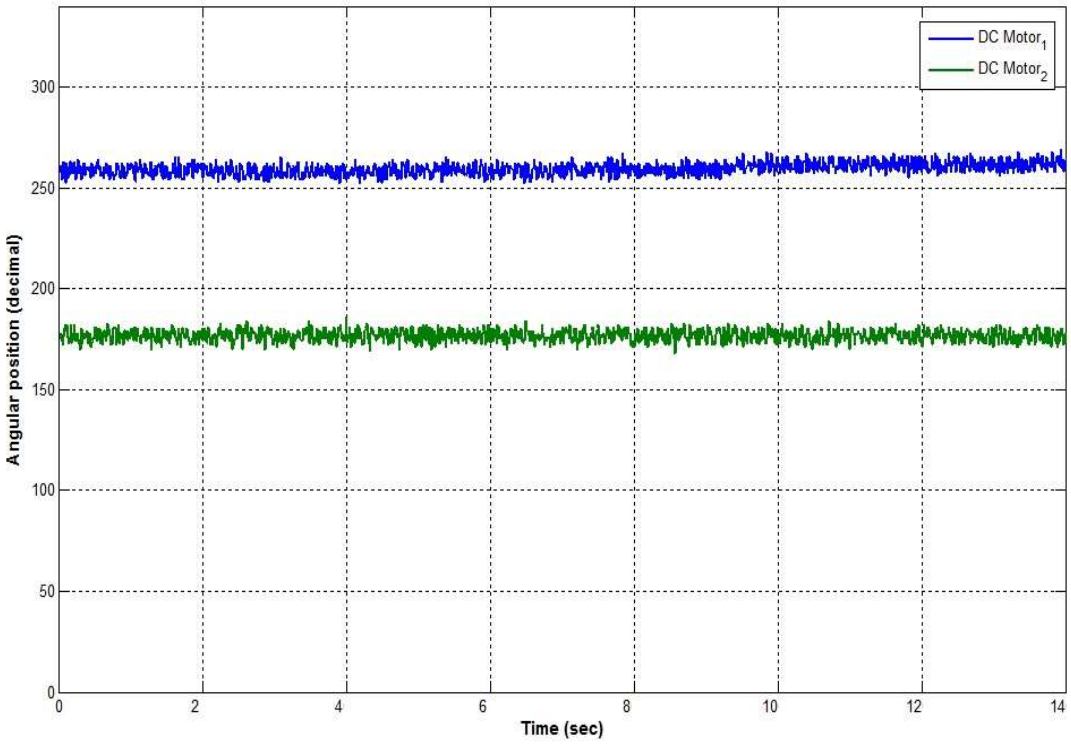


Figure 6.11 Swash Plate position in steer right mode

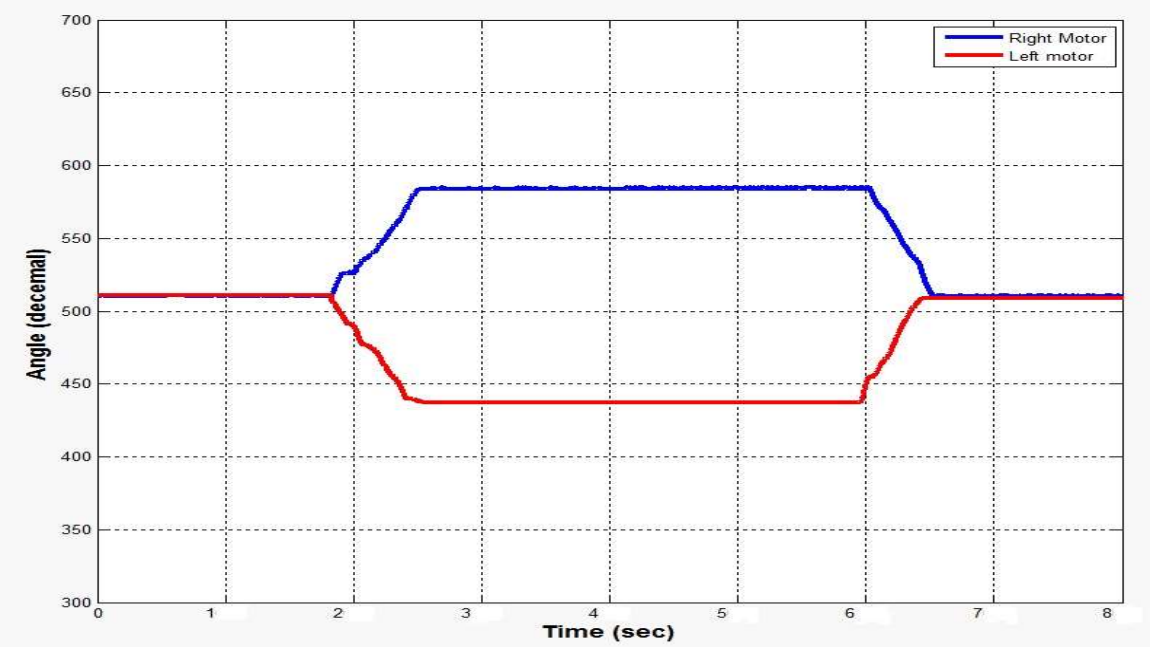


Figure 6.12 Swash Plate position in steer right mode

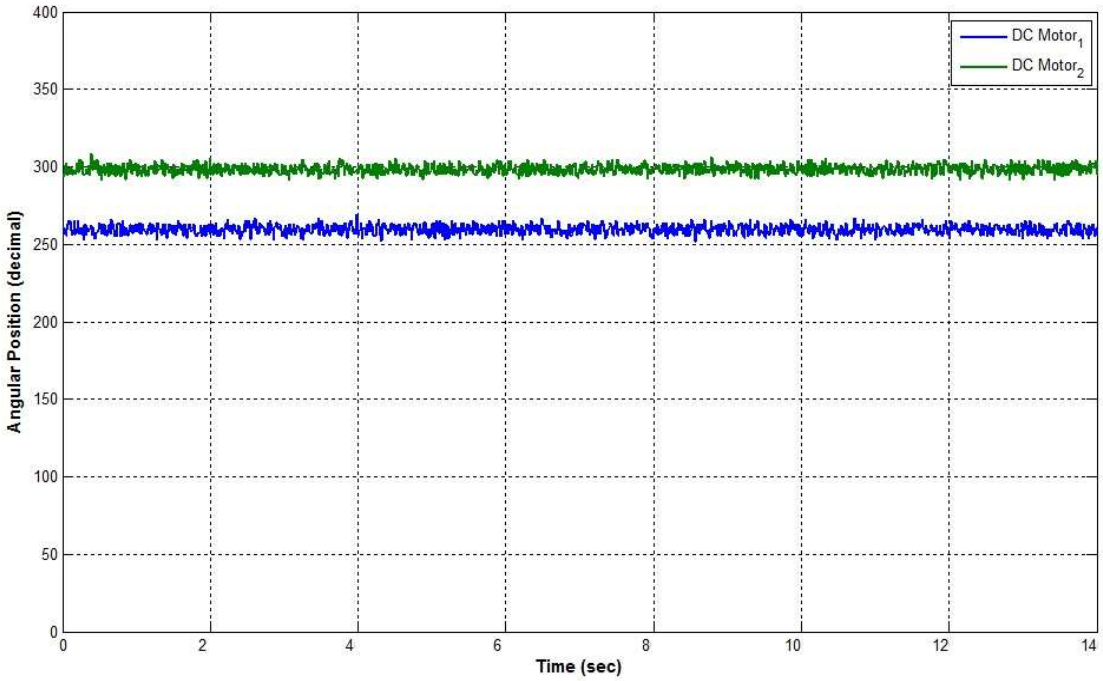


Figure 6.13 Swash Plate position in steer left mode

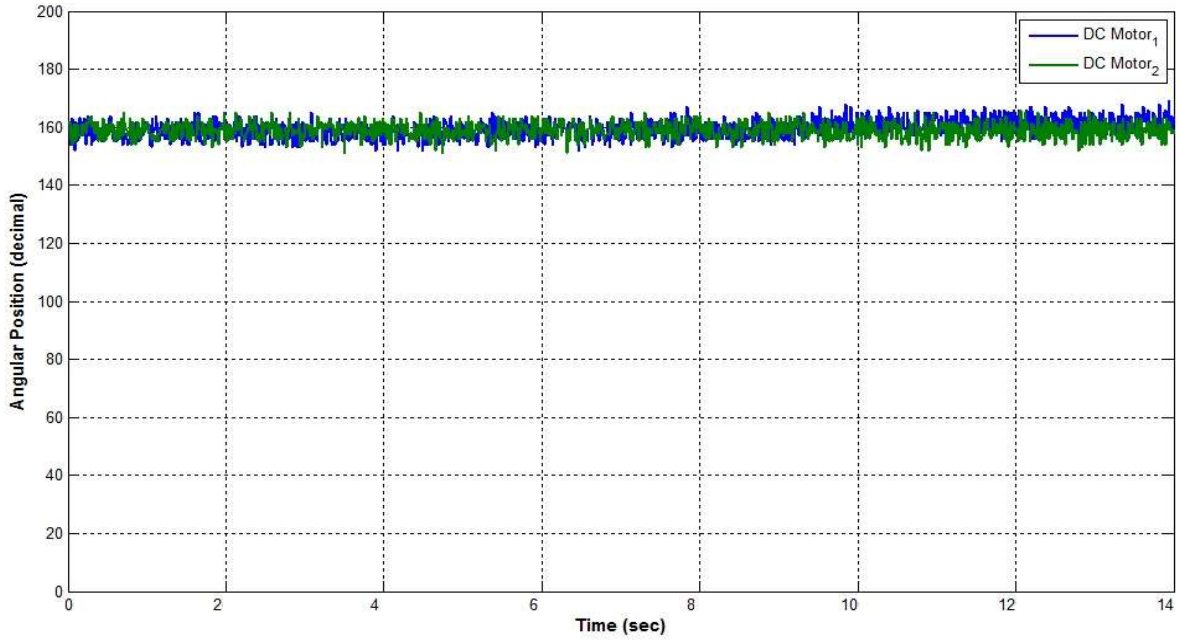


Figure 6.14 Swash Plate position in backward driving mode

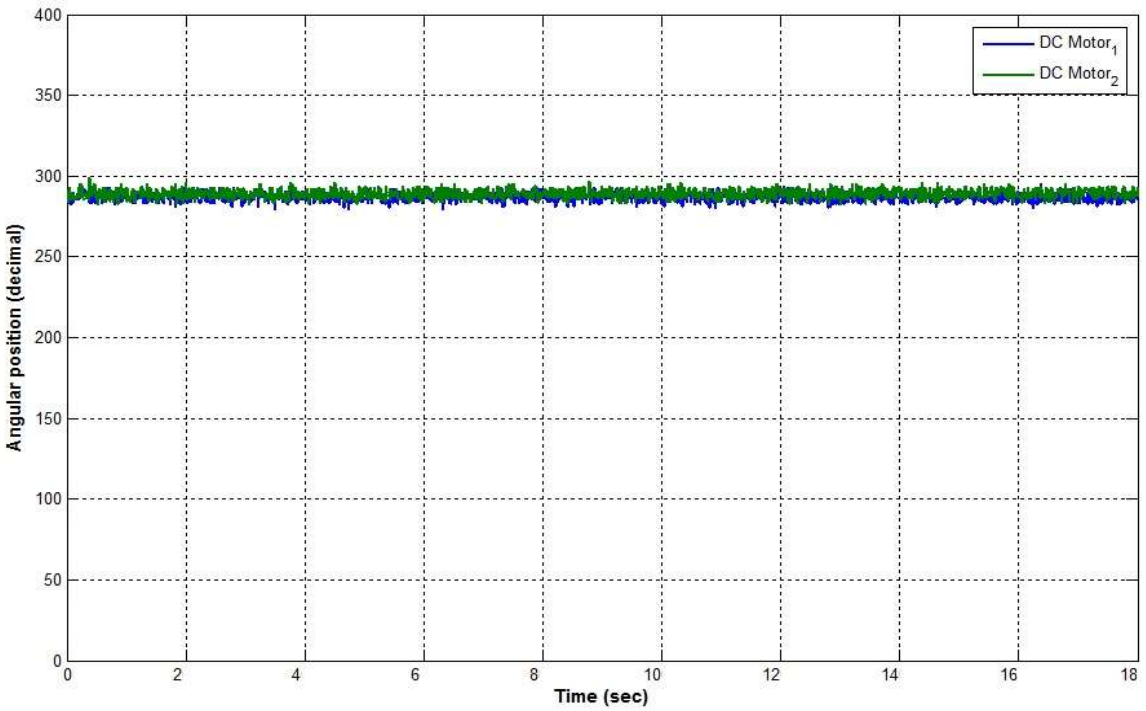


Figure 6.15 Swash Plate position in forward and middle speed

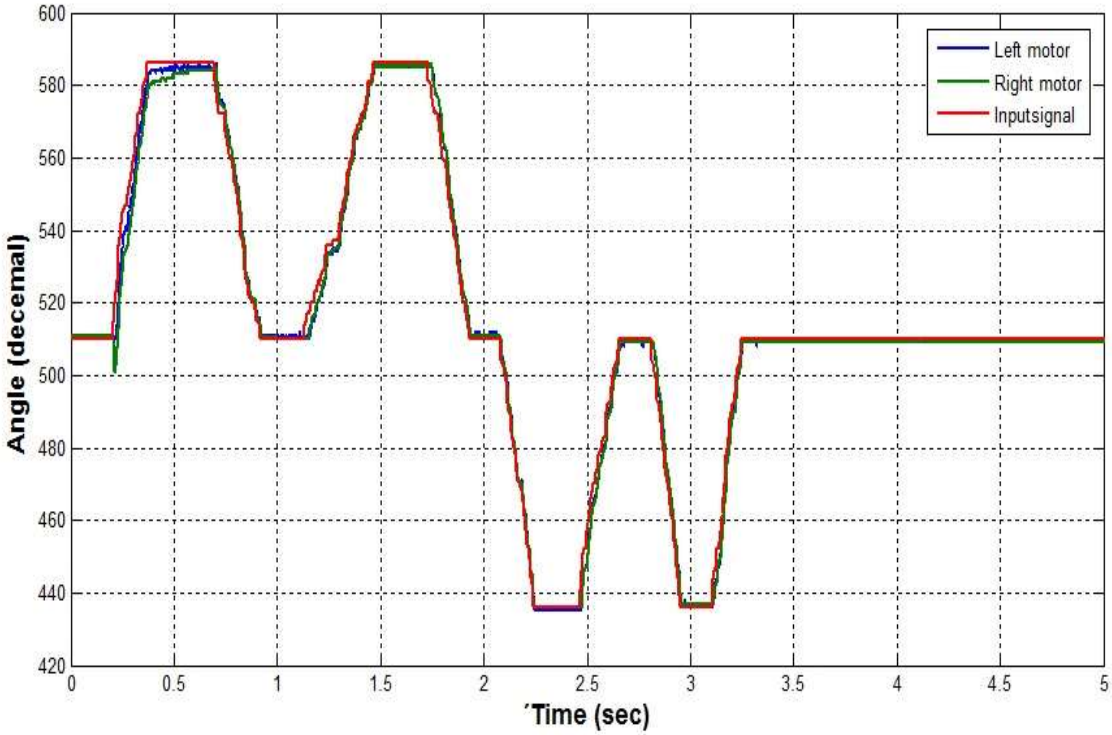


Figure 6.16 Swash plate response to the input signal

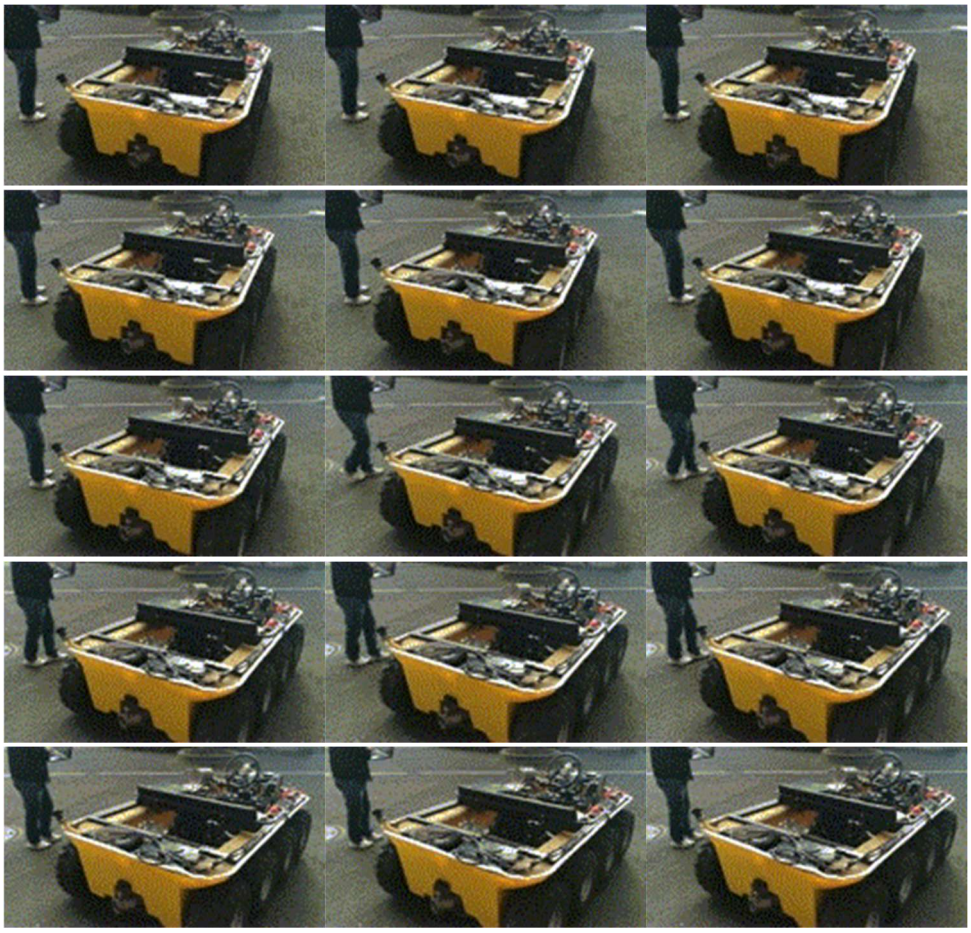

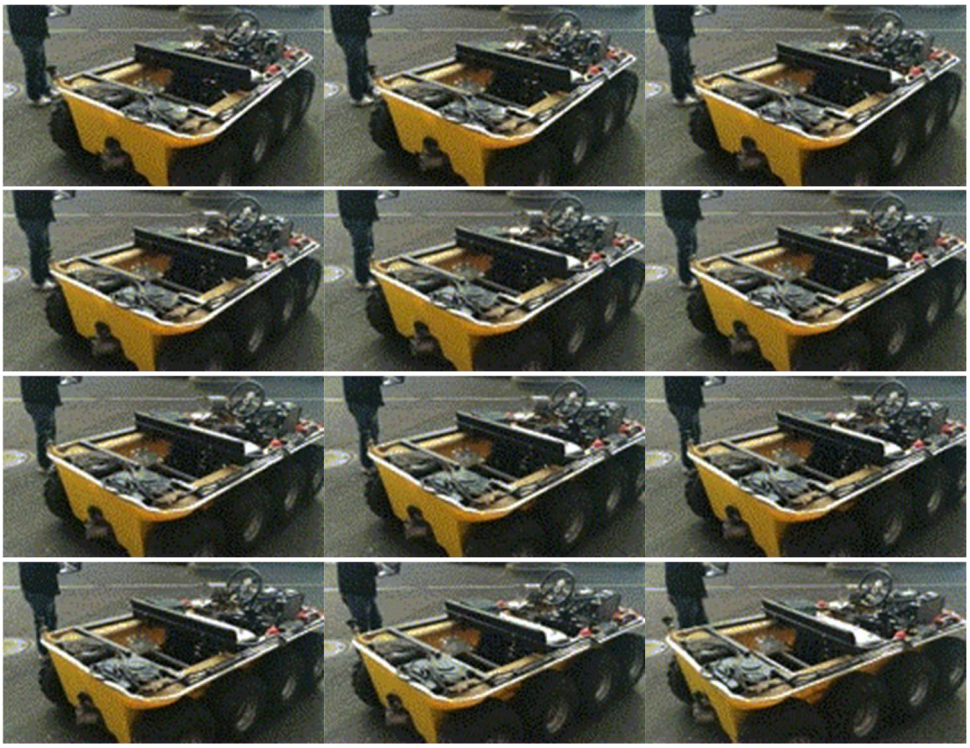

Figure 6.17 Right side skid steer scene

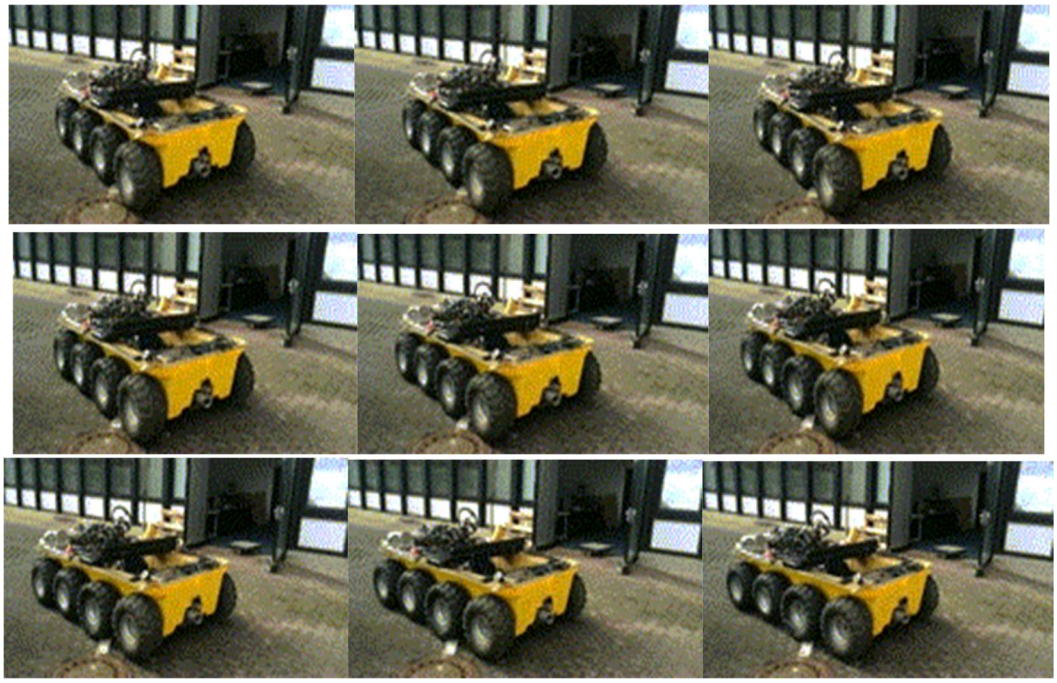

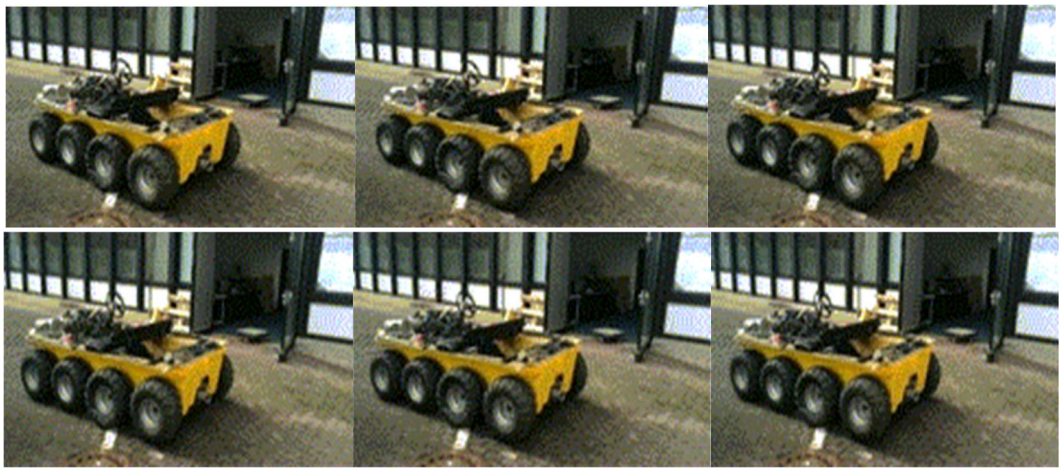

Figure 6.18 Left side skid steer scene

# Chapter 7

# Obstacle Avoidance using Fuzzy Logic Control System

When the Amphibious Autonomous Vehicle is moving in unknown and changing environment, the task of the Fuzzy logic system is to guide the robot without colliding with obstacles in the surrounding. For obstacle avoidance is a basic requirement of Autonomous Vehicle navigation, it is a key issue in Amphibious Autonomous Vehicle to design a fast and efficient obstacle avoidance navigation algorithm with the presence of obstacles, which needs to coordinate lots of sensors and actuators to work together. In general, the robot needs to acquire surrounding information via sensors onboard such as laser range finder that can be used to detect obstacles. In the past decades, researchers have exploited many obstacle avoidance navigation algorithms utilizing these sensors. Generally speaking, these methods can be divided into the following categories: model-based method, fuzzy logic method and reactive method based on neural network [Ren, L., et al., 2012]. The obstacle avoidance method based on fuzzy logic reacts quickly and is robust to sensor measuring errors. The algorithm proposed in this paper is on the foundation of fuzzy logic principle. Fuzzy logic intelligent obstacle avoidance strategy is addressed to solve obstacle avoidance problem for Amphibious Autonomous Vehicle tracking a target in unknown environment. Fuzzy obstacle avoidance controller strategy is based on a fuzzy reactive control principle to dominate robot's obstacle avoidance action, and run-to-goal fuzzy controller utilizes fuzzy control to dominate robot's approaching target action. When the robot is approaching the target with the presence of obstacles, run-to-goal fuzzy controller and fuzzy obstacle avoidance controller compete with each other. Therefore, intelligent coordinator is designed to coordinate the two actions mentioned above to generate robot's ultimate control command. Simulations and experiments validate the effectiveness and feasibility of the fuzzy intelligent obstacle avoidance control strategy presented in this chapter. Many works applied fuzzy logic systems to mobile robot a obstacle avoidance [Lian, S.H. 1996].

## 7.1 Steering Fuzzy Logic Controller Design

FLC is proposed to move the amphibious autonomous vehicle to its target smoothly. The inputs of FLC are the angle between the robot and the target (error angle), and the distance from the robot to the target. The outputs of FLC are the angular position of the hydraulic pump swash plate which controls the hydraulic motor speed. FLC is implemented with five membership functions for each input as illustrated in figures 7.1 and 7.2, these membership functions are for left Motor and right Motor can be the same [Faisal, M., et al., 2013].

The linguistic variables used for the angle between the robot and the targets (angle) are: L: Left, ML: Middle left, M: Middle, MR: Middle right and R: Right. The linguistic variables used for input distance are: Z: Zero, NZ: Near Zero, M: Medium, F: Far and VF: Very Far.

Angle = {R, MR, M, ML, L}

Distance {Z, NZ, M, F, VF}

FLC is implemented with five membership functions for each output as in figure 7.3 (Left Motor LM and Right Motor RM). The linguistic variables used for the fuzzy rules of FLC are: Z: Zero, S: Slow, M: Medium, H: High and VH: Very High. The membership functions rules for the left and the right motors are shown in table 7.1. LM Output = {Z, S, M, H, VH}. The fuzzy logic rule statements aimed at achieving a well-defined set of objectives are:

Motor_1 = RM, Motor_2 = LM

Rule 1: IF (angle is R) AND (distance is Z) THEN (Motor_1 is z) and (Motor_2 is h)

Rule 2: IF (angle is MR) AND (distance is Z) THEN (Motor_1 is z) and (Motor_2 is vh)

Rule 3: IF (angle is M) AND (distance is Z) THEN (Motor_1 is vh) and (Motor_2 is z)

Rule 4: IF (angle is ML) AND (distance is Z) THEN (Motor_1 is vh) and (Motor_2 is z)

Rule 5: IF (angle is L) AND (distance is Z) THEN (Motor_1 is h) and (Motor_2 is z)

Rule 6: IF (angle is R) AND (distance is NZ) THEN (Motor_1 is s) and (Motor_2 is vh)

Rule 7: IF (angle is MR) AND (distance is NZ) THEN (Motor_1 is z) and (Motor_2 is h)

Rule 8: IF (angle is M) AND (distance is NZ) THEN (Motor_1 is h) and (Motor_2 is z)

Rule 9: IF (angle is ML) AND (distance is NZ) THEN (Motor_1 is vh) and (Motor_2 is z)

Rule 10: IF (angle is L) AND (distance is NZ) THEN (Motor_1 is vh) and (Motor_2 is z)

Rule 11: IF (angle is R) AND (distance is M) THEN (Motor_1 is m) and (Motor_2 is vh)

Rule 12: IF (angle is MR) AND (distance is M) THEN (Motor_1 is s) and (Motor_2 is vh)

Rule 13: IF (angle is M) AND (distance is M) THEN (Motor_1 is S) and (Motor_2 is S)

Rule 14: IF (angle is ML) AND (distance is M) THEN (Motor_1 is h) and (Motor_2 is S)

Rule 15: IF (angle is I) AND (distance is M) THEN (Motor_1 is M) and (Motor_2 is M)

Rule 16: IF (angle is R) AND (distance is NF) THEN (Motor_1 is m) and (Motor_2 is m)

Rule 17: IF (angle is MR) AND (distance is NF) THEN (Motor_1 is S) and (Motor_2 is S)

Rule 18: IF (angle is M) AND (distance is NF) THEN (Motor_1 is S) and (Motor_2 is S)

Rule 19: IF (angle is ML) AND (distance is NF) THEN (Motor_1 is s) and (Motor_2 is s)

Rule 20: IF (angle is L) AND (distance is NF) THEN (Motor_1 is m) and (Motor_2 is m)

Rule 21: IF (angle is R) AND (distance is F) THEN (Motor_1 is h) and (Motor_2 is h)

Rule 22: IF (angle is MR) AND (distance is F) THEN (Motor_1 is h) and (Motor_2 is h)

Rule 23: IF (angle is M) AND (distance is F) THEN (Motor_1 is m) and (Motor_2 is m)

Rule 24: IF (angle is ML) AND (distance is F) THEN (Motor_1 is h) and (Motor_2 is h)

Rule 25: IF (angle is L) AND (distance is F) THEN (Motor_1 is h) and (Motor_2 is h)

The all fuzzy logic Rules for the left and right motor illustrates in figure 7.6 and 7.7. The relationship between the two inputs and the output shows in figure 7.4 and 7.5.

Table 7.1 Fuzzy rules for obstacle avoidance

| Angle / Dis. | R | MR | M | ML | L |
|---|---|---|---|---|---|
| **Z** | $LM^{z}$ | $LM^{z}$ | $LM^{h}$ | $LM^{vh}$ | $LM^{h}$ |
| | $RM^{h}$ | $RM^{vh}$ | $RM^{z}$ | $RM^{z}$ | $RM^{z}$ |
| **NZ** | $LM^{s}$ | $LM^{z}$ | $LM^{vh}$ | $LM^{vh}$ | $LM^{vh}$ |
| | $RM^{vh}$ | $RM^{h}$ | $RM^{z}$ | $RM^{z}$ | $RM^{s}$ |
| **M** | $L^{Mm}$ | $LM^{s}$ | $LM^{s}$ | $LM^{h}$ | $LM^{m}$ |
| | $RM^{vh}$ | $RM^{vh}$ | $RM^{s}$ | $RM^{s}$ | $RM^{m}$ |
| **NF** | $LM^{m}$ | $LM^{s}$ | $LM^{s}$ | $LM^{s}$ | $LM^{m}$ |
| | $RM^{m}$ | $RM^{s}$ | $RM^{s}$ | $RM^{s}$ | $RM^{m}$ |
| **F** | $LM^{h}$ | $LM^{h}$ | $LM^{m}$ | $LM^{h}$ | $LM^{h}$ |
| | $RM^{h}$ | $RM^{h}$ | $RM^{m}$ | $RM^{h}$ | $RM^{h}$ |

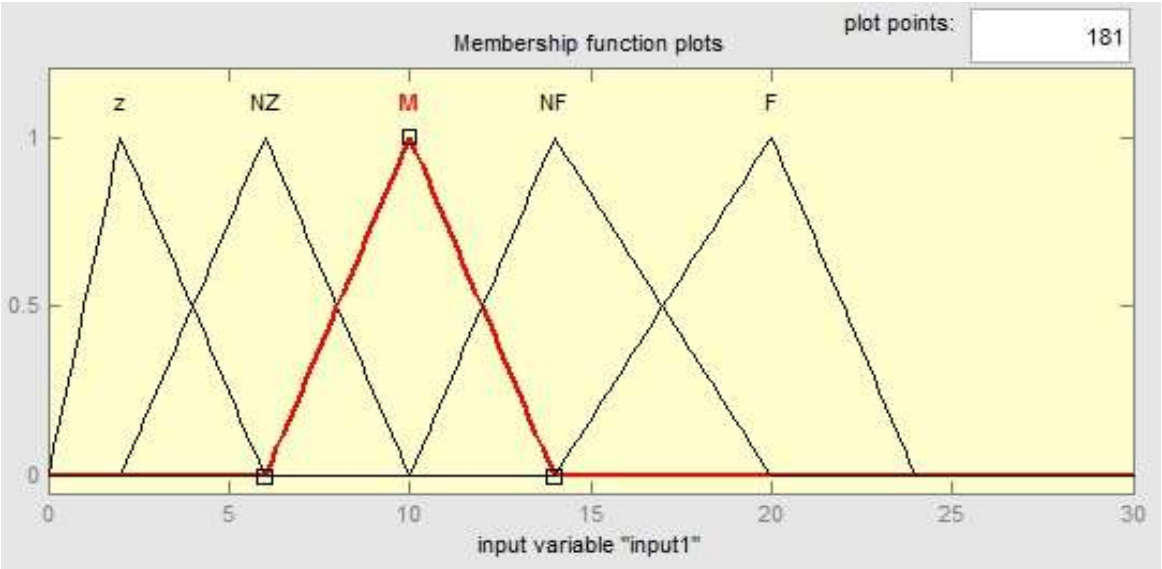


Figure 7.1 Membership function for input_1 (distance)

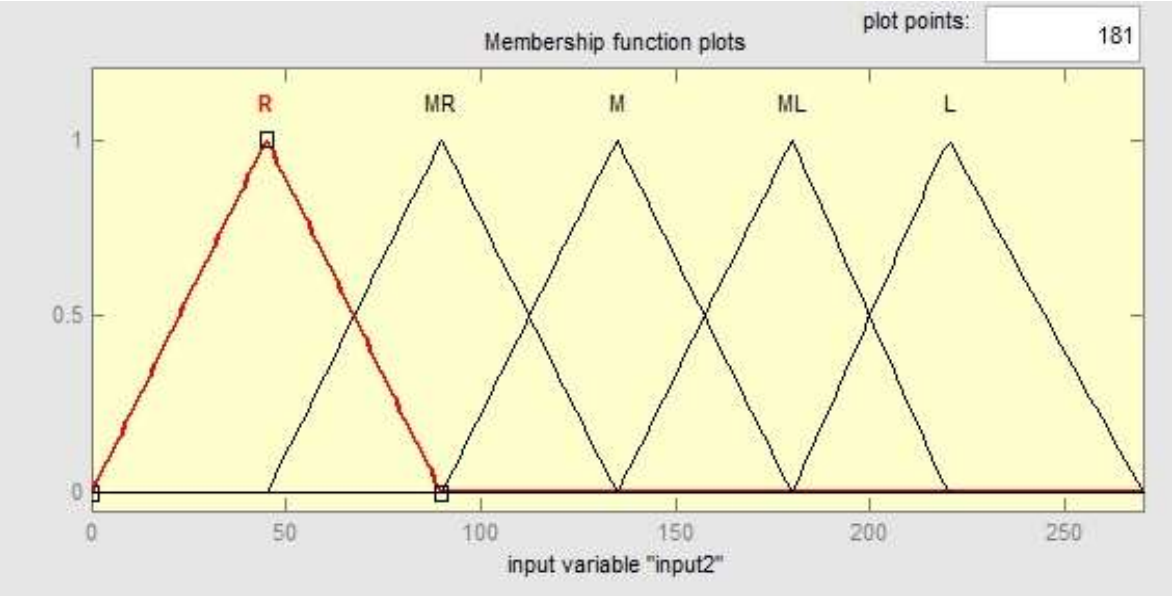


Figure 7.2 Membership function for input_2 (angle)

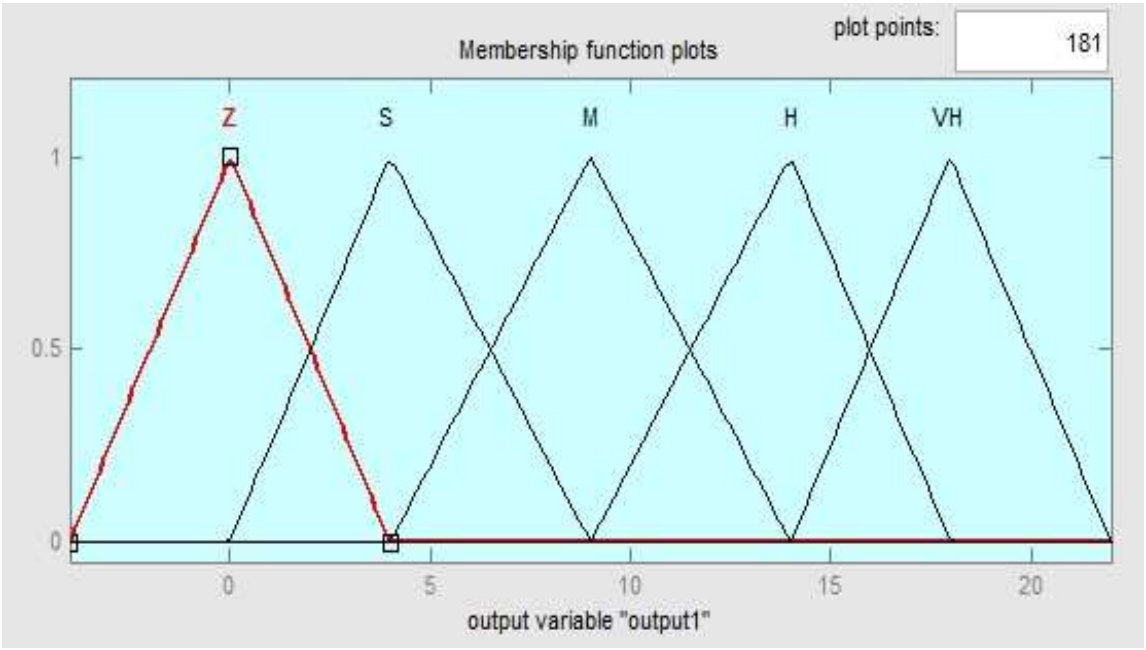


Figure 7.3 Membership function for output (Swash plate position)

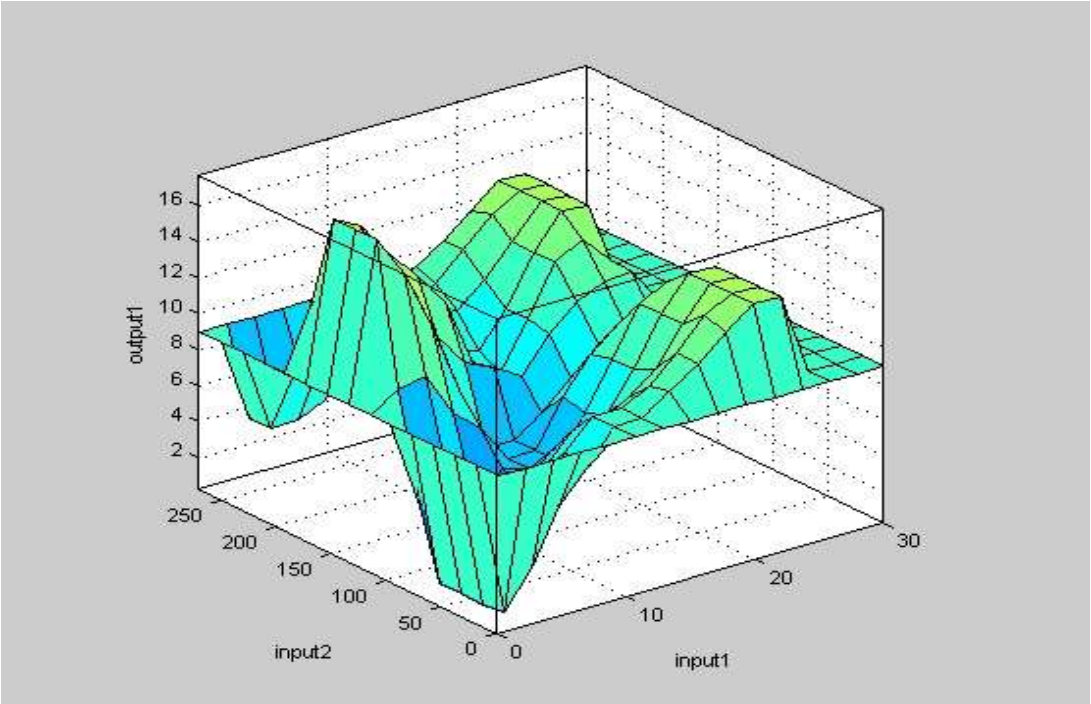


Figure 7.4 Fuzzy Logic surface for right motor

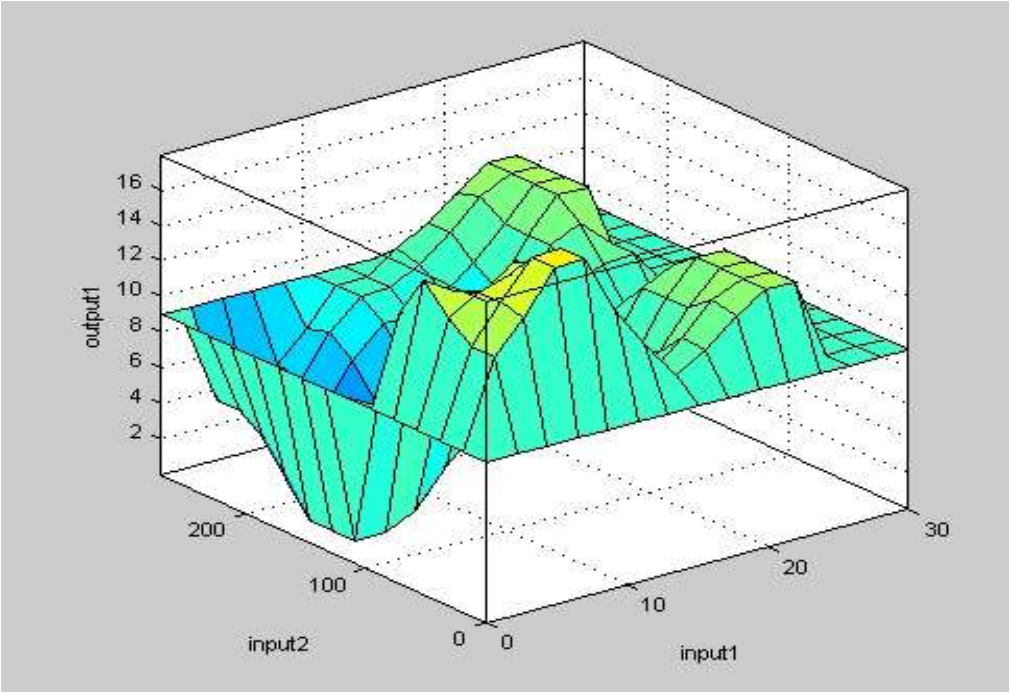


Figure 7.5 Fuzzy Logic surface for left motor

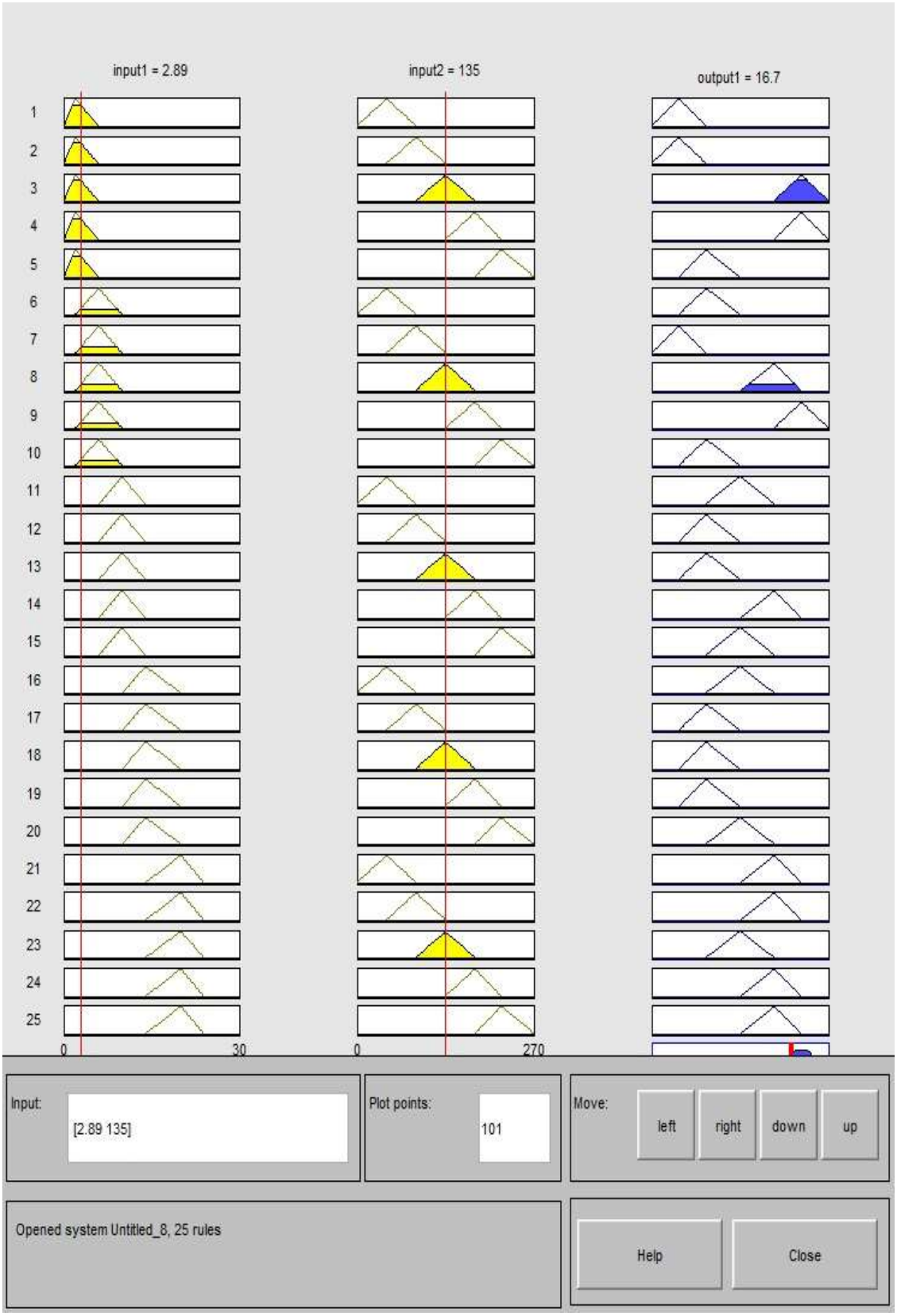


Figure 7.6 Fuzzy Logic rule for left motor

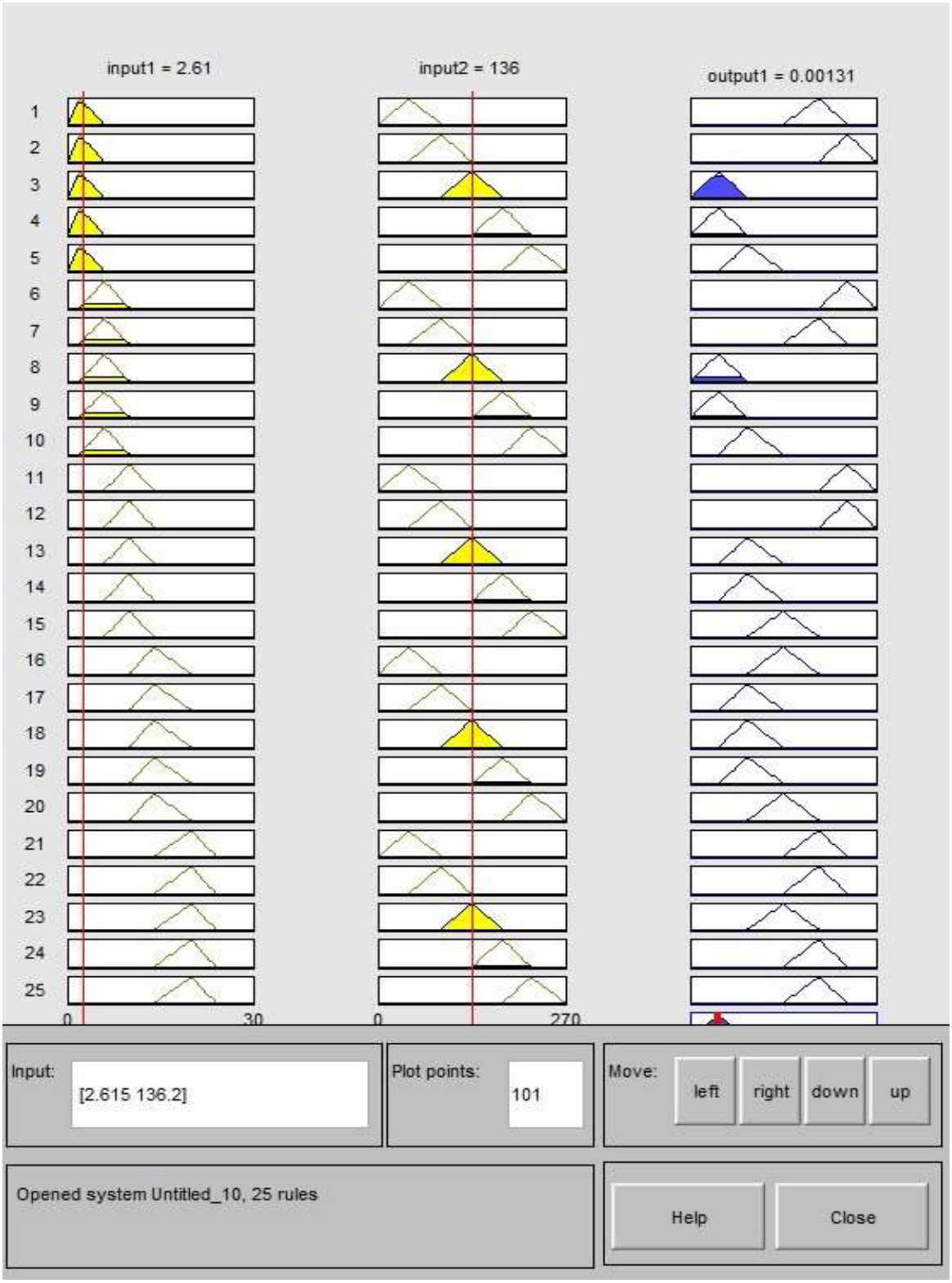


Figure 7.7 Fuzzy Logic rule for right motor

## 7.3 Strategy of Obstacle Detection

It is important to define what an obstacle is before we discuss how an obstacle may be detected. We define an obstacle as something that will cause dangerous or undesirable behaviour if hit by the host vehicle. Three general classes of obstacles are:

1. people
2. vehicles
3. roadway obstacles

The third class of obstacles can include anything like a rock lying in the middle of Vehicle road or at the sides of the Vehicle road. An object should only be considered an obstacle as shown in figure 7.8 if the host vehicle will probably collide with that object in the near future. For example, on a regular suburban road, parked cars are not obstacles, but the slow moving vehicle in-front is. This rather obvious statement has a very significant implication for an obstacle detection system i.e. an obstacle detection system must have some idea of how its host vehicle will move in the future in order to declare a detected object an obstacle [Roberts, J., et al., 2013].

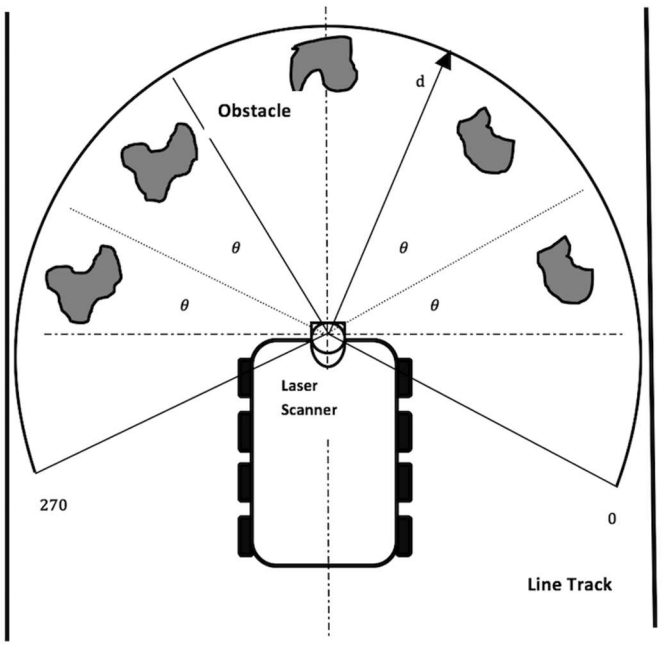


Figure 7.8 Obstacle detection strategy

## 7.3 Laser Scanner

In a Hokuyo UTM-30LX Laser Scanner as in figure 7.10 Processing section we get the raw data from the laser scanner as shown in figure 7.9. Then we cluster the data given by the laser scanner by a clustering algorithm, on that basis we get the distance and angle of the obstacles. The laser scanner gives us a field of view showing the complete 270° sweep made by the laser beam as shown in figure 7.9. The laser beam starts from the right and goes to the left. So at every angle, depending on the resolution set, we can get the distance and position of the objects along the robot's path; with these values we know exactly at what angle an obstacle is present and what its size is. The fuzzy logic can then decide the path the robot must follow and the angle it must turn to avoid the obstacle.

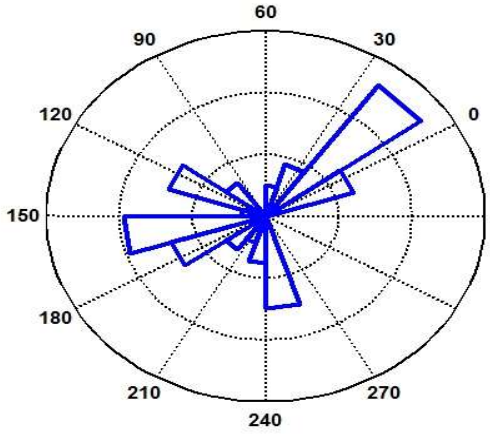


Figure 7.9 Laser scanner pattern

Figure 7.10 Hokuyo laser scanner

## 7.4 Experiments and Results

The performance of the fuzzy controller has been tested in real time, under different working conditions. Before that the system was simulated using Matlab Tools as shown in 7.11. The simulation results from Matlab/Simulink show the hydraulic pump swash plate angle for hydraulic pump_1 (right side) and hydraulic pump_2 (left side) for different inputs. Figure 7.12 shows the swash plate angles when the obstacle is on the right side and the distance is near zero, the hydraulic pump_2 will close and hydraulic pump_1 will open causing the vehicle to skid away from the obstacle to the left side. Figure 7.13 shows the swash plate angles for middle left side and the distance is in middle, the hydraulic pump_1 is in the small angle (small speed) and hydraulic pump_2 in high speed this will cause the vehicle to skid away to the right side and avoid the obstacle. Figure 7.14 and figure 7.15 show the real swash plate angle for the simulated result discussed above. Figure 7.16 shows the Vehicle during skid left when the obstacle is on the right side and figure 7.17 shows the vehicle during skid to the right when the obstacle is on the left side. Figure 7.18 shows the flow chart for obstacle avoidance, which was implemented on the robot.

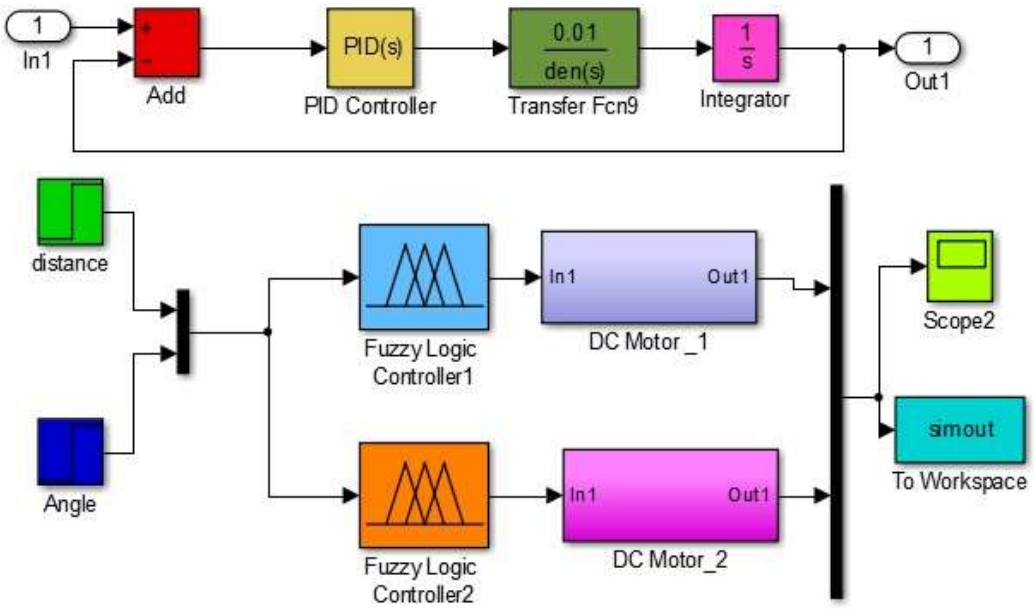


Figure 7.11 Hokuyo Laser Scanner

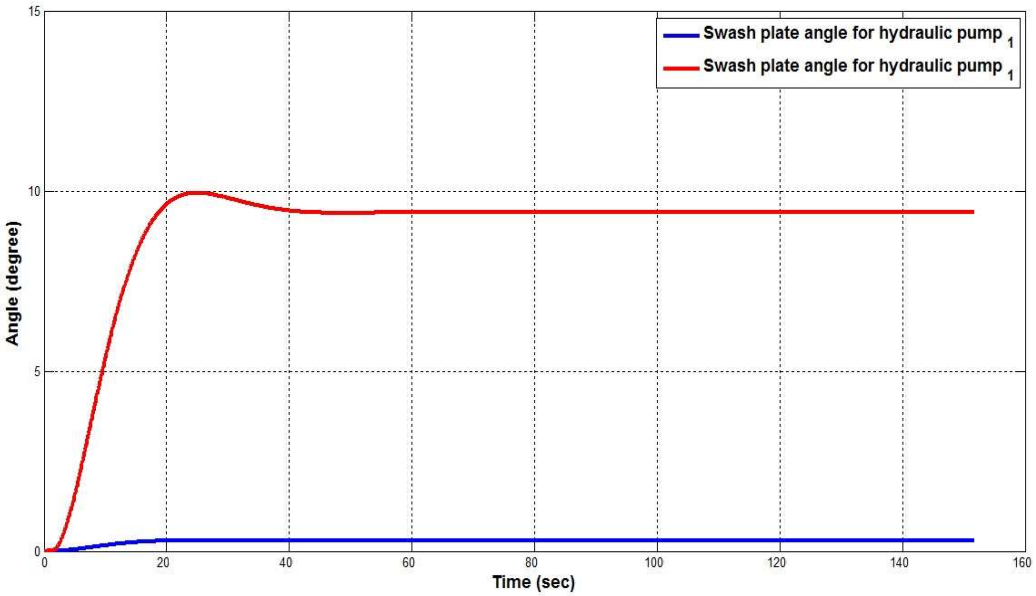


Figure 7.12 Simulation Block diagram of Fuzzy Logic Controller(obstacle case)

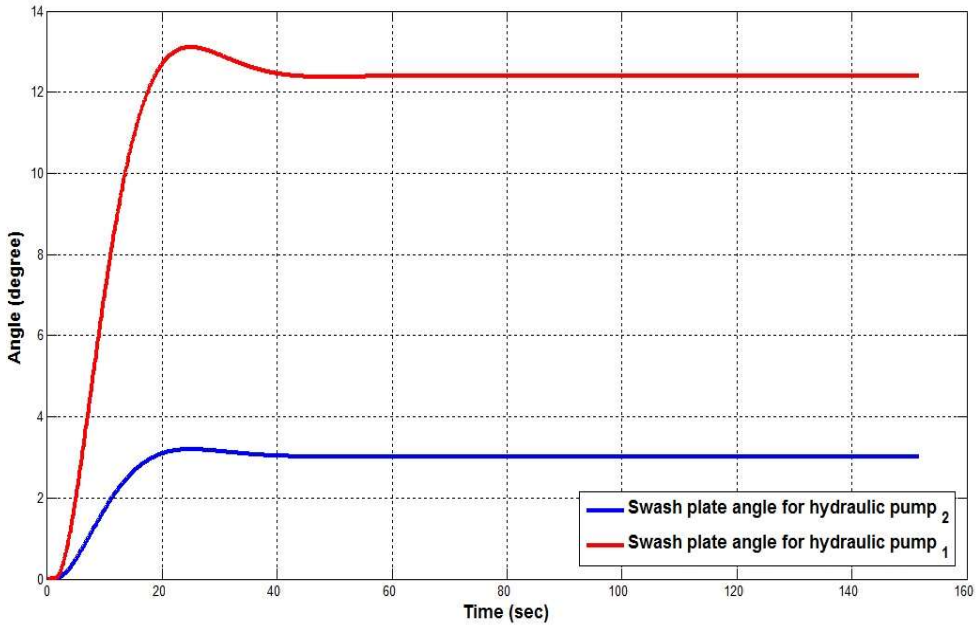


Figure 7.13 Swash plate angle for hydraulic pump 1_2 (Simulation)

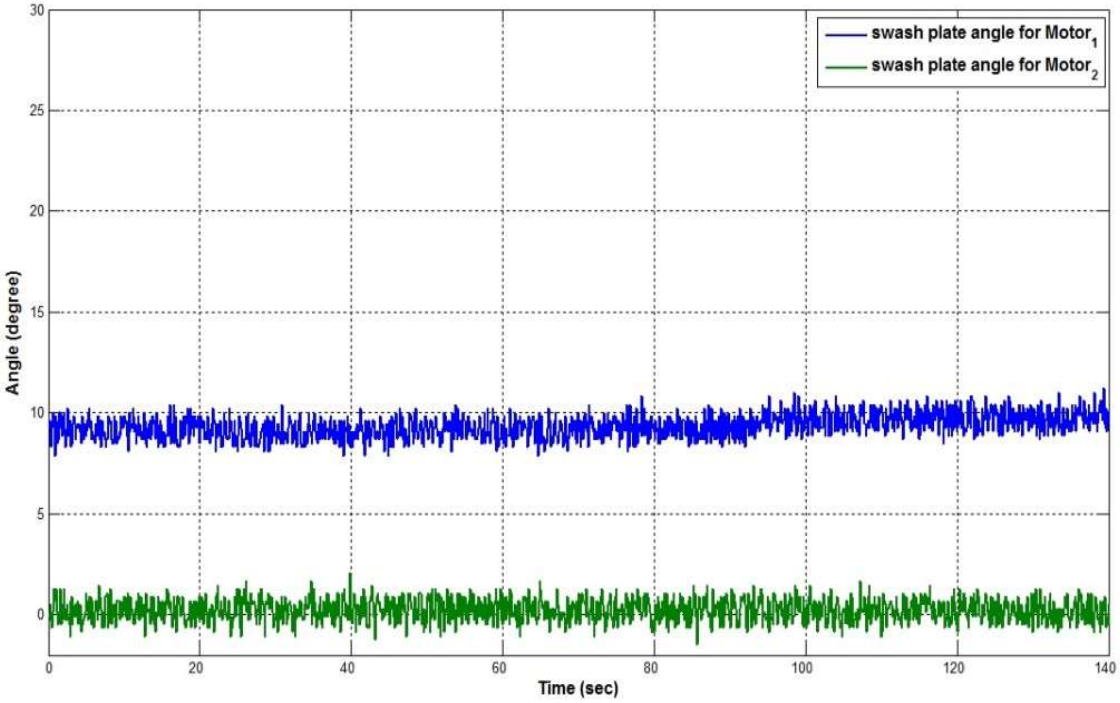


Figure. 7.14 Swash plate angle for hydraulic pump 1_2 (Experiment)

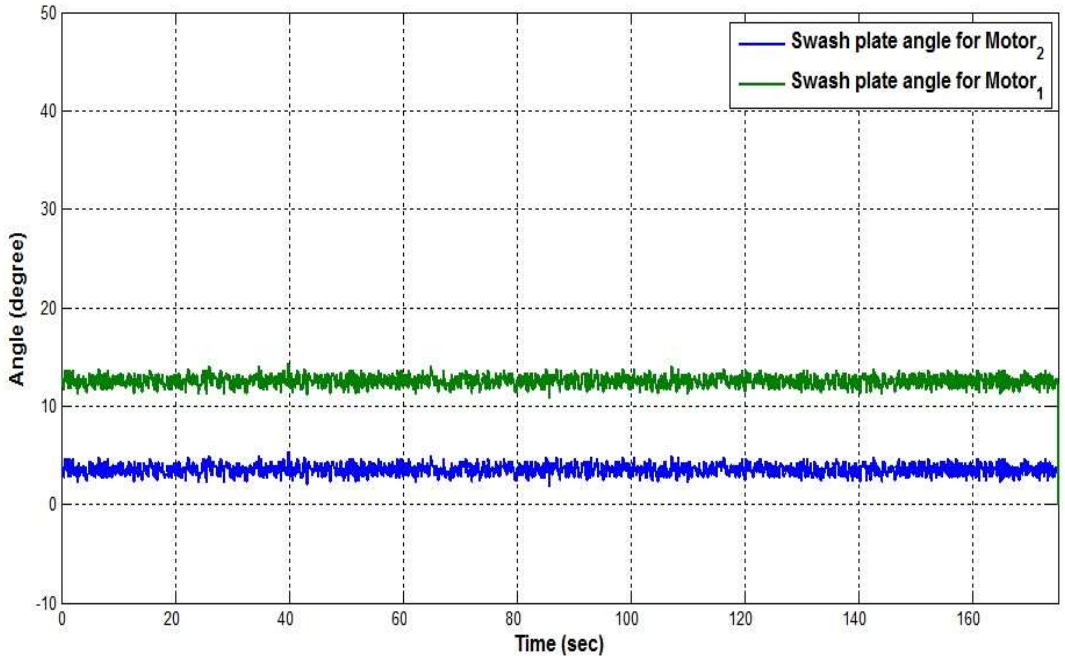


Figure. 7.15 Swash plate angle for hydraulic pump 1_2 (Experiment)

Figure 7.16 Obstacle on the right side (Experiment)

Figure 7.17 Obstacle on the left side (Experiment)

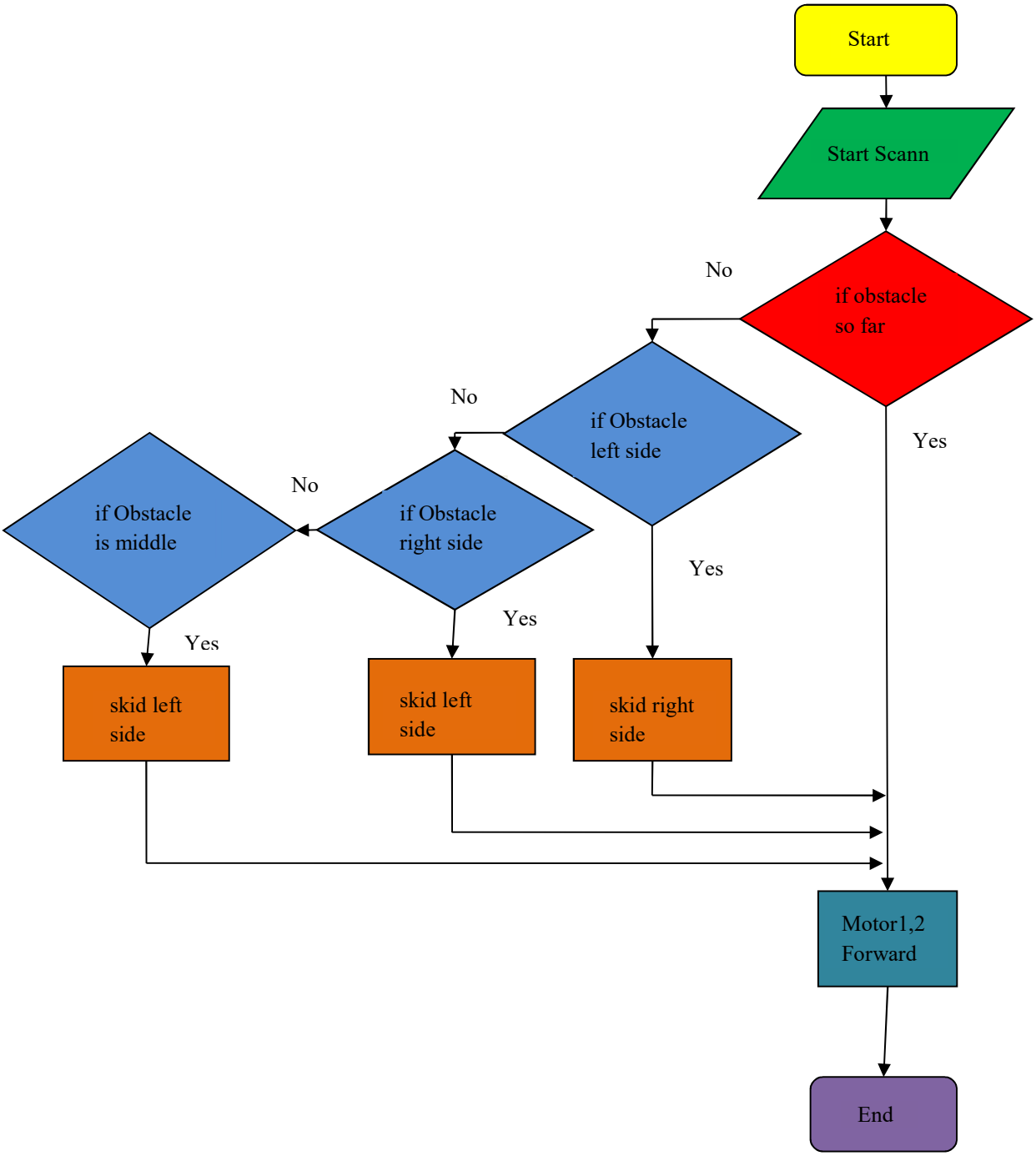


Figure 7.18 Obstacle avoidance flow chart

# Chapter 8

# Water Jet Control System

The main principle of a water jet engine is to take advantage of Newton's third law of motion. To every action there is always an equal and opposite reaction. By creating a jet stream of the fluid, the jet stream will produce a forward motion in the opposite direction of the jet stream. One of the basic amphibious vehicle systems, which have a decisive meaning for effectiveness and safety of navigation, is propulsion and steering system. Several kinds of propulsion systems are applied on board modern inland waterways ships as mention down [Dymarski, C. 2007]:

• Conventional one fitted with a combustion engine, toothed gear and fixed or controllable pitch propeller

• Combustion-electric one fitted with an electric transmission and frequency converter, making it possible to variably control rotational speed of the propeller, which may be fixed one

• Combustion-hydraulic one fitted with a hydrostatic transmission and fixed propeller

• Propulsion system fitted with two azimuthally propellers (rotatable thrusters) driven by combustion engines through a toothed, electric or hydrostatic transmission

• Propulsion system fitted with cycloid (Yoith-Schneider) propellers

• Propulsion system fitted with water jet propellers

## 8.1 Combustion-Hydraulic Propulsion System

Figure 8.1 shows schematic diagram of the propulsion system fitted with hydrostatic transmission. The system is driven by a gasoline engine type, Suzuki. The engine, through a flexible coupling, directly drives unit of two variable displacement pumps, the right Pump feeding a fixed displacement hydraulic motor as in figure 8.3 through 6/2 Directional Valve as shown in figure 8.2.

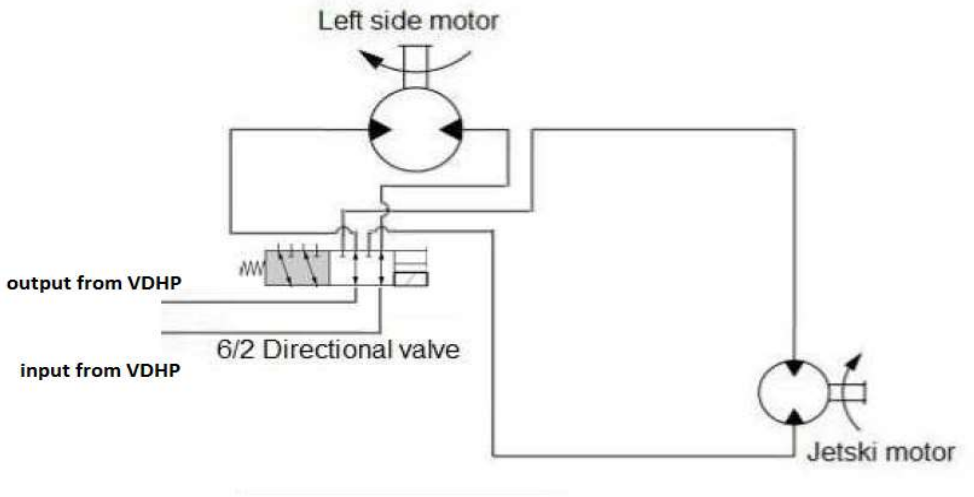


Figure 8.1 Hydraulic circuit of water jet

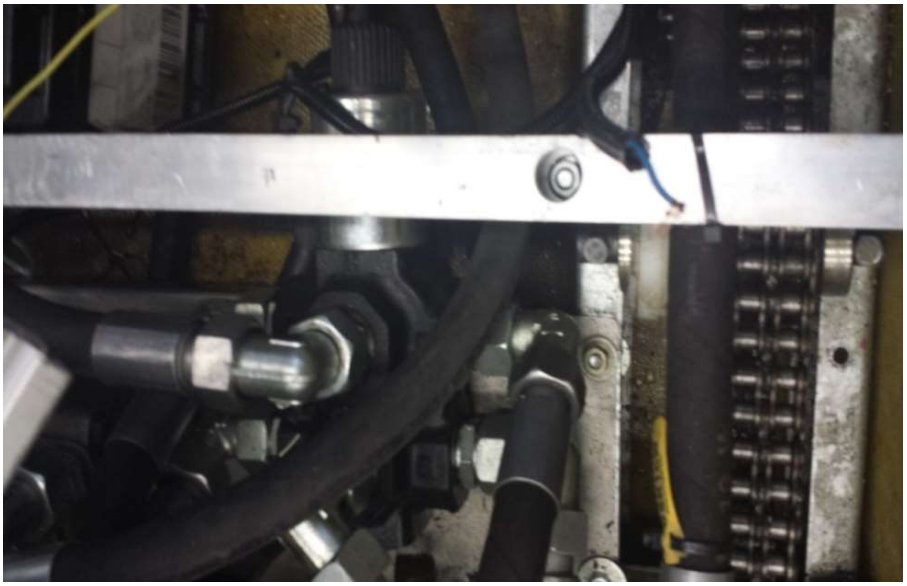

Figure 8.2 6/2 Directional valve


Figure 8.3 Fixed displacement hydraulic motor

The steering unit provides manoeuvrability of the Amphibious Vehicle by redirecting the jet stream. This is achieved by adding a box outside the nozzle that the jet stream can pass through as shown in figure 8.4. The box rotates around its point of attachment and redirects the jet stream in the desired direction by using electrical motor provided with position sensor and linear actuator, by doing this the thrust will push the boat and steering is achieved. Controlling the DC Motor position is achieved using a traditional PID controller and to activate the water jet system, the engine servo, the hydraulic pump motors, the solenoid valve and the Steering Motor should be active. The flow chart in figure shows the signal flow for the water jet system. [Örtegren, V. 2014]

Figure 8.4 Water jet steering box

## 8.2 Water Jet Layout

Water jet installation as used in commercial applications can be divided into four components: the inlet, the pump, the nozzle and the steering device. Figure 8.5 shows typical water jet installation with the main components displayed. The main component is the pump, which delivers the moment to produce the jet at the nozzle exit. In general the stator bowl and the nozzle are integrated in one part, the combination of the pump unit and the nozzle is regarded as the water jet pump. Downstream of the nozzle there is a steering device, which can deflect the jet in order to create steering and reversing forces. There are also installations for the deflection of the jet, possible with only the reversing option; this can be useful for quick crash-stop manoeuvres. If the water jet has no steering device at all, it is called booster water. [Bulten, N.W.H. 2006]

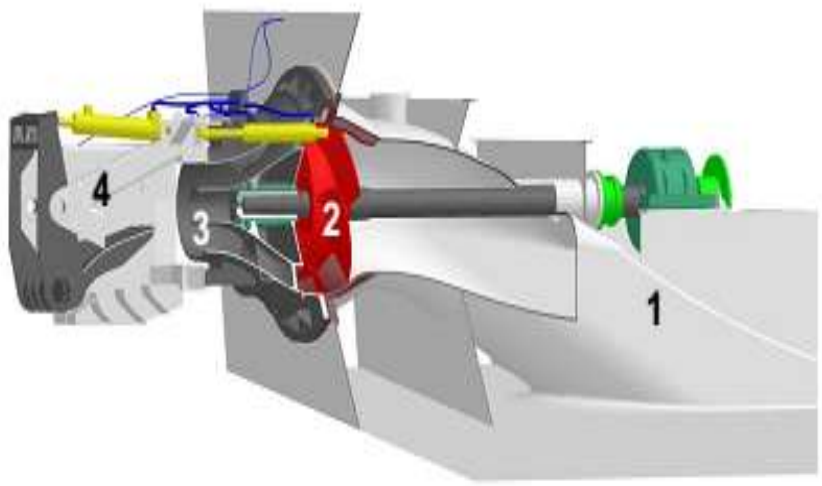


Figure 8.5 Typical water jet

## 8.3 Modelling of Water Jet Control System

The application of water jets is rapidly growing and they are increasingly being chosen for propulsion in high-speed crafts. Water jet as a propulsion system for amphibious vehicles is also favourable when it comes to manoeuvring, appendage drag, draft and fuel consumption at high speeds. Furthermore, water jet system has recently gained more credibility for its acceptable efficiency because of the advent of more efficient and large pumps.

A water jet is operated by the gasoline engines that drive a hydrostatic transmission system attached with it a jet water pump. Water is taken in through a water pick up on the bottom

of the water jet, drawn into an internal propeller (an impeller) that creates a jet of high pressure water which exits through a nozzle on the back of the water jet.

The selection of water jet propulsion pump needs to determine the main parameters: pump flow pressure head spout area and pump type. The equilibrium equations considering main engine water jet propulsion system and hull are as follows Thrust equation is [Li, B., et al, 2013]:

$$T = \rho Q(V_j - V_i) \tag{8.1}$$

Power Equilibrium equation is

$$P_i = \gamma Q \frac{H}{\eta_p} \tag{8.2}$$

The equilibrium equation of head and loss is

$$H = (1 - \xi)\frac{V_j^2}{2g} - \frac{V_i^2}{2g} \tag{8.3}$$

The jet velocity corresponding to the best ratio of jet velocities is

$$V_j = K_{opt} V_i \tag{8.4}$$

Head is:

$$H = \frac{V_i^2}{2g}(k^2 - \xi - 1) \tag{8.5}$$

The flow is:

$$Q = \frac{T}{\rho(V_j - V_i)} \tag{8.6}$$

The spout diameter is:

$$D = \sqrt{\frac{4Q}{\pi V_j}} \tag{8.7}$$

Where

$\rho$ is the density (kg/m3) of liquid;

$Q$ is the flow (m3 /s) of jet pump;

$V_j$ is the jet velocity (m/s) of flow at the spout;

$V_i$ is the flow speed (m/s) at entrance;

$k$ is the ratio of jet velocity to entering speed;

$\zeta$ is the loss coefficient of system head.

T is the pump thrust

P is the equilibrium Power (W)

H is the Pump Head (m)

g is the earth gravity (m/s2)

$\eta_p$ is the Pump efficiency

$\gamma$ is the equilibrium coefficient

### 8.3.1 Pump Controlled Motor System

Pump controlled motors are the preferred power element in applications which require considerable horsepower for control purposes. This type of closed hydrostatic transmission gives much higher efficiency compared to a valve-controlled actuator, since there are no flow orifices in the main circuit. However, the comparatively slow response of the pump displacement controller, limit their use in high performance systems. In figure 8.6 a pump controlled motor used as an angular position Motor is shown. The variable displacement pump is controlled through controlling the swash plate position, a DC Motor is used to operate and control the swash plate angular position, where the speed of the hydraulic motor is controlled through controlling the hydraulic pump swash plate position, which is discussed in details in the previous chapters. [Rydberg, K.-E.2008]

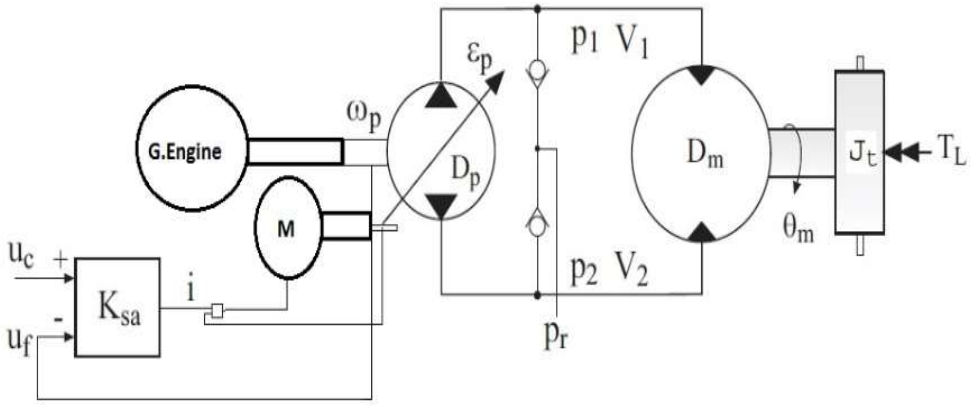


Figure 8.6 Pump controlled motor system

### 8.3.2 Mathematical Model of Pump Motor

The mathematical model of the pump motor is derived by [Rydberg, K.-E. 2008]; the block diagram of the closed loop for the hull system shown in figure 8.7. The transfer function consists of the transfer function of the DC Motor, hydraulic pump, directional valve, hydraulic motor and disturbance transfer function.

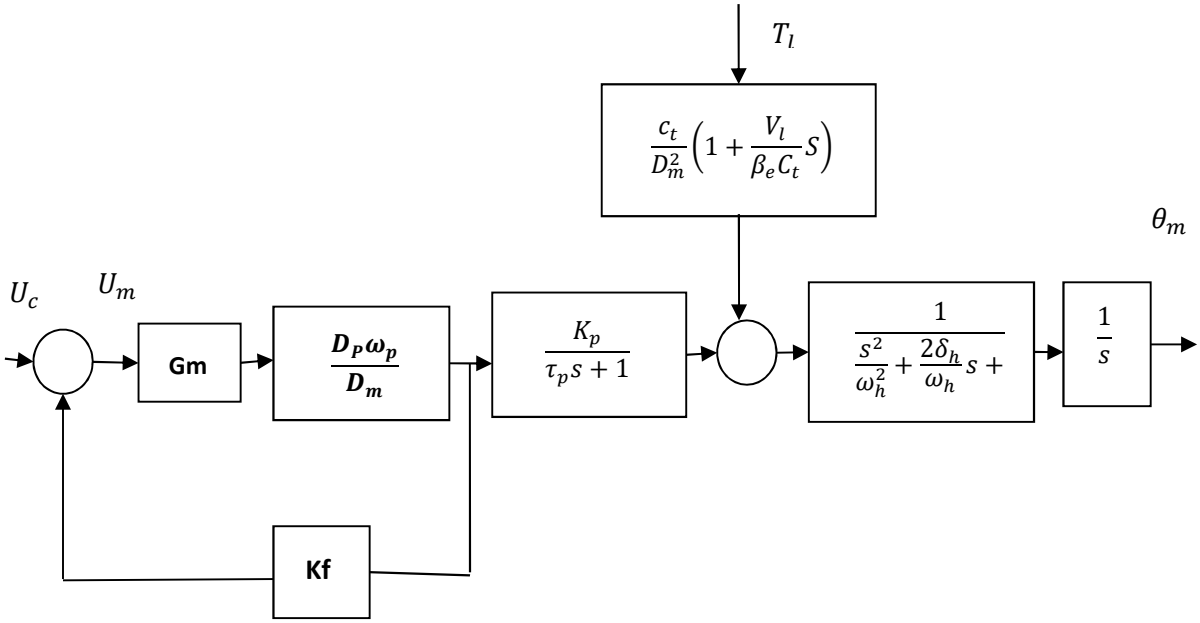


Figure 8.7 block diagram of the pump controlled motor transfer functions

$$A_u(s) = \frac{K_a D_P \omega_P \frac{K_f}{D_m}}{Gm(s).\left(\frac{s^2}{\omega_h^2}+\frac{2\delta_h}{\omega_h}S+1\right)}\frac{1}{S} = \frac{K_v}{Gv(s)Gm(s).S.\left(\frac{s^2}{\omega_h^2}+\frac{2\delta_h}{\omega_h}S+1\right)}\frac{1}{S} \quad (8.8)$$

From [Sailan, K., et al., 2013] the Dc Motor transfer function is:

$$Gm(s) = \frac{1}{0.05s^2 + 3.8s + 0.78} * \frac{1}{s} \tag{8.9}$$

Where:

$$\omega_h = \sqrt{\frac{\beta_e D_m^2}{J_t}\left(\frac{1}{V_1} + \frac{1}{V_2}\right)}$$

$$\omega_h = \sqrt{\frac{4\beta_e D_m^2}{J_t V_t}}$$

$$\delta_h = \frac{C_t}{D_m}\sqrt{\frac{\beta_e J_t}{V_t}} + \frac{B_m}{4D_m}\sqrt{\frac{V_t}{\beta_e J_t}}$$

The valve behaves as if it were linear and that the dynamic performance could be approximated by the linear transfer function [Dobchuk, J.W. 2004]

$$G_p(s) = \frac{\Delta P}{V} = \frac{K_p}{\tau_p s + 1} \tag{8.10}$$

Table 8.1 shows the most important parameters for the system transfer function.

Table 8.1System Parameters

| Sym | Description | Unit |
|---|---|---|
| $K_v$ | Proportional gain | ----- |
| $\omega_p$ | Pump angular speed | Rad/sec |
| $J_t$ | Inertia of motor and load | Kg.m2 |
| $V_t$ | Total fluid volume in pipes | m3 |
| $B_m$ | Motor viscous damping coefficient | N.m.sec./rad |
| $D_m$ | Motor displacement | m3/rad |
| $\rho$ | Density of the Hydraulic oil | Kg/m3 |
| $C_t$ | Total leakage coefficient for pump and motor | m3/sec. Pa |
| $D_P$ | Pump displacement | m3/rad |
| $\beta_e$ | Effective bulk modulus | N/m2 |
| $\omega_m$ | Motor rotational speed | rpm |

## 8.4 Speed control system

The water jet pump speed does not control directly, it controls through the gasoline engine speed and through the variable displacement pump swash plate position which is described in details in the previous chapters, the directional valve used to enable and disable the water jet system which is connected between the pump and hydraulic motor. The block diagram of the hull system is illustrated in figure 8.8.

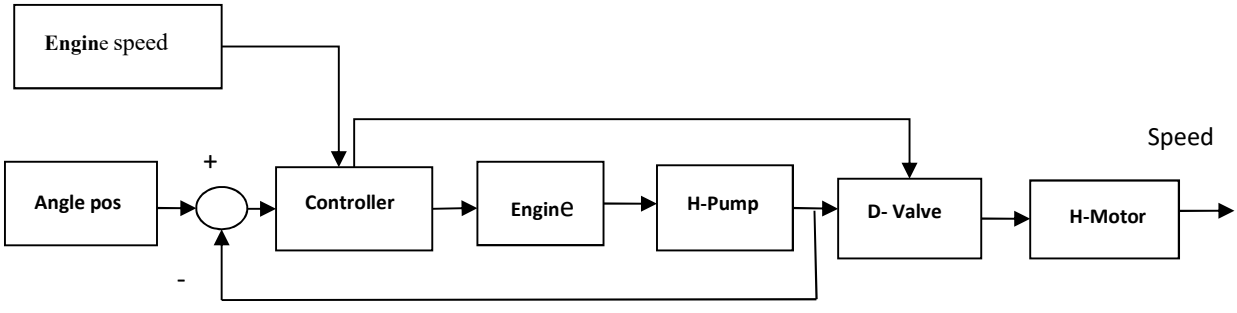


Figure 8.8 Block diagram of the water jet control system

## 8.5 Steering control system

To steer the vehicle on the water a steering device is mounted on the water jet nozzle as shown in figure 8.4. The steering box attached to a metal cable connected to linear actuator, the linear actuator has been driven with DC Motor which is used to position the steering box through controlling the DC Motor position, the block diagram of the steering system shows in figure 8.9 and for that a PID controller is used to control the DC Motor position. Figure 8.10 shows the DC Motor control unit and the communication between this unit and the Master unit.

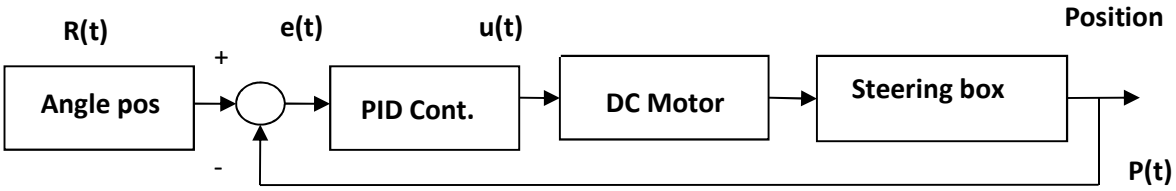


Figure 8.9 Block diagram of the water jet steering system

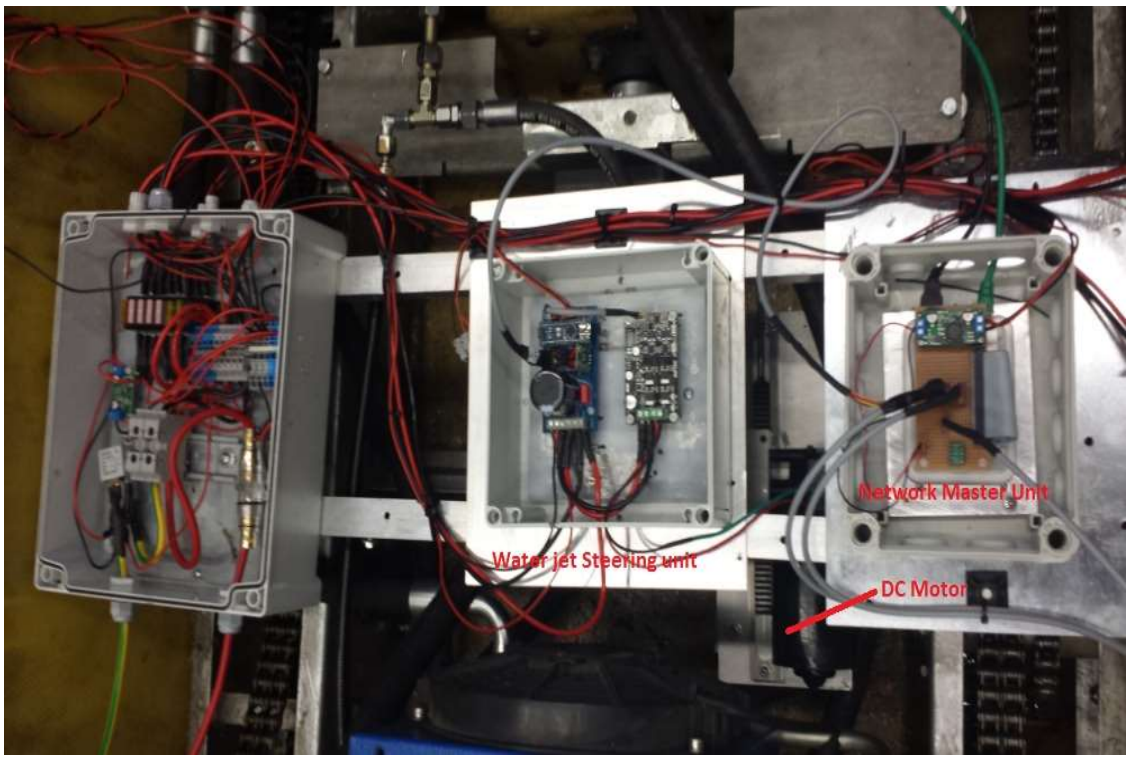


Figure 8.10 Steering control system

### 8.5.1 PID Controller for steering system

PID controllers are commonly used to regulate the time-domain behaviour of many different types of dynamic plants. These controllers are extremely popular because they can usually provide good closed-loop response characteristics. Consider the feedback system architecture that is shown in figure 8.11 where it can be assumed that the plant is a DC motor with the steering box whose position must be accurately regulated. The PID controller is placed in the forward path, so that its output becomes the voltage applied to the motor's armature the feedback signal is a position, measured by angular position sensor .The output position signal P (t) is summed with a reference or command signal R (t) to form the error signal e (t). Finally, the error signal is the input to the PID controller as shown in figure 8.10

$$u = KPe + Ki \int edt + Kd \frac{de}{dt}$$

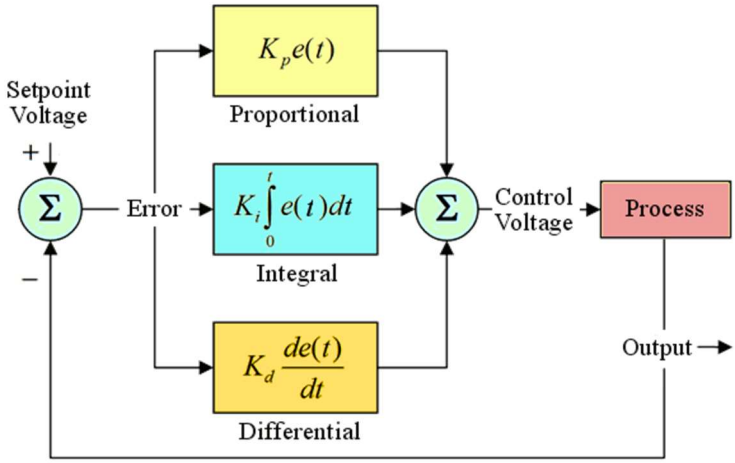


Figure 8.11 PID controller diagram

## 8.6 Experiment and Results

From Figure 8.12, we can see that the response of the DC motor which drives the Jet Ski hydraulic motor follows the input signal which fulfils the system requirement. For the task of stable control, a PID controller is used. For controlling the Jet Ski steering box PID controller used with the parameters of Kp =5.0, Kd = 0.00, Ki = 0.00, as shown in figure 8.16; the response of PID controlled DC motor for the input signal is nearly symmetric as shown in figure 8.15 in the second part. We can see that by using a PID controller type P,

the settling time is 1s which is enough for the task of our Amphibious Autonomous vehicle. Figure 8.17 shows the jet ski motor current and figure 8.13 shows the Left and Right Motor current, the maximum current is 900mA when the Motors runs freely and also when it reaches the swash plate opening end, but when the Motors are connected to the hydraulic pumps swash plate pivot, the current increase in the beginning to overcome the pivot inertia as shown in figure 8.14. The Jet-ski DC Motor response to the step input signal shows in figure 8.18. Because the mechanical connection and between the DC motor and opening shaft specially the shaft key are not symmetric this make the both motor response in some stage not typical. The table below shows the hull PID controller parameters, figure 8.19 shows the steering control system flow chart and Table 8.2 shows the hull PID controller parameters.

Table 8.2 PID Controller Parameters

| parameters | value |
|---|---|
| P | 5.0 |
| I | 0.00 |
| D | 0.00 |
| Step response | 0.5 second |
| Overshoot | 7.1% |
| Steady state error | 0.02 |

The method of tuning the PID parameters is based on experiments on a real or simulated control system. A benefit of the method as compared to the Ziegler-Nichols' closed loop method is that it does not require the control system to be brought into sustained oscillations in the tuning phase. The procedure described below assumes a P controller, which is the most commonly used controller function. Ensure that the controller is a P controller with Kp = 0. Increase Kp until the control loop gets satisfactory stability as seen in the response in the measurement signal after e.g. a step in the set point or in the disturbance. If you do not want to start with Kp = 0, you can try Kp = 1 (which is a good initial guess in many cases) and then increase or decrease the Kp value until you observe a slight overshoot but a well damped response.

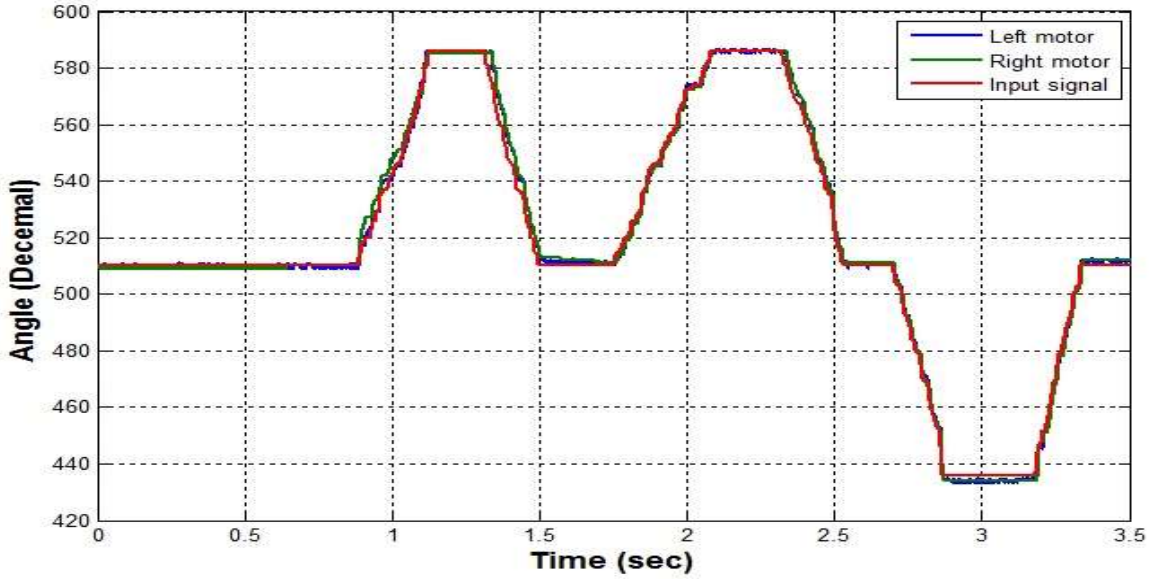


Figure 8.12 PID controller for pumps motors

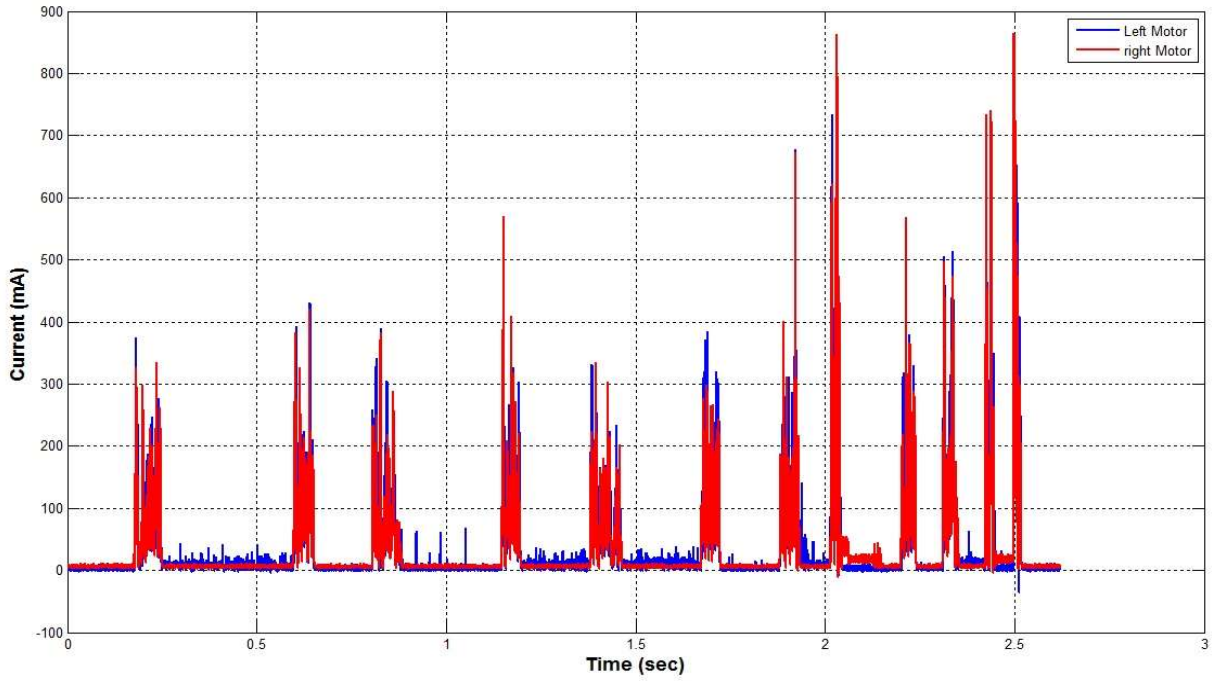


Figure 8.13 Left and right motor current free running

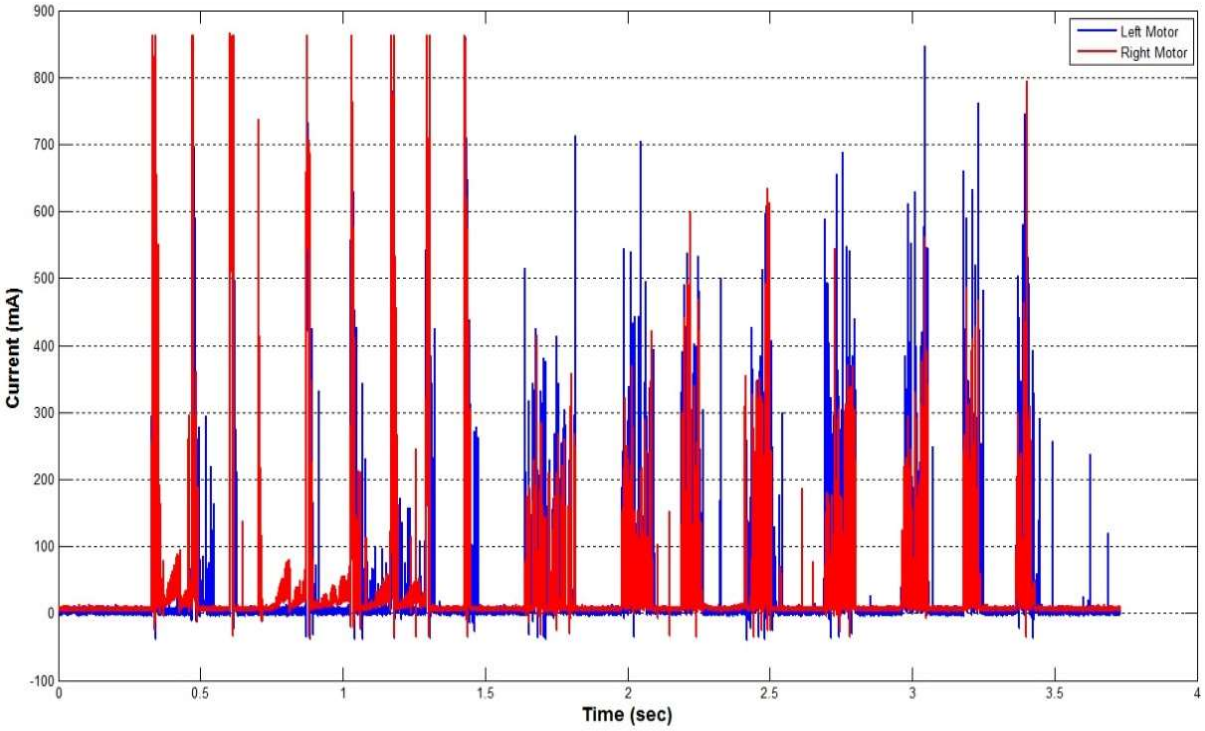


Figure 8.14 Left and right motor current connected to the pump

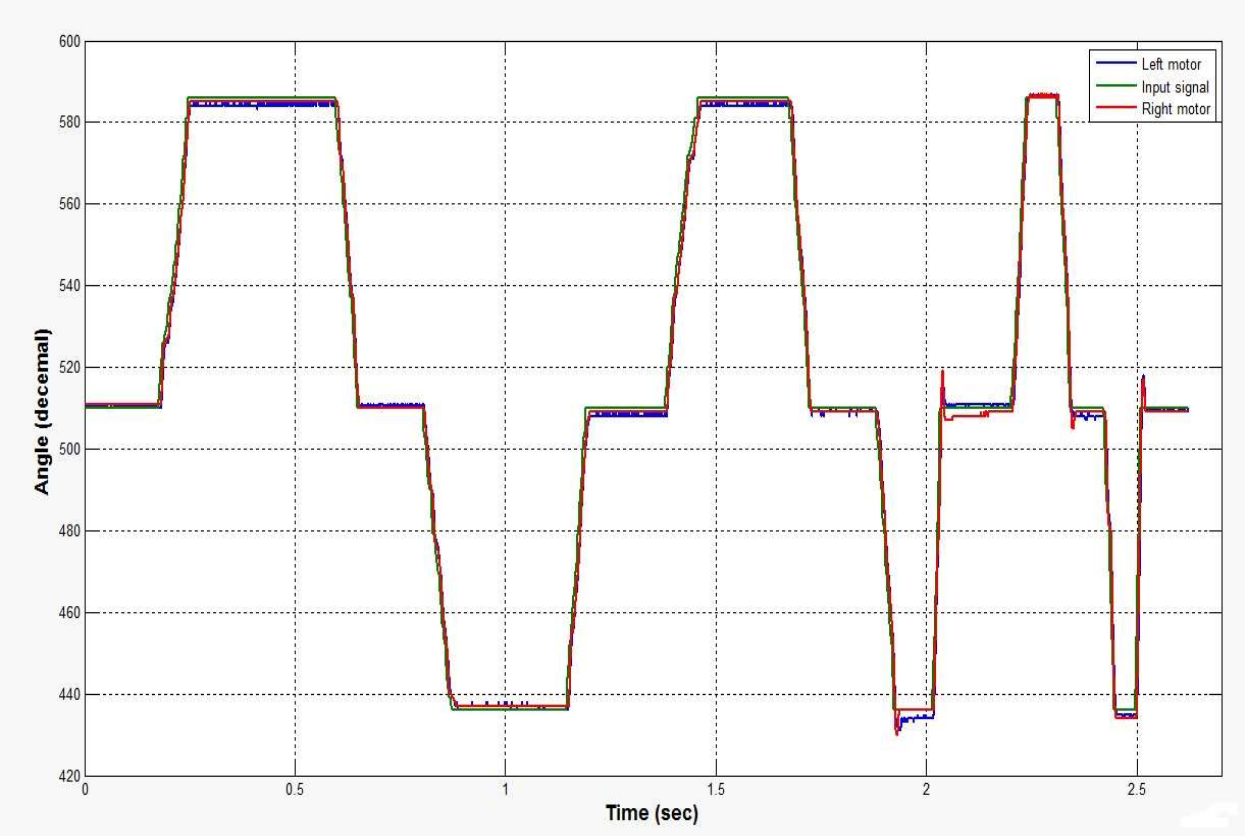


Figure 8.15 Left and right motor response to the input signal

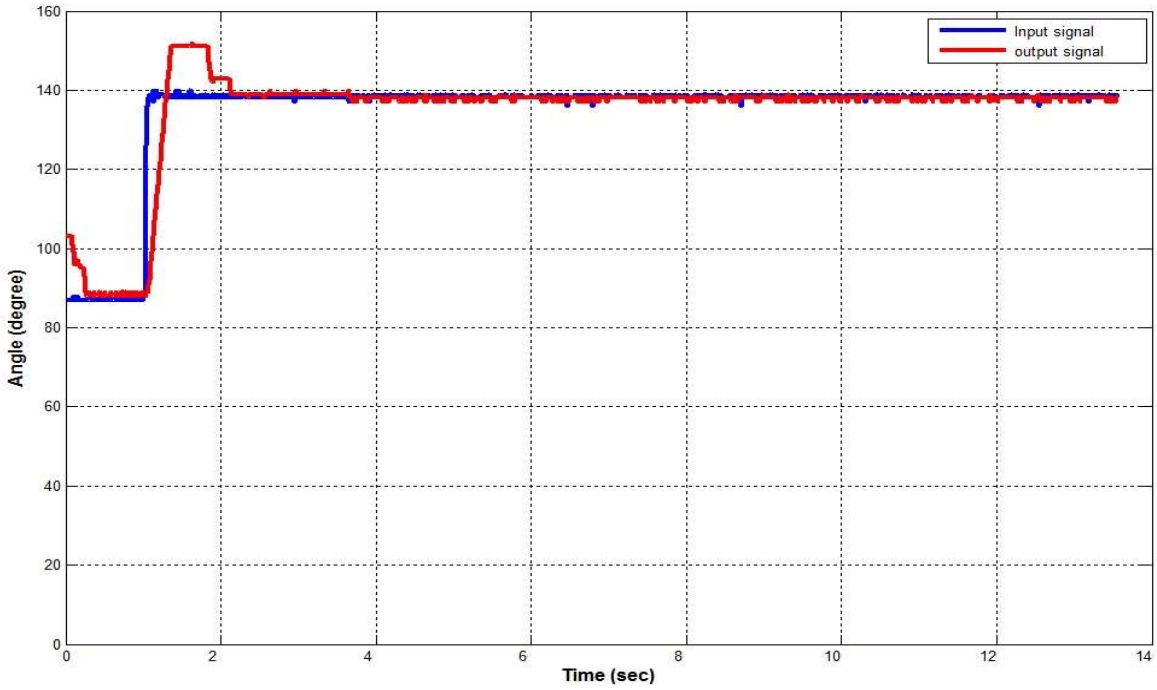


Figure 8.16 Jet ski steering box PID controller step response

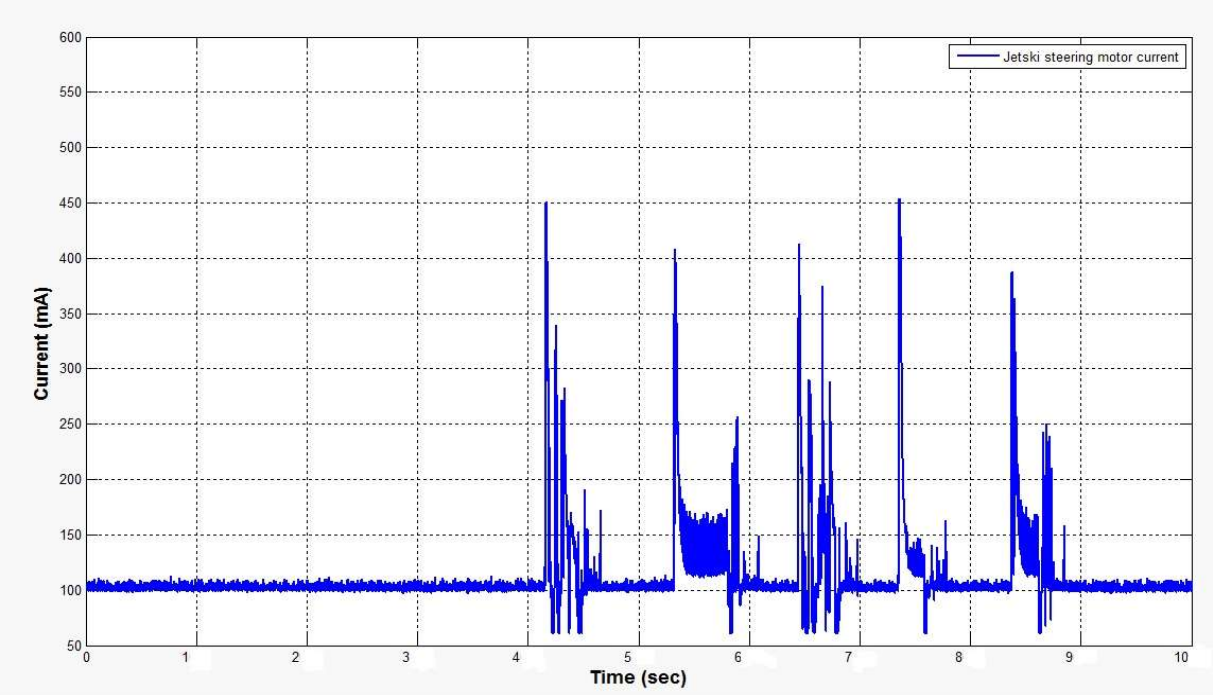


Figure 8.17 Jet ski motor current during steering

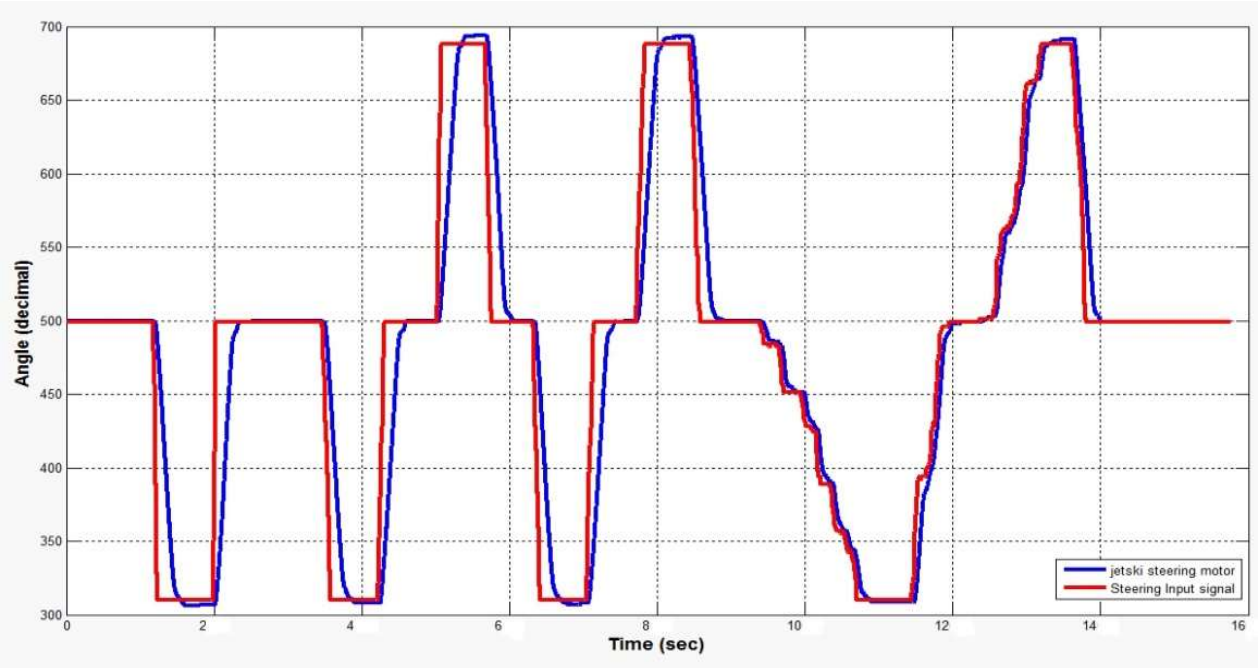


Figure 8.18 Jet ski steering box PID controller response to the input signal

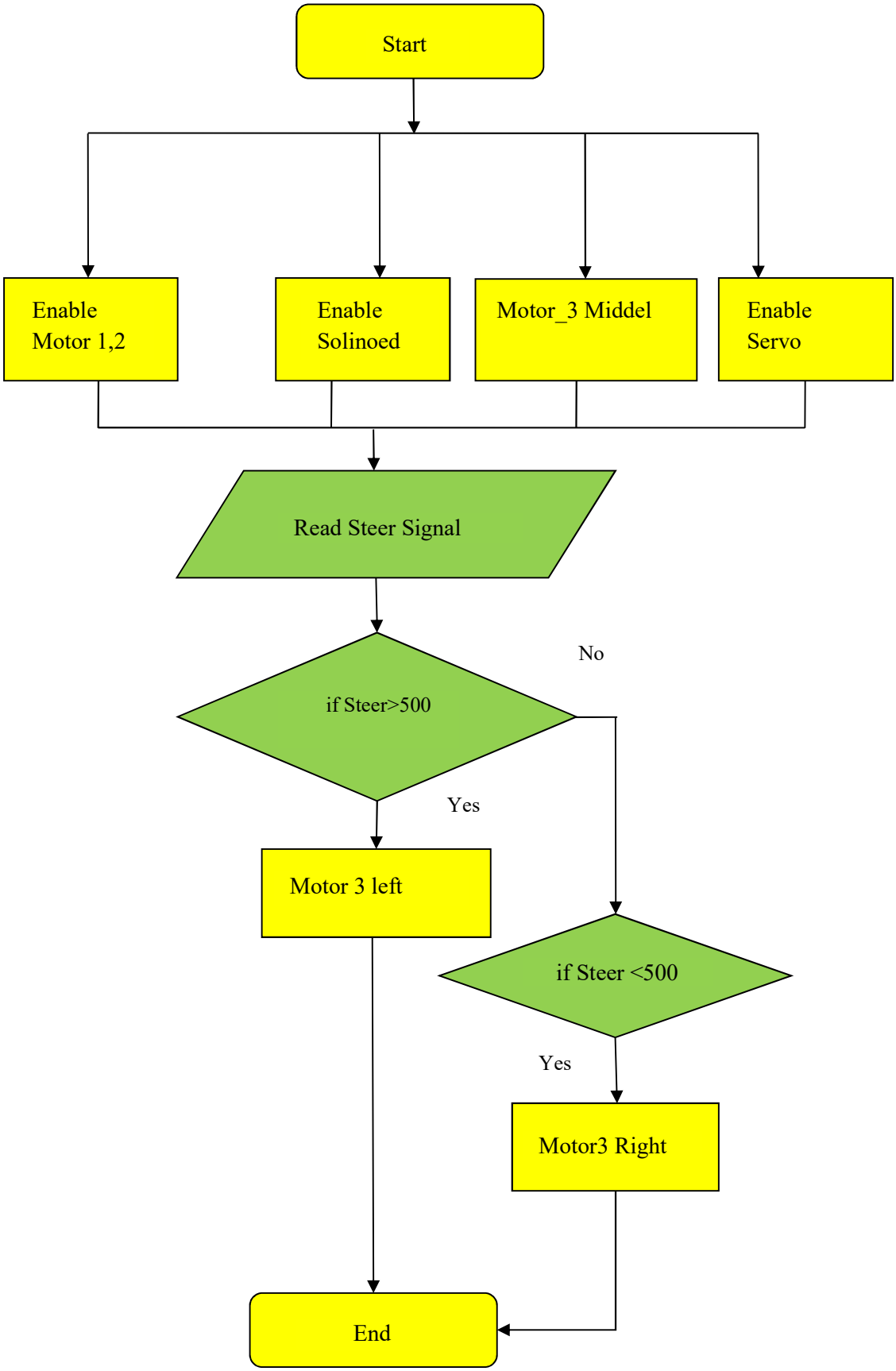


Figure 8.19 Jet ski steering box PID controller

# Chapter 9

# Conclusion and Further Work

## 9.1 Conclusion

Popularity of the research on amphibious autonomous vehicle has been recently increasing, due to their possible use in different outdoor environments. Planetary explorations, search and rescue missions in hazardous areas, surveillance, humanitarian demining, and the need for large-scale robotic vehicles arises in the exploration of hazardous sites as well as in exploring on land and on the water. Both applications require a vehicle that can operate continuously for several hours, cover large distances at speeds of up to 25 metre per second, carry a payload of several hundred kilograms, and drive at precisely controlled speeds. To meet these needs, Institute of Real Time Learning Systems in Siegen University has procured the DORIS Robot with the intention of converting them to driverless operation for use as amphibious autonomous vehicle. Speed control of autonomous amphibious and ground vehicles is very challenging tasks. For 8x8 Vehicle with payload of several hundred kilograms, controlling speed is achieved using either Hydrostatic transmission system or electro servo hydraulic system. In the Hydrostatic transmission system the speed of the vehicle wheels is controlled through controlling the variable displacement pump swash plate angle, there are many methods to control the swash plate angle, mechanically using levers, hydraulically using pneumatic servo, hydraulic servo, digital servo and using DC Motors to actuate the swash plate, this method (hydraulically using DC Motor) is our proposed method for controlling the swash plate angle, the DC Motor actuates the swash plate in a small angular position range between +18 to -18 degrees. This angle is proportional to +5mm to -5mm travelling distance, to control the angular position which controls the wheel speed, this very small distances become big challenging, because we are using two DC Motors with Gear box and couplings, we have to prevent any small differences between the Motors during driving forward and backward, 0.25 mm difference produce 8 RPM difference between left and right side, this difference comes from the mechanical systems that connect the DC Motors to the variable displacement pump and comes from the mechanical systems between the hydraulic motors and the wheel, like the chains and the shaft. This thesis offers a comprehensive look at semi-autonomous speed control applied to amphibious vehicles, a more difficult problem than those previously solved by virtue of its complicated power train

and suspension dynamics. The analyses and designs produced in this work result in a simple control algorithm that enables stable and wide-bandwidth power train control for an amphibious vehicle hydraulic power terrain system**.**

## 9.2 Principal Contributions

There are many contributions made in this thesis - fundamentals and demonstratives. Fundamental contributions are untried method in the field, and have a full grounding in either physical or mathematical theory. Demonstrative contributions show the controller systems and their results on the vehicle platform by many successfully tests.

The contributions presented by the research and development in this thesis are outlined below.

This thesis has demonstrated successfully the use of (two) speed control system for amphibious vehicle using two control systems; PID with Fuzzy logic controller and Dead beat with Fuzzy logic controller, the hardware and software were implemented successfully on the vehicle platform. System simulation demonstrated the hydrostatic transmission system and the effect of different surfaces on the hydraulic pump actuator torque and the vehicle speed. A comparison between the two systems was demonstrated in this thesis.

This thesis analyzed the hydrostatic transmission system which is used as a power train system for DORIS, an Amphibious Autonomous Vehicle (AAV), this thesis also analyzed the effect of the pressure difference from skid steering and from rolling driving on the variable displacement pump swash plate presented. The torque needed to open the hydraulic variable displacement pump swash plat was also studied and defined.

Fuzzy control has been used successfully in the steering control systems. The fuzzy speed controller uses two inputs to the system, the steering and the Gas signal applied to the conventional closed loop, a conventional inside closed loop treats the steady state error between the input and the output.

A fuzzy logic obstacle-avoidance subsystem based on the use of obstacle factors has been developed successfully. These obstacle factors are based not on the steering angle of the wheels but on the obstacle angle and the angles adjacent to the steering angle. This method has been designed to control both the speed and steering of the vehicle to avoid collisions with obstacles.

Tele-operation system has been successfully developed using joystick in cooperation with ROS, the communication between the system controllers was achieved with SPI and UART Protocols.

This thesis shows the design and implementation of a water jet control system for driving the vehicle on water, the system is modelled and designed, a steering control system for steering the vehicle on water was achieved using PID controller.

## 9.3 Research Objectives Answers

1. Can a robot such as DORIS be automated, and what complexity of both software and electronic and mechanical components are required?

Yes, DORIS Robot can be automated, two electronics circuits, two software systems, two power train systems hase been designed and the table below briefly describes that.

| Characteristic / Hardware and software | Controllability | Stability | Complexity | Robustness |
|---|---|---|---|---|
| Dead Beat with Fuzzy logic control system | controllable | stable | complex | - |
| PID with Fuzzy logic control system | controllable | stable | not complex | - |
| Arduino with MD Motor drivers | | | not complex | robust |
| ELZS Motor drivers and controller Board | | | complex | less robust |
| Hydrostatic transmission power train system | controllable | stable | complex | less robust |
| Electro-Hydraulic Servo power train System | controllable | stable | not complex | robust |

2. What level of accuracy can be expected from a skid-steering system and to what extent is a control system more or less accurate than a human operator?

The control system is so accurate and the Tele-operation system is more accurate than human operator, in that in human operation, the vehicle vibration can have an effect on the driver and may cause him to give a wrong input signal which would make the vehicle move in an unexpected direction.

3. What effects does surface type have on the operation of the vehicle?

Chapter 3 demonstrates the effect of surface type on the controller actuators, the hardest surface produce high pressure difference, which produce high torque and of course high voltage and current which can damage the electronic circuit; for this reason, high current Motor drivers are used to avoid this effect, the effect on the speed is neglected.

## 9.4 Further Work

Although the speed control of the amphibious Robot was achieved, there are still some improvements in accuracy and efficiency possible by future research

- To avoid the speed, differentiate between both sides caused by the mechanical systems, another close loop control system can be added to the speed control system by attaching tachometer to the wheels and measuring the wheel speed directly and then sending the signal to the microcontroller and treating the error from the swash plate angular position as shown in figure 9.1.
- Convert the Amphibious Vehicle to Autonomous Amphibious Vehicle.
- Implement the Electro-hydraulic servo system on the DORIS Vehicle.
- Human operator dynamics in the time delayed control loop can be catastrophic. Compensating for these performance-degrading effects must be accomplished by using a Delay Compensation technique, e.g. using Smith Predictor as used for the time delay.

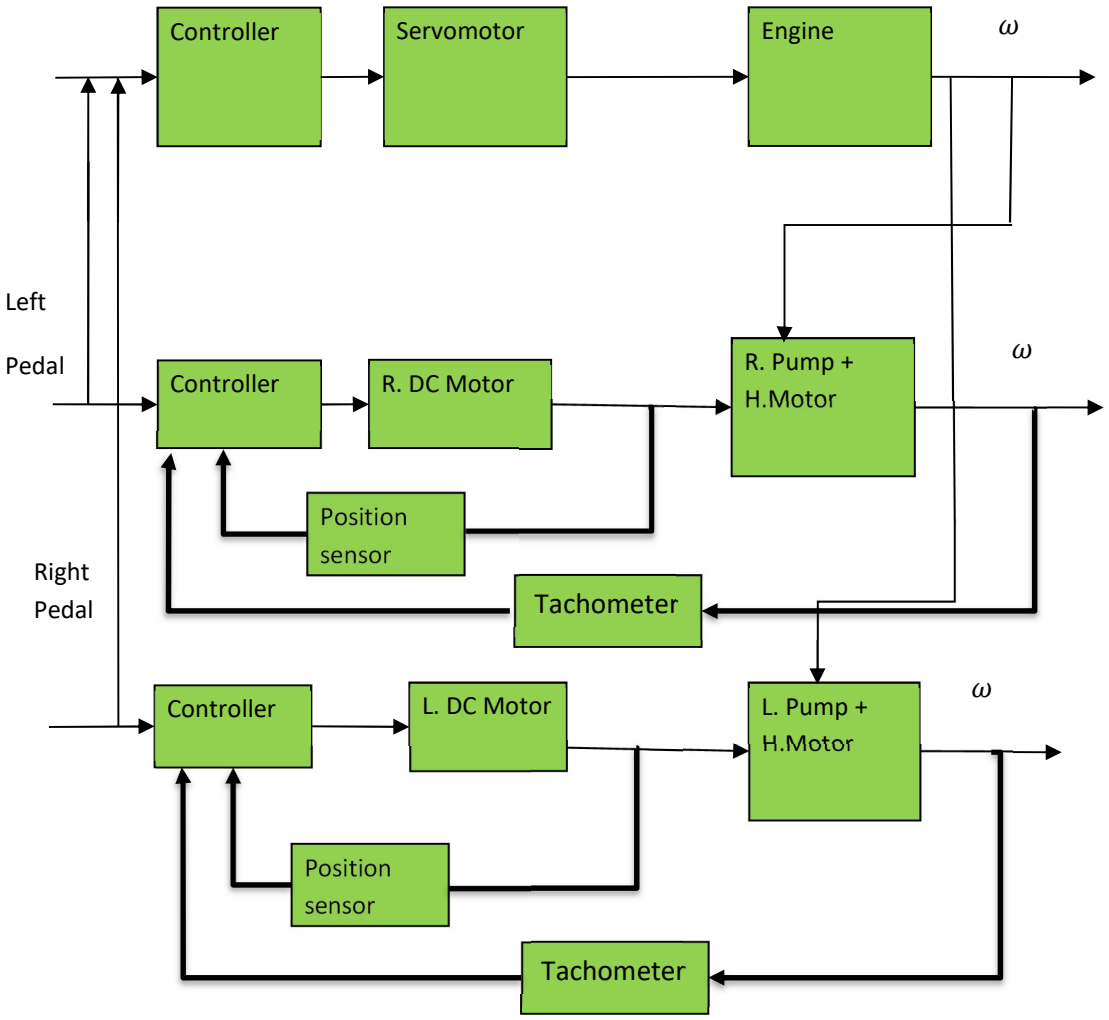


Figure 9.1 Cascade control system with tachometer

## References


1. Abdelhameed, M.M.; Abdelaziz, M.A. and Bakarman, A., "The Velocity Control of the Electro-Hydraulic Servo System," International Journal of Research in Engineering and Technology (IJRET), Vol. 3, pp. 73-79, Issue No. 11, 2014.

2. Adam, E.J. and Marchetti, J.L., "Feed-forward Controller Design Based on H∞ Analysis," Proceedings of ENPROMER, Dynamics, Operability and Process Control, Vol. 1, pp. 271-276, 2001.

3. Ahmed, A. and Bhutia, D.D., "Propulsion System Design and Sizing of a Electric Vehicle," International Journal of Electronics and Electrical Engineering, Vol. 3 , pp.14-18, Issue No. 1, 2015.

4. Angue-Mintsa, H.; Venugopal, R.; Kenne, J.-P. and Belleaub, C., "Adaptive Position Control of an Elecotro-Hydraulic Servo System with Load Disturbance Rejection and Friction Compensation," Journal of Dynamic Systems, Measurement, and Control, Vol. 133, 2011.

5. Aung, W.P., "Analysis on Modeling and Simulink of DC Motor and its Driving System Used for Wheeled Mobile Robot," Proceedings of World Academy of Science: Engineering & Technology, Vol. 1, pp.1141-1148, 2007.

6. Babuìka, R. and Stramigioli, S., "Matlab and Simulink for Modeling and Control," Control Laboratory, Faculty of Information Technology and Systems Delft University of Technology, Netherlands, November 1999.

7. Barber, R.; Rosa, D.R. and Garrido, S., "Adaptive Control of a DC Motor for educational Practices," 10th IFAC ACE, Symposium Advances in Control Education, Sheffield, pp.244-249, UK, 28.-30. August 2013.

8. Basilio, J.C. and Matos, S.R., "Design of PI and PID Controllers With Transient Performance Specification," Transactions on Education, IEEE, Vol. 45, pp. 364 - 370, Issue No. 4, November 2002.

9. Bindu R. and Namboothiripad, M.K., "Tuning of PID Controller for DC Servo Motor using Genetic Algorithm," International Journal of Emerging Technology and Advanced Engineering, Vol. 2, pp.310-314, Issue No. 3, ISSN 2250-2459, 2012.

10. Boxerbaum, A.S.; Werk, P.; Quinn, R.D. and Vaidyanathan, R., “Design of an Autonomous Amphibious Robot for Surf Zone Operation: Part I Mechanical Design for Multi-Mode Mobility,” Proceedings of the 2005 International Conference on Advanced Intelligent Mechatronics (IEEE/ASME), Monterey, California, pp.1459-1464, USA, 24.-28. July 2005.

11. Bulten, N.W.H., “Numerical Analysis of a Waterjet Propulsion System,” PhD Thesis, Eindhoven University of Technology, Netherlands, 2006.

12. Carrier, D., “Soviet Rover Systems,” Proceedings of the AIAA Space Programs and Technologies Conference, Huntsville, Alabama, USA, 1992.

13. Chang, S.-H., “Implementation and Control Logic Design of Intelligent Electric Power Steering System,” World Electric Vehicle Journal, Vol. 3, pp.711-718, ISSN 2032-6653, 2009.

14. Cherroun, L. and Boumehraz, M., “Designing of Goal Seeking and Obstacle Avoidance Behaviors for a Mobile Robot Using Fuzzy Techniques,” Journal of Automation & Systems Engineering, pp. 164-171, 2014.

15. Choudhury, S.; Singh, G.K. and Mehra R.M., “Design and Verification Serial Peripheral Interface (SPI) Protocol for Low Power Applications,” International Journal of Innovative Research in Science, Engineering and Technology, Vol. 3, pp.16750-16758, Issue No. 10, 2014.

16. Clarke, M. and Blanchard, T., “Development of a Control System for a Skid-Steer Amphibious Vehicle”, Proceedings of TAROS 2010, Plymouth, UK, pp. 41-46, September 2010.

17. Corriveau, D., “Techniques de Conduite avancée,” Nicolet: Editions dynamiques, pp. 199-201, 1987.

18. Cortner, A.; Conrad, J.M. and BouSaba, N.A., “Autonomous All-Terrain Vehicle Steering,” Proceedings of IEEE Southeastcon, IEEE, 15-18. March 2012.

19. Crespi, A.; Badertscher, A.; Guignard, A. and Ijspeert, A.J., “Swimming and Crawling with an Amphibious Snake Robot,” Proceedings of the 2005 IEEE International Conference on Robotics and Automation (ICRA), 18.-22. April 2005.

20. Danapalasingam, K.A.; La Cour-Harbo A. and Bisgaard, M., “Disturbance Effects in Nonlinear Control Systems and Feedforward Control Strategy,” International Conference on Control and Automation, IEEE, Christchurch, New Zealand, 9.-11. December 2009.

21. Dobchuk, J.W., “Control of a Hydraulically Actuated Mechanism Using a Proportional Valve and a Linearizing Feedforward Controller,” Phd Thesis, University of Saskatchewan, Saskatoon, Canada, August 2004.

22. Dorf, R.C. and Bishop, R.H., “Modern Control Systems,” Prentice Hall, Pearson Education, Inc., New Jersey, 12th Edition, 2010.

23. Dymarski, C., “Analysis of Two Design Kind of Propulsion for an Inland Vessel,” Journal of Polish CIMAC, Vol. 2, Issue No. 1, pp.107-116, 2007.

24. Eliewa, A.; Atef, M.; Elhadad, M. and Khodary, R., “A Proposed Control System for a Autonomous Unmanned Ground Vehicle,” 13th International Conference on Aerospace Science and Aviation Technology, May 26–28, 2009.

25. Escobar, A.D., “Addaptive fuzzy control applied to a speed control,” The Online Journal on Electronics and Electrical Engineering (OJEEE), Vol. 2, pp.229-233, Issue No. 2, 2009.

26. Faisal, M.; Hedjar, R.; Al Sulaiman, M. and Al-Mutib, K., “Fuzzy Logic Navigation and Obstacle Avoidance by a Mobile Robot in an Unknown Dynamic Environment,” International Journal of Advanced Robotic Systems, Vol. 10, pp.371-379, Issue No. 37, September 2013.

27. Fang, G.; Xiwen, L. and Hongxia, X., “Compound Gear Box Torque Analysis of Vertical Mixer,” Proceedings of 2012 International Conference on Mechanical Engineering and Material Science,pp.581-584, 2012.

28. Fong, T. and Thorpe, C., “Vehicle Teleoperation Interfaces,” Autonomous Robots, Kluwe Academic Publishers, pp. 9-18, 2001.

29. Gage, D., “A brief History of Unmanned Ground Vehicle (UGV) Development Efforts,” Unmanned Systems Magazine, Vol. 13, Issue No. 3, pp. 9-16, 1995.

30. Grabe, V.; Riedel, M.; Bulthoff, H.H.; Giordano, P.R. and Franchi, A., "The TeleKyb framework for a modular and extendible ROS-based quadrotor control," European Conference on Mobile Robots (ECMR), 25.-27. September 2013.

31. Guo, W., "A Novel Methodology of Displacement Calculation for the Swash Plate Axial Piston Pump with Angle Cylinder Block," Danfoss Power Solutions (Zhejiang), IFPE Paper 9.2, 2010.

32. Guptal, G.S.; Mukhopadhyay, S.C. and Finnie, M., "WiFi-Based Control of a Robotic Arm with Remote Vision," Conference Record of the IEEE Instrumentation and Measurement Technology Conference, June 2009.

33. Ha; Q.P.; Tran, T.H.; Scheding, S; Dissanayake, G. and Whyte, H.F.D., "Control Issues of an Autonomous Vehicle," 22nd International Symposium on Automation and Robotics in Construction ISARC, Ferrara (Italy), September 11-14, 2005.

34. Hetthéssy, J.; Barta, A. and Bars, R., "Dead Beat Controller Design," (https://avalon.aut.bme.hu/education/contheor/contheor2/DeadBeat2004.pdf) November, 2004.

35. Ibrahim, D., "Microcontroller Based applied Digital Control," John Wiley & Son Ltd., 2006.

36. Ioannou, P. and Sun, J., "Robust Adaptive Control," Prentice Hall, Pearson Education, Inc., 1996.

37. Jacoba, J.S.; Gunderson, R.W., Fullmer, R.R., "Conversion and Control of an All-terrain Vehicle for use as an Autonomous Mobile Robot", Proceedings of the International COnference on Robotic and Semi-Robotic Ground Vehicle Technology, Orlando, Florida, 13. April, 1998.

38. Jamshidi, M.; Vadiee, N. and Ross, T., "Fuzzy Logic and Control: Software and Hardware Applications," Prentice Hall, Pearson Education, Inc., New Jersey, pp. 89-101, 1993.

39. Jamshidi, M.; Vadiee, N. and Ross, T., "Fuzzy Logic Control," Prentice Hall, Pearson Education, Inc., New Jersey, pp. 89-101, 1993.

40. Jayasree, P.V.Y.; Poojita, G.R. and Priya, J.C., “Design of Active Electromagnetic Interference Filter to Eliminate Common-mode Noise in Conducted Interference,” International Journal of Computer Applications, Vol. 43, pp.10-15, Issue No. 11, April 2012.

41. Karnik, A., “Performance of TCP Congestion Control with Rate Feedback: TCP/ABR and Rate Adaptive TCP/IP,” Master Thesis, Indian Institute of Science, Bangalore, India, 1999.

42. Kenaya, R. and Chabaan R., “Fuzzy Controllers for Electrical Power Steering Systems,” Proceedings of the World Congress on Engineering and Computer Science, Vol. 1, WCECS, San Francisco, USA, 20.-22. October, 2010.

43. Klocke, C., “Control Terminology for Hydrostatic Transmissions,” Sauer-Danfoss (US) Company, 2012.

44. Krishnamurthi, K.; Thapa, S.; Kothari, L. and Prakash, A., “Arduino Based Weather Monitoring System,” International Journal of Engineering Research and General Science, Vol. 3, Issue No. 2, March-April, pp. 2091-2730, 2015.

45. Kumar, S., “Design and Implementation of UART using FIFO for Serial Communication,” International Journal of Scientific Engineering and Technology, Vol. 3, Issue No. 7, pp. 737-740, 2013.

46. Lewis, P.H. and Yang, C., “Basic Control System Engineering,” Prentice Hall, Pearson Education, Inc., New Jersey (USA), 2005.

47. Lian, S.H., “Fuzzy Logic Control of an obstacle Avoidance Robot,” Proceedings of IEEE 5th International Fuzzy Systems, IEEE, Vol. 3, pp.26-30, New Orleans, Louisiana, USA, 8.-11. September 1996.

48. Lin, P.I.-H.; Hwang, S. and Chou, J., “Comparison of Fuzzy Logic and PID Controls For a DC Motor Position Controller,” Conference: Industry Applications Society Annual Meeting, IEEE, 2-6. October 1994.

49. Maclaurin, B., “A Skid Steering Model using the Magic Formula,” Journal of Terramechanics, Vol. 48, Issue No. 4, pp. 247-263, August 2011.

50. Mahajan, S.; Bhosale, R. and Kulkarni P., "Obstacle Detection using Mono Vision Camera and Laser Scanner," International Journal of Research in Engineering and Technology, Vol. 02, pp 284-290. Issue No. 12, December 2013.

51. Maiti, R. and Narayan, P., "An experimental investigation on Swash Plate Control Torque of A pressure Compensated Variable Displacement Inline Piston Pump," Proceedings of the 8th JFPS International, Symposium on Fluid Power, pp.220-227, Okinawa, Japan, 25-28. October 2011

52. Mayannavar, S.; Desai, A. and Wali, U.V., "Design of a High Level Protocol for Serial Peripheral Interface and its Implementation in a CAN Controller IC," International Journal of Engineering Science and Innovative Technology (IJESIT), Vol. 3, pp.346-353, Issue No. 4, July 2014.

53. Mohammed, J.A., "Pulse Width Modulation for DC Motor Control, Based on LM324," Eng. &Tech. Journal, Vol. 31, Part (A), Issue No.10, 2013.

54. Nazari, V. and Naraghi, M., "Sliding Mode Fuzzy Control of a Skid Steer Mobile Robot for Path Following," 10th International Conference on Control, Automation, Robotics and Vision, Hanoi, pp.549-554 Vietnam, 17.-20. December 2008.

55. Nhivekar, G.S.; Nirmale, S.S. and Mudholker, R.R., "Implementation of Fuzzy Logic Control Algorithm in embedded Microcomputers for dedicated Application," International Journal of Engineering, Science and Technology, Vol. 3, Issue No. 4, pp. 276-283, 2011.

56. Örtegren, V.; "Water Jet Steering Concept," Master Thesis, Karlstadt University, 2013.

57. P. M. Meshram; Rohit G. Kanojiya, "Tunning of PID Controller using Ziegler-Nichols Method for Speed Control of DC Motor," International Conference On Advances In Engineering, Science And Management (ICAESM), IEEE, 30.-31. March 2012.

58. Ren, F.; Liu, X.-H.; Chen, J.-S.; Zeng, P.and Jia, X.-F., "Analysis of Skid Steer Loader Steering Characteristic," Hindawi Publishing Corporation Advances in Mechanical Engineering, Article ID 245713, November 2014.

59. Ren, L.; Wang, W. and Du, Z., "A New Fuzzy Intelligent Obstacle Avoidance Control Strategy for Wheeled Mobile Robot," Proceedings of International Conference on Mechatronics and Automation, IEEE, Chengdu, China, 5.-8. August 2012.

60. Riedewald, F., “Comparison of Deterministic, Stochastic and Fuzzy Logic Uncertainty Modelling for Capacity Extension Projects of DI/WFI Pharmaceutical Plant Utilities with Variable/Dynamic Demand,” PhD Thesis, University College Cork, 2011.

61. Roberts, J. and Corke, P., “Obstacle Detection for a Mining Vehicle using a 2D Laser,” Proceedings of the Australian Conference on Robotics and Automation (ACRA 2000), Australian Robotics & Automation Association, Melbourne, Australia, pp. 185-190, 2000.

62. Rohit, G.; Ruchika, l.; Subhransu, P., “Thyristor Based Speed Control Techniques of DC Motor: A Comparative Analysis,” International Journal of Scientific and Research Publications, Vol. 2, pp.1-6, Issue No. 6, June 2012.

63. Rydberg, K.-E., “Hydraulic servo systems”, Linköpings Universitet, 2008.

64. Sailan, K. and Kuhnert, K.-D., “Design and Implement of Powertrain Control System for the All Terrian Vehicle,” International Journal of Control, Energy and Electrical Engineering (CEEE), Copyright IPCO, Vol. 1, pp. 50-56, 2014.

65. Sailan, K. and Kuhnert, K.-D, “DC Motor Angular Position Control using PID Controller for the Purpose of Controlling the Hydraulic Pump,” International Conference on Control, Engineering, Information Technology (CEIT´13), copyright IPCO, Vol. 1, pp. 22-26, 2013.

66. Sailan, K.; Kuhnert, K.-D. and Karelia, H., “Modelling, Design and Implement of Steering Fuzzy PID Control System for DORIS Robot,” International Journal of Computer and Communication Engineering, Vol. 3, pp.57-62, Issue No. 1, 2014.

67. Shuang, G.; Cheung, N.C.; Cheng, K.W.E., Lei, D. and Xiaozhong, L., “Skid Steering in 4-Wheel-Drive Electric Vehicle, “Proceedings of the International Conference on Power Electronics and Drive Systems, December 2007.

68. Shukla, S. and Tiwari, M., “Fuzzy Logic of Speed and Steering Control System for Three Dimensional Line Following of an Autonomuse Vehicle,” International Journal of Computer Science and Information Security, Vol. 7, pp.101-108, Issue No. 3, 2010.

69. Sieben, V., “A High Power H-Bridge,” ARVP-Autonomous Robotic Vehicle Project, 2003.

70. Tanaka, T. and Shiraishi, T., “Development of Automated Shoreline Surveying System Using Amphibious Walking Robot,” Proceedings of the 23rd ISARC, Tokyo, Japan pp. 46-51, 2006.

71. Tee, Y.; Tan, Y.; Teoh, B.; Tan, E. and Wong, Z., “A Compact Design of Zero-Radius Steering Autonomous Amphibious Vehicle with Direct Differential Directional Drive - UTAR-AAV,” IEEE Conference on Robotics Automation and Mechatronics (RAM), 28.-30. June 2010.

72. Tekorius, T. and Levisauskas, D., “Comparative Investigation of Feed Forward Control Algorithms,” Electronic and Electrical Engineering, ISSN1392-1215, No. 9 (115), pp. 79-82, 2011.

73. Tran, T.H.; Ha, Q.P.; Grover, R. and Scheding, S.J., “Modelling of an Autonomous Amphibious Vehicle,” ARC Centre of Excellence in Autonomous Systems (CAS), December 2004.

74. Tran, T.H., “Modeling and Control of Unmanned Ground Vehicle,” PhD Thesis, September 2007.

75. Trebi-Ollennu, A.; Dolan J.M. and Khosla, P., “Adaptive Fuzzy Throttle Control for an All Terrain Vehicle”, Carnegie Mellon University, Institute for Complex Engineered Systems, Pittsburgh, Vol. 215 Part I, pp 189-198, 2001.

76. Van de Van, J.D.; Olson, M.W. and Li, P.Y., “Development of a Hydro-Mechanical Hydraulic Hybrid Drive Train with Independent Wheel Torque Control for an Urban Passenger Vehicle,” Engineering Research Center for Compact and Efficient Fluid Power (CCEFP), EEC-0540834.

77. Voyles, R.M.; Povilus, S.; Godzdanker, R. and Chun, W., “Heterogeneous Drive System for Macro/Micro Exploration of Deconstructed Environments”, Proceedings of the AUVSI Unmanned Systems, North America, Denver, Colorado, 2010.

78. Wang, W. A, “Speed Regulation System of DC Motor Based on PWM Technology,” Applied Mechanics and Materials, Vols. 29-32, pp. 2194-2199, 2010.

79. Yu, M.; Lin, Y. and Wang, X., “Human-Robot Interaction Based on Gaze Gestures for the Drone Teleoperatio,” Journal of Eye Movement Research, Vol. 7, Issue No. 4, pp. 1-14, 2014.

80. Zadeh, R.L.A., “Fuzzy Sets,” Information Control, Vol. 8, pp. 338-353, 1965.

81. Zavlangas, P.G.; Tzafestas, S.G. and Althoefer, K., “Fuzzy Obstacle Avoidance and Navigation for Omnidirectional Mobile Robots,” ESIT, Aachen, Germany, pp 375-382, 14.-15. September 2000.

82. Zhang, J.; Zhang, Y. and Chen, L., “A Fuzzy Control Strategy and Optimization for Four Wheel Steering System,” International Conference on Vehicular Electronics and Safety, IEEE, 13.-15. December 2007.

83. Zhang, X.D., “The Principle of the Potentiometer and its Applications in the Vehicle steering,” International Conference on Vehicular Electronics and Safety, IEEE, 14.-16. October 2005.

84. Wikipedia.org/wiki/PID_controller

85. Bühler Motor Gmbh, Technical notes regarding DC Motor

86. http://www.kemmericelektromotoren.de/fileadmin/images/pdfs_und_grafiken/gleichstrommotoren/A176_Abmessungen_MP.pdf

87. http://ctms.engin.umich.edu/CTMS/index.php?example=MotorSpeed&section=ControlPID.

88. http://sauerdanfoss.cohimar.com/OMR.pdf

89. http://www.hydromot.lu/pdf/deutsch/HM2_de.pdf

90. http://powersolutions.danfoss.com/stellent/groups/publications/documents/product_literature/520l0344.pdf

91. https://www.engineeringtoolbox.com/rolling-friction-resistance-d_1303.html